XXII POLISH CONFERENCE ON BIOCYBERNETICS AND BIOMEDICAL ENGINEERING

Abstract Book

Warsaw, May 19-21, 2021

Committee of Biocybernetics and Biomedical Engineering of the Polish Academy of Sciences

Polish Society of Biomedical Engineering

Nalecz Institute of Biocybernetics and Biomedical Engineering PAS, Warsaw

XXII Polish Conference

on Biocybernetics and Biomedical Engineering

(PCBBE)

Honorary Patronage

Prof. Jerzy Duszyński

President of the Polish Academy of Sciences

Abstract Book

Warsaw, May 19-21, 2021

Program Committee

Chair

Prof. Adam Liebert, Chair of the Committee of Biocybernetics and Biomedical Engineering of the Polish Academy of Sciences, Warsaw, Poland

Co-chairs

Prof. Marek Darowski, President of the Polish Society of Biomedical Engineering, Warsaw, Poland

Prof. Dorota Pijanowska, Nalecz Institute on Biocybernetics and Biomedical Engineering PAS, Poland

Members

Prof. Piotr Augustyniak, AGH University of Science and Technology, Poland

Prof. Romuald Będziński, University of Zielona Góra, Poland

Prof. Ryszard Białecki, Silesian University of Technology, Poland

Prof. Piotr Bogorodzki, Warsaw University of Technology, Poland

Prof. Gerard Cybulski, Warsaw University of Technology, Poland

Prof. Agnieszka Dardzińska, Bialystok University of Technology, Poland

Prof. Krzysztof Fujarewicz, Silesian University of Technology, Poland

Prof. Adam Gacek, Institute of Medical Technology and Equipment, Poland

Prof. Marek Gzik, Silesian University of Technology, Poland

Prof. Adrian Horzyk, AGH University of Science and Technology, Poland

Prof. Janusz Jeżewski, Institute of Medical Technology and Equipment, Poland

Prof. Janusz Kacprzyk, Systems Research Institute PAS, Poland

Prof. Mariusz Kaczmarek, Gdańsk University of Technology, Poland

Prof. Krzysztof Kędzior, Central Institute for Labour Protection – National Research Institute, Poland

Prof. Józef Korbicz, University of Zielona Góra, Poland

Prof. Małgorzata Kotulska, Wrocław University of Science and Technology, Poland

Prof. Piotr Ładyżyński, Nalecz Institute on Biocybernetics and Biomedical Engineering PAS, Poland

Prof. Bogusław Major, Institute of Metallurgy and Materials Science PAS, Poland

Prof. Roman Major, Institute of Metallurgy and Materials Science PAS, Poland

Prof. Roman Maniewski, Nalecz Institute on Biocybernetics and Biomedical Engineering PAS, Poland

Prof. Olivier Meste, University of Nice, France

Prof. Tomasz Moskalewicz, AGH University of Science and Technology, Poland

Prof. Antoni Nowakowski, Gdańsk University of Technology, Poland

Prof. Tadeusz Pałko, Warsaw University of Technology, Poland

Prof. Zbigniew Paszenda, Silesian University of Technology, Poland

Prof. Elżbieta Pamuła, AGH University of Science and Technology, Poland

Prof. Jolanta Pauk, Bialystok University of Technology, Poland

Prof. Wojciech Penczek, Institute of Computer Science PAS, Poland

Prof. Ewa Piętka, Silesian University of Technology, Poland

Prof. Halina Podbielska, Wrocław University of Science and Technology, Poland

Prof. Jan Poleszczuk, Nalecz Institute on Biocybernetics and Biomedical Engineering PAS, Poland

Prof. Jacek Rumiński, Gdańsk University of Technology, Poland

Prof. Alina Sionkowska, Nicolaus Copernicus University, Poland

Prof. Paweł Strumiłło, Lodz University of Technology, Poland

Prof. Andrzej Świerniak, Silesian University of Technology, Poland

Prof. Zdzisław Tabor, Cracow University of Technology, Poland

Prof. Ryszard Tadeusiewicz, AGH University of Science and Technology, Poland

Prof. Ewaryst Tkacz, Silesian University of Technology, Poland

Prof. Władysław Torbicz, Nalecz Institute on Biocybernetics and Biomedical Engineering PAS, Poland

Prof. Milan Tysler, Slovak Academy of Sciences, Slovakia

Prof. Joerg Vienken, Usingen, Germany

Prof. Jerzy Walecki, Center of Postgraduate Medical Education, Poland

Prof. Bogdan Walkowiak, Lodz University of Technology, Poland

Prof. Jacek Waniewski, Nalecz Institute on Biocybernetics and Biomedical Engineering PAS, Poland

Dr. Krzysztof Zieliński, Nalecz Institute on Biocybernetics and Biomedical Engineering PAS, Poland

Program at a glance

Conference schedule
May 18 – 21, 2021

	May 18, Tuesday	May 19, Wednesday		May 20, Thursday		May 21, Friday	
		Track 1	Track 2	Track 1	Track 2	Track 1	Track 2
09:00 - 10:00		Opening Ceremony Plenary Lecture 1 - Prof. Frąckowiak (Track 1)		Plenary Lecture 3 - Prof. Legallais (Track 1)		Plenary Lecture 5 - Prof. Marraro (Track 1)	
10:00 - 11:00	Preconference workshop: "Good practice in research"	S1. Biomedical imaging	S2. Bioinformatics	S6. Bio-micro, nano technologies	S7. Artificial Organs	S10. Biomaterials I	S11. Biomechanics and biorobotics
11:00 - 11:30		Coffee Break		Coffee Break		Coffee Break	
11:30 -12:30		**Team Leaders Session 1 (Track 1)**		**Team Leaders Session 2 (Track 1)**		**Team Leaders Session 3 (Track 1)**	
12:30 - 13:30		Lunch Break Sygnis Bio Technologies - video		Lunch Break		Lunch Break Sygnis Bio Technologies - video	
13:30 - 14:30		S3. Biomedical signal processing I	SS1. Dlaczego Polska nie produkuje respiratorów?	SS3. IBBE PAS 45 anniversary (Track 1)		S12. Biomaterials II	S13. Biosensors and bioinstrumentation
14:30 - 15:30		Plenary Lecture 2 - Prof. Miklavcic (Track 1)		Plenary Lecture 4 - Prof. Pijanowska (Track 1)		Plenary Lecture 6 - Prof. Schoening (Track 1)	
15:30 - 16:00		Coffee Break	Poster Session I (15:45 - 17:30)	Coffee Break	Poster Session II (15:45 - 17:30)	Coffee Break	Poster Session III (15:45 - 17:30)
16:00 - 17:30		SS2. Clinical Engineering		SS4. Prof. Roman Maniewski Anniversary		SS5. Shared Ventilation	
17:30-18:30		S4. Biomedical signal processing II	S5. Modeling of biological systems	S8. Neural and rehabilitation engineering	S9. Molecular, cell and Tissue engineering	S14. E-health and telemedicine	SS6. PTIB Awards
18:30						Closing Ceremony	

PLENARY LECTURES

PL1: Prof. Richard Frąckowiak, *Non-invasive exploration of the human brain in health and disease*
PL2*:* Prof. Damijan Miklavčič, *Electroporation in biomedicine*
PL3*:* Prof. Cécile Legallais, *Building an external (bio)artificial liver : multi-scale and biomechanical considerations*
PL4: Prof. Dorota G Pijanowska, *Challenges in biosensing technologies*
PL5: Prof. Giuseppe A Marraro, *Respiratory support strategy of severe failure caused by sars-cov-2 infection*
PL6: Prof. Michael Schöning, *25 years with capacitive field-effect biosensors – a short review and current trends*

18 May, PRECONFERENCE WORKSKOP „Good practice in research”

Chairman: P. Ładyżyński

10:00 – 10:45 Prof. Jörg Vienken, *Designing medical devices: current concepts and their disqualification by fake news*
10:45 – 12:15 Prof. Adam Liebert, *How to write a good scientific article*?
14:00 – 15:30 Prof. Marek Wroński, *Naruszenia dobrych praktyk badawczych w biomedycynie*

SESSIONS

11:30 – 12:30. Team Leaders Session 1 – May 19, 2021

Chairman: A. Liebert

1. Elżbieta Pamuła "*Multifunctional biomaterials for tissue engineering and drug delivery*".
2. Paweł Sajkiewicz "*Biodegradable polymers as scaffolds and drug delivery systems for tissue engineering*".
3. Ludomira Granicka "*Nanomembranes and nanobiosystems for therapeutic purposes*".
4. Katarzyna Arkusz "*Biomechanics and nanobiomaterials at the University of Zielona Gora*".
5. Celina Pezowicz "*Tissue Biomechanics*".
6. Marta Kopaczyńska "*Changes of biomechanical properties of cancer cells induced by cytostatic agents*".
7. Marek Gzik "*From the Biomechanics of the 20th to the Biomechatronics of the 21st century*".
8. Jolanta Pauk "*Trends, research and technologies in the area of biomedical engineering*".
9. Zbigniew Paszenda / Marcin Kaczmarek "*Scientific potential and R&D experience of the Department of Biomaterials and Medical Devices Engineering*".
10. Ewa Piętka „Multimodal techniques in diagnostics, therapy and rehabilitation".

11:30 – 12:30. Team Leaders Session 2 – May 20, 2021

Chairman: A. Liebert

1. Andrzej Czyżewski "*Applications of multimedia technology in medicine*".
2. Robert Iskander "*New concepts in corneal imaging - when noise is not noise*".
3. Anna Korzyńska "*Artificial intelligence and deep learning in pathology*".
4. Tomasz Markiewicz "*Medical image analysis: selected topics*".
5. Jerzy Litniewski "*Quantitative ultrasound. Application in cancer diagnostics and therapy*".
6. Zbisław Tabor "*Statistics and machine learning for radiotherapy*".
7. Gerard Cybulski "*Biosignals detection and event prediction*".
8. Piotr Augustyniak "*Assisted living aspects of physiological signal processing*".
9. Adam Liebert/Piotr Sawosz "*Biomedical optics for assessment of tissue prefusion and oxygenation*".

11:30 – 12:30. Team Leaders Session 3 – May 21, 2021

Chairman: A. Liebert

1. Andrzej Skalski "*Mixed Reality and Image Registration in medicine - IPAL AGH experiences*".
2. Jacek Rumiński "*Ambient Intelligence in Healthcare*".
3. Jacek Waniewski/Jan Poleszczuk "*Mathematical modeling of physiological processes*".
4. Małgorzata Kotulska "*Amyloids - harmful or desirable proteins?*".
5. Tomasz Lipniacki "*Dissecting innate immune responses at single cell level*".
6. Krzysztof Fujarewicz "*Department of System Biology and Engineering at Silesian University of Technology*".
7. Piotr Ładyżyński "*Biomedical systems supporting the diagnosis and treatment of diabetes and its complications*".
8. Paweł Strumiłło "*Computer analysis of images of different modalities in medicine*".
9. Józef Korbicz "*Computer-aided medical diagnosis*"
10. Andrzej Swinarew "*Application of advanced methods of molecular analysis in medical diagnostics*"

May 19, 2021

10:00 - 11:00

S1. Biomedical imaging

Chairmen: A.Korzyńska, I.Buzalewicz

O1.1 Guy Perkins, Samuel J. E. Lucas and Hamid Dehghani. *Subject Specific Atlas Based Frequency Domain Diffuse Optical Tomography*

O1.2 Dawid Borycki, Egidijus Auksorius, Sławomir Tomczewski, Kamil Liżewski, Piotr Węgrzyn and Maciej Wojtkowski. *Spatiotemporal optical coherence (STOC) manipulation for structural and blood flow imaging of the human retina in vivo*

O1.3 Stanislaw Wojtkiewicz, Karolina Bejm and Adam Liebert. *Homodyne detection of brain-origin signals in near infrared spectroscopy*

O1.4 Jakub Zak, Krzysztof Siemion, Lukasz Roszkowiak and Anna Korzynska. *Fourier Transform Layer for fast foreground segmentation in samples images of tissue biopsies*

S2. Bioinformatics

Chairmen: A.Dardzińska, A.Horzyk

O2.1 Agata Wilk, Krzysztof Łakomiec, Krzysztof Psiuk-Maksymowicz and Krzysztof Fujarewicz. *Individualized mathematical models for Covid-19 pandemic in European countries*

O2.2 Katarzyna Hubicka and Małgorzata Kotulska. *Choosing representative subsets of amyloid proteins dataset*

O2.3 Marek Kochańczyk, Frederic Grabowski, Maciej Czerkies, Zbigniew Korwek, Wiktor Prus and Tomasz Lipniacki. *Antagonism between viral infection and innate immunity at the single-cell level*

O2.4 Leon Bobrowski and Tomasz Łukaszuk. *Functionally similar groups of features (genes) in a complex layer of formal neurons*

13:30 - 14:30

S3. Biomedical signal processing I

Chairmen: G.Cybulski, A.Uryga

O3.1 Tomasz Hawro, Ewelina Turczak, Reinhard König and Cezary Sielużycki. *ML classification of auditory evoked responses for task-related hemispheric lateralization*

O3.2 Anna M Stecka, Marcin Michnikowski, Elżbieta M Grabczak, Monika Zielińska-Krawczyk, Rafał Krenke and Tomasz Gólczewski. *Cough: is this seemingly unfavorable phenomenon profitable during thoracentesis?*

O3.3 Agnieszka Uryga, Marek Czosnyka and Magdalena Kasprowicz. *The utility of using non-invasive arterial blood pressure to estimate the time constant of cerebral arterial bed*

O3.4 Jacek Jurkojć, Piotr Wodarski, Robert Michnik, Wojciech Marszałek, Kajetan J. Słomka and Marek Gzik. *The use of FFT and STFT analysis in assessment of ability to maintain balance in sensory conflict conditions as a complementary element for time domain analyses*

SS1. Dlaczego Polska nie produkuje respiratorów?

Moderatorzy sesji:
Prof. Marek Gzik, Prof. Adam Liebert

Paneliści:
prof. Jarosław Fedorowski, prezes Federacji Szpitali Polskich, kardiolog,

prof. Tomasz Topoliński, rektor Uniwersytetu Technologiczno-Przyrodniczego im. Jana i Jędrzeja Śniadeckich w Bydgoszczy w kadencji 2016–2020, pomysłodawca polskiego respiratora,

dr inż. Krzysztof Zieliński, Instytut Biocybernetyki i Inżynierii Biomedycznej im. prof. Macieja Nałęcza PAN, kierownik zespołu wdrażającego polskie urządzenie Ventil, które może pozwolić na wentylację dwóch pacjentów z użyciem jednego respiratora.

Michał Janasik, wiceprezes Centrum Łukasiewicz ds. Finansów i Komercjalizacji

16:00 - 17:30

SS2. Inżynieria kliniczna w Polsce – jak przeskoczyć lukę pokoleniową

Chairman: Prof. E. Zalewska

SS2.1 Ewa Zalewska *„Inżynieria kliniczna – filar nowoczesnej ochrony zdrowia "*

SS2.2 Tadeusz Pałko, Kazimierz Pęczalski *„Zawód inżyniera medycznego – regulacje prawne"*

SS2.3 Zbigniew Paszenda, Marek Gzik, Witold Walke "*Inżynier medyczny - realia i perspektywy*"

SS2.4 Piotr Augustyniak *„Inżynieria kliniczna w planowaniu kariery absolwenta i programowaniu toku studiów "*

Poster Session I
(15:45 - 17:30)

17:30 - 18:30

S4. Biomedical signal processing II

Chairmen: P.Augustyniak, M.Kowal

O4.1 Zalewska Ewa. *Differentiation between single fiber potential (SFP) from one muscle fiber and SFP contaminated by other fibers*

O4.2 Aleksandra Królak and Edyta Pilecka. *Analysis and comparison of heart rate variability signals derived from PPG and ECG sensors*

O4.3 Nikodem Hryniewicz, Marcin Sińczuk, Rafał Rola, Ewa Piątkowska-Janko, Danuta Ryglewicz and Piotr Bogorodzki. *Manual and automatic epilepsy events selection in EEG-fMRI studies*

O4.4 Katarzyna Minta-Bielecka and Jolanta Pauk. *Gait patterns classification in hemiplegia patients based on biclustering algorithm*

S5. Modeling of biological systems

Chairmen: K.Fujarewicz, M.Dębowska

O5.1 Emilia Kozłowska and Andrzej Świerniak. *The stochastic mathematical model predicts angio-therapy could delay the emergence of metastases in lung cancer*

O5.2 Jaroslaw Smieja, Krzysztof Psiuk-Maksymowicz and Andrzej Swierniak. *A framework for modeling and efficacy evaluation of treatment of cancer with metastasis*

O5.3 Mauro Pietribiasi, Jacek Waniewski and John Leypoldt. *Modelling bicarbonate and CO2 dialysance in the haemodialyzer*

O5.4 Leszek Pstraś and Jacek Waniewski. *Contribution of albumin and globulins to plasma oncotic pressure*

May 20, 2021

10:00 - 11:00 S6. Bio-micro, nano technologies

Chairmen: M.Kopaczynska, L.Granicka

O6.1 Katarzyna Reczyńska, Magdalena Bialik, Natalia Nowosińska and Elżbieta Pamuła. *Solid lipid nanoparticles loaded with antibacterial peptides as versatile drug delivery systems for the treatment of bacterial infections*

O6.2 Katarzyna Arkusz, Marta Nycz, Ewa Paradowska and Dorota G. Pijanowska. *Corrosive and antibacterial properties of titanium nanotubes surface-modified thermally and with silver nanoparticles*

O6.3 Maxime Fages-Lartaud, Joanna Doskocz, Magdalena Przybyło, Maciej Łukawski and Marek Langner. *Development of the effective iron delivery vehicle*

O6.4 Krzysztof Makuch, Jolanta Zegarlińska, Aleksander Czogalla, Tomasz Borowik, Magdalena Przybyło and Marek Langner. *Liposomal carrier as a phospholipid depot for tear film lipid layer supplementation in patients with evaporative Dry Eye Syndrome*

S7. Artificial Organs

Chairmen: A.Jung, J.Poleszczuk

O7.1 Maria Rocchi, Libera Fresiello, Bart Meyns, Steven Jacobs, Anna Stecka, Maciej Kozarski and Krzysztof Zielinski. *An In Vitro System To Study Suction Events In Ventricular Assist Devices In Different Pathophysiological Conditions*

O7.2 Jacek Waniewski, Joanna Stachowska-Pietka and Roman Cherniha. *Hydration and swelling of non-perfused tissue: spatially distributed mathematical model for nonlinear poroelasticity*

O7.3 Anna Ciechanowska, Piotr Foltyński, Ilona Marcelina Góra, Stanislawa Sabalińska and Piotr Ładyżyński. *Design and optimization of the system controlling glucose concentration in a model of the artificial blood vessel*

O7.4 John Leypoldt, Joerg Kurz, Jorge Echeverri, Markus Storr, Mauro Pietribiasi and Kai Harenski. *Modeling acid-base balance for in-series extracorporeal carbon dioxide removal and continuous venovenous hemofiltration devices*

13:30 - 14:30 SS3. IBBE PAS 45 anniversary

Chairman: A.Liebert

SS3.1 Piotr Ładyżyński. *45-years of the Institute of Biocybernetics and Biomedical Engineering Polish Acedemy of Sciences*

SS3.2 Kamila Sadowska. *Implantable biofuel cells for self-powered biosensors*

SS3.3 Piotr Sawosz. *Cerebral oxygenation – clinical aspects*

SS3.4 Jan Poleszczuk. *Computational oncology: how close are we to performing in silico clinical trials?*

16:00 - 17:30 SS4. Prof. Roman Maniewski Anniversary

Chairman: A.Liebert

Poster Session II (15:45 - 17:30)

17:30 - 18:30 S8. Neural and rehabilitation engineering

Chairmen: P.Strumiłło, T.Bem

O8.1 Jolanta Zuzda, Jakub Kacpura, Jakub Dziura, Piotr Borkowski and Robert Latosiewicz. *An innovative approach for a hip disorders rehabilitation*

O8.2 Piotr Wodarski, Jacek Jurkojć and Marek Gzik. *Wavelet Decomposition in Analysis of Impact of Virtual Reality Head Mounted Display Systems on Postural Stability*

O8.3 Kacper Ogórek, Paweł Poryzała and Paweł Strumiłło. *EEG Based Image Reconstruction Using Transformers*

O8.4 Katarzyna Koter and Witold Szulc. *Examination of pneumatic bellows for the rehabilitation of the human jaw*

S9. Molecular, cell and Tissue engineering

Chairmen: M.Kotulska, K.Pluta

O9.1 Małgorzata Krok-Borkowicz, Bartosz Mielan and Elżbieta Pamuła. *Dynamic vs. static cell culture PLGA microspheres for "bottom-up" tissue engineering*

O9.2 Ilona Marcelina Góra, Anna Ciechanowska and Piotr Ładyżyński. *Activation of NLRP3 Inflammasome in Type 2 Diabetes*

O9.3 Małgorzata Kotulska, Michał Burdukiewicz, Witold Dyrka, Marlena Gąsior-Głogowska, Katarzyna Hubicka, Monika Szefczyk, Natalia Szulc and Jakub Wojciechowski. *Identification of amyloid proteins and their interactions – bioinformatics versus experiment*

O9.4 Natalia Szulc, Marelena Gąsior-Głogowska, Jakub W. Wojciechowski, Monika Szefczyk, Andrzej M. Żak, Michał Burdukiewicz and Malgorzata Kotulska. *The effect of deuterium oxide on the aggregation process of CsgA fragments*

May 21, 2021

10:00 - 11:00

S10. Biomaterials I

Chairmen: B.Major, A.Sionkowska

- O10.1 Aleksandra Jędrzejewska. *Corrosion properties of double-walled TiO2 nanotubes measured in 0.9% NaCl - preliminary results*
- O10.2 Marcin Elgalal, Piotr Komorowski and Bogdan Walkowiak. *Custom implants for the reconstruction of complex cranial and maxillofacial bone tissue defects*
- O10.3 Justyna Gargaś, Justyna Janowska, Karolina Ziąbska, Małgorzata Ziemka-Nałęcz and Joanna Sypecka. *An in vitro model of perinatal asphyxia: the influence of different biomaterials on proliferation and morphology of oligodendrocytes and astrocytes*
- O10.4 Beata Niemczyk-Soczyńska and Paweł Sajkiewicz. *Thermosensitive hydrogel/short electrospun fibers as a smart scaffold for tissue engineering*

S11. Biomechanics and biorobotics

Chairmen: J.Pauk, M.Gzik

- O11.1 Kamila Wiśniewska, Aleksandra Jędrzejewska, Monika Ratajczak and Tomasz Klekiel. *Analysis of the mechanical properties of impact absorbing structures used in military helmets*
- O11.2 Joanna Rymek and Adam Ciszkiewicz. *Analyzing the sensitivity of a procedure for obtaining a spherical contact pair to model the hip joint*
- O11.3 Marek Gzik, Wojciech Wolański, Kamil Joszko, Bożena Gzik-Zroska, Michał Burkacki and Sławomir Suchoń. *Multivariate analysis the blast injury of soldiers*
- O11.4 Monika Palmerska, Tomasz Klekiel and Agnieszka Mackiewicz. *Characteristics of nerve roots mechanical properties exposed to uniaxial stretching tests*

13:30 - 14:30

S12. Biomaterials II

Chairmen: J.Vienken, J.Sypecka

- O12.1 Konrad Kwiecień, Katarzyna Reczyńska, Katarzyna Bąk, Daria Niewolik, Katarzyna Jaszcz and Elżbieta Pamuła. *Manufacturing of poly(ester-anhydride) microparticles as drug delivery systems for pulmonary administration*
- O12.2 Aleksandra Jastrzębska, Marta Kamińska and Bogdan Walkowiak. *Assessment of changes in biological and antimicrobial properties of double-doped TiO2 coatings produced by anodic oxidation*
- O12.3 Angelika Zaszczynska and Paweł Sajkiewicz. *Designing of Three-Dimensional Piezoelectric Scaffolds for Neural Tissue Engineering*
- O12.4 Roman Major, Adam Byrski, Maciej Gawlikowski, Katarzyna Kasperkiewicz, Marcin Dyner, Juergen M. Lackner and Boguslaw Major. *The demands for designing the patient-specific, anti-microbial bioactive finger implants for durable functional reconstruction after amputation*

S13. Biosensors and Bioinstrumentation

Chairmen: K.Sadowska, F. Vahidpour

- O13.1 Rene Welden, Michael J. Schöning, Patrick H. Wagner and Torsten Wagner. *Light-addressable electrodes induce pH changes in microfluidic channels*
- O13.2 Igor Buzalewicz, Łukasz Zadka, Anna Matczuk and Halina Podbielska. *Optical phenotyping and characterization of macro- and micro-scale biological objects*
- O13.3 Dua Özsoylu, Tugba Isik, Mustafa M. Demir, Michael J. Schöning and Torsten Wagner. *A cell-based biosensor: "All-in-one" and "off-the-shelf" format for on-site monitoring of cell response*
- O13.4 Agnieszka Paziewska-Nowak, Marcin Urbanowicz, Anna Sołdatowska, Kamila Sadowska and Dorota Genowefa Pijanowska. *A multimodal, optical and electrochemical, approach towards detection of endogenous immunomodulators*

16:00 - 17:30

SS5. Shared Ventilation

Chairman: M.Darowski

- SS5.1 Giuseppe Marraro. *Flow diverters for lung ventilation in clinical practice: state of the art and future perspectives*
- SS5.2 Peter Khan. *Split Ventilation – Lessons from the COVID-19 Pandemic*
- SS5.3 Shriya Srinivasan et. al. *iSAVE Ventilator Multiplexing System*
- SS5.4 Krzysztof Zieliński. *Ventil - the system for independent lungs ventilation in splitted ventilation*

Poster Session III
(15:45 - 17:30)

17:30 - 18:30

S14 E-health and telemedicine

Chairmen: J.Rumiński, P.Foltyński

- O14.1 Piotr Foltynski and Piotr Ladyzynski. *An internet service system for automatic wound area measurement: preliminary tests*
- O14.2 Jan Poleszczuk, Niklas Krupka and Benjamin Misselwitz. *Microsimulation-based optimization of colorectal cancer screening strategies*
- O14.3 Mariusz Kaczmarek, Adam Bujnowski, Kamil Osiński, Tomasz Neumann and Jacek Rumiński. *eBathtub and eChair sensor subsystems supporting the elders*
- O14.4 Jakub Niemczuk, Dawid Michałowski, Bartosz Pośpiech and Marek Langner. *Novel Bluetooth Low Energy wireless endoscopic capsule for gastrointestinal diagnostics*

SS6. PTIB Awards

Chairman: M.Darowski

- SS6.1 Aleksandra Maria Osowska-Kurczab. *Differentiation of the Renal Cancer Types Based on the Analysis of CT Images*
- SS6.2 Wiktoria Wojnarowska. *Analysis of PEEK applications in knee endoprosthesis modeling*
- SS6.3 Paweł Czekała. *Construction of a voice communication device in production conditions for deaf people*
- SS6.4 Krzysztof Andrzej Gromada. *Construction and research of pulse pump with magneto-hydraulic levitation applied to artificial heart*
- SS6.5 Agnieszka Dubiel. *Attempt to develop a technology for the production of personalized polylactide plates for bone anastomosis reinforced with glass fiber*

May 19, 2021	**Poster Session I**	
	Chairmen: M.Kaczmarek, J.Stachowska-Piętka, M.Antosiak-Iwańska	
15:45 - 17:30	P1.1	Ilona Karpiel and Klaudia Duch. *BOLD-fMRI study of auditory cortex in young women*
	P1.2	Paweł Bzowski, Daniela Schwedka-Nowak and Damian Borys. *Analysing of breast deformations in different patient positions using FEM*
	P1.3	Marcin Skobel, Marek Kowal and Józef Korbicz. *Cell nuclei detection in breast cancer cytology images with U-Net neural network*
	P1.4	Damian Wanta, Mateusz Midura, Przemysław Wróblewski, Grzegorz Domański, Jacek Kryszyn and Waldemar T. Smolik. *Capacitively coupled electrical tomography for anatomical and functional imaging of thorax*
	P1.5	Anna Pawłowska, Norbert Żołek, Katarzyna Dobruch-Sobczak, Ziemowit Klimonda, Hanna Piotrzkowska-Wróblewska and Jerzy Litniewski. *The outcome of breast chemotherapy based on Gray Relational Coefficient of ultrasound images*
	P1.6	Lukasz Fura, Norbert Zolek and Tamara Kujawska. *Numerical simulations of the ultrasonic tissue ablation process*
	P1.7	Dominika Gabor, Rafał Doniec, Szymon Sieciński, Natalia Piaseczna, Konrad Duraj and Ewaryst Tkacz. *Automatic Assessment of Benton Visual Retention Test Results*
	P1.8	Krzysztof Psiuk-Maksymowicz, Martyna Szczyrba and Damian Borys. *Automatic detection of intracranial aneurysms on MRA data sets*
	P1.9	Kamil Kawoń, Zuzanna Setkowicz, Agnieszka Dróżdż, Krzysztof Janeczko and Joanna Chwiej. *Biochemical anomalies of nervous tissue resulting from mechanical brain injury can be characterized using the techniques of vibrational microspectroscopy*
	P1.10	Mateusz Midura, Damian Wanta, Przemysław Wróblewski, Jacek Kryszyn and Waldemar Smolik. *Web Application with Semiautomatic Algorithm for Renal Blood Flow Estimation in Dynamic Scintigraphy*
	P1.11	Lukasz Roszkowiak, Jakub Zak, Krzysztof Siemion, Antonina Pater and Anna Korzynska. *Split point assessment for HRnet dual model*
	P1.12	Marta Borowska. *Multiscale entropy in the analysis of enveloped uterine EMG signals*
	P1.13	Karolina Bejm, Stanislaw Wojtkiewicz, Żanna Pastuszak and Adam Liebert. *Decrease of hemodynamic responses to visual stimulation in the human brain under hypoxia*
	P1.14	Aleksandra Jung. *Influence of compartment model structure simplification on radiation dose calculation for C-14 urea breath test*
	P1.15	Katarzyna Hajdowska, Damian Borys and Andrzej Świerniak. *Spatial 3D simulations of tumour progressionmodel using evolutionary game theory*
	P1.16	Jolanta Zuzda, Jakub Kacpura, Jakub Dziura, Manuel Sillero Quintana and Robert Latosiewicz. *The Influence of Hip Conditioning Program with Rotational Movements on Thermal Response of Lower Limbs*
	P1.17	Agnieszka Mackiewicz, Tomasz Klekiel, Jagoda Kurowiak, Tomasz Piasecki and Romuald Będziński. *Mechanical properties of New Zealand White Rabbit urethra tissue under urinal fluid flow*
	P1.18	Mikołaj Schabowski and Adam Ciszkiewicz. *Analyzing the geometry of the articular surfaces of the bones in the radioulnar and the radiohumeral joint*
	P1.19	Anna Kasperczuk and Agnieszka Dardzinska. *Decision support system for IBD*
	P1.20	Marlena Gąsior-Głogowska, Natalia Szulc, Oliwia Polańska, Monika Szefczyk and Witold Dyrka. *Aggregation determination of bacterial amyloid signaling motifs using ATR-FTIR spectroscopy*
	P1.21	Jakub W. Wojciechowski and Małgorzata Kotulska. *Statistical potential and energy maps in prediction of amyloids*
	P1.22	Katarzyna Orzechowska and Tymon Rubel. *An SVM-based peptide identification algorithm integrated into a database search engine*
	P1.23	Michał Burdukiewicz, Katarzyna Sidorczuk, Przemyslaw Gagat, Filip Pietluch, Jakub Kała, Dominik Rafacz, Mateusz Bąkała, Jadwiga Słowik, Rafał Kolenda, Stefan Rödiger and Paweł Mackiewicz. *Negative data set sampling as the source of bias in prediction of antimicrobial peptides*

May 20, 2021	**Poster Session II**	
15:45 - 17:30	**Chairmen: A.Kaczorowska, A.Wencel, M.Antosiak-Iwańska**	
	P2.1	Agnieszka Kolodziejczyk, Paulina Sokolowska, Aleksandra Zimon, Magdalena Grala, Marcin Rosowski, Malgorzata Siatkowska, Piotr Komorowski and Bogdan Walkowiak. *Atomic force spectroscopy as a nanoscopic tool for assessing nanomaterials toxic effects in vitro*
	P2.2	Farnoosh Vahidpour, Torsten Wagner and Michael Josef Schöning. *A combined chemical/biosensor for simultaneous online monitoring and sterility assurance in aseptic food packaging*
	P2.3	Marcin Urbanowicz, Bartłomiej Lemieszek, Kamila Sadowska, Anna Sołdatowska, Agnieszka Paziewska-Nowak, Marek Dawgul and Dorota Pijanowska. *A new low-range biosensor for glutamate based on hyperbranched linkers*
	P2.4	Małgorzata Siatkowska, Paulina Sokołowska, Kamila Białkowska, Aleksandra Zimon, Magdalena Grala, Marcin Rosowski, Kinga Kądzioła-Długołęcka, Piotr Komorowski, Krzysztof Makowski, Daniel Reda and Bogdan Walkowiak. *Impact of micron-sized diamond particles on barrier cells of the human small intestine*
	P2.5	Anna Grzeczkowicz, Agata Lipko and Ludomira Granicka. *Nanothin Polyelectrolyte Membranes for Biomedical Purposes*
	P2.6	Magdalena Walkowiak-Przybyło, Marta Walczyńska, Marta Kamińska, Małgorzata Siatkowska, Piotr Komorowski and Bogdan Walkowiak. *Quantitative real-time polymerase chain reaction (qRT-PCR) technique as a useful tool for the assessment of cancer risk caused by medical implants*
	P2.7	Krzysztof Pietryga, Angelika Kiełbasa and Elżbieta Pamuła. *Indirect 3D-printing of viscous hydrogel in poly(vinyl alcohol) molds as a method to obtain tissue engineering scaffolds*
	P2.8	Anna Miklewska, Eleonora Kruglenko, Ryszard Tymkiewicz, Marcin Krajewski and Barbara Gambin. *Magnetic ferrofluids and ferrogel as sample materials for hyperthermia study*
	P2.9	Julia Lisoń, Anna Taratuta, Marcin Basiaga, Magdalena Antonowicz and Zbigniew Paszenda. *Various approaches to modify Ti13Nb13Zr alloy surfaces for improving biocompatibility*
	P2.10	Natalia Janik-Olchawa, Agnieszka Dróżdż, Damian Ryszawy, Maciej Pudełek, Karolina Płaneta, Zuzanna Setkowicz, Maciej Śniegocki, Andrzej Żądło, Beata Ostachowicz and Joanna Chwiej. *Assessment of the toxicity and possible therapeutic effects of iron oxide nanoparticles in in vitro cellular models*
	P2.12	Mateusz Kopec, Adam Brodecki and Zbigniew L. Kowalewski. *Microstructural analysis of fractured orthopedic implants*
	P2.13	Ved Prakash Dubey, Mateusz Kopec and Zbigniew L. Kowalewski. *Insight of magnesium matrix nanocomposites for biomedical applications- a synthetic review*
	P2.14	Marta Kamińska, Magdalena Walkowiak-Przybyło, Marta Walczyńska, Piotr Komorowski and Bogdan Walkowiak. *Effect of surface structuring of metallic materials on their thrombocompatibility*
	P2.15	Malgorzata Debowska, Mauro Pietribiasi, Jan Poleszczuk, Wojciech Zaluska, Wojciech Dabrowski and Alicja Wojcik-Zaluska. *Bioimpedance measurements in estimation of fluid removal during hemodialysis*
	P2.16	Joanna Stachowska-Pietka, Beata Naumnik, Ewa Suchowierska, Jacek Waniewski and Bengt Lindholm. *Mathematic modeling of automated peritoneal dialysis: Effect of schedules with variable temporal patterns of administration of dialysis fluid with different* glucose concentration
	P2.17	Barbara Stankiewicz, Krzystof J. Pałko and Marek Darowski. *Lung function impairment in CDH – from fetus diagnostics to young child examination*
	P2.18	Grzegorz Żurek, Mateusz Gąbka, Paulina Dałek, Magdalena Przybyło and Marek Langner. *The method for the approximation of AUC curve for supplements of endogenous biologically active substances*
	P2.19	Daria Hemmerling, Magdalena Wójcik-Pędziwiatr and Łukasz Paluch. *The classification system for Parkinson's disease based on EMD using voice signals*
	P2.20	Marzena Rugieł, Justyna Kutorasińska, Agnieszka Dróżdż, Zuzanna Setkowicz and Joanna Chwiej. *The use of FTIR microspectroscopy for the investigation of molecular changes in the hippocampal formation after repetitive electrical stimulation*
	P2.21	Bogdan Walkowiak, Magdalena Walkowiak-Przybyło and Piotr Komorowski. *Can molecular biology and photoelectron spectroscopy methods be used to identify nanotechnology products?*
	P2.22	Karolina Planeta, Zuzanna Setkowicz-Janeczko, Damian Ryszawy, Natalia Janik-Olchawa, Agnieszka Dróżdż and Joanna Chwiej. *Biomolecular topography of glioblastoma multiforme developed in the rat brain – a FTIR study*
	P2.23	Katarzyna Kramek-Romanowska, Agata Dorosz, Anna Stecka and Piotr Okrzeja. *Numerical simulations of air flow and particle deposition in the model human airways during independent lung ventilation*

May 21, 2021	**Poster Session III**	
15:45 - 17:30	**Chairmen: A.Korzyńska, M.Jablonski, M.Antosiak-Iwańska**	
	P3.1	Monika Drabik, Anna Grzeczkowicz, Paweł Bącal, Angelika Kwiatkowska, Magdalena Antosiak-Iwańska, Beata Kazimierczak, Ewa Godlewska and Ludomira Granicka. *Composite Membrane Scaffolds with Incorporated Metallic Nanoparticles for Supporting Fibroblastic Cell Growth*
	P3.2	Karolina Orzeł, Tomasz Gajowik and Magdalena Zielińska. *Customizable transepithelial/endothelial electrical resistance device with integrated multi-microelectrodes for the measurement of cellular barrier integrity*
	P3.3	Denise Molinnus, Kevin A. Janus, Aleksander Drinic, Heiko Iken, Nadja Kröger, Max Zinser, Ralf Smeets, Marius Köpf, Alexander Kopp and Michael J. Schöning. *Flexible electrochemical biosensor fabricated from Bombyx mori silk*
	P3.4	Melanie Jablonski, Jasmina Nork, Denise Molinnus, Likas Muschallik, Johannes Bongaerts, Torsten Wagner, Michael Keusgen, Petra Siegert and Michael J. Schöning. *Biosensoric acetoin detection in alcoholic beverages and fermentation broths*
	P3.5	Yasamin Ziai, Chiara Rinoldi, Paweł Nakielski, Tomasz Kowalewski and Filippo Pierini. *Bioinspired glucose sensor based on a smart nanoarchitecture hydrogel composite*
	P3.6	Anna Sołdatowska, Marcin Urbanowicz, Agnieszka Paziewska-Nowak, Kamila Sadowska and Dorota Pijanowska. *Bioplatform development for DNA-azathioprine interaction studies*
	P3.7	Adam Mirek, Paulina Korycka, Katarzyna Kramek-Romanowska, Marcin Grzeczkowicz and Dorota Lewinska. *How to create the electrospun polymeric mats of desired structure for biomedical applications?*
	P3.8	Aleh Sudakou, Anna Gerega, Helene Isler, Piotr Sawosz, Daniel Ostojic, Martin Wolf and Adam Liebert. *Hemoglobin spectra affect estimation of concentration and oxygen saturation: blood-lipid phantom study*
	P3.9	Antonina Pater, Łukasz Roszkowiak, Krzysztof Siemion and Anna Korzyńska. *Estimation of the fraction of area covered by cells and cell clusters in WSI patches*
	P3.10	Krzysztof Siemion, Anna Korzyńska, Łukasz Roszkowiak, Jakub Żak, Antonina Pater and Joanna Reszeć-Giełażyn. *Application of image analysis methods to evaluate histopathological slides in the study of prognostic factors of inflammatory spindle cell lesions*
	P3.11	Marcin Sińczuk, Jacek Rogala, Nikodem Hryniewicz, Ewa Piotrowska-Janko and Piotr Bogorodzki. *Feasibility analysis of suppressed water peak in single voxel 1-H MRS thermometry*
	P3.12	Elham Fazliazar, Piotr Sawosz, Aleh Sudakou and Adam Liebert. *Validation of a method to improve depth sensitivity of diffuse reflectance measurements to absorption changes in an optically turbid medium*
	P3.13	Kamil Wołos and Jan Poleszczuk. *Pulse wave propagation modeling for non-invasive assessment of heart function*
	P3.14	Piotr Okrzeja, Krzysztof Zieliński, Marcin Michnikowski and Marek Darowski. *Independent Lungs Ventilation impact on the cardiovascular system – a computer simulations*
	P3.15	Julia Grajek, Iñaki Schniewind, Claudia Peitzsch and Jan Poleszczuk. *Cellular plasticity upon proton irradiation*
	P3.16	Raman Pasledni and Krzysztof Zielinski. *Hybrid cardiovascular simulator - an application for the mechanical assistance by an intra-aortic balloon pump*
	P3.17	Małgorzata Jakubowska, Monika Wiśniewska, Agnieszka Wencel, Dorota Genowefa Pijanowska and Krzysztof Dariusz Pluta. *Evaluation of Polysulfone Capillary Membranes Used for Hepatic Cells Culturing in Dynamic Conditions*
	P3.18	Monika Wiśniewska, Małgorzata Jakubowska, Agnieszka Wencel, Dorota Pijanowska and Krzysztof Pluta. *Construction of Hollow Fiber Bioreactors for Hepatic Cell Culture*
	P3.19	Joyce Pinto, Malgorzata Debowska and Jacek Waniewski. *Mathematical modelling of phosphate kinetics, its peculiarity and adequacy indices for patients on maintenance hemodialysis*
	P3.20	Akanksha Jaiswar, Maria Grześ, Magdalena Oroń and Dawid Walerych. *Functional transcriptomics analysis of driver's oncogenes molecular programs in human neoplasia*
	P3.21	Saeed Samaei, Neda Mogharari, Dawid Borycki, Adam Liebert and Michal Kacprzak. *Non-invasive brain perfusion and oxygenation assessment with combined use of time-domain diffuse correlation spectroscopy and time-domain near-infrared spectroscopy*
	P3.22	Neda Mogharari, Saeed Samaei, Stanislaw Wojtkiewicz, Adam Liebert and Michał Kacprzak. *Hybrid diffuse optical system for the tissue perfusion and oxygenation assessment*
	P3.23	Dominika Szuberla, Włodzimierz Łukasik, Elżbieta Magdalena Grabczak, Krzysztof Jakub Pałko and Tadeusz Pałko. *Two methods for recording and classifying cough signals*

Location

The conference is organized by the the Nalecz Institute of Biocybernetics and Biomedical Engineering, Polish Academy of Sciences in Warsaw,
Ks. Trojdena 4 Str.
02-109, Warsaw, Poland

Due to the Covid-19 pandemic situation, the conference is held **ONLINE**.

Organizning Committee:

Krzysztof Zieliński, PhD, **Chairman**

Magdalena Antosiak-Iwańska, PhD

Anna Stecka, MSc

Piotr Okrzeja, MSc

Marta Baranowska, MSc

Barbara Wolff, MSc

Łukasz Wasilak

Marek Rudnicki

Content

(abstracts are listed in the alphabetical order of the first author)

PLENARY LECTURES

LECTURES

SPECIAL SESSION LECTURES

PLENARY LECTURES

Non-invasive exploration of the human brain in health and disease

Richard Frackowiak
EPFL, Geneve, Switzerland
richard.frackowiak@gmail.com

CV: Prof. Richard Frackowiak studied at Cambridge University as head of the Department of Clinical Neurosciences at the Centre Hospitalier Universitaire Vaudois in 2015. Previously, he served as Professor of Cognitive Neurology at University College London, Director of the Department of Cognitive Studies at the Ecole Normale Superieure, Paris and Vice-Provost of UCL. He founded the Wellcome Department of Imaging Neuroscience in 1994. A pioneer of human brain imaging research, he has investigated human brain structure-function relationships in health and disease. He headed up the medical informatics platform of "The Human Brain Project" His papers are highly cited (H-index Google 209).

Abstract: Organisationally, the human brain is massively redundant. When brain systems are damaged, or when reinforced by learning, they reorganise at the level of synaptic connection strength, or by selection of new preferred connections between cortical regions. In adults, up to 50% of brain cell loss can be accommodated, if gradual, with little obvious effect on clinically observed features. This fact generates hypotheses of potential clinical interest. Can we monitor these mechanisms or their effects precisely? Can they be enhanced or modulated? What are the implications after the appearance of symptoms and for any potential recovery?

Clinical scientists deploy novel non-invasive functional imaging techniques to examine brain reorganisation and to detect pre-clinical neuronal loss. MR images are now analysed with artificial intelligence techniques in a standard anatomical space making integration with clinical and biological data possible. The eventual clinical ambition is to link genetic and proteomic levels of brain organisation with rules that govern the cellular segregation of protein expression. From protein expression rules that determine cellular morphology should predict connectivity and so on, until a constructive process of predictive simulation discovers the mechanisms of emergent behaviours.

Frackowiak RSJ, Markram H. (2015) The future of human cerebral cartography: a novel approach. Phil.Trans. R. Soc. B 370: 20-32.

Building an external (bio)artificial liver : multi-scale and biomechanical considerations

Cécile Legallais
University of Technology, Compiegne, France
cecile.legallais@utc.fr

CV: Dr Cécile Legallais is Head of the CNRS/University of technology of Compiègne (FR) joint laboratory "Biomechanics & Bioengineering". She coordinates research on "Bioartifical liver". Her group possesses a large experience on hepatic cells culture (cell lines, primary from human or animal origin) on different 3D scaffolds perfused or not. The multidisciplinary nature of her work reveals her expertise in biomedical engineering and tissue engineering for the design of bio-artificial organs, fluid mechanics and microfluidics, transport phenomena, and the interactions between cells and tissues with biomaterials. Bronze Medal of CNRS in 2003, she published more than 100 papers in peer reviewed journals. She has supervised 25 PhD thesis. She is Past-President of the European Society of Artificial Organs.

Abstract: For patients with acute liver failure, the gold standard treatment, i.e. transplantation, suffers from a huge organs' shortage. Liver assist devices are either purely artificial (replacing functions) or bioartificial (in an integrated structure/function approach). For the liver, the challenge is very high since this organ is in charge of more than 500 functions in a healthy organism, coming from the presence of several cell types with a complex 3D organisation.

After a review of artificial extracorporeal systems, we will present several approaches currently under investigation in liver tissue engineering at the organ scale or at the tissue scale.
In these reconstruction attempts, biomechanics should not be forgotten: indeed, liver is a highly perfused organ with both venous and arterial blood, with a significant influence of local pressure and oxygen content on cell activities. In addition, this organ is very soft and most of its related diseases results in an alteration of its mechanical properties.

We will summarize how several bioinspired approaches at different scales to offer to the cells the "best" biomechanical environment. This means that both artificial matrix and bioreactor can be designed to meet the physiological conditions encountered in the native liver.

Respiratory support strategy of severe failure caused by sars-cov-2 infection

Giuseppe Marraro
University of Milan, Italy
gmarraro@picu.it

CV: Giuseppe A Marraro is Distinguished Professor at Department of Pulmonary and Critical Care Medicine, Department of Neonatology and Pediatrics, the Second Affiliated Hospital of Fujian Medical University, Quanzhou, China. Is Prof. Emeritus and Adjunct Professor at Center for Medical Simulation, DY Patil University, Navi Mumbai, India. He is associated to the "Healthcare Accountability Lab" at the University of Milan. He served as Chief of Department of Anesthesia and Intensive Care and Pediatric Intensive Care, Fatebenefratelli and Ophthalmiatric University Affiliated Hospital, Milan Italy; as President of the Italian Society of Anesthesia, Intensive Care, Emergency and Pain Society – SIARED.

His clinical and experimental scientific researches interests include Respiratory and Critical Care Medicine and Anesthesia in neonates, children and adults (e.g. protective lung ventilation strategy in human and animals; non-invasive ventilation; lung ultrasonography in children and neonate; biomarkers for lung diseases and pediatric sepsis; liquid ventilation; independent lung ventilation in pediatric age; clinical use of surfactant in lung pathologies in adults, pediatric age and neonates).
He acts as Associate Editor of Pediatric Critical Care Medicine and Member of the Editorial Boards and Reviewer of several scientific medical journals. He is authors/editor/co-author of 38 books, 7 scientific video-film; 300 scientific publications. He is deeply involved in basic and advanced education and training, and in the use of advance simulation systems in medical education.
He has been awarded with the Yandang Friendship Award and the West Lake Friendship Award. in China.

Abstract: Coronavirus disease 2019 (COVID-19), caused by the SARS-CoV-2 infection, is a systemic disease characterized by severe respiratory failure, similar to Acute Respiratory Distress Syndrome (ARDS).

The rapid spread of the COVID-19 pandemic on a global level has put national health systems in crisis, also highlighting considerable differences between countries in the proven effectiveness to deal with major emergencies, especially in the initial phase of the first pandemic wave.
COVID-19 has a great variability in severity ranging from a simple flu-like event with fever, cough, severe asthenia, shortness of breath up to severe ARDS.
The SARS-CoV-2 infection simultaneously infected a large number of patients and rapidly spread all over the world, also due to the initial lack of recognition of its severity which has led to dramatic consequences.

The severity and the very wide spread of the pandemic found everyone unprepared because, in addition to the symptomatic treatment, it was not known which treatments could be effective compared to others that were proposed from time to time. There has been enormous confusion in the treatments applied with extremely conflicting results in relation to the patients treated. Essentially there was a very wide use of O2, sometimes at high concentrations that could probably be toxic. Anti-inflammatory generics, antivirals, hydrochloroquine, plasma transfusion obtained from patients who had overcome the syndrome were used, as well to specific and in some cases traditional medicines in the countries where they are still used. The results on careful analysis were negative.

The WHO has defined the pharmacological treatments as certainly effective, resolving the great confusion that had arisen. Antipyretics have been described as useful in the initial stages and in home treatments. The use of O2 had to be supplemented at non-toxic dosages. In the advanced stages, non-invasive and invasive ventilatory support was indicated.

After the first autopsies it was revealed that the patients who died of severe SARS CoV-2 infection revealed not only the presence of diffuse alveolar damage consistent with ARDS but also with a higher thrombus burden in pulmonary capillaries. Following this evidence, the use of anticoagulants was suggested to avoid the formation of thrombus and facilitate their resolution.

Steroids that from the beginning had been widely used without any specific indication even in non-severe cases, were limited to advanced stage ARDS only.

The advanced stages of COVID-19 required hospitalization in ICU and in most cases support with non-invasive – continuous positive airway pressure (CPAP) through the use of Helmet and high flow nasal cannula (HFNC) – and invasive ventilation. The recommended ventilatory model has been the low tidal volume strategy, the appropriate level of positive end expiratory pressure (PEEP) and prone position.

The large number of patients who simultaneously required intensive care and artificial ventilation to treat the severe respiratory failure exerted on ICU a considerable pressure. Two main shortcomings were highlighted: lack of suitable spaces and mechanical ventilators for which it was necessary to proceed with the choice of patients to be hospitalized and ventilated in the ICU based on age and any associated pathologies.

Electroporation in biomedicine

Damijan Miklavčič
University of Ljubljana, Faculty of Electrical Engineering, Slovenia
Damijan.Miklavcic@fe.uni-lj.si

CV: Damijan Miklavčič was born in Ljubljana, Slovenia, in 1963. He received his PhD degree in electrical engineering from the University of Ljubljana in 1993. He is currently a tenured Professor at the Faculty of Electrical Engineering of the University of Ljubljana. His current research interests include electroporation-based treatments and therapies, including cancer treatment by means of electrochemotherapy, cardiac tissue ablation by irreversible electroporation, and gene transfer for gene therapy and DNA vaccination. His research involves biological experimentation, numerical modelling of biological processes, and hardware development. http://lbk.fe.uni-lj.si/en/damijan-en/

Abstract: Application of short high-voltage electric pulses causes transient increase of membrane permeability for molecules that otherwise are deprived of transport mechanisms. The phenomenon is known as electroporation and can be reversible – cell survives, or irreversible – cell dies. Reversible electroporation can be successfully used in introducing molecules such as RNA and DNA into cells for gene therapy and DNA vaccination, or chemotherapeutic drugs thus increasing their cellular accumulation and cytotoxicity in a treatment named elecrochemotherapy. Irreversible electroporation is on the other hand used successfully as a non-thermal tissue ablation method in local tumor treatment. Of particular interest is its potential that is bringing in cardiac tissue ablation as it promises fast and safe ablation of arrhythmogenic substrate with little or no damage to collateral tissues, e.g. lungs, esophagus and phrenic nerve in atrial fibrillation treatment by pulmonary vein isolation. Although final proof of its efficacy is still awaited, it has triggered enormous interest in cardiac electrophysiology arena. I will review the electroporation phenomenon at the membrane, cell and tissue level and highlight current challenges in making electroporation-based therapies safe and efficient.

Challenges in biosensing technologies

Dorota Pijanowska
Nalecz Institute of Biocybernetics and Biomedical Engineering PAS, Warsaw, Poland
dorota.pijanowska@ibib.waw.pl

CV: Dorota G. Pijanowska is a full professor at the Nalecz Institute of Biocybernetics and Biomedical Engineering, Polish Academy of Sciences (IBBE PAS), where she received PhD and DSc degrees in 1996 and 2006, respectively. Currently, she is the deputy director for research at IBBE PAS. She received postdoctoral fellowship at the Biosensors Group, University of Twente, The Netherlands. In 2007 she has got a position of associate professor at the IBBE PAS and she became the head of Biosensors Lab and Department of Hybrid and Analytical Microbiosystems. In 2017 she was awarded with title of full professor. Her research interests include development, fabrication and characterization of chemical sensors and biosensors as well as micro total analysis systems (μTAS, lab-on-a-chip), and their biomedical applications.

Abstract: Talking about biosensing technologies (bioSTs) anyone can think of different research aspects, including micro/nanotechnologies, molecular recognition, bioaffinity, enzymatic reactions, as well as plenty of biochemical species and biomarkers to be determined. Regardless various points of view, bioSTs are aimed at formation of specifically responding (bio)active sensing layers and sample processing systems. This can be achieved particularly through formation of biorecognition layers using natural or synthetic (bio)receptors deposited on active area of the transducer, and microfluidic based systems for bioassays. Particular interests are focused on development of sensor and microfluidic based bioanalytical microtools for brain metabolites analysis and non-specific and specific markers of cardiovascular and Alzheimer diseases as well as for bioactive substances (cytostatics, psychoactive drugs). These include recent and perspective research concerning microfluidic based systems for biomedical applications, in particular for determination of selected markers in biological samples of very small volume, such as cell lysates. A future direction of the research is related to theranostics, integrating many technologies, such as organs-on-a-chip, and microanalytical tools for monitoring the cell cultures.

25 years with capacitive field-effect biosensors – a short review and current trends

Michael Schoening
Aachen University of Applied Sciences, Germany
schoening@fh-aachen.de

CV: Michael J. Schöning received his diploma degree in electrical engineering (1989) and his PhD in the field of semiconductor-based microsensors for the detection of ions in liquids (1993), both from the Karlsruhe University of Technology. In 1989, he joined the Institute of Radiochemistry at the Research Centre Karlsruhe. Since 1993, he has been with the Institute of Thin Films and Interfaces (now, Institute for Biological Information Processing, IBI-3) at the Research Centre Jülich, and since 1999 he was appointed as full professor at Aachen University of Applied Sciences, Campus Jülich. Since 2006, he serves as a director of the Institute of Nano- and Biotechnologies (INB) at the Aachen University of Applied Sciences. His main research subjects concern silicon-based chemical and biological sensors, thin-film technologies, solid-state physics, microsystem and nano(bio-)technology.

Abstract: Among the multitude of concepts and different types of chemical sensors and biosensors discussed in the literature, the strategy to integrate chemical or biological recognition elements together with semiconductor-type field-effect devices is one of the most attractive approaches. In this context, typical examples are represented by the capacitive EIS (electrolyte-insulator-semiconductor) sensor, the LAPS (light-addressable potentiometric sensor) or the ISFET (ion-sensitive field-effect transistor). This presentation gives a 25 years review as well as considers current trends in the area of capacitive field-effect chemical and biological sensing. The sensors have been dealing with different receptor molecules (such as enzymes, polyelectrolytes or DNA molecules), various immobilization strategies and fabrication techniques as well as the detection of charged macromolecules by their intrinsic molecular charge.

LECTURES

Corrosive and antibacterial properties of titanium nanotubes surface-modified thermally and with silver nanoparticles

Katarzyna Arkusz[1], Marta Nycz[1], Ewa Paradowska[1], Dorota G. Pijanowska[2]
[1]Department of Biomedical Engineering, Faculty of Mechanical Engineering, University of Zielona Gora, Zielona Gora, Poland.
[2]Nalecz Institute of Biocybernetics and Biomedical Engineering, Polish Academy of Sciences, Warsaw, Poland.
k.arkusz@iimb.uz.zgora.pl

The rejection of long-term orthopedic/dental implant rejection is associated with infection caused by immune system imbalance or bacterial infection. Therefore, finding appropriate implantable biomaterials combining high corrosion resistance and antibacterial properties is important nowadays. The most common antibacterial agents used in implantology are silver nanoparticles, but their influence on corrosion and the resultant antimicrobial effect with thermally modified titania nanotubes have not been demonstrated yet [1-2].

This work aimed to elaborate and corrosive properties (corrosion rate, polarization resistance) in sodium chloride (0.9% NaCl) and phosphate buffered saline (0.01 M PBS) of titanium dioxide nanotubes (TNT) before thermal modification in an argon atmosphere (TNT NW and TNT WYZ, respectively) and chemical modification with silver nanotubes (AgNPs) both. Additionally, the antibacterial activity was tested against *Staphylococcus epidermidis* [Gramm(+)] and *Pseudomonas Aeruginosa* [Gramm(-)] after 24-hour incubation.

Corrosion rates and polarization resistance obtained using Tafel extrapolation of polarization curves are presented in Table. 1. The antibacterial efficiency against *Staphylococcous epidermidis* [Gramm(+)] were as follow: 62.58±2.66% (TNT NW), 91.57±1.03% (TNT WYZ), 54.00±4.69% (AgNPs/TNT NW), 9.33±2.13% (AgNPs/TNT WYZ), while against *Pseudomonas Aeruginosa* [Gramm(-)] as follow: 98.65±6.75% (TNT NW), 88.88±0.97% (TNT WYZ), 3.73±0.35% (AgNPs/TNT NW), 5.27±0.81% (AgNPs/TNT WYZ).

Table 1. The results of the corrosion test obtained using Tafel extrapolation of polarization curves.

	Corrosion rate [mm/year]		**Polarization resistance [Ω]**	
	0.01 M PBS	**0.9% NaCl**	**0.01 M PBS**	**0.9% NaCl**
Ti	0.0103±0.0014	0.0195±0.0095	346400±48270	619047±190262
TNT NW	0.0031±0.0001	0.0039±0.0021	9898±1414	21935±7713
TNT WYZ	0.0040±0.0024	0.0036±0.00196	26188±10847	30978±2283
AgNPs/TNT WYZ	0.0026±0.0004	0.00032±0.00013	23612±4652	109115±40304

The positive shift of anodic-polarization curves of titanium dioxide nanotubes modified thermally and chemically by silver nanoparticles indicates higher corrosion resistance than pure titanium or nonmodified-TNT. The lower corrosion rate and the higher corrosion resistance indicate the TNT annealed in argon and deposited with silver nanoparticles.
In this contribution, the better antibacterial activities of non-modified TNT against Gramm(+) were confirmed, while the thermal modification improves the antibacterial efficiency against Gramm-positive bacteria. Silver nanoparticles deposited on TNT significantly improve the antibacterial properties against each of the bacterial strains, however, a greater antibacterial effect of AgNPs/TNT WYZ on gram-negative bacteria was demonstrated than that of gram-positive bacteria.

References:
[1] Coman A.N., Mare A., Tanase C., Bud E., Rusu A., *Silver-Deposited Nanoparticles on the Titanium Nanotubes Surface as a Promising Antibacterial Material into Implants*. Metals 2021, 11(92), pp. 1-16.
[2] Arkusz K., Paradowska E., Nycz M., Mazurek-Popczyk J., Baldy-Chudzik K., *Evaluation of the Antibacterial Activity of Ag- and Au-Nanoparticles Loaded TiO_2 Nanotubes,* Journal of Biomedical Nanotechnology 2020, 16(9), pp. 1416-1425.

Decrease of hemodynamic responses to visual stimulation in the human brain under hypoxia

Karolina Bejm[1], Stanisław Wojtkiewicz[1], Żanna Pastuszak[2],Adam Liebert[1]

[1]Nalecz Institute of Biocybernetics and Biomedical Engineering PAS, 4 Trojdena Street, 02-109 Warsaw, Poland
[2]Department of Neurosurgery, Mossakowski Medical Research Center PAS, 5 Pawińskiego Street, 02-106 Warsaw, Poland
kbejm@ibib.waw.pl

Introduction: Hypoxia is a condition where the tissues are not getting enough oxygen**.** Cerebral hypoxia may occur in many life-threatening conditions such as ischemic stroke or heart attack [1].
Aims: The aim of this study is to investigate the effect of hypoxia and hyperoxia on hemodynamic of visual cortex under stimulation.

Methods: We have carried out series of visual stimulations on a group of six healthy volunteers. The cortical activity was recorded with high-density diffuse optical tomography (HD-DOT) measurement setup, which was developed in-house [2]. An optical fibres fixing system, including 12 detectors and 16 sources, was placed on the surface of a head above the occipital. A hypoxicator system Go2Altitude® (Biomedtech Australia Pty Ltd, Australia) was used to control the oxygen level in a breathing gas mixture. The stimulation of the visual cortex was induced by a reversing checkerboard at the frequency of 8 Hz, following the protocol: 60-second of baseline followed by epochs of stimulation (10 seconds of stimulation and 10 seconds of rest). The visual cortex activation was registered under three subsequent conditions: normal breathing conditions (20% oxygen in the gas mixture), hypoxia (12 % oxygen) and hyperoxia (40% oxygen).

Results: All registered parameters (heart rate, respiratory rate, arterial oxygen saturation and haemoglobin concentration change) were stable at the normoxia. The following symptoms have been observed under the hypoxia: an increase in the heart rate and deoxyhaemoglobin concentration and a decrease in oxyhaemoglobin concentration and arterial saturation. Under the hypoxia condition, a decrease in the amplitude of the brain hemodynamic response to the visual stimulation is visible in both (oxy and deoxy) haemoglobin concentrations. Furthermore, the highest amplitude of the visual cortex hemodynamic response to stimulation is observed during the hyperoxia, following the hypoxia challenge.

Conclusion: We validated the HD-DOT system as a method for high-resolution imaging of cortex activity under hypoxia and hyperoxia. We observed decrease in hemodynamic reaction amplitude during hypoxia. Obtained results follow functional magnetic resonance observations [3]. However, the NIRS can be applied outside the laboratory and allows to evaluate the effect of hypoxia and hyperoxia on both forms of haemoglobin which may allow deepening of knowledge about brain function under harsh condition. Furthermore, our results may help in the prediction of a saturation level, where the hemodynamic response to visual cortex stimulation is no longer visible during hypoxia and the critical saturation is hit.

Acknowledgments:
This study was partially supported by the National Science Centre – project number 2016/21/N/ST7/03117

References:

1. P. Ferdinand and C. Roffe, "Hypoxia after stroke: a review of experimental and clinical evidence," Experimental & translational stroke medicine **8**, 1-8 (2016).
2. S. Wojtkiewicz, P. Sawosz, M. Kacprzak, A. Gerega, K. Bejm, R. Maniewski, and A. Liebert, "Towards Optical Tomography of an Adult Human Head," in *Optical Tomography and Spectroscopy*, (Optical Society of America, 2016), OM4C. 2.
3. F. Rodrigues Barreto, S. Mangia, and C. E. Garrido Salmon, "Effects of reduced oxygen availability on the vascular response and oxygen consumption of the activated human visual cortex," Journal of Magnetic Resonance Imaging **46**, 142-149 (2017).

Functionally similar groups of features (genes) in a complex layer of formal neurons

Leon Bobrowski[1,2], Tomasz Łukaszuk[2]
[1] Faculty of Computer Science, Bialystok University of Technology,
[2] Institute of Biocybernetics and Biomedical Engineering, PAS, Warsaw, Poland
l.bobrowski@pb.edu.pl

Datasets consisting of a small number of multivariate feature vectors often appear in practice. Genetic data sets, among others, have such a structure. Learning datasets consisting of a small number of high-dimensional feature vectors can usually be separated linearly. For this reason, linear classifiers (formal neurons) play a fundamental role in the processing of small samples of multidimensional vectors.

Margins maximization is one of the basic principles of designing linear classifiers. Maximizing Euclidean (L_2) margins is a fundamental concept in the design of support vector machines (*SVM*) classifiers. An alternative approach to designing linear classifiers was based on maximizing the margins determined according to the L_1 norm. Groups of features (genes) characterized by large margins of the L_1 type can be selected from a given data set by minimizing the perceptron criterion function with regularization [1].

The perceptron criterion function belongs to the family of convex and piecewise (*CPL*) criterion functions. The basis exchange algorithm enables the efficient and precise minimization of the *CPL* criteria functions. This approach can also be used to design complex layers of linear classifiers from small samples of multidimensional vectors [2]. A complex layer of linear classifiers makes it possible to increase the accuracy of classification in pattern recognition tasks. Such a property has been described in many works on classifier assemblies.

The complex layer is designed on the basis of a small number of m vectors with a large dimension n ($m << n$). The complex layer consists of formal neurons (linear classifiers) that are defined on disjoint groups of m features and are characterized by large L_1 margins. Designing complex layers of low-dimensional linear classifiers can be related to the ergodic theory. According to the proposed approach, averaging over a small number of m vectors of features (patients, objects) is replaced by averaging over a large number of functionally similar subsets of m features (genes).

The article proposes a method of forming functionally similar subsets of genes by designing a complex layer of formal neurons. The layer is designed by using two opposing groups of patients which are represented by genetic vectors. The two opposing groups of m patients may reflect various diseases or other medical problems of interest. Subsets of m selected genes allow for linear differentiation with a large margin of the same two groups of patients. Selected gene subsets can be treated as alternative diagnostic keys for diseases represented by particular groups of patients.

The functional similarity of gene groups means that one group of genes can be replaced with another group without changing differentiation between fixed groups of patients. The number and structure of diagnostic keys may allow for inference about the genetic basis of particular diseases. It can be expected that under certain conditions, the diagnostic keys used for differentiation between opposite groups of patients can be generalized as an important property of an organism [3].

References:
[1] Bobrowski, L. *Data Exploration and Linear Separability*, pp. 1 – 172, Lambert Academic Publishing, 2019.
[2] Bobrowski, L. Complexes of low dimensional linear classifiers with L_1 margins, *ACIIDS* 2021, Springer 2021 (*to appear*).
[3] Collins, S.C., Mikhaleva, A., Vrcelj, K. *et al.* Large-scale neuroanatomical study uncovers 198 gene associations in mouse brain morphogenesis. *Nat Commun* **10,** 3465 (2019). https://doi.org/10.1038/s41467-019-11431-2.

Multiscale entropy in the analysis of enveloped uterine EMG signals

Marta Borowska
Faculty of Mechanical Engineering, Bialystok University of Technology, Białystok, Poland
m.borowska@pb.edu.pl

Physiological systems are regulated by many mechanisms operating at different spatial and temporal scales. The signals generated by these systems often exhibit complex fluctuations that are not due to noise in them, but contain information about the dynamics of the system. Multiscale entropy (MSE) is a measure of complexity based on the quantification of information on multiple scales [1]. For a given time series $\{x_n\}$ represents biological system is constructed time series $\{y^{\varepsilon}\}$ dependent on scaling parameter ε expressed by the formula:

$$y_j^{\varepsilon} = \frac{1}{\varepsilon} \sum_{i=(j-1)\varepsilon+1}^{j\varepsilon} x_i$$

For the first scale, we have the original time series. The length of each time series corresponds to the length of the original time series divided by the scaling parameter ε. The quantitative measure calculation is based on sample entropy which expressed by the formula:

$$\mathrm{Samp_{en}} = \ln \frac{\Phi^{\mathrm{m}}(\mathrm{r})}{\Phi^{\mathrm{m+1}}(\mathrm{r})}$$

where $\Phi^{\mathrm{m}}(\mathrm{r})$ is the probability that two sequences match for *m* points is computed by counting the average number of vector pairs for which the distance is lower than the tolerance *r*.

In this study, multiscale entropy was applied in describing the dynamics of the uterus taking into account the non-linear and non-stationary nature of electromyography uterine (uEMG) signals. The uEMG signals come from an open access database (TPEHGDB) located on Physionet Web [2]. Two groups of uEMG signals were used from 3rd channel (E3): delivering on term (>37 weeks of pregnancy, before the 26th week of gestation) - group A (n = 19) and delivering prematurely (≤37 weeks of pregnancy, before the 26th week of gestation) - group B (n = 19. The first signals were filtered using 4-pole band-pass Butterworth filter with cutoff frequency of 1–3 Hz. From the filtered uEMG signals were removed the first and the last 180s length of signals in order to avoid transient effects due to filtering process. After that, the envelope and smoothed of the signals were obtained with the help of Hilbert transform. In this way, uterine contractions were detected from uEMG signals. In the next step, the multiscale entropy measure (MSE) of enveloped uEMG signals was computed in 20 scales in order to test its suitability for the detection of preterm labor. Statistical analysis was performed by means of a t-student test.

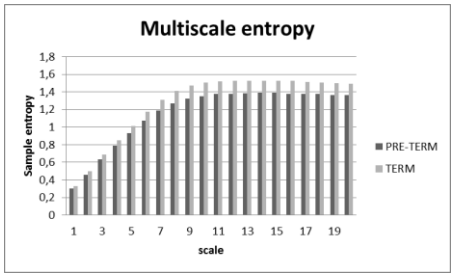

Fig. 1. The results of multiscale entropy of uEMG signals.

The mean values of sample entropy in Group A are significantly higher than those in Group B for all scales ($p<0.05$) (Fig. 1). Sample entropy measures of uEMG signals increase for all scales both in Group A and Group B. The result indicates that uEMG signals are more complex in the term state than in the preterm state. MSE is a simple method for quantifying the dynamical changes of uEMG signals and can be useful for other types of biomedical signal analysis.

References:

[1] M. Costa, A. L. Goldberger, and C.-K. Peng, Multiscale entropy analysis of complex physiologic time series, Physical Review Letters, vol. 89, no. 6, pp. 068102, 2002.

[2] Goldberger, A. L., Amaral, L. A., Glass, L., Hausdorff, J. M., Ivanov, P. C., Mark, R. G., ... & Stanley, H. E. (2000). PhysioBank, PhysioToolkit, and PhysioNet: components of a new research resource for complex physiologic signals. Circulation, 101(23), e215-e220.

Spatiotemporal optical coherence (STOC) manipulation for structural and blood flow imaging of the human retina *in vivo*

Dawid Borycki, Egidijus Auksorius, Sławomir Tomczewski, Kamil Liżewski,
Piotr Węgrzyn, and Maciej Wojtkowski
Institute of Physical Chemistry, Polish Academy of Sciences, Warsaw, Poland,
International Centre for Translational Eye Research, Warsaw, Poland
dborycki@ichf.edu.pl

Optical coherence tomography (OCT) is a well-established modality providing cross-sectional images of the human retina non-invasively. However, OCT does not provide high-resolution *en face* images of the outer retinal layers due to eye aberrations and the fundamental tradeoff between axial imaging range and transverse resolution. Furthermore, OCT is challenging to depict blood flow of the deep retina layers, like choroid.

To solve this problem, we developed spatiotemporal optical coherence (STOC) manipulation [1-3] that provides high-resolution, aberration-free volumetric images of the retina and cornea with a voxel rate of 8 GHz. In STOC imaging, the interferometer is supplemented by the spatial light modulator (SLM). The time-varying phase masks displayed on the SLM modulate the incident light to alter the interferometric images [Fig. 1]. These images are then corrected with digital aberration correction [2], and integrated coherently to produce crosstalk-free, aberration-free volumetric images of the sample. We have recently applied this approach for *in vivo* human retinal and corneal imaging [2,3].

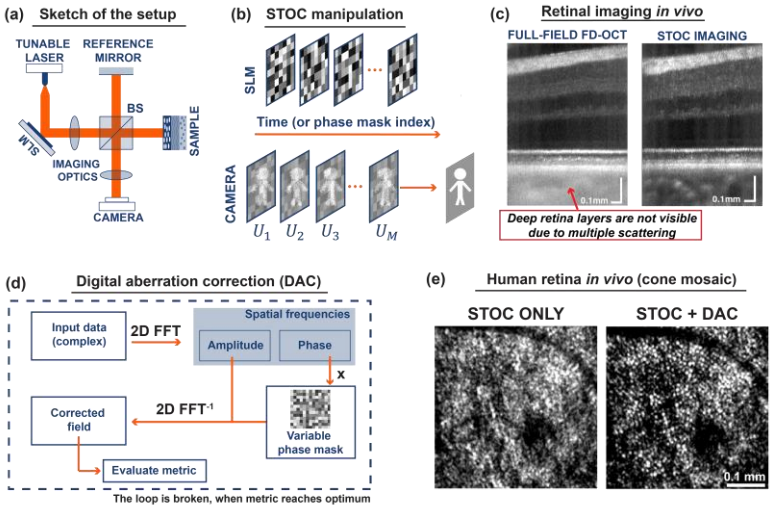

Fig. 1. Spatiotemporal optical coherence (STOC) imaging. (a) Sketch of the optical setup, which is the FD-FF-OCT supplemented by the SLM. (b) The SLM sequentially displays inhomogeneous phase patterns, which alter the spectral fringe patterns. Fringe patterns are processed to yield complex approximations of the fields scattered from the sample $U_1, U_2, \ldots, U_M$. They are integrated to get crosstalk-free images (c). The phase of the STOC images is corrected in post-processing (d) to remove aberrations and reveal otherwise invisible sample features

Here, we extend our work to demonstrate that our datasets can be processed digitally to remove the phase shifts from laser tuning and ultimately estimate Doppler broadening. We show that this approach enables visualization of the choroidal blood vessels, located deep in the human retina [Fig. 2].

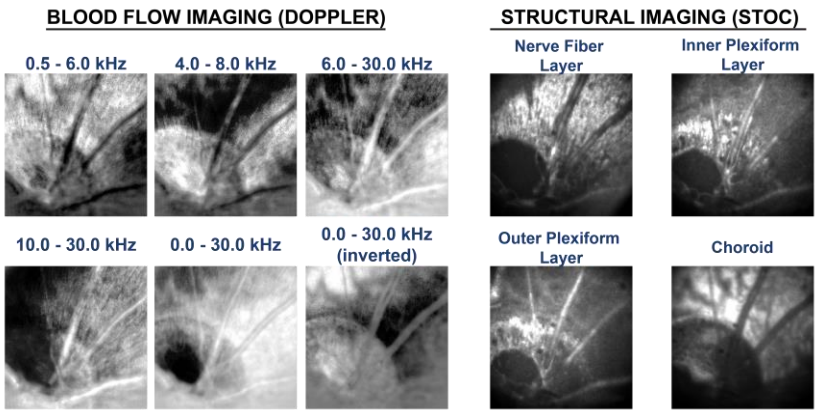

In summary, we showed that spatiotemporal phase modulation can be used to improve imaging depth of the human eye *in vivo*. We could further enhance the transverse image resolution with digital aberration correction. Finally, we depicted deep blood flow through Doppler broadening analysis.

[1] D. Borycki, M. Hamkalo, M. Nowakowski, M. Szkulmowski, and M. Wojtkowski, Biomed Opt Express 10, 2032 (2019).
[2] D. Borycki, E. Auksorius, P. Węgrzyn, M. Wojtkowski, Opt. Lett., 45(6), 1293 (2020).
[3] E. Auksorius, D. Borycki, P. Stremplewski, K. Liżewski, S. Tomczewski, P. Niedźwiedziuk, B. L. Sikorski, M. Wojtkowski, Biomed Opt Express 11 (5), 2849-2865 (2020).

Negative data set sampling as the source of bias in prediction of antimicrobial peptides

Michał Burdukiewicz[1,5], Katarzyna Sidorczuk[2], Przemysław Gagat[2], Filip Pietluch[2], Jakub Kała[3], Dominik Rafacz[3], Mateusz Bąkała[3], Jadwiga Słowik[3], Rafał Kolenda[4], Stefan Rödiger[5], Paweł Mackiewicz[2]
[1]Medical University of Białystok, Białystok, Poland
[2]University of Wrocław, , Poland
[3]Warsaw University of Technology, Warsaw, Poland
[4]Wrocław University of Environmental and Life Sciences Wrocław, Poland,
[5]Brandenburg University of Technology Cottbus-Senftenberg, Cottbus, Germany
michalburdukiewicz@gmail.com

Aims: Antimicrobial peptides (AMPs), an important alternative to traditional antibiotics, are molecules that participate in host defense and/or microbial competition by disrupting negatively charged bacterial membranes. To reduce the costs of experimental research, robust machine learning models for AMP prediction (as our model AmpGram [1]) are essential. However, such models require training data and although positive cases (AMPs) are widely available in the database of antimicrobial peptides (e.g., DBAASP), the negative data has to be sampled from more general databases. The aim of this work is to compare the impact of negative data sampling strategies on the on the performance of machine learning models.
Methods: We have implemented 13 negative data sampling strategies and 15 model architectures employed by the state-of-art AMP predictors. Next, we have trained 195 models for each combination of the model architecture and negative data set sampling method and benchmarked them (Figure 1). To obtain better estimates of performance measures, we have repeated this whole procedure five times.

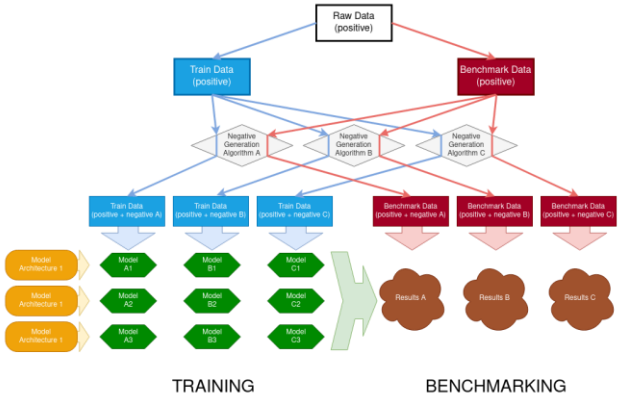

Results: Despite superficial similarities, the negative data set sampling methods considered in our analysis generated drastically different data sets. From 13 methods, only two were generating negative data with amino acid composition indistinguishable by statistical testing (p-value with the Benjamini-Hochberg correction above 0.05). Moreover, three out of 13 methods were unstable enough to generate negative data that was significantly different in each repetition. Our results confirmed that negative data sampling has a dramatic effect on the performance of the model. Models trained using negative data sampled with one method are in general handicapped when benchmarked on the data sampled with another method. Our analysis has also shown patterns in the performance of model architectures. The best performing architectures are based on the k-mer (n-gram) counts and significantly outperforms architectures employing only the physicochemical properties of amino acids or their variants as pseudo amino acid composition (PseAA). The average AUC of k-mer based models is 0.91 compared to 0.81 of models based on other metrics. Moreover, the models trained using deep approaches (as convolutional neural networks) had similar performance or lower measures to non-deep architectures as random forests (the difference between mean AUC of 0.91 compared to 0.90 was found insignificant by the Friedman test).

Conclusion: Our analysis has shown that the majority of benchmarks of the model for AMP prediction are biased. Thus, to fairly compare two different models, one should train them and benchmark using negative data sampled with the same method. Additionally, some of the methods for sampling negative data sets (e.g.,

employed by amPEP and iAMP-2L) are very variable. Here, to obtain an unbiased estimate of the model performance, the benchmark procedure should be repeated at least a few times. Moreover, the deep models for the prediction of AMPs cannot significantly outperform non-deep approaches.

References:

[1] Burdukiewicz, M., Sidorczuk, K., Rafacz, D., Pietluch, F., Chilimoniuk, J., Rödiger, S., and Gagat, P. (2020). Proteomic Screening for Prediction and Design of Antimicrobial Peptides with AmpGram. International Journal of Molecular Sciences 21, 4310.

Optical phenotyping and characterization of macro-and micro-scale biological objects

Igor Buzalewicz[1], Łukasz Zadka[2], Anna Matczuk[3], Halina Podbielska[1]

[1]Department of Biomedical Engineering, Faculty of Fundamental Problems of Technology, Wroclaw University of Science and Technology, 27 Wybrzeże S. Wyspiańskiego St., 50-370, Wroclaw, Poland
[2] Histology and Embryology Division, Department of Human Morphology and Embryology, 6a Chałubińskiego St., 50-368 Wrocław, Poland
[3] Department of Pathology, Division of Microbiology, Faculty of Veterinary Medicine Wrocław University of Environmental and Life Sciences, 31 C.K. Norwida St. 51-375 Wrocław, Poland
igor.buzalewicz@pwr.edu.pl

Three-dimensional imaging is crucial for the investigation of cell and tissue biology and provides valuable information about the mechanisms behind the pathophysiology of cells and tissues. Recent advances in the field of optical diffraction tomography (ODT) and digital holographic tomography (DHT) have demonstrated the potential for the examination of different biological objects in a quantitative and label-free manner [1]. DHT enables the reconstruction of the 3D refractive index (RI) distribution, which can provide unique information about the local density and chemical composition changes. The presented study aims to demonstrate the potential of the DHT in the examination of various biological objects: *E.coli* cells, colonic tissues, extracellular vesicles (EVs), or cytopathic effects in cells caused by viruses (EAV- Equine Arteritis Virus) as an alternative for the common microscopic techniques.

In this study, we used the commercial off-axis Mach-Zehnder interferometric setup with a rotatable scanning mirror (3D Cell Explorer, Nanolive, Switzerland). For different angles of the monochromatic illumination beam (520 nm) the series of digital holograms (DHs) resulting from the interference of the reference beam and object beam (diffracted on analyzed samples) were registered, while the camera and the sample remained at the fixed locations. Next, the projections needed for acquiring the 3D-RI tomograms were numerically reconstructed from individual DHs taking advantage of the concepts of the quasi 2π-holographic detection and complex convolution [2]. The RI data were processed in MATLAB software. The biological samples were provided by Wroclaw Medical University and Wroclaw University of Environmental and Life Sciences.

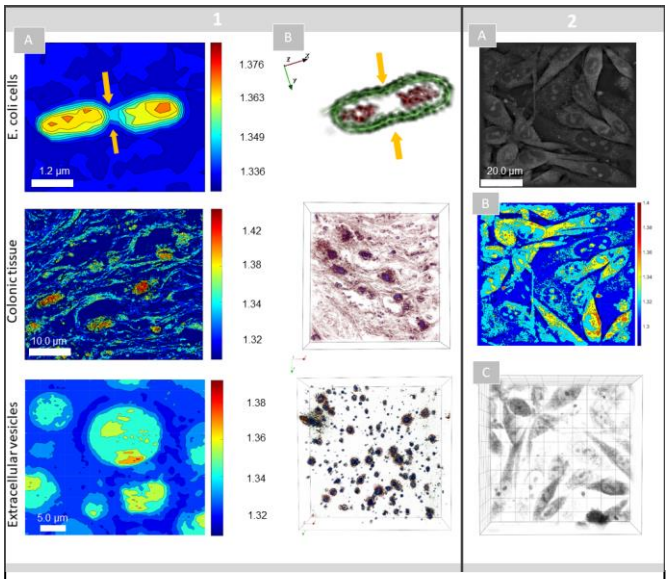

Fig.1 The representative experimental results: (1) processed 2D-RI maps (A) and rendered 3D-RI maps of E. coli cells, colonic tissue and extracellular vesicles, (2) cytopathic effect of hamster fibroblast cells infected by a virus: 2D-RI gray-scale map (A), processed 2D-RI map, rendered 3D-RI map (C).

The exemplary results in Fig. 1 are showing that 3D-RI data can provide additional quantitative information for biological objects examination. It enabled the examination of the process of bacteria single-cell division, characterization differences between the post-mortem and healthy colonic tissue, analyze the spatial heterogeneity of EVs or characterize the cytopathic effect and morphological changes of the fibroblast cells cause by virus infection.

DHT enables sensitive, objective, rapid, and reproducible measurement and the data could be easily compared to conventional imaging like confocal fluorescence microscopy. We demonstrate a label-free method for the functional and physiological research of the cellular processes in real-time without any exogenous labeling agents or dyes, such as fluorescence proteins, organic/inorganic dyes, and quantum dots.

References:

[1] K. Kim et al. Optical diffraction tomography techniques for the study of cell pathophysiology, *Journal of Biomedical Photonics & Engineering*, vol. 2(2), p. 020201.
[2] Y. Cotte et al. Marker-free phase nanoscopy. *Nature Photonics* 7, pp. 113–117.

Analysing of breast deformations in different patient position using FEM

Paweł Bzowski [1,2,3], Daniela Schwedka-Nowak[4] , and Damian Borys[1,2,3]

[1] Silesian University of Technology, Faculty of Automatic Control, Electronics and Computer Science, Department of Systems Biology and Engineering, Gliwice, Poland
[2] Silesian University of Technology, Biotechnology Center, Gliwice, Poland
[3] Maria Sklodowska-Curie National Research Institute of Oncology, Nuclear Medicine Department, Gliwice, Poland
[4] University of Silesia, Faculty of Science and Technology, Katowice, Poland

Breast cancer is one of the most common types of cancer in the XXI century. Late detected could be mortal. According to GLOBOSCAN [1], only in 2020 were more than 2 million new breast cancer cases. Image processing methods are used to enhance diagnosis and to compare studies in different modalities or patient positions. Using new technologies and image processing methods, the detectability of cancer is much higher. The primary imaging modalities in breast diagnosis are computed tomography with positron emission tomography, magnetic resonance imaging, and mammography [2]. Each of these studies gives different information about structures and physiology. The best way is to compare these images in one coordinate system, but these studies are acquired in different patient positions: supine, prone, and upright standing.

This work aims to create an algorithm to evaluate breast deformation in different patient positions. In this work, the Finite Element Method was used for breast examination [3]. The breast is a specific organ due to its flexibility, so in different positions, the breast shape could be not the same. This property makes that comparison of various studies could be difficult or impossible. Breast modelling using the Finite Element Method could solve this problem and improve diagnostics in breast cancers.

The algorithm uses DICOM images acquired on PET/CT Siemens mCT Biograph. In the next step, we have created an STL model using Horos software. The model was imported to FreeCAD (open-source software). Using the FEM module in FreeCAD, the deformations in different positions were calculated. The gravity's force was used as an external force that was acting on an object. The back of the breast has been stabilized

The model can simulate different breast positions during the study. Obtained new nodes positions present breast deformation in a supine position. To better describe deformation, the nipple movement was calculated for each breast in each position. A bigger breast is more flexible than a smaller one. For bigger breast maximum displacement in the z-axis was 57.30 mm, and for smaller, it was 2.50 mm to 10.70 mm in the z-axis.

The proposed algorithm allows deforming images depended on different patient positions, which can be useful in comparing various studies.

References:

[1] Sung, H., Ferlay, J., L.Siegiel, R., Laversanne, M., Soerjomataram, I., Jemal, A., Bray, F.: Global cancer statistics 2020: Globocan estimates of incidence and mortality worldwide for 36 cancers in 185 countries. CA CANCER J CLIN (0), 1–41 (2021).

[2] Lima ZS, Ebadi MR, Amjad G, Younesi L. Application of Imaging Technologies in Breast Cancer Detection: A Review Article. *Open Access Maced J Med Sci*. 2019;7(5):838-848. Published 2019 Mar 14. doi:10.3889/oamjms.2019.171.

[3] Sturgeon GM, Kiarashi N, Lo JY, Samei E, Segars WP. Finite-element modeling of compression and gravity on a population of breast phantoms for multimodality imaging simulation. *Med Phys*. 2016;43(5):2207. doi:10.1118/1.4945275.

Design and optimization of the system controlling glucose concentration in a model of the artificial blood vessel

Anna Ciechanowska, Piotr Foltyński, Ilona Marcelina Góra, Stanisława Sabalińska, Piotr Ładyżyński
Nalecz Institute of Biocybernetics and Biomedical Engineering, Polish Academy of Sciences,
4, Trojdena Str., 02-109 Warsaw, Poland
aciechanowska@ibib.waw.pl

Aims

Hyperglycemia and glucose variability increase the risk of developing diabetes-related late complications. An artificial blood vessel model based on a capillary bioreactor was constructed to investigate the effect of constant and variable glucose concentrations in the culture medium on endothelial cells in vitro. The aim of the work was to design and optimize the system controlling glucose concentration in this model. We investigated what volume of circulating medium needs to be replaced in order to achieve the new target concentration of glucose.

Methods

The system consists of the control unit (CS), two pumps (P1, P2), two valves (V1, V2), two containers with culture medium with minimum (C1) and maximum (C2) glucose concentration, the waste medium container (C4) and the circulation circuit (CC) (Fig. 1). CC consists of the bioreactor (B), container with target glucose concentration (C3) and two pumps ensuring the flow of the culture medium through the inner and outer part of the bioreactor (P3, P4). The task of CS is to replace the culture medium in C3 with the medium of the target glucose concentration during the continuous circulation of the medium. The CS controls valves V1, V2 and pump P1 so that it takes the appropriate volumes of culture medium from C1 and C2. At the same time, CS controls P2 to remove the correct volume of medium from the C3. The CS was designed based on input parameters like glucose concentration in C1 and C2, target glucose concentration, volume of CC, period of media switching. It calculates the pumping time of the media with the maximum and minimum concentration in a set period and the total working time of the pumps P1 and P2. During the tests, the glucose levels in C1 and C2 were 5 mM and 20 mM, respectively. The medium in CC with a volume of 28.6 ml was changed 2, 3 and 4 times. Tests were carried out for the following changes in glucose concentration (mM): 0, 5, 10, 15, 20, 15, 10, 5, 20 and 5, and then the relative error (δ) of the target glucose concentration was calculated.

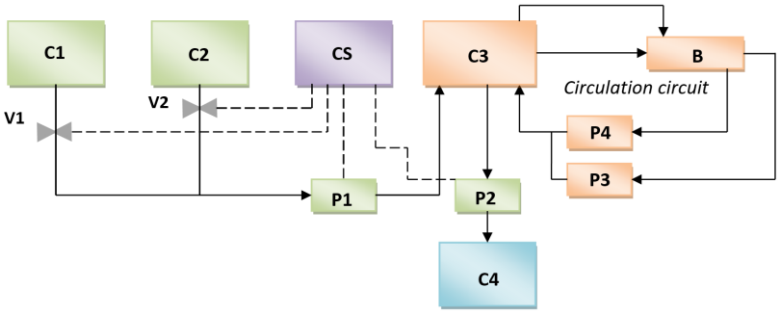

Fig. 1. Schema of the system (see description in text).

Results

The best result was obtained when the medium was changed 4 times ($\delta < 0.1\%$). Assuming that $\delta < 10\%$ is acceptable, a two-fold exchange of the culture medium was sufficient when increasing the glucose concentration every 5 mM from 5 to 20 mM. Changing the culture medium twice is sufficient during reducing the glucose concentration every 5 mM from 20 to 10 mM, and also if the glucose concentration changes from 5 to 20 mM. To decrease the concentration from 10 to 5 mM, the medium must be changed 3 times, and to decrease it from 20 to 5 mM, the medium must be changed at least 3.3 times.

Conclusions

To achieve the target glucose concentration in the circulation circuit, for a designed control system, the volume of medium changed depends on the initial glucose concentration in the circuit.

Acknowledgments

This research was founded by National Science Centre Poland, grant no. 2017/27/B/ST7/00269.

Antagonism between viral infection and innate immunity at the single-cell level

Maciej Czerkies, Frederic Grabowski, Marek Kochańczyk, Zbigniew Korwek, Wiktor Prus, and Tomasz Lipniacki

All authors are with the Institute of Fundamental Technological Research, Polish Academy of Sciences, Pawińskiego 5B, 02-106 Warsaw, Poland.
tlipnia@ippt.pan.pl (T.L.)

Background. Recognition of viral RNA in some cells initiates a signaling cascade culminating in activation of transcription factors IRF3 and NF-κB that jointly trigger synthesis of type I and III interferons (IFNs). By activation of STAT1/2 transcription factors in surrounding cells, secreted IFNs prompt them to prepare for viral infection before they encounter a virus. Many viruses convey nonstructural proteins to impede innate immune response.

Results. We observed that this mutual inhibition leads to bistability, giving rise to high spatiotemporal heterogeneity of cellular responses. We put forward and parameterized an agent (single cell)-based, stochastic, computational model of innate immune response to the respiratory syncytial virus (RSV) infection based on experimental results from cell-population techniques (Western blot, ELISA, dPCR). Then, based on results obtained with single-cell techniques (immunostaining, live fluorescent imaging), we validated the model and used it to explain how a population of cells can spontaneously divide into "sentinel cells" (primary responders that get IRF3 active and secrete IFNs) and "fortifying cells" (secondary responders in which activated STAT1/2 upregulate IFN-stimulated genes).

Conclusion. The model reproduces experimentally observed complex spatial patterns of RSV spread and dichotomous cell responses, and allows for investigation of signaling network perturbations that could potentially facilitate eradication of the viral infection.

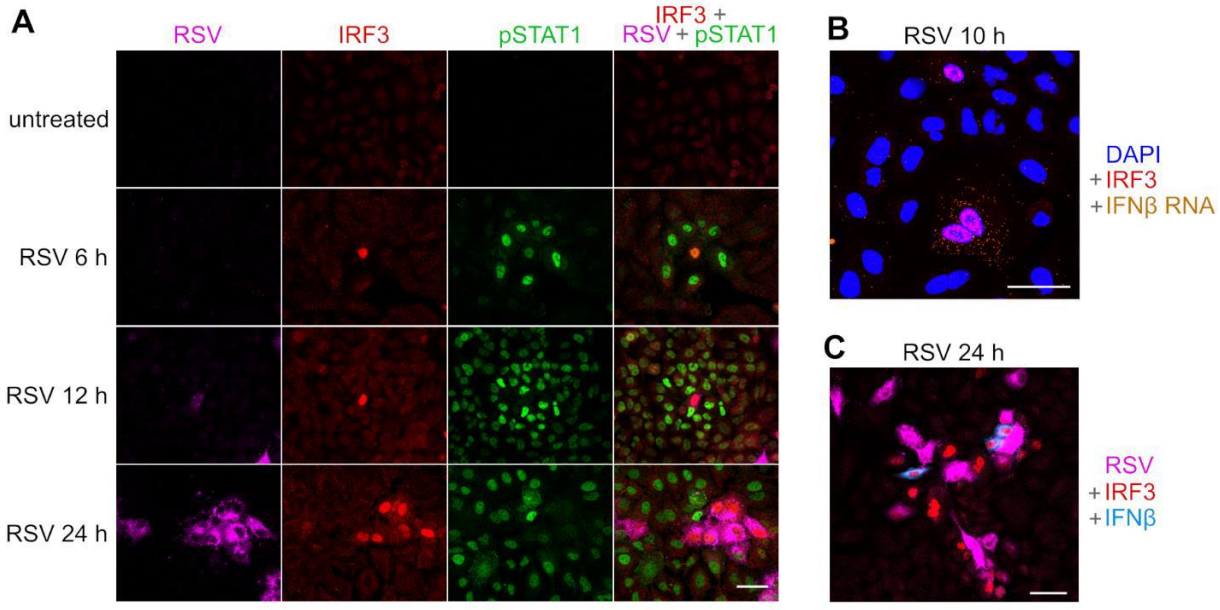

Figure: A549 cells infected with RSV at MOI = 0.01 immunostained for: (**A**) p-IRF3, p-STAT1, and RSV protein F; (**B**) p-IRF3, IFNβ (RNA FISH), and DAPI (merge); (**C**) RSV protein F, p-IRF3, and IFNβ (merge). Scale bar: 50 μm.

Bioimpedance measurements in estimation of fluid removal during hemodialysis

Malgorzata Debowska[1*], Mauro Pietribiasi[1], Jan Poleszczuk[1], Wojciech Zaluska[2], Wojciech Dabrowski[3], Alicja Wojcik-Zaluska[4]
[1]Nalecz Institute of Biocybernetics and Biomedical Engineering, Polish Academy of Sciences, Ks. Trojdena 4 St., 02-109 Warsaw, Poland
Departments of [2]Nephrology, [3]Anaesthesiology and Intensive Care, [4]Physical Therapy and Rehabilitation, Medical University of Lublin, Jaczewskiego 8 St., 20-090 Lublin, Poland
[*]mdebowska@ibib.waw.pl

Aims. In renal failure, in patients without urine output, the excess of fluid is removed by dialysis. In conventional hemodialysis, during 2 - 3 days of interdialytic time patient gains water (2 - 3 L), which is removed in a short time of treatment (3 - 5 hours) carried out asymmetrically 3 times per week. In our study we used bioimpedance method to investigate fluctuations of body water as fluid management is a crucial objective of dialysis treatment.
Methods. Two consecutive hemodialysis session (average duration 239.0 ± 14.0 min), with the first hemodialysis after a 3-day and the second after a 2-day interdialytic interval, were monitored in 42 anuric, prevalent hemodialysis patients (mean age 62.5 ± 14.6 year; 36% men; body mass 69.4 ± 19.9 kg). Fluid status was assessed using whole-body, multi-frequency (from 5 kHz to 1 MHz) bioimpedance spectroscopy (Body Composition Monitor, BCM, Fresenius Medical Care, Germany). Volumes of overhydration, extracellular, intracellular and total body water (being the sum of extra- and intracellular volumes) were measured before and after two monitored hemodialysis sessions (in total 168 measurements). Measurement accuracy of the device was +/- 1 L for extracellular water (reference method: sodium bromide dilution), +/- 1 L for intracellular water (reference method: total body potassium) and +/- 1.5 L for total body water (reference method: deuterium dilution). The difference of body mass, that corresponds to the removed fluid, was calculated by weighing the patient before and after each hemodialysis.
Results. Significant differences in body mass, volumes of extracellular and total body water and overhydration were observed when comparing values before and after hemodialysis as well as comparing pre-dialytic values of hemodialysis sessions performed after 3-day and 2-day interdialytic periods, Fig. 1. The set ultrafiltration (on the machine) differed significantly from fluid removal derived from change in patient mass and bioimpedance measurements ($p < 0.05$). However, we found correlations between ultrafiltration and changes in body mass, extracellular water volume and overhydration ($p < 0.001$).

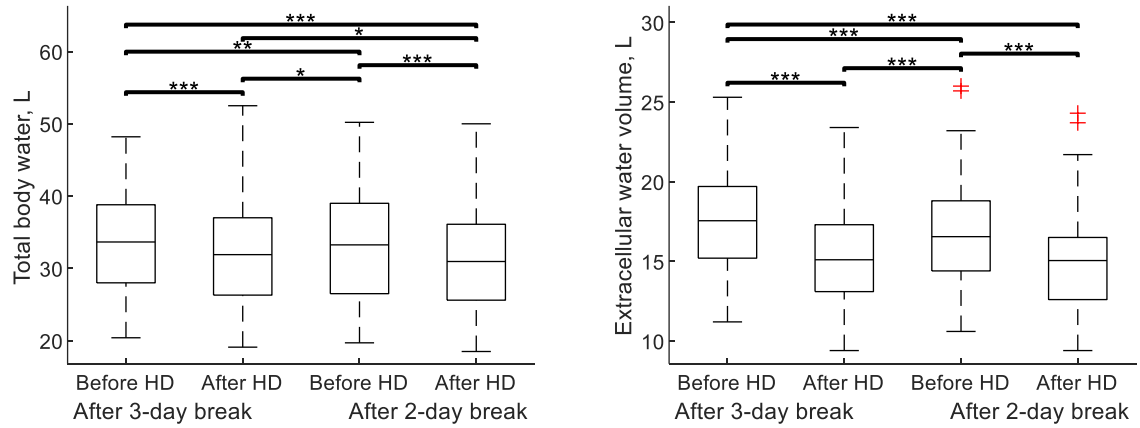

*Fig. 1. Total body water (left panel) and volume of extracellular water (right panel) before and after hemodialysis (HD) performed after 3-day and 2-day interdialytic intervals. ***, **and * denote p-value < 0.001, < 0.01 and < 0.05, respectively.*

Conclusions. Asymmetric, thrice weekly hemodialysis causes significant fluctuations of water in different body compartments. Clinical assessment of hydration status in patients with renal failure can be facilitated by bioimpedance. However, accurate assessment of hydration status in hemodialysis patients requires further investigation.

Composite Membrane Scaffolds with Incorporated Metallic Nanoparticles for Supporting Fibroblastic Cell Growth

Monika Drabik, Anna Grzeczkowicz, Paweł Bącal, Angelika Kwiatkowska, Magdalena Antosiak-Iwańska, Beata Kazimierczak, Ewa Godlewska, Ludomira H. Granicka
Nalecz Institute of Biocybernetics and Biomedical Engineering, PAS, Trojdena 4 st., Warsaw, Poland
lgranicka@ibib.waw.pl

Aims: A lot of global emergence and dissemination of antibiotic-resistant strains causes substantial loss of benefits offered by these agents. Alternative nonantibiotic solutions to fight bacterial diseases need to be explored [1]. We previously reported, that metal nanoparticles showed bacteriostatic properties and can be considered when design materials for biomedical and biotechnological purposes [2, 3]. The aim of this study was to develop a nanocomposite membrane for the immobilization of biologically active material for applications in dressings. Membranes with incorporated gold or silver nanoparticles as a bacteriostatic agent were constructed to cooperate with the chosen cells. The functioning of eukaryotic cells on the constructed membranes was studied. The influence of the bacteriostatic elements on the physicochemical properties of the membrane was assessed.
Methods: The layered membrane scaffolds based on polyethyleneimine with silver or gold nanoparticles incorporated within were produced. We applied the deep coating method and layer-by-layer approach to construct membrane scaffolds. Next, the structure of designed membranes was examined with microscopic and spectroscopic techniques including scanning electron and transmission electron microscopies and energy-dispersive X-ray spectroscopy. Moreover, the physicochemical properties of the designed systems were determined. To estimate the membrane transport properties, the alginate cores coated with evaluated membrane were used. Dextrans of molecular weight of 70 kDa and 150 kDa were used as the model particles in these studies. Additionally, the water contact angle of the designed membranes was evaluated. To assess the biocompatibility of the developed membrane scaffolds in terms of their cytotoxicity, *in vitro* studies were performed. The viability of human dermal fibroblasts (HDF) maintained in the presence of constructed membranes with AgNPs or AuNPs incorporated within, was evaluated by flow cytometry during 7-day culture.
Results: SEM images of immobilized cells indicated that the membranes involving AuNPs facilitated cells to form the shape characteristic for the adhesion phase and allowing for higher adhesion of immobilized cells comparing with the membranes containing AgNPs.
On the other hand, among the studied materials, the layer-by-layer coating, based on polyethyleneimine with incorporated silver nanoparticles, indicated the best performance in cell viability studies. Nevertheless, cells immobilized on all membrane scaffolds showed viability comparable with a control group. All investigated membrane scaffolds were hydrophilic.

Conclusion: We demonstrated that applied membranes with chosen metallic nanoparticles in investigated concentration did not exert a cytotoxic effect on the HDF cells. The applied membrane composites with silver and gold nanoparticles can be used for supporting bandages in biomedical applications.

Acknowledgements: This study was partially supported by ESF**, POWR.03.02.00-00-I028/17-00.**

References:

1. A. R. Hauser, J. Mecsas, D. T. Moir, Beyond antibiotics: New therapeutic approaches for bacterial infections. *Clinical Infectious Diseases*. **63**, 89–95 (2016).
2. M. Antosiak-Iwańska *et al.*, Polyelectrolyte Membrane with Hydroxyapatite and Silver Nanoparticles as a Material for Modern Wound Dressings. *Journal of Biomedical Nanotechnology*. **16**, 702–714 (2020).
3. A. Kwiatkowska *et al.*, Gold nanoparticle-modified poly(vinyl chloride) surface with improved antimicrobial properties for medical devices. *Journal of Biomedical Nanotechnology*. **14**, 922–932 (2018).

Insight of magnesium matrix nanocomposites for biomedical applications- a synthetic review

Ved P. Dubey[1], Mateusz Kopec [1,2], Zbigniew L. Kowalewski[1]
[1] Institute of Fundamental Technological Research, Polish Academy of Sciences, Pawińskiego 5B, 02-106 Warsaw, Poland.
[2] Department of Mechanical Engineering, Imperial College London, London SW7 2AZ, UK.
vdubey@ippt.pan.pl

Abstract:
Traditional biomaterials, such as Ti alloys, Co-based alloys and stainless steel, often show unsatisfactory results such as metal ion release and stress shielding in biomedical applications [1]. Orthopedic implants are divided into permanent and temporary implants. After healing the body part and to avoid long-term exposure of the toxic implant contents to the body, secondary surgical operation(s) are normally needed to remove the implants [2]. As a result, bio-dissolvable implants are an absolute necessity for resolving these issues. The synthesis of biodegradable materials, such as metals, alloys, and nanocomposites, is revolutionizing metallic biomaterials.
In this article, we had done a detailed analysis on the important aspects of Mg matrix nanocomposites (MMNCs) and the effects of nano reinforcements on the biocompatibility, mechanical properties and degradation behavior of MMNCs as future biodegradable implant materials. MMNCs exhibit compatible mechanical and physical properties to human bone in comparison to the traditionally used biomaterials. Mg alloys have Young's modulus (40–45 GPa) nearly to cortical bone (10–27 GPa) whereas the Young's modulus of Ti-based and 316L stainless steel are 110 and 193 GPa, respectively. Mg has the density of 1.74 g/cm3 similar to the density of cortical bone (2.0 g/cm3), whereas densities of Ti and stainless steel are 4.5 and 8 g/cm3, respectively [3]. Also, Magnesium implants can decay during healing as Mg is an essential mineral in the human body.
The findings of this work lead to the conclusion, that the properties and behavior of Mg-based biomaterials are influenced by the synthesis methods used and the components chosen. MMNCs can replace present commercially used biomaterials as having better compatibility to bone and eliminating further surgical operation(s) for implant removal if its fundamental problem of undesirably fast degradation within a living system can be solved.

Keywords: *Magnesium nanocomposites, biomaterials, biomedical applications, orthopedic implants, biodegradable*

References:

[1] Kujur, Milli Suchita, et al. "Development of rare-earth oxide reinforced magnesium nanocomposites for orthopaedic applications: A mechanical/immersion/biocompatibility perspective." *Journal of the Mechanical Behavior of Biomedical Materials* 114 (2021): 104162.
[2] Zhao, Dewei, et al. "Current status on clinical applications of magnesium-based orthopaedic implants: A review from clinical translational perspective." *Biomaterials* 112 (2017): 287-302.
[3] Jahani, Babak, et al. "Biodegradable magnesium-based alloys for bone repair applications: prospects and challenges." *Biomed Sci Instrum* 56 (2020): 292-304.

Custom implants for the reconstruction of complex cranial and maxillofacial bone tissue defects

Marcin Elgalal[1,2], Piotr Komorowski[1], Bogdan Walkowiak[1,3]
[1]Custom Medical Implants Unit, Molecular and Nanostructural Biophysics Laboratory, Bionanopark sp. z o.o., Dubois 114/116, 93-465 Lodz, Poland
[2]Department of Diagnostic Imaging, Radiation and Isotope Therapy, Medical University of Lodz, Pomorska 251, 92-215 Lodz, Poland
[3]Division of Biophysics, Institute of Materials Science, Lodz University of Technology, Lodz, Poland; m.elgalal@bionanopark.pl

The first attempts to design and manufacture personalized medical implants were made by the authors around ten years ago. From the outset it was the intention to use these implants in patients requiring non-standard treatment [1]. Over the following years, the authors developed innovative methods of creating custom implants for the reconstruction of complex bone tissue defects of the cranial and maxillofacial skeleton. These patient specific implants were designed on the basis of computer tomography imaging and made from medical grade Ultra High Molecular Weight Polyethylene (UHMWPE) and titanium alloy.

To date, 120 patients in total have been treated with the following implants: Craniotech® UHMWPE implants for reconstruction of cranial tissue defects, Orbitech® UHMWPE implants for reconstruction of orbital bone tissue defects and Facialtech® UHMWPE implants for reconstruction of facial bone tissue defects. These products are manufactured in accordance with ISO 13485 and have been registered as medical devices with the Office for Registration of Medicinal Products, Medical Devices and Biocidal Products. The Custom Medical Implants Unit also designs and produces patient specific mandibular as well as TMJ (Temporomandibular Joint) titanium alloy/UHMWPE prostheses, however these are not medical devices and can only be used by a surgeon who has received bioethics committee approval to carry out a medical (therapeutic) experiment.
All patients underwent computer tomography of the cranial and/or maxillofacial skeleton in accordance with an established CT protocol. The acquired imaging data was then analyzed and patient data was coded. Segmentation of the CT data was performed (Amira 5.5, ThermoFisher Scientific) and detailed three dimensional models of the relevant bone structures were prepared. These 3D models were then imported into reverse engineering software (Geomagic Studio. Geomagic Design X) in which they were repaired and surface model optimization was carried out. In the next stage, custom implants were designed using a combination of reverse engineering, CAD (Computer Assisted Design) and freeform modelling software. Most tissue defects were virtually reconstructed on the basis of the patients' own geometry. This was achieved by using the technique of mirroring the relevant, unaffected, contralateral bone fragment onto the tissue defect. These mirrored bone fragments were then modified to accurately fit and optimally reconstruct the unique geometry of the tissue defects. The patients' surgical team was consulted during the different stages of the design process and the final version of each implant was confirmed by the referring surgeon. Following this, the models had to be converted into a format that could be imported into CAM (Computer Assisted Manufacturing) software. Finally, the implants were manufactured via a CNC (Computer Numeric Control) milling process from medical grade UHMWPE or titanium alloy.

All patients were successfully treated using these patient specific implants and no significant problems were reported during their clinical application, with surgeons having to make only very minor, intraoperative modifications in sporadic cases. Furthermore, there have been no complications in their long-term use.
Our experience shows that it is possible to design and manufacture custom, patient specific implants that can be used to accurately reconstruct complex tissue defects, which are very difficult, and in many cases impossible, to treat using standard of-the-shelf implants. The benefits of using such personalized implants include shortening the time of the surgical procedure as well as the recovery period, significantly improved aesthetic effects and no need for repeat or additional procedures.

References: [1] Elgalal MT, Kozakiewicz M, Loba P, Walkowiak B, Olszycki M, Stefańczyk L. Patient specific implants, designed using Rapid Prototyping and diagnostic imaging, for the repair of orbital fractures. Med Sci Monit, 2010; 16(Suppl.1): 75-79.

Development of the effective iron delivery vehicle

Maxime Fages-Lartaud[1], Joanna Doskocz[1,2], Magdalena Przybyło[1,2], Maciej Łukawski[1], Marek Langner[1,2]

[1]Lipid Systems sp. z o.o., 54-613 Wrocław, ul. Krzemieniecka 48C, Poland
[2]Department of Biomedical Engineering, Faculty of Fundamental Problems of Technology, Wrocław University of Science and Technology, 50-377, Wrocław, pl. Grunwaldzki, 13, Poland
joanna.doskocz@pwr.edu.pl

Aims

There are numerous medical conditions requiring the supplementation of iron, which can be delivered via oral or intravenous routes. The currently available oral formulations are frequently inefficient, whereas intravenous route is associated with high risk of toxicity. The delivery of iron, both oral and intravenous can be improved by application of delivery vehicle engineered with the consideration for physiological limitations. The major challenge in developing such delivery vehicle for iron is achieving a sufficient payload. The payload depends predominantly on the production processes of a vehicle. The engineering aspects of designing the iron carrier are illustrated by the formation of spherical lipid aggregates (liposome). The traditional and widely used passive or active encapsulation methods cannot be easily applied in this case.

Method

In the paper, the systematic studies leading to the development of liposomal iron formulation with high encapsulation efficiency and capable to overcome physiological barriers is presented. The high encapsulation efficiency was possible thanks to the application of new liposome formation technique. Specifically, the high quantity of lipids is dissolved in poly-ethyl glycol, which is then hydrated with iron containing aqueous phase. Then the dispersion is extruded to achieve high encapsulation efficiencies and physiologically acceptable size.

Result

The resulting formulation contains uniform liposomes, which has been thoroughly characterized and its formation process optimized. Liposomal gel encapsulates more than 50% of iron. The average size of liposomes equals to 125 nm ensuring effective absorption. The formulation is stable for a more than five weeks (no liposomes leakage was observed).

Conclusion

The major outcome of presented studies is the method that can be readily upscaled to provide high encapsulation efficiency in physiologically effective liposomal iron formulation designed to treat anemia.

Validation of a method to improve depth sensitivity of diffuse reflectance measurements to absorption changes in an optically turbid medium

Elham Fazliazar, Piotr Sawosz, Aleh Sudakou and Adam Liebert
Nalecz Institute of Biocybernetics and Biomedical Engineering, Trojdena 4, 02-109 Warsaw, Poland
efazli@ibib.waw.pl

A serious drawback of a near infrared spectroscopy (NIRS) technique, used in a brain oxygenation assessment, is that measured signals are contaminated by changes in oxygenation of an extracerebral tissue. In this study we aim to validate a theoretical study to improve depth sensitivity of diffuse reflectance measurements through a series of phantom experiments.

Methods for discrimination of superficial and deep absorption changes from data obtained by NIRS techniques were developed by several research groups and after the proposal of subtraction-based approach [1], recently a modified theoretical technique based on multi−distance approach with two detection spots and two sources was proposed [2,3]. In this method, differences between the signals obtained for both detectors are calculated independently for both sources and afterwards the results are summed up for both source positions. This theoretical technique revealed a major advance over single-distance geometry in depth selectivity of time-resolved and frequency domain NIRS techniques.

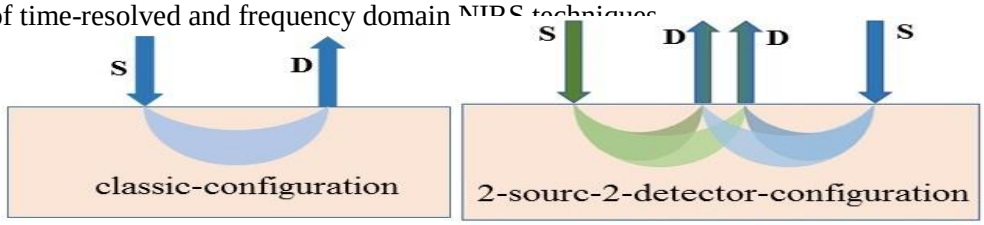

Right: the geometry of measurement (two sources with two detectors for each the sources) and left: The classic geometry. [2]

To validate this two-source-two-detector based method, the optical signals were measured on a homogeneous, optically turbid medium (a fish tank filled with a solution of water, milk and black ink. μa =0.1, μs' =7cm^{-1}) while introducing local absorbtion inclusion. Finally, sensitivity to absorption changes in the medium were obtained for different positions of the absorption inclusion in the medium in both classic and two-source-two-detector methods.

The spatial sensitivity profile of the first statistical moment of distribution of time of flight of photons (DTOF) obtained from the new measuring geometry was compared to that obtained from classic measurement geometry. The resulted sensitivity profiles show that areas with positive sensitivities of mean time of flight of photons are located just between both detection spots and cover the compartment located deeply in the medium. The sensitivity in superficial compartments of the medium is negative.

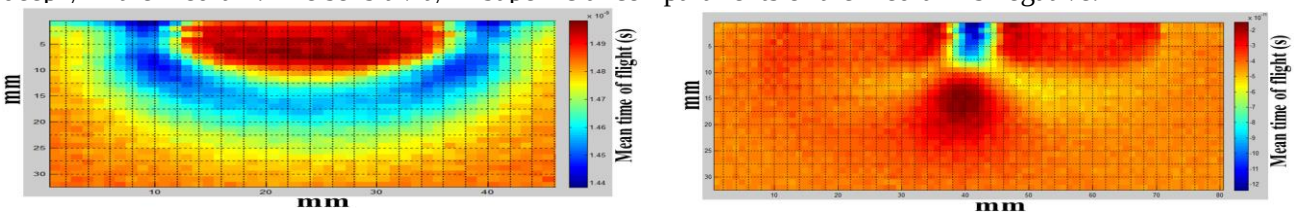

2D distribution of sensitivity of time of flight of photons for the standard measuring geometry (left) and the 2-source-2-detector geometry (right)

The phantom experiments show the advance of the proposed two_sources_two_detectors technique over the classic measuring geometry in discrimination of optical signals related to the change in absorption located deeply in the medium. The technique is promising and may allow to avoid a serious obstacle in application of the NIRS technique in assessment of the brain oxygenation or perfusion.

References:

1-D. Milej, A. Abdalmalak, P. McLachlan, M. Diop, A. Liebert, and K. St Lawrence, "Subtraction-based approach for enhancing the depth sensitivity of time-resolved NIRS," Biomed. Opt. Express 7(11), 4514–4526 (2016).

2- Sawosz, Piotr, and Adam Liebert. "Method to improve the depth sensitivity of diffuse reflectance measurements to absorption changes in optically turbid medium." Biomedical optics express 10.10 (2019): 5031-5041.

3- Sassaroli, Angelo, Giles Blaney, and Sergio Fantini. "Dual-slope method for enhanced depth sensitivity in diffuse optical spectroscopy." JOSA A 36.10 (2019): 1743-1761.

An internet service system for automatic wound area measurement: preliminary tests

Piotr Foltyński, Piotr Ładyżyński
Nalecz Institute of Biocybernetics and Biomedical Engineering, Polish Academy of Sciences,
4, Trojdena Str., 02-109 Warsaw, Poland
pfoltynski@ibib.waw.pl

Aims

Wound surface area change over time is important prognostic parameter for wound closure and may be used for healing procedure assessment [1]. Accurate and precise wound area measurement is important for proper tracking of area changes. The time needed for a single measurement is also important for a busy medical personnel. Thus, devices with automatic wound border detection which decreasing the measurement time are the most preferred. Most of the measurement systems require manual wound border tracing and calibration [2]. Therefore the aim of the present study is to present a new concept of such a measurement system.

Methods

The wound area measurement in the proposed system was based on the digital photoplanimetry with newly developed adaptive calibration procedure for curved surfaces [3]. A picture showing the wound and calibration markers, placed at its opposite sites, is taken by a smart device with software able to send it to a cloud folder (Fig. 1). This location is monitored by the developed software and each new image file is analyzed. The output data are saved in a database and also sent to the user who provided the image file for analysis. Four self-adhesive stickers in the shape of real wounds (i.e. phantoms of wounds) were placed at different parts of the human body: the wrist, forearm, sole of the foot, and calf. Two calibration markers were also placed near the phantom. Pictures of the phantoms and calibration markers were taken and sent to the cloud folder. Each picture was automatically analyzed. The efficacy of an algorithm for detection of calibration markers and the region of interest (ROI) and calculating the calibration coefficients was tested.

Results

The software correctly recognized calibration markers and ROIs in all 16 pictures. The calibration coefficients were also correctly calculated. The output pictures and digital data were sent back via e-mail and also stored in the database. The time needed to analyze a single image and send the result back ranged from 5 to 8 seconds. More than 70% of this time was needed to upload the image.

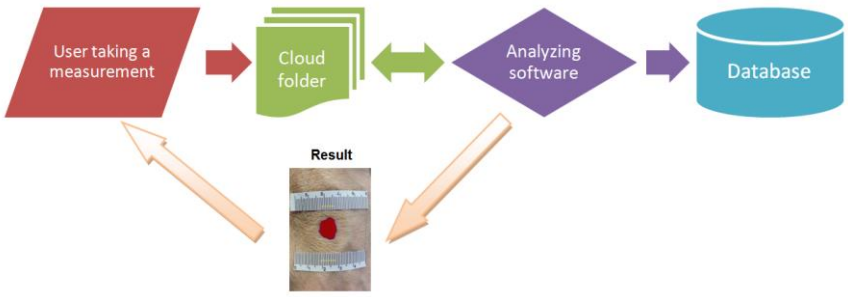

Fig. 1 Scheme of the internet service for wound area measurement system

Conclusion

The tests of the system revealed that it was efficient in the first stages of data analysis and once the wound margin detection module is ready, the system may be a useful tool in automatic wound area measurement.

References

[1]. Hingorani A, LaMuraglia GM, Henke P, Meissner MH, Loretz L, Zinszer KM et al. The management of diabetic foot: A clinical practice guideline by the Society for Vascular Surgery in collaboration with the American Podiatric Medical Association and the Society for Vascular Medicine. J Vasc Surg. 2016, 63(2 Suppl):3S-21S.

[2]. Foltyński P, Ciechanowska A, Ładyżyński P. Wound surface area measurement methods. Biocyb Biomed Eng, 2021, *accepted April 14, 2021*.

[3]. Foltynski P, Ladyzynski P. Digital Planimetry With a New Adaptive Calibration Procedure Results in Accurate and Precise Wound Area Measurement at Curved Surfaces. Journal of Diabetes Science and Technology. October 2020. doi:10.1177/1932296820959346.

Numerical simulations of the ultrasonic tissue ablation process

Lukasz Fura, Norbert Zolek, Tamara Kujawska
Institute of Fundamental Technological Research Polish Academy of Sciences
Pawińskiego St. 5B; 02-106 Warsaw, Poland
lfura@ippt.pan.pl

Ultrasonic tissue ablation is based on rapidly (<3s) raising the temperature in a small volume (around 13mm^3) of tissue by a single exposure to a beam of high-intensity focused ultrasound (HIFU). The process does not thermally destroy tissue outside the focus of the beam. Thermal ablation of a larger volume of tissue (e.g. a tumor) requires the planning and execution of multiple individual exposures of the tissue to the HIFU beam so that the entire volume intended for thermal destruction is covered by the necrosis. HIFU has been used in clinical practice for the thermal destruction of various solid tumors (e.g. prostate, breast, liver, and uterine fibroids) [1]. Predicting the location and extent of planned thermal ablation of tissue will ensure treatment efficacy and safety. The aim of this study was to create a theoretical tool for predicting the location and the volume of the necrosis developed inside the *ex vivo* tissue as a result of its exposure to the pulsed HIFU beam using the ultrasound imaging-guided HIFU ablation system [2] for different duty cycle values.

The proposed model is based on a numerical simulation of non-linear propagation of acoustic waves and heat transfer in heterogeneous media using a k-wave toolbox [3]. The wave propagation equations were solved in a box of the size 7cm x 7cm x 10cm. The source of acoustic waves (bowl-shaped HIFU transducer with a diameter of 64 mm and focal length of 62.6mm simulating the one used in real experiments [2]) was located at the border of the region and directed along with the longest size of the simulation box. The frequency of the transmitted wave was 1.08MHz. Numerical discretization allowed to simulate propagation taking into account frequencies up to 6.48MHz, (6 harmonics could be included). The distribution of heat sources in the simulated two-layered structure (water (50mm) - tissue (40mm)), based on the calculated acoustic pressure distribution of the propagating wave, was determined. Additionally, the temperature distribution after a 3-second exposure of the medium to the HIFU beam for three duty cycle values and the cooling curves at 120s were computed. This allowed to calculate the thermal dose received by the simulated tissue and to determine from this the size of the necrosis formed.

Experimental results from previous studies and the results of simulations were compared. The difference between the length of the simulated necrotic lesion and the experimental necrotic lesion was less than 0.5 mm on average, as did the difference between the iameter of the simulated and experimental necrotic lesions. The ablation volumes obtained showed a 90% agreement between the simulation and experimental results on average.

The consistency of numerical simulation and experimental results is sufficient to proceed with further studies aimed at numerical optimization of the temporal and spatial thermal ablation of larger tissue volumes.

Acknowledgements
The work was partially supported by the National Science Centre (Grant 2016/21/B/ST8/02445) and ESF (POWR.03.02.00-00-I028/17-00) grants.

References:

[1] Y.-F. Zhou, "High intensity focused ultrasound in clinical tumor ablation," *World J. Clin. Oncol.*, vol. 2, no. 1, p. 8, 2011, doi: 10.5306/wjco.v2.i1.8.
[2] T. Kujawska, W. Dera, and C. Dziekoński, "Bimodal ultrasonic instrument for non-invasive destruction of solid neoplastic tumors in small animals", Pat.233294, 2019.
[3] B. E. Treeby and B. T. Cox, "k-Wave: MATLAB toolbox for the simulation and reconstruction of photoacoustic wave fields," 2010, doi: 10.1117/1.3360308.

Automatic Assessment of Benton Visual Retention Test Results: A Pilot Study

Dominika Gabor, Rafał Doniec, Szymon Sieciński, Natalia Piaseczna, Konrad Duraj and Ewaryst Tkacz
Evertop sp. z o.o., Chorzów, Poland
Silesian University, Faculty of Biomedical Engineering, Department of Biosensors and Processing of Biomedical Signals, Zabrze, Poland
szymon.siecinski@polsl.pl

Visual memory plays an important role in learning to read, write, spell or draw. The dysfunctions of visual memory can be detected by applying tests, such as Benton Visual Retention Test (Benton Test, BVRT), which is based on displaying ten patterns for ten seconds per each pattern and asking the subject to reproduce the displayed patterns. The purpose of our study is automation of Benton Test by developing a desktop application.

We automated the assessment of the hand-drawn geometrical shapes (triangles, circles, rectangles) by applying machine learning and image processing techniques, namely the ResNet50 network trained for recognition of triangles, circles, rectangles and other shapes, filling in the shape, and determining the type of triangle. Proposed algorithm proved its reliability on subjects with limited ability to draw shapes and was the part of a desktop application which may find its use in screening the visual perception and visual memory.
The study group consists of 9 residents at the nursing home in Borowa Wieś, the neighborhood in Mikołów (Poland) which represent three groups of people with diagnosed disability: mild (A), moderate (B) and severe (C).

The ability to reproduce a shown pattern as accurately as possible is measured by the number of errors found in the reproduced shapes. These errors are divided into six categories (omission, distortions, repetition, shifts, rotations, and wrong size) indicate disorders of visual perception [1]. In our study we automated the assessment of geometrical shapes reproduced by a subject by preprocessing and applying deep neural network (DNN) to recognize them. The results of BVRT were evaluated based on the description published in [2]. The number of correctly recognized rotations, distortions, changes of size, omissions, triangles, circles, and rectangles was 10 out of 10 evaluated geometrical shapes for each category. The number of correctly recognized incorrect rotations was 6.

Proposed algorithm proved its reliability on subjects with limited ability to draw shapes in a careless and sloppy manner. However, in some cases, the algorithm classified the geometric shapes incorrectly because some hand-drawn geometric shapes such as a circle, square, or triangle may look quite similar [3]. The most significant limitations were the small number of subjects in the study group (only 9 people) and incorrect recognition of triangle rotations in some cases. In future work, we consider including the recognition of more geometrical shapes, their modifications (distortions, rotations, and scales), and extending the study groups by including more subjects.

References:
[1] Sivan, A.B., Levin, H.S., Hannay, J.: Arthur L. Benton, Ph.D.: Pioneer, Col-league, Mentor, and Friend. Journal of the International Neuropsychological Soci-ety13(04) (June 2007).
[2] Benton, A.L.: A Visual Retention Test For Clinical Use. Archives of Neurology & Psychiatry 54(3) (Sep 1945) 212–216.
[3] Verdine, B.N., Lucca, K.R., Golinkoff, R.M., Hirsh-Pasek, K., Newcombe, N.S.:The shape of things: The origin of young children's knowledge of the names andproperties of geometric forms. Journal of Cognition and Development17(1) (March2015) 142–161.

An *in vitro* model of perinatal asphyxia: the influence of different biomaterials on proliferation and morphology of oligodendrocytes and astrocytes

Justyna Gargaś, Justyna Janowska, Karolina Ziąbska, Małgorzata Ziemka-Nałęcz, Joanna Sypecka
Mossakowski Medical Research Institute Polish Academy of Sciences, NeuroRepair Department, Warsaw, Pawińskiego 5 Street
jgargas@imdik.pan.pl

Aims: Perinatal asphyxia (hypoxic-ischemic encephalopathy; HIE) is one of the leading causes of all child deaths under the age of 5-years. Temporary lack of oxygen and glucose affects several body organs, including the developing brain. Unfortunately, there is no effective therapy to treat consequences of HIE. The newest research shows that the glial cells may play important roles in reparative processes after HIE event [1].

Methods: To evaluate response of glial cells to HIE, an *in vitro* model of perinatal asphyxia was used. The brain hemispheres were isolated from 1-2 days old Wistar rats for establishing the primary mixed glial culture. After 11-12 days, the individual glial fractions were isolated (oligodendrocyte progenitor cells-OPCs, astrocytes), cultured on the selected biomaterials and subjected to the OGD procedure (oxygen-glucose deprivation) which mimics HIE *in vitro*. Afterwards, the cells were cultured in physiologically normoxic conditions for additional 24 hours and subjected to detailed immunocytochemical analyses. Among others, the influence of different biomaterials on survival, proliferation and morphology of the cells under HIE conditions was assessed. The tested biomaterials included: poly-L-lysine (PLL), fibronectin (FBR), laminin (LAM) and Extracellular Matrix gel (ECM Gel). PLL was used as a standard plate-cover compound which enables adherence of the cells. FBR is an extracellular matrix component, while LAM is a constituent of the basement membrane. ECM Gel contains various extracellular matrix components, especially different types of collagens.

Results: The tested biomaterials exerted diversified influence on the survival, proliferation and morphology of the cultured glial cells. FBR seemed to be the most beneficial compound for *in vitro* culturing of astroglia which exhibited fibroblastic morphology and better survival than on PLL-coated surface. When cultured on ECM Gel, the cells aggregated and were cultured in a form of clusters, to some extent resembling processes occurring in the selected pathological conditions. Contrary, no effects on survival, proliferation or morphology of OPCs were observed with application of the tested biomaterials. However, the influence of OGD procedure was the most strongly pronounced when the both types of glial cells were cultured on PLL-coated surface. Namely, the applied temporary limitation of oxygen and glucose supply led to approx. 62% increase in OPCs and approx. 77% increase in astrocyte numbers during three days in vitro after the insult.

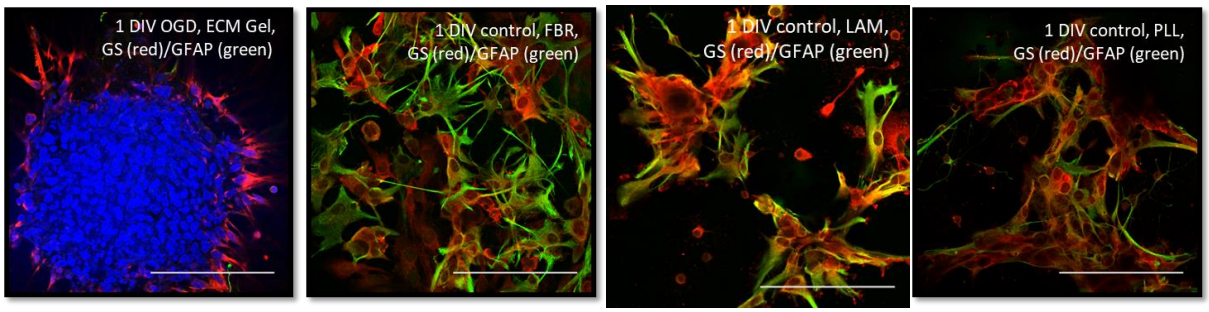

Conclusion: The results show that the culturing cells on various biomaterials exerts diversified effects on their morphology and survival. This observation could be especially useful when aiming at mimicking *in vitro* physiological conditions or creating selected disease-in-a-dish models for both basic research and pre-clinical studies.

References:

[1] J. Janowska, J. Sypecka. Therapeutic Strategies for Leukodystrophic Disorders Resulting from Perinatal Asphyxia: Focus on Myelinating Oligodendrocytes, Mol Neurobiol (2017) 55(5):4388-4402, doi: 10.1007/s12035-017-0647-7.

Aggregation determination of bacterial amyloid signaling motifs using ATR-FTIR spectroscopy

Marlena Gąsior-Głogowska[1], Natalia Szulc[1], Oliwia Polańska[1], Monika Szefczyk[2], Witold Dyrka[1]
[1]Department of Biomedical Engineering, Faculty of Fundamental Problems of Technology, Wroclaw University of Science and Technology, 50-370 Wroclaw, Poland
[2]Department of Bioorganic Chemistry, Faculty of Chemistry, Wroclaw University of Science and Technology, Wybrzeże Wyspiańskiego 27, 50-370 Wrocław, Poland
marlena.gasior-glogowska@pwr.edu.pl

Aims: With the aim to characterize amyloid properties of fungal and bacterial amyloid signaling motifs (BASS), we used the Attenuated Total Reflectance – Fourier-Transform InfraRed (ATR-FTIR) spectroscopy as a rapid tool for indication of the presence of fibrillar aggregates in different solutions. BASS motifs occur specifically in filamentous Actinobacteria, Cyanobacteria and Euryarchaeota species, where they play a crucial role in programmed cell death processes. Some of these sequences display a high similarity with the Rip Homotypic Interaction Motif (RHIM) [1][2]. It was found recently that BASS motifs are capable to form fibrils *in vitro* [2], yet the mechanism of fibril assembly is not fully understood and may be highly affected by environmental conditions.

Methods: Secondary structure investigations have been carried out on the dataset of BASS sequences detected by a novel machine learning grammatical model [3]. Peptides were synthesized on the solid support, purified using preparative HPLC in water/acetonitrile eluent system to obtain >95% purity and lyophylized. Peptides were dissolved in different media: water, deuterium oxide or in the initial solvent (such as NaOH or HCl) and next diluted by adding the phosphate buffered saline to adjust the mixed solution to desired pH. Spectroscopic studies have been conducted under different experimental conditions (e.g, pH, solvent, temperature) to identify the key factors affecting the physical stability of formed fibrils.

Results: We observed a significant variability in the amyloidogenic properties of studied peptides depending on fibril growing conditions. As might be expected, even a slight increase in temperature enhanced self-assembly processes. Structure of aggregates formed *in vitro* was also contingent on the initial particle size.
The assembly pathways started from the monomer phase resulted in forming oligomers up to 50 nm length and did not yield mature fibrils. Generally, ATR-FTIR spectra of BASS peptides exhibited an intense absorption in 1630-1620 cm^{-1} range, corresponding to the cross-β amyloid architecture. In addition, strong bands between 1670 and 1660 cm^{-1} were also noticed, which indicated the presence of turn and loops structures. These findings suggest that these fragments adopted beta solenoid conformations reported before for the HET-s and PrP^{Sc} prion motifs.

Conclusions:
These results are consistent with previous findings for amyloid and amyloid-like peptides, that aggregation processes are promoted by increasing the temperature and concentration. Additionally, we showed the oligomers did not undergo further assembly to fibrils, when the aggregation process started from monomers.

Acknowledgements: The work was partially supported by the National Science Centre, Poland, Grant No. 2017/26/D/ST5/00341 (to M.S.), National Centre for Research and Development, Poland under POWR.03.02.00-00-I003/16 (to N.S.).

References:
[1] Kajava, A., Klopffleisch, K., Chen, S. et al. Evolutionary link between metazoan RHIM motif and prion-forming domain of fungal heterokaryon incompatibility factor HET-s/HET-s. Sci Rep 4, 7436 (2014).
[2] Dyrka W, Coustou V, Daskalov A, Lends A, Bardin T, Berbon M, Kauffmann B, Blancard C, Salin B, Loquet A, Saupe SJ. Identification of NLR-associated Amyloid Signaling Motifs in Bacterial Genomes. J Mol Biol. Nov 432, 6005 (2020).
[3] Dyrka, W., Gąsior-Głogowska, M., Szefczyk, M. et al. Searching for universal model of amyloid signaling motifs using probabilistic context-free grammars. BMC Bioinformatics 22, 222 (2021).

Activation of NLRP3 Inflammasome in Type 2 Diabetes, Inflammation and Endothelial Dysfunction

Ilona Marcelina Góra, Anna Ciechanowska, Piotr Ładyżyński
Nalecz Institute of Biocybernetics and Biomedical Engineering PAS,
4 Trojdena Street, 02-109, Warsaw, Poland
igora@ibib.waw.pl

Aims

Type 2 diabetes mellitus (T2DM) is one of the most serious chronic diseases affecting more than 450 mln people worldwide. T2DM is characterized by insulin resistance or dysfunction of pancreatic islet β-cells. Several studies have shown that chronic tissue inflammation is a key contributor to the development of T2DM [1]. Pioneering studies have demonstrated that the NLRP3 inflammasome complex acts as a primary initiator of inflammatory responses and plays an important role in endothelial dysfunction, and in the development of diabetes and its complications [2]. The aim of this work is to present a review of links between activation of NLRP3 inflammasome in T2DM, inflammation and endothelial dysfunction, and identify new therapeutic possibilities for people with T2DM.

Methods

We conducted a narrative literature review to summarize the findings to date regarding the mechanisms of NLRP3 inflammasome activation in T2DM, inflammation and endothelial dysfunction.

Results

Elevated levels of inflammatory proteins such as C-reactive protein (CRP), interleukin 1β (IL1 β), interleukin 6 (IL6) and monocyte chemoattractant protein 1 (MCP1) have been shown to be predictive of T2DM. NLRP3 expression positively correlated with insulin resistance. There is a growing number of reports showing that expression of several, the same, microRNAs is deregulated in both, T2DM and inflammation, strengthening the notion that T2DM is an inflammatory disease stimulated by pro-inflammatory cytokines. Inflammation is the first response of the immune system to infection or tissue damage and is central to the pathogenesis of many vascular diseases, such as atherosclerosis and diabetic angiopathy [3]. NLRP3 inflammasome regulates a few metabolic pathways, which are affected in T2DM, inflammation and endothelial dysfunction. Endothelial cells become active participants and regulators of the inflammatory response in the event of inflammation or infection as they are among the first cells to come into contact with endogenous particles or microbes. Endothelial dysfunction is the first key step to activate NLRP3 inflammasome, which develops at a very early stage of T2DM with a complex mechanism including altered cell signaling, increased oxidative stress, pro-inflammatory activation, and mitochondrial dysfunction. This pathological condition in diabetes has been associated with high glucose and high fat levels in the blood. Several studies identified hyperglycemia as one of the primary signals initiating activation of NLRP3 inflammasome. All this evidence demonstrates that suppressing NLRP3 inflammasome could be a new approach in depletion of hyperglycemic toxicity and averting the onset of vascular complication in people with T2DM.

Conclusion

Understanding the molecular mechanisms of NLRP3 inflammasome activation increases the chances of developing new therapies for patients with inflammatory diseases that may also prove effective in treating people with type 2 diabetes.

Acknowledgments

This research was partially founded by National Science Centre Poland, grant no. 2017/27/B/ST7/00269.

References

[1] Eguchi K., Nagai R. Islet Inflammation in Type 2 Diabetes and Physiology, *Journal of Clinic Investigation*, vol. 127, no. 1, pp. 14–23.
[2] Im H., Ammit A.J. The NLRP3 Inflammasome: Role in Airway Inflammation, *Clinical and Experimental Allergy*, vol. 44, no. 2, pp. 160–172.
[3] Hansson G.K., Libby P., Schönbeck U., Yan Z.Q. Innate and Adaptive Immunity in the Pathogenesis of Atherosclerosis, *Circulation Research*, vol. 91, no. 4, pp. 281–291.

Cellular plasticity upon proton irradiation

Julia Grajek, Iñaki Schniewind, Claudia Peitzsch, Jan Poleszczuk
Institute of Biocybernetics and Biomedical Engineering, Polish Academy of Sciences,
Księcia Trojdena 4, 02-109 Warsaw
jgrajek@ibib.waw.pl

Conventional photon-based radiotherapy, one of the main treatment options for cancer patients, has two main limitations: radioresistance of certain cancer cells and radiation-induced damage of healthy tissues. Proton-based radiotherapy, a newer form of radiation treatment, allows for a superior control of radiation dose distribution compared to photon-based radiotherapy, thus targeting the tumor more precisely and minimizing collateral damage. However, while the physical differences between photons and protons have been extensively studied, it is not fully understood how these differences influence radioresistance [1].

It is known that one of the factors driving resistance in conventional radiotherapy is the existence of cancer stem cells (CSC), who confer radioresistance [2]. In [3] Peitzsch et al. showed that upon X-ray irradiation prostate cancer cells undergo a phenotypic switch towards stem cell like cells. The aim of our work was to investigate whether this phenotypic switch occurs upon proton irradiation and which therapy has a higher potential of eliminating CSC and thereby minimizing radioresistance.

We proposed a differential equation model of irradiated and non-irradiated cancer stem cell like cells (CSCs) and non-stem cancer cells (CCs). The model accounts for radiation damage as well as plasticity events, i.e. the phenotypic switch from CC to CSC and reverse plasticity events, i.e. the phenotypic switch from CSC to CC. The number of equations depends on the proliferation capacity of cells. We calibrated the model with in vitro data describing changes in the ratio of ALDH+ cells in a population coming from six cell lines of three different cancer types subjected to photon- or proton-based irradiation (ALDH is a stemness marker). We showed that while the ratio of CSC did not differ significantly between the two therapies, in accordance with data, the rate of reverse plasticity events was consistently lower following proton therapy than X-ray therapy. Moreover, we were able to rigorously show that the model has to include reverse plasticity events in order to reproduce experimental data.

Our model's predictions indicate that plasticity events are a crucial factor differentiating the influence of proton therapy and X-ray therapy on the CSC population. Targeting of these events may reduce radioresistance following radiotherapy.

References:
[1] Konings K, Vandevoorde C, Baselet B, Baatout S, Moreels M. Combination Therapy With Charged Particles and Molecular Targeting: A Promising Avenue to Overcome Radioresistance, *Front Oncol*, 2020;10:128.
[2] Kim BM, Hong Y, Lee S, et al. Therapeutic Implications for Overcoming Radiation Resistance in Cancer Therapy, *Int J Mol Sci*, 2015;16(11):26880-26913.
[3] Peitzsch C, Cojoc M, Hein L et al. An Epigenetic Reprogramming Strategy to Resensitize Radioresistant Prostate Cancer Cells, *Cancer Res*, 2016;76(9):2637-51.

Nanothin Polyelectrolyte Membranes for Biomedical Purposes

Anna Grzeczkowicz, Agata Lipko, Ludomira Granicka
Nalecz Institute of Biocybernetics and Biomedical Engineering Polish Academy of Sciences
Ks. Trojdena 4 st.Warsaw,
lgranicka@ibib.waw.pl

Nanothin polyelectrolyte membranes (PEM) have a vast number of applications in pharmaceutical, chemical and food industries as well as in environmental and biomedicinal engineering particularly in tissue engineering and gene/drug delivery. Such membranes can be applied to the various surfaces, e.g. eukaryotic and prokaryotic cells[1,2], glass, ceramics, metals, natural and synthetic polymers [3], textiles, hydrogels or nanofibers for specific purposes like cells or bilogically active material immobilization. Immobilization consists in partial or complete limitation of free movement by binding particles, substances or biological materials to the carrier. A number of biodegradable polymers are used for the production of PEM coatings, including: chitosan, alginate, polyallylamine hydrochloride (PAH), polystyrene sulfonate (PSS), polyethyleneimine (PEI), poly-L-lysine (PLL).
The aim of the project was to support the growth of human dermal fibroblasts (HDF) cells utilizing constructed by us polyelectrolyte membrane scaffold based on alginate or chitosan with incorporated hydroxyapatite (HAP) NPs for their immobilization.
The layer-by-layer (LbL) technique based on the alternate adsorption of positively and negatively charged polyelectrolytes was applied to build the multi-layered films. After 7 days of culture the immobilized cells were analysed. The microscopic techniques were applied for morphology assessment. For that purpose the samples were fixed with 4% paraformaldehyde (for phalloidin staining using fluorescence microscopy) or 2.5% glutaraldehyde (for scanning electron microscopy assessment).

The use of the developed membranes allowed to achieve proper adhesion of fibroblasts. Microscopic observations revealed significant morphological differences between the control (cells grown on coverslips) and cells grown on nanothin polyelectrolyte membranes.

Polyelectrolyte membranes as elements of the scaffolds for immobilization of eukaryotic cells give ability to maintain directed cell growth.

References:
[1] Grzeczkowicz A., Granicka L.H., Maciejewska I., Strawski M., Szklarczyk M., Borkowska M.: The Experimental Study of the Performance of Nano-Thin Polyelectrolyte Shell for Dental Pulp Stem Cells Immobilization. *J Nanosci Nanotechnol.* 2015 Dec;15(12):9531-9538.
[2] Granicka L.H., Borkowska M., Grzeczkowicz A., Stachowiak R., Szklarczyk M., Bielecki J., Strawski M.: The targeting nanothin polyelectrolyte shells in system with immobilized bacterial cells for antitumor factor production. *J Biomed Mater Res A.* 2014 Aug;102(8):2662-2668.
[3] Kwiatkowska A., Granicka L.H., Grzeczkowicz A., Stachowiak R., Bącal P., Sobczak K., Darowski M., Kozarski M., Bielecki J.. Gold Nanoparticle-Modified Poly(vinyl chloride) Surface with Improved Antimicrobial Properties for Medical Devices. *J Biomed Nanotechnol*. 2018 May 1;14(5):922-932.

Multivariate analysis the blast injury of soldiers

Marek Gzik, Wojciech Wolański, Kamil Joszko, Bożena Gzik-Zroska, Michał Burkacki, Sławomir Suchoń
Faculty of Biomedical Engineering, Silesian University of Technology, Roosevelt Str. 40, 41-800 Zabrze, Poland
Wojciech.wolanski@polsl.pl

Abstract:
The aim of this article is to present a multivariate numerical analysis of blast injury of soldiers. The research was carried out as part of the NCBiR grant No. DOBR-BIO4 / 022/13149/2013 of 20/12/2013 which the main task was to evaluate the safety of polish soldiers on missions in Iraq and Afghanistan in which the IED explosion occurred [1].

As part of the research extensive model research was carried out using the Multibody and Finite Element Method. The model of a wheeled armoured personnel carrier, including the crew and their equipment, was developed. Model allowed to analyze a number of factors that affected soldiers safety during the blast.

The simulations show that the use of 4 point belt harness provides a sufficient level of security compared to other systems analyzed in the dissertation. Adjusting the backrest of the seat at an angle of 1000 allows obtaining lower injury criteria relative to other seat positions during an explosion. Simulation results indicate the need to mount all loose items of equipment in the vehicle, as they can cause serious injuries to soldiers during an explosion. The most dangerous scenarios for head and leg injury have been selected for detailed analysis using the FEM method. The model of the human head allowed the analysis of dynamic effects on individual head structures. The results of the simulations made it possible to assess the parameters determining head injury of the soldier during the IED explosion which will enable the development of guidelines to improve their safety. The developed model allows determining the parameter of stress, strain and pressure acting on the human head.
In future studies, it is planned to use the model to carry out simulations, the results of which can be used to improve the construction of both military helmets and helmets to minimize the possibility of head injury. Carried out work will be applied as guidelines to improve the safety of soldiers in aspects of vehicle construction, ergonomics and soldier behavior.

References:
[1] Sławiński G., Malesa P., Świerczewski M., Analysis Regarding the Risk of Injuries of Soldiers Inside a Vehicle during Accidents Caused by Improvised Explosive Devices. *Appl. Sci.* 2019, 9, 4077. https://doi.org/10.3390/app9194077.

Spatial 3D simulations of tumour progression model using evolutionary game theory

Katarzyna Hajdowska, Damian Borys, Andrzej Świerniak
Silesian University of Technology, Faculty of Automatic Control, Electronics and Computer Science,
Department of Systems Biology and Engineering, Gliwice, Poland
{katarzyna.hajdowska,damian.borys,andrzej.swierniak}@polsl.pl

Cancer cells have characteristic traits, among them altered glucose metabolism, which is less efficient than citrate cycle in terms of energy, but it allows cells to survive in hypoxic environment. Game theory can be utilised to study how interactions between phenotypes affect outcome of tumour progression or assess the possibility of population becoming homo- or heterogenous. Evolutionary game theory differs from traditional game theory in how it defines conflict and strategy; strategy is understood as a phenotype of individual acquired through evolution, while payoff is the average success of reproduction. Individuals compete or cooperate for resources in the population. Over generations, the population may attain stable state – a situation where a phenotype is adopted by the majority of the population and is unable to be repressed by other phenotypes [1].

All tumor cells are assumed to be initially characterized by autonomous growth (AG phenotype); they can change to anaerobic glycolysis for energy production (GLY) or become increasingly motile and invasive (INV) [2]. Fitness of a cell depends on its interaction with surrounding cells. Every generation, a number of cells are chosen to die (according to one of three updating methods: asynchronous, semi-synchronous and synchronous) and are replaced with cell identical to one chosen in deterministic or probabilistic manner [3]. We intended to investigate whether choice between *2D* and *3D*, and reproduction method changes the outcome.

The results obtained show that in *3D* spatial games, as opposed to *2D* games, outcome does not depend on reproduction method of cells – it only affects time needed to attain stable state. The model is very sensitive to variable values, however, said values are strongly related – changing them should be done deliberately. Mixed and not-mixed games end results differ, even given same starting values. There is no correlation between outcomes obtained for *2D* and *3D* simulations.

Although more computationally expensive, *3D* model is much closer to reality of human body than *2D* model – also results are much more reliable. We suggest using *3D* games, since *2D* can give misleading results.

References:
[1] A. Swierniak and M. Krzeslak. Application of evolutionary games to modeling carcinogenesis. *Mathematical biosciences and engineering*, 10 (3):873–911, 2013. https://doi.org/10.3934/mbe.2013.10.873.
[2] D. Basanta, M. Simon, H. Hatzikirou, and A. Deutsch. Evolutionary game theory elucidates the role of glycolysis in glioma progression and invasion. *Cell proliferati*on, 41(6):980–987, 2008. https://doi.org/10.1111/j.1365- 2184.2008.00563.x.
[3] L. A. Bach, D. J. T. Sumpter, J. Alsner, and V. Loeschcke. Spatial evolutionary games of interaction among generic cancer cells. *Journal of Theoretical Medicine*, 5(1):47–58, 2003. https://doi.org/10.1080/10273660310001630443.

ML classification of auditory evoked responses for task-related hemispheric lateralization

Tomasz Hawro[1*], Ewelina Turczak[1*], Reinhard König[2], and Cezary Sielużycki[1]
[1]Department of Biomedical Engineering, Wrocław University of Science and Technology,
Wybrzeże Wyspiańskiego 27, 50-370 Wrocław, Poland
[2]Research Group Comparative Neuroscience, Leibniz Institute for Neurobiology,
Brenneckestr. 6, 39118 Magdeburg, Germany
[*]Tomasz Hawro and Ewelina Turczak contributed equally to this work.
cezary.sieluzycki@pwr.edu.pl

Aims: The processing of acoustic stimuli in the auditory cortex (AC) in humans and animals is known to reveal features beyond the mere processing of the physical properties of sounds. Several works reported on the ability of AC to categorize incoming stimuli with respect to their characteristics (see [1] and references therein). For example, the right AC was found to be important for the categorization of frequency-modulated tones (FMs) with regard to the direction of frequency modulation when subjects were actively involved in the discrimination task [2, 3]. In this work, we sought to improve the quality of the related data analysis by employing advanced classification methods based on machine learning (ML) algorithms, with the aim to automatically classify signals from left and right AC and from two experimental conditions.
Methods: We analyzed the same set of magnetoencephalographic (MEG) recordings acquired from 16 subjects exposed to FMs as described in Ref. [3]. In the active condition, subjects were asked to discriminate FMs with regard to the direction of frequency modulation, whereas in the passive condition, they merely listened to the same FMs. Data were acquired with a whole-head MEG system (Magnes 2500WH, 4-D Neuroimaging, USA). For each hemisphere, the sensor that revealed the strongest M100 response was selected for further analysis. Trial-averaged MEG signals were processed in four ML classification schemes: 1) active vs passive listening for the left AC, 2) active vs passive listening for the right AC, 3) left vs right AC for active discrimination, and 4) left vs right AC for passive listening. Two ML classification approaches were applied: one based on extracted scalar features of the MEG signals, such as the M100-peak amplitude and latency, and the other one acting on the entire time course of the MEG signal in a 150-ms and a 200-ms time window after stimulus onset. Several ML classifiers were used, such as logistic regression, decision tree, random forest, *k*-nearest neighbors, naïve Bayes, support vector machines, as well as were deep neural networks, both recurrent and convolutional.

Results: We found that ML classification with the two approaches applied to the auditory evoked responses enables signal discrimination of both the two ACs and the two experimental conditions. Even though classification accuracies differed between the two ML approaches and certain classifiers, as well as between particular sets of features in the scalar approach, the highest accuracies obtained confirm the experimental findings that the right AC plays a dominant role in FM categorization. The scalar approach was capable of providing somewhat higher accuracies than the window approach, with values of about 0.8 vs about 0.7, respectively. Both values are remarkable considering the relatively small dataset, as sample size is a pivotal limitation in ML classification.

Conclusion: Using MEG recordings of auditory evoked responses, we have demonstrated the applicability of ML classification as a powerful analysis tool for an auditory categorization task, despite the small sample size of the data set and the subtle differences between the signals of the two experimental conditions and from the two hemispheres. To the best of our knowledge, this is the first ML approach to discern such differences in the context of the task-related hemispheric lateralization of AC activity recorded by means of MEG.
References:
[1] Brechmann A. and Scheich H. Hemispheric shifts of sound representation in auditory cortex with conceptual listening, *Cerebral Cortex*, vol. 15, no. 5, pp. 578–587, 2005.
[2] Ohl F.W. and Scheich H. Learning-induced plasticity in animal and human auditory cortex, *Current Opinion in Neurobiology*, vol. 15, no. 4, pp. 470–477, 2005.
[3] König R., Sielużycki C, Simserides C., Heil P., and Scheich H. Effects of the task of categorizing FM direction on auditory evoked magnetic fields in the human auditory cortex, *Brain Research*, vol. 1220, pp. 102–117, 2008.

The classification system for Parkinson's disease based on EMD using voice signals

Daria Hemmerling[1], Magdalena Wójcik-Pędziwiatr[2,3], Łukasz Paluch[3]
[1]AGH University of Science and Technology, Krakow, Poland
[2]Department of Neurology, The John Paul II Hospital, Krakow, Poland
[3]Department of Neurology, Andrzej Frycz Modrzewski Krakow University, Krakow, Poland
hemmer@agh.edu.pl

Aims

The aim of this research is the application of empirical mode decomposition (EMD) of voice signals acquired from people suffering from Parkinson's disease (PD) to find abnormalities in voice signals. Further signal processing on intrinsic mode functions (IMFs) lead to features origination, which are used for classification whether the signals represented healthy or PD person.

Recent advances in artificial intelligence are being applied to diagnose and timely deal with degenerative disorders such as e.g. Parkinson's disease, Alzheimer's disease, parkinsonian syndromes, Huntington's disease and multiplesclerosis by analysing EEG signals, MRI images, and other data types. This investigation focuses on Parkinson's Disease and proposes a method based on the machine learning approach to its early detection through the analysis of audio signals.

Methods

The speech signals were acquired from PC-GITA database [1], which includes recordings of 50 healthy people and 50 suffering from PD balanced in age and gender. The signals used for the purpose of this research were 3 vowels pronounced in sustained phonation: /a/, /e/, /o/. The EMD enabled the signals' decomposition into intrinsic mode functions, the number of which differs depending on the complexity of the signal. We have chosen for each voice signal 3 IMFs, which contains the most dominant signal's frequencies. The classification was performed using support vector machines algorithm, random forest, C-support vector classification and XGBoosts classifier.

Results

The classification was performed and underwent 10-fold cross-validation. The average classification accuracy of the proposed solution ranges from 80-86%. The developed models were subjected to use extra validation on polish database, we used a set that did not participate in the training or validation. The polish database included 15 people suffering from PD and 15 healthy controls balanced in age and gender. Accuracy for additional evaluation criteria is 60 to 78%.

Conclusion

Parkinson's disease is the second most frequent neurodegenerative disease in the world. Early diagnosis of the disease is an open research and many research try to get the highest accuracy for its detection in non-invasive way. Voice processing can be done remotely, the sound of vowels is very easy to phonate by elderly people. The results obtained for the new test kit indicate that the proposed method could be used to indicate changes in voice signals and could indicate the presence of a neurodegenerative Parkinson's disease.

References:

[1] R. Orozco-Arroyave, J. D. Arias-Londoño, J. F. Vargas-Bonilla,M. C. Gonzalez-Rátiva, and E. Nöth, ''New Spanish speech corpus database for the analysis of people suffering from Parkinson's disease,''in Proc. LREC, 2014, pp. 342–347

Manual and automatic epilepsy events selection in EEG-fMRI studies

Nikodem Hryniewicz[1], Marcin Sińczuk[1], Rafał Rola[2], Ewa-Piątkowska Janko[1,3], Danuta Ryglewicz[2,4], Piotr Bogorodzki[1,3]

[1]Nalecz Institute of Biocybernetics and Biomedical Engineering Polish Academy of Sciences, Warsaw, Poland, [2]Neurology Department of The Military Institute of Aviation Medicine, Warsaw, Poland, [3]Faculty of Electronics and Information Technology, The Institute of Radioelectronics and Multimedia Technology, Warsaw, Poland,
[4]Institute of Psychiatry and Neurology, Warsaw, Poland.
nhryniewicz@ibib.waw.pl

Epilepsy is one of the most common chronic neurological diseases. We use the EEG-fMRI technique to study epilepsy patients who were not characterized by external symptoms. EEG acquisition during fMRI examination allows to determine seizure onset times and to use them in the statistical analysis of MR images obtaining maps of activation in the brain [1]. In EEG-fMRI epilepsy studies, epileptic events are usually manually delineated by an experienced neurologist. This time-consuming procedure requires manual inspecting of the EEG signal. In order to automate this process, we examined 5 epileptic events regressors, which were later used in the fMRI analysis.

17 subjects underwent the same EEG-fMRI scanning sessions (64-channel Neuroscan SynAmps RT EEG system and GE Discovery MR750w 3T MR scanner) consisting of anatomical T1w sequence and from two to four 10 min lasting resting state series. After acquisition, EEG and fMRI data were preprocessed in Curry7, SPM12 and FieldTrip and 6 types of General Linear Model (GLM) regressors were calculated using: 1) manually selected events (BasicReg), 2) global mean field amplitude signal (GMFAReg) from FP1, FP2, F7, F8, T7, T8, C5, C6, P5 and P6 EEG channels , 3) peak value of the T7 channel EEG envelope, PeakReg(L), 4) peak value of the T8 channel EEG envelope, PeakRegR, 5) root mean square value of the T7 channel EEG envelope, RMSReg(L) 6) root mean square value of the T7 channel EEG envelope, RMSReg(R). Subsequently, for each of the types of regressor a SPM12 analysis was performed giving the following results (FWE corrected, $P<0.05$): average number of the clusters (C), maximum cluster size (MC) and maximum T score Tmax. The mean results are summarized in Table 1 divided for groups according to the type of epilepsy [2].

Table 1. The results of SPM analysis with the use of different regressors

	BasicReg			GMFAReg			PeakReg(L)			PeakReg(R)			RMSReg(L)			RMSReg(R)		
Epilepsy type	**C**	**MC**	**T**	**C**	**MC**	**T**	**C**	**MC**	**T**	**C**	**MC**	**T**	**C**	**MC**	**T**	**C**	**MC**	**T**
Generalized	7	510	5,9	2,6	19	3,37	3,6	24,6	2,38	2	11,2	2,38	6,2	40,8	2,86	2,4	14,8	2,46
Temporal	17,2	220,33	6,01	10,17	77,5	4,58	3	54,67	3,44	8,17	68,33	4,43	8,83	97,67	4,62	11	71,67	4,53
Focal	11	47,33	3,52	4,5	75,33	5,64	3,83	48,17	3,27	2,17	37,33	3,78	5,67	30,33	4,25	5,67	39,33	4,13

The results showed that automatically calculated regressors are less sensitive than manual (in most cases higher values of C, MC and T were shown for BasicReg compared to the rest of the regressors) For generalized epilepsy, the most sensitive regressor was the RMSReg(L), for temporal epilepsy the least effective was the PeakReg(L). For focal epilepsy, the use of GMFAReg resulted in a visibly large cluster size and the value of the T statistic.

In summary, the use of automatic epilepsy event detection methods may be useful in the analysis of EEG-fMRI data but should not replace the manual method. Our study was limited by the small sample size and group heterogeneity.

References:

[1] Ritter P, Villringer A. Review Simultaneous EEG–fMRI, *Neuroscience and Biobehavioral Reviews* (2006), vol 30 , pp. 823–838.

[2] Berg A.T., Berkovic S.F., Brodie M.J., Buchhalter J., Cross J.H., van Emde Boas W., Engel J., French J., Glauser T.A., Mathern G.W., Moshé S.L., Nordli D., Plouin P., Scheffer I.E. Revised terminology and concepts for organization of seizures and epilepsies: report of the ILAE Commission on Classification and Terminology, *Epilepsia* (2010), vol. 51, no.4, pp. 676-85.

Choosing representative subsets of amyloid proteins dataset

Katarzyna Hubicka, Małgorzata Kotulska
Department of Biomedical Engineering, Wroclaw University of Science and Technology,
27 Wybrzeże Wyspiańskiego st., 50-370 Wrocław
katarzyna.hubicka@pwr.edu.pl

Choosing a representative and non-redundant subset of protein sequences is an important step in creating bioinformatics tools, such as selecting training sets for machine learning models. Commonly used general methods for this task include CD-HIT, PICES and UCLUST, which are threshold-dependent algorithms. Libbrecht et al. [1] proposed a new approach of selecting representative and non-redundant subsets based on submodular optimization, where objective function consists of quality measures responsible for representativeness and non-redundancy of sets.

The above mentioned method was used for creation of representative subsets of amyloid protein sequences dataset. The full dataset contained peptide instances representing two classes: amyloids and non-amyloids, which is characterized by a relatively small number of samples and imbalance in the number of instances in each class. Such datasets constitute databases used for developing computational predictors, however their redundancy and representativeness is a difficult problem to evaluate. Three objective functions were applied for constructing the representative subsets: function $f_1(R)$ responsible for subset representativeness and checking if every sequence from the whole dataset S has its representative in subset R; function $f_2(R)$ responsible for the subset non-redundancy and punishing for too much similarity within a subset R; function $f_3(R)$ – a mixture of these 2 functions. In addition to different forms of objective functions, we studied if the full representation of sequences is crucial for choosing the representative subsets of amyloids. Therefore, two representations of sequences were considered: standard 20 letters of amino acid alphabet and reduced alphabet with 6 letters, which was revealed by AmyloGram [2] – the bioinformatics predictor of amyloids.

Six subsets, depended on the objective function and sequences representations, were obtained. To validate the quality of determined subsets, first the proportion of amyloid and non-amyloid instances was verified with proportion of the whole data set. Results showed, that applying the reduced alphabet representation gave more balanced representative subsets than the standard alphabet. The subsets created with $f_1(R)$ or $f_3(R)$ functions had similar frequency of amyloids as that in the whole data set, while using $f_2(R)$ created a subset predominantly populated with non-amyloidogenic peptides. However, in contrast to the subset built with $f_3(R)$, the order of sequences added to the subset built with $f_1(R)$ strongly depended on their position in the whole dataset. A classification using AmyloGram was also performed on the most representative and non-representative sets. The most representative samples gave better values of accuracy (above 0.85) and specificity (about 0.95) than the least representative sequences (accuracy: around 0.8, specificity: around 0.85). Interestingly, a higher level of sensitivity (about 0.85) was obtained in a limited range of the least representative sequence of instances, then the value sharply decreased, while the most representative samples stably kept the value around 0.7.

The method has the potential for further modifications, such as creation of a subset of pairs of sequences, which could be useful in proteins interaction models. Moreover, determined subsets can be used not only in creating training sets for bioinformatical models. They can be also applied in the step of data collection, such as choosing representative samples, which would give the most informative and valuable experimental results.

Acknowledgements: This work was partially supported by the National Science Centre, Poland, Grant 2019/35/B/NZ2/03997.

References:

[1] Libbrecht MW, et al. Choosing non-redundant representative subsets of protein sequence data sets using submodular optimization, *Proteins* 86,4 (2018): 454-466.

[2] Burdukiewicz Michał, et al. Amyloidogenic motifs revealed by n-gram analysis, *Scientific reports* 7.1 (2017): 1-10.

Biosensoric acetoin detection in alcoholic beverages and fermentation broths

Melanie Jablonski [1,2], Jasmina Nork [1], Denise Molinnus [1], Lukas Muschallik [1], Johannes Bongaerts [1], Torsten Wagner [1,3], Michael Keusgen [2], Petra Siegert [1], Michael J. Schöning [1,3]
[1]Institute of Nano- and Biotechnologies (INB), Aachen University of Applied Sciences, Heinrich-Mußmann-Straße 1, 52428 Jülich, Germany
[2]Institute of Pharmaceutical Chemistry, Philipps University Marburg, Marbacher Weg 8, 35032 Marburg, Germany
[3]Institute of Biological Information Processing (IBI-3), Forschungszentrum Jülich GmbH, 52425 Jülich, Germany
m.jablonski@fh-aachen.de

In food industry, one important parameter for quality control is maintaining a specific taste. To ensure this, flavoring agents are frequently utilized, such as acetoin with its butter-like aroma (e.g., present in cheese, yoghurt or alcoholic beverages). During the production of wine and beer, the acetoin concentration varies at different fermentation stages, thereby, it can be used as an indicator of how far the fermentation is progressed. As the flavor maturation is the rate-limiting factor in beer maturation, unnecessary maturation time can be avoided by measuring the acetoin concentration. Separate from its impact in alcoholic beverages, acetoin detection has a significant role in biotechnological applications: its concentration gives information about the metabolic activity of bacteria during fermentation processes [1]. Additionally, acetoin was found to be a potential biomarker in patients with Parkinson disease [2].

"Off-line" acetoin determination by gas chromatography (GC) enables the precise quantification of the acetoin concentration, but this technique is time-consuming because sample preparation is necessary and equipment and trained staff is required, whereby high costs can arise. A biosensor could avoid these drawbacks by enabling on-site measurements with a fast response time. Our group developed a field-effect biosensor based on an enzyme-modified electrolyte-insulator-semiconductor (EIS) sensor [1,3]. In the present work, the storage stability of this acetoin biosensor was studied and acetoin was detected in real samples of beer, red wine and fermentation broths.

For sensor fabrication, capacitive EIS sensors, consisting of an Al/p-Si/SiO_2/Ta_2O_5 layer structure, have been modified with a novel acetoin reductase by means of cross-linking. The acetoin reductase (from *Alkalihalobacillus clausii* DSM 8716T) catalyzes the reduction of acetoin to 2,3-butanediol, using NADH as a cosubstrate. The acetoin biosensor has been electrochemically characterized by capacitance-voltage- and constant-capacitance measurements in buffer solution, beer-, red wine- and fermentation-broth samples spiked with varying acetoin concentrations. For the detection of naturally formed acetoin during fermentation, samples were taken from two in-house fermenters producing subtilisin proteases with *Bacillus subtilis* DB104. The acetoin concentration was also determined by GC as an additional reference method.

Acknowledgements: The authors thank the Ministerium für Innovation, Wissenschaft und Forschung des Landes Nordrhein-Westfalen for financial support (funding program FH-Struktur 2016). The authors thank Heiko Iken, Felix Münstermann, Inga Recker, and Fabian Falkenberg for technical support and providing the fermentation broths.

References:

[1] M. Jablonski, F. Münstermann et al. Capacitive Field-Effect Biosensor Applied for the Detection of Acetoin in Alcoholic Beverages and Fermentation Broths, *Phys. Status Solidi A*, 2021, 2000765.
[2] S. Kumari, V. Goyal et al. Quantitative Metabolomics of Saliva using Proton NMR Spectroscopy in Patients with Parkinson's Disease and Healthy Controls. *Neurol. Sci.*, 2020, 41 1201–1210.
[3] D. Molinnus, L. Muschallik et al. Development and Characterization of a Field-Effect Biosensor for the Detection of Acetoin, *Biosens. Bioelectron.,* 2018, 115, 1.

Functional transcriptomics analysis of driver's oncogenes molecular programs in human neoplasia

Akanksha Jaiswar, Maria Grześ, Magdalena Oroń, Dawid Walerych
Laboratory of Human Disease Multiomics, Mossakowski Medical Research Institute,
Pawinskiego 5, 02-106 Warsaw, Poland
ajaiswar@imdik.pan.pl

Cancer is the primary cause of maximum death in western countries [1]. According to the study, in Europe, cancers of the lung, colon, breast, prostate, and pancreas are the primary causes of cancer-related deaths in men and women altogether (according to WHO reports, 2021). Tendencies of improving diagnosis and treatment in breast and prostate cancer in the European countries allow predicting that in the upcoming decade the cancers of the lung, colon/rectum, and pancreas will be the primary causes of deaths in the European Union [2].

The main objective of this study to build a systematic, transcriptomics and proteomics map of molecular pathways to determine the leading oncogenes such as cellular proteasome machinery, mutated TP53, KRAS, and hyperactive CMYC in human neoplasia. Large-scale transcriptomics and proteomics analysis (RNA-sequencing and whole-cell lysate proteomics procedures) were performed in a panel of cancer cell lines with CRISPR-Cas9 knockouts of the oncogenes.

Bioinformatics approaches were followed to obtain the results which included pre-processing and mapping of reads, expression counts, and statistical analysis. We had followed a bioinformatics approach to analyze three different cancer types (lung, colon, and pancreatic) with three different oncogenes (mutant TP53, KRAS, and CMYC). Data quantification had been done by FastQC and trimmomatic tool then processed for the mapping with HISAT2 tool. Differentially regulated genes were predicted by the DEseq2 method and separately submitted to Cytoscape plugin ClueGO for pathway analysis.

After the removal of insignificant reads, data quantification resulted in 96.47% good quality reads. Mapping of the obtained significant reads with the reference dataset leads to a significant score of ~ 97-98 %. The obtained score value shows the successful mapping of the reads with the reference genome. To find common pathways between up and down differentially regulated genes predicted by the Deseq2 method observed a total of 204 up and 4 down common pathways. Finally, with the above approach total of 73 signatures with the broadest potential meaning for cancer progression core genes including 42 up and 19 down-regulated genes common in each cell line have been selected for in vitro validation to choose possible therapeutic targets to confirm the effect of oncogene editing on transcript and protein levels first in the studied cancer cell lines.
The importance of this work is mainly focusing on the traditional and current development of new drug targets and identify already known targets for drug combinations in specific cancer types using molecular and bioinformatics approaches.

Keywords: Cancer, Oncogene, CRISPR-Cas9, Transcriptomics, Proteomics, Differential Gene Expression Analysis.

References:

1. University of Adelaide. World's 'better' countries have higher rates of cancer, 2017, October 11. *ScienceDaily*.
2. Carioli G, Malvezzi M, Bertuccio P, et al. European cancer mortality predictions for the year 2021 with focus on pancreatic and female lung cancer, Ann Oncol. 2021;32(4):478-487.

Evaluation of Polysulfone Capillary Membranes Used for Hepatic Cells Culturing in Dynamic Conditions

Małgorzata Jakubowska, Monika Wiśniewska, Agnieszka Wencel, Dorota G. Pijanowska, Krzysztof D. Pluta
Laboratory of Tissue Engineering, Nalecz Institute of Biocybernetics and Biomedical Engineering Polish Academy of Sciences, Ks. Trojdena 4 st., 02-109 Warsaw
mjakubowska@ibib.waw.pl

Aims

Liver diseases that lead to its failure are one of the most frequent causes of death worldwide. Taking into account liver's complexity, there are no effective medical solutions for acute or chronic liver failure. The only long-term cure for fulminant liver failure is orthotopic transplantation. Unfortunately donor shortage is a main problem of this therapy. According to the Organ Procurement and Transplantation Network approximately 12 000 patients are currently on the transplant waiting list in the USA and circa 10% of patients die each year while waiting. One of the most promising alternative for liver transplantation are bioartificial liver devices (BALs). They constitute a bridging therapy for patients until liver regeneration or transplantation. ELAD, the most advanced device among BALs, came to the third phase of clinical trials, but did not live up to expectations. The ELAD utilizes the C3A hepatocellular carcinoma cell line with non-functional urea cycle and this could be a reason for the clinical therapy failures. Therefore, we attempted to construct BAL devices, which utilize genetically modified C3A cells with the restored urea cycle obtained in our laboratory. The aim of this study was to evaluate the properties of polysulfone capillary membranes used in hollow fiber bioreactors constructed in the cooperation with the Laboratory of Semipermeable Membranes and Bioreactors IBBE PAS and to establish the appropriate conditions for cell growth using mathematical modeling tool.

Methods

In order to evaluate the properties of polysulfone membrane the measurement of retention of albumin and polystyrene microbeads was conducted. Moreover, wettability of membrane was checked. Importantly, the biocompatibility of this material was also evaluated. In order to simulate the changes of albumin, urea, and glucose concentration in different areas of membrane mathematical modeling of polysulfone fiber was performed using COMSOL Multiphysics 5.5. Additionally, the effect of applying different flow rates (from 1 to 10 mL/min) on albumin, urea, and glucose diffusion was checked.

Results

The studies confirmed that the substances with the particle size smaller than 0,1 μm passed freely through the membrane. It allows for free albumin (crucial hepatic marker) transfer through the membrane and hence for monitoring cell growth. The studies also confirmed the hydrophilicity of polysulfone membrane, what suggests that cells should easily adhere to the capillary surface. Importantly, obtained results indicated that polysulfone material is non-toxic to cells. Conducted simulations showed the increase in albumin concentration after three days, whereas in case of urea and glucose concentration there were no big differences between initial values and results obtained after three days. Interestingly, mathematical modeling indicated that flow rate does not strongly affect albumin, urea, and glucose diffusion.

Conclusion

To sum up, obtained results indicated that chosen polysulfone membrane, and hence, constructed hollow fiber bioreactors, are suitable for hepatic cells culture. The next step of our experiments will be to culture the C3A cells with restored urea cycle and their unmodified counterparts (as a control) in dynamic conditions in order to compare culture parameters of both cell lines.

Assessment of the toxicity and possible therapeutic effects of iron oxide nanoparticles in *in vitro* cellular models

Natalia Janik-Olchawa[1], Agnieszka Drozdz[1], Damian Ryszawy[2], Maciej Pudełek[2], Karolina Planeta[1], Zuzanna Setkowicz[3], Maciej Śniegocki[4], Andrzej Żądło[2], Beata Ostachowicz[1], Joanna Chwiej[1]

[1]Faculty of Physics and Applied Computer Science, AGH University of Science and Technology, al. Mickiewicza 30, 30-059, Krakow, Poland.
[2]Faculty of Biochemistry Biophysics and Biotechnology, Jagiellonian University, Gronostajowa 7, 30-387 Krakow, Poland.
[3]Institute of Zoology and Biomedical Research, Jagiellonian University, Gronostajowa 9, 30-387, Krakow, Poland.
[4]Collegium Medicum in Bydgoszcz, Curie Skłodowskiej 9, 85-094, Bydgoszcz, Poland.
natalia.janik-olchawa@fis.agh.edu.pl

Increasing interest in the application of superparamagnetic iron oxide nanoparticles (IONPs) in biomedicine including medical diagnostics and therapy, involve the necessity of assessing the safety and toxicity profile of these nanomaterials. Therefore, the potential therapeutic effects and toxicity mechanisms of ultrasmall IONPs are a subject of many scientific research and still rise a lot of controversies[1,2]. The *in vitro* studies constitute the basic method for the assessment of nanotoxicity, they produce reproducible and reliable results without the use of animal model, are rapid, simple, and inexpensive[3].

In our research, the influence of PEG-coated NPs with 5, 10 and 30 nm magnetite core on six different cell lines was examined. Cell lines were carefully chosen for the study to determine both possible toxic effects on normal cells and therapeutic potential in case of cancerous ones. These were: human bronchial fibroblasts (NHLF), human embryonic kidney cells (HEK293T), mouse macrophages, two glioblastoma multiforme (GBM) cell lines (T98G, U87MG) as well as GBM cells isolated from a brain tumor of patient (KJT23I). The influence of IONPs in two doses (5 and 25 μg Fe/ml) and at two exposure times (24 and 72 hours) on the viability, proliferation and migration activity, ROS production and actin cytoskeleton rearrangements was examined. The cytotoxicity of nanomaterials were determined using the MTT assay and trypan blue staining, fluorescence microscopy and time-lapse video microscopy.

The obtained results clearly show that the observed changes in cell life parameters are different for various cell lines and strongly depends on the used dose, exposure time and IONPs core diameter. Nanoparticles can stimulate the proliferation of some cells, including glioma cells, however they have negative impact on their viability. IONPs often increase the cell motility and change the architecture of their actin cytoskeleton.

References:

[1] Malhotra N, Lee JS, Liman RAD, Ruallo JMS, Villaflores OB, Ger TR, Hsiao CD. Potential Toxicity of Iron Oxide Magnetic Nanoparticles: A Review. Molecules. 2020 Jul 10;25(14):3159. doi: 10.3390/molecules25143159. PMID: 32664325; PMCID: PMC7397295.

[2] Vakili-Ghartavol R, Momtazi-Borojeni AA, Vakili-Ghartavol Z, Aiyelabegan HT, Jaafari MR, Rezayat SM, Arbabi Bidgoli S. Toxicity assessment of superparamagnetic iron oxide nanoparticles in different tissues. Artif Cells Nanomed Biotechnol. 2020 Dec;48(1):443-451. doi: 10.1080/21691401.2019.1709855. PMID: 32024389.

[3] Arami H, Khandhar A, Liggitt D, Krishnan KM. In vivo delivery, pharmacokinetics, biodistribution and toxicity of iron oxide nanoparticles. Chem Soc Rev. 2015 Dec 7;44(23):8576-607. doi: 10.1039/c5cs00541h. Epub 2015 Sep 21. PMID: 26390044; PMCID: PMC4648695.

Assessment of changes in biological and antimicrobial properties of double-doped TiO_2 coatings produced by anodic oxidation

Aleksandra Jastrzębska, Marta Kamińska, Bogdan Walkowiak
Lodz University of Technology, Mechanical Faculty, Institute of Materials Science and Engineering, Department of Biophysics, Stefanowskiego 1/15 St., 90-924 Lodz, Poland
jastrzebska.aleksandra1@gmail.com

Currently, many surface modification techniques and strategies are used in surface engineering, thanks to which the modified surfaces of biomaterials reduce colonization by microbes and have a positive effect on human cells. Among them, the modification of titanium (one of the most commonly used metallic biomaterials) uses techniques that improve the physicochemical and biological properties of this material, consisting in the modification of titanium dioxide (TiO_2) layers [1]. One of the possible solutions to the problem is the electrochemical modification of titanium and its alloys, widely described in the literature in recent years [2], and doping becomes the most popular strategy, which significantly extends the range of possible applications of these materials in biomedical applications [3].

Our previous research on titanium dioxide coatings with different morphology (barrier, porous and nanotube) doped with various elements with biomedical potential (silver, copper, strontium and zinc) showed a large and varied influence of the coating morphology and chemical composition on the physicochemical properties, but above all on the photocatalytic properties and biological response of cells exposed to contact with these surfaces. The aforementioned tests were performed only for the cases of single-element doping. Currently presented research was carried out with the use of double doping during one electrochemical process.

In the current research, we conducted a high-voltage anodic oxidation process with the participation of two admixtures: one that may affect the surface biocompatibility (calcium) and one that has an antibacterial effect (copper or zinc). The successful introduction of admixtures into all types of coatings has been confirmed by the XPS test. Analysis of microbial biofilm formation, proliferation and viability of osteoblasts was also performed. For the obtained coatings, a significant reduction in microbial colonization with a simultaneous positive antibacterial (against *E.coli* strain) and antifungal (against *C.albicans* strain) effect was demonstrated. Moreover, all coatings allowed for good proliferation and high viability of the osteoblasts grown on their surfaces.

The obtained results show that it is possible to control the anodic oxidation process in such a way as to obtain titanium dioxide coatings with porous morphology, additionally doped with additives introduced into the electrolyte. The introduction of an admixture of calcium, copper or zinc to TiO_2 coatings affects their properties in contact with biological objects. Interestingly, only calcium-doped coatings showed the worst properties compared to other surfaces. Despite good antimicrobial properties, they showed the lowest biocompatibility assessed on the basis of cytotoxicity and proliferation potential of bone cells in contact with them.

References:
[1] X. Liu et al., Materials Science and Engineering: R: Reports 47(3-4), 2014, s.: 49-121.
[2] C. Yao, T.J. Webster, Journal of Nanoscience and Nanotechnology 6 (9-10), 2006, s.: 2682-2689.
[3] A.P. Ross, T.J. Webster, International Journal of Nanomedicine 8, 2013, s.: 109-117.

Corrosion properties of double-walled TiO_2 nanotubes measured in 0.9% NaCl - preliminary results

Aleksandra Jędrzejewska[1,2]
[1]Science and Technology Park of University of Zielona Góra, ul. A. Syrkiewicza 6 – Nowy Kisielin, 66-002 Zielona Góra, Poland.
[2]Department of Biomedical Engineering, Faculty of Mechanical Engineering, University of Zielona Góra, ul. prof. Z. Szafrana 4, 65-516 Zielona Góra, Poland.
a.jedrzejewska@pnt.uz.zgora.pl

Titanium and its alloys have good corrosion resistance and biocompatibility and are often used in biomedical applications. The corrosion resistance of these materials can be improved, thereby increasing their usability and durability. The aim of this study was to improve the corrosive properties of titanium by developing a coating of double-walled titanium dioxide nanotubes (dTNT) on its surface. The dTNT layers were prepared by electrochemical anodization of titanium foils in 85% ethylene glycol solution with 0.65% wt. NH_4F and 7.5% H_3PO_4 in time 4 h using potentials: 10, 30 and 60 V. Based on the electrochemical and scanning electron microscopy studies, it was found that dTNT layer improves corrosion resistance, and the best protection was confirmed for dTNT formed at 60 V. The dTNT layer due to its good anti-corrosion, protective properties and stability can expand the applicability and extend durability of titanium in aircraft structures, medicine or chemical industries.

Influence of compartment model structure simplification on radiation dose calculation for ^{14}C urea breath test

Aleksandra Jung
AGH University of Science and Technology, Mickiewicza Av. 30, Cracow, Poland
jung@fis.agh.edu.pl

Simplification of mathematical model structure is often used for clinical purposes e.g. in hepatology, where single-compartment model for bile acid kinetics is used for treatment dose calculation during extracorporeal liver treatment. Lately the renewed interest of breath tests among physicians and the need to estimate doses received by patients for various radiopharmaceutical procedures by medical physicists to prepare practical recommendations and methodology of calculations has been observed [1,2]. The aim of this study was to verify if simplification of the model presented by Stubbs and Marshall [3] gives acceptable results of radiation dose for the ^{14}C labeled urea breath test used for diagnosis of *Helicobacter pylori* (*H.pylori*) and if patient dose estimation gives the results consistent with ICRP recommendations.

Three simplified models were adopted to estimate radiation dose for the ^{14}C labeled urea breath test used in the diagnosis of *H. pylori*: one-compartment model, two one-compartment submodels and a three-compartment model using two sets of coefficient and distinguishing the effective dose for *H.pylori* positive and negative patients.

Obtained results were compared to the effective doses calculated using the model presented by Stubbs and Marshall to estimate the radiation absorbed by positive and negative patients with the ^{14}C-urea breath test. The reference model consisted of two submodels and it was much more complex than the simplified models what probably caused an order of magnitude difference between own results and literature model doses (range 4.6-7.6 μSv). Unfortunately, the values of doses obtained in this study are underestimated compared to the original model, what does not predispose them for practical application. If the calculated doses were higher than in the complex model, then simplified models would have been useful since from the radiological protection point of view, it is better when the calculated dose is overestimated as it protects the patient.

The results shows that the more complex model, the more identical doses to reference values and the dose underestimation is smaller. This means in practice that only verified models should be used in accordance with ICRP recommendations for accurate dose estimation during diagnostic tests using radiotracers, given dose underestimation is unfavorable for the patient.

References:
[1] Jung A., Korohoda P., Krisper P., Stadlbauer V., Stauber R.E., Schneditz D. Bile acid kinetic modeling in end-stage liver support patients. *Biocybernetics and Biomedical Engineering*, 2020, vol. 40, pp. 764-73
[2] Matusiak K., Jung A. Zastosowanie modelowania kompartmentowego do szacowania dawek promieniowania jonizującego w diagnostyce medycznej. *Bio-Algorithms and Med-Systems,* 2010, vol. 6, pp. 125-6
[3] Stubbs J.B., Marshall B.J. Radiation dose estimates for the carbon-14-labeled urea breath test. *J Nucl Med,* 1993, vol. 34, pp. 821-5

The use of FFT and STFT analysis in assessment of ability to maintain balance in sensory conflict conditions as a complementary element for time domain analyses

Jacek Jurkojć[1], Piotr Wodarski[1], Robert Michnik[1], Wojciech Marszałek[2], Kajetan J. Słomka[2], Marek Gzik[1]
[1] Silesian University of Technology, Biomechatronics Department, ul. Roosevelta 40, 41-800 Zabrze
[2] Academy of Physical Education, Institute of Sport Sciences ul. Mikołowska 72a, 40-065 Katowice
Jacek.Jurkojc@polsl.pl

Assessment of human balance is one of the most common diagnostic tests, however the analysis of results is mainly based on the values obtained in time domain. As long as such an analysis may be sufficient for the most common tests - standing motionless with eyes open and closed – the measurements in sensory conflict conditions require more sophisticated analysis. This is due to the fact that the increased values of the analyzed parameters may be related not only to balance problems but also to the natural behavior of a participant affected by destabilizing stimuli. The aim of the work was to develop a methodology for the practical use of frequency-domain analyses to quantify the ability to maintain body balance during measurements in sensory conflict conditions introduced by means of oscillating virtual 3D scenery.
27 healthy volunteers (13 women and 14 men, mean age 21) took part in the study. The three-dimensional scenery, presented by means of the Oculus system, oscillated in the sagittal plane with frequencies equal to 0.7 Hz and 1.4 Hz. 4 trials were conducted by each participant – the frequency value was constant during the measurement or changed in the middle of the test. Each trial lasted 60 seconds. Oscillation started at the 15th second and was stopped at the 45th. Analyzed 30 seconds were divided into first and second 15 seconds for the statistical analyses reason. Measurements of Centre of Pressure (COP) were conducted on the FDM Zebris platform. Successive coordinates of the COP were treated as a signal for frequency analyses.
The results were analyzed using developed coefficients determined on the basis of the Short-time Fourier transform (STFT; window width 10 seconds, window shift step 0.1 seconds, windowing method: Hamming window). Balance Disturbances Coefficient (D) was calculated as $D = \sum_{n=1}^{N} A_n^2 \cdot f_n$ (where A_n is an amplitude value of the nth cyclic component on the FFT chart, f_n - value of frequency of the nth cyclic component and N - total number of cyclic components detected excluding the component appearing at the frequency equal to the frequency of scenery movements) and Sensitivity Coefficient (S) was determined as square of the amplitude value of the cyclic component appearing at the frequency equal to the frequency of scenery movement (0.7 Hz or 1.4 Hz). Values of both parameters were calculated for each moment of time using STFT chart. S describes the subject's movement of following the scenery, whereas D takes into account movements with other frequencies. For each parameter the median, quartiles and the max and min values were calculated. Tests of the significance of statistical differences were carried out using the Wilcoxon paired order test assumed the significance limit p = 0.05. The MATLAB environment program and the STATISTICA 13 were used.

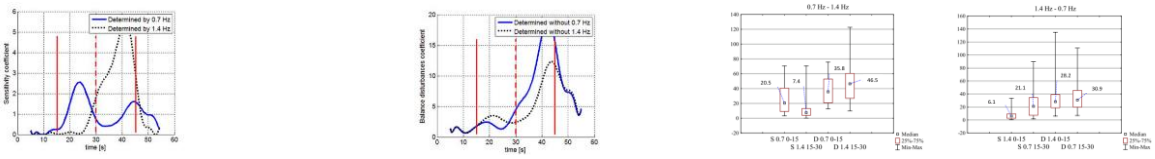

a) b) c) d)

Courses of a) Sensitivity Coefficient S, b) Balance Disturbances Coefficient D obtained for a selected person for a measurement with changing frequency from 0.7 Hz to 1.4 Hz – dashed line: change of the frequency of the scenery movement. Medians of the areas under curves of coefficients obtained for all participants c) changing frequency from 0.7 to 1.4 Hz, d) changing frequency from 1.4 to 0.7 Hz

Obtained results showed that the changes in the average COP speed (time domain parameter) that occur during the measurement in sensory conflict conditions can result from changes related to the movement of following the scenery as well as additional body movements indicating a greater or lesser loss of balance. It was also found out that differences in the COP movement depend on values of the introduced frequencies.

The conducted research proved that in measurements involving the ability to maintain one's balance conducted in sensory conflict conditions, standard time-domain analyses should be supplemented with other types of data analysis, e.g. frequency domain analyses.

References:

[1] Jurkojć J., Wodarski P., Michnik R., Marszałek W., Słomka K.J., Gzik M. The Use of Frequency Analysis as a Complementary and Explanatory Element for Time Domain Analysis in Measurements of the Ability to Maintain Balance, *Journal of Human Kinetics*, 76/2021, pp. 117-129.

[2] Keshner E.A., Kenyon R.V., Langston J.: Postural responses exhibit multisensory dependencies with discordant visual and support surface motion. Journal of Vestibular Research 14, 2004, p. 307-319.

eBathtub and eChair sensor subsystems supporting the elders

Mariusz Kaczmarek, Adam Bujnowski, Kamil Osiński, Tomasz Neumann, Jacek Rumiński
Gdańsk University of Technology, Narutowicza 11/12, 80-233 Gdańsk
mariusz.kaczmarek@pg.edu.pl

The aim of the project is to develop Ella4Life system for supporting the elders and chronically ill. Ella4Life integrates three technologies that all have a wide applicability and robust implementation. It combines Anne of Virtask (NL), Emma of Medicine Men (NL) and the sensors subsystem: eBathtub and eChair of the Gdansk University of Technology (PL). People and in particular older people with chronic diseases often have a sedentary lifestyle. Therefore, the role of the support system should be to activate the elderly, both for physical activity and for social contacts. At the same time, the system can use habits to a sedentary lifestyle and measure vital signals while resting. In study [1] researchers have been developing a non-conscious physiological monitor installed in a bath, a lavatory, and a bed for home health care. The combination of data from multiple sensors from home health monitoring systems is described in [2]. Data fusion gives more objective predictive factors than signals analyzed separately. The capacitive-coupled electrocardiography (CECG) technology is also described in the literature: requires ultra-high impedance probes and high CMRR input amplifier [3].
eBathtub and eChair subsystems are designed to record vital signals during rest and relaxation, without the need to connect measuring electrodes to the body or perform other additional activities related to measurements. Measurements are performed automatically in the background. The only thing the user has to remember is to charge the batteries powering the electronic measuring systems. The eChair is a device for electrode-less monitoring of cardiac action potential embedded into a classical deep armchair. The device can monitor electrical bio-potentials through clothing, it can monitor and report heart-rate and its derivatives like HRV of the person sitting in the chair. Data is available on-line via the a wireless network. For Ella4Life system we used ZigBee as the transport mechanism. The eChair send data to a hub-host (Rapberry Pi Zero) and authenticated clients can read data by means of various protocols. Available data are always representing the actual situation – presence of the person on a chair, measured waveforms and parameters like HR, HRV etc. eBathtub - device for monitoring vital signs of a bathing person. Device is in the form of an anti-slip mat with embedded electrodes placed at the bottom of ordinary bathtub. The mat is longer than usual anti-slip mat as it is folded to the top of bathtub where it has integrated controller. Technique of detection can indicate presence of the person in the bathtub with presence of different water ingredients like bathing salts, soap, shampoo etc. Additionally monitoring of the activity of the person in the bathtub is possible – in sense – “Is he or she moving or not ?”. In cases of weak activity it is possible to monitor heart activity by measuring biopotentials. Additionally temperature of the water in the bathtub can be monitored – Fig. 1.

Detection of the presence of a person in the bathtub allows us to reduce risk of accidents in the bathtub. Bath process can be supervised and via speech synthesis provided by Anne; “I advise you to leave the bathtub soon, is everything okay?”, “Do You need assistance while leaving bathtub ?” In case of prolonged stay in bathtub, lack of activity and no reaction for communicates a request for help can be raised.

a)  b) 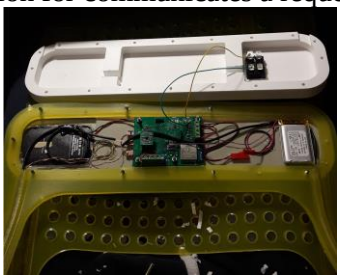 c) 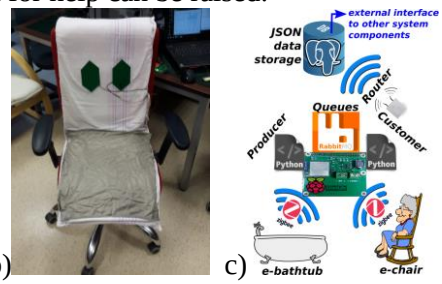

Fig. 1. The eBathtub – a), eChair – b) subsystem prototypes and communications between components – c)

References:

[1] S. Majumder, E. Aghayi, M. Noferesti, H. Memarzadeh-Tehran, T. Mondal, Z. Pang, M. Deen, Smart Homes for Elderly Healthcare-Recent Advances and Research Challenges, Sensors, 31;17(11):2496, 2017.

[2] K. Motoi et al., A fully automated health-care monitoring at home without attachment of any biological sensors and its clinical evaluation, 2009 Annual International Conference of the IEEE Engineering in Medicine and Biology Society, pp. 4323-4326, 2009.
[3] Y. Sun, X. B. Yu, Capacitive biopotential measurement for electrophysiological signal acquisition: A review, IEEE Sensors Journal, 16(9): 2832–2853, 2016.

Effect of surface structuring of metallic materials on their thrombocompatibility

Marta Kamińska[1], Magdalena Walkowiak-Przybyło[1], Marta Walczyńska[1], Piotr Komorowski[2], Bogdan Walkowiak[1,2]
[1]Department of Biophysics, Institute of Materials Science and Engineering, Lodz University of Technology Stefanowskiego 1 St., 90-924 Lodz, Poland
[2]Bionanopark Ltd., Dubois 114/116 St., 93-465 Lodz, Poland
marta.kaminska@p.lodz.pl

The implant surface topography is a very important element moderating biological response necessary for the proper functioning of the whole organism. Interaction of blood with the biomaterial surface causes, between others, adhesion and activation of platelets [1]. This may stimulate the integrating process of the implant with the tissue, but may also lead to thromboembolic complications. At the same time, contact of platelets with the surface of the biomaterial may cause changes in their proteome and loss of their functionality [2]. Structuring biomaterial surface with laser gives it new properties. The aim of the current research was to determine the effect of surface structuring on the thrombocompatibility of commonly used biomaterials.

Three types of alloys were tested: AISI 316L, Ti6Al4V, Ti6Al7Nb. Four types of samples surface structuring were employed: A – after machining (Ra 1.1 ÷ 1.2 μm), B - after grinding (Ra 0.5 ÷ 0.8 μm), C and D - two types of laser modification with different radiation power. Blood was obtained from healthy volunteers who had abstained from an antiplatelet medication for 14 days prior blood donation. The materials were contacted with blood 20 min after blood collection. The research was carried out with the consent of the Local Bioethics Committee of the Medical University of Lodz granted to the Department of Biophysics (no. RNN / 46/06 / KB 21.02.2006).

The test surfaces were in contact with whole citrated blood for one hour at 37° C under gentle flow conditions. After dehydrating and drying the samples were sprayed with a thin layer of gold. In order to accurately assess the shape of the adhered platelets, photos of the surfaces of the materials were taken using a scanning electron microscope. After the contact with biomaterials the remaining citrated whole blood was tested with a flow cytometer for determining of spontaneous blood platelets activation and aggregation. For this purpose three fluorescence labeled antibodies were used: anti-CD61-perCP, anti-CD62-PE, and anti-PAC-1-FITC. Platelet aggregation was assessed by analysis of forward and side scattered light.

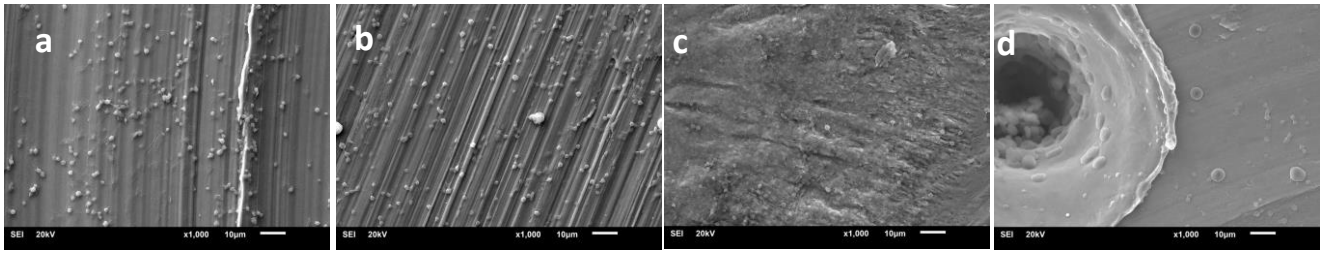

Fig. 1. Representative photos of SEM analysis of the studied surfaces. a) to d) randomly selected areas of four types of surface modification of the Ti6Al7V alloy.

The degree of platelet activation was assessed on the basis of Goodman classification [3]. The highest number of not activated platelets was found on all materials with D-type laser modified surfaces. Also for this modification the lowest number of platelets with a high degree of activation was recorded for both titanium alloys. Fewest platelet aggregates in whole blood were formed after contact with type B modified materials, and laser modified C type causes the highest platelet activation in the whole blood for all materials. The lowest activation of blood platelets in the whole blood were observed after contact with B and D types of modified materials - and these were comparable levels.

References:

[1] M. Walkowiak-Przybyło, *et al.*, Adhesion, activation, and aggregation of blood platelets and biofilm formation on the surfaces of titanium alloys Ti6Al4V and Ti6Al7Nb, Journal of Biomedical Materials Research - Part A, 2012 Volume 100 A, Issue 3, 768-775.

[2] Walkowiak B. *et al.*, Effect of Uremia and Hemodialysis on Proteome Profile of Blood Platelets and Plasma, Clin Appl Thromb Hemost. 2013, vol. 19, 541-549.

[3] Goodman S.L**.** Sheep, pig, and human platelet–material interactions with model cardiovascular biomaterials, Juranl of Biomediacal Materials Research, 1999, 45(3), s. 240-250.

BOLD-fMRI study of auditory cortex in young women

Ilona Karpiel[1], and Klaudia Duch[2]
[1]Łukasiewicz Research Network – Institute of Medical Technology and Equipment, Zabrze, Poland, [2]Faculty of Science and Technology, Institute of Biomedical Engineering, The Silesian Centre for Education and Interdisciplinary Research, The University of Silesia in Katowice, Chorzow, Poland
ilona.karpiel@itam.lukasiewicz.gov.pl

Abstract. In the last 25 years, there has been a development of neuroimaging techniques - especially functional magnetic resonance imaging (fMRI). Current-ly, functional magnetic resonance imaging is used in two areas - cognitive neu-roscience and clinical applications. fMRI is based on the BOLD (Blood Oxy-genation Level-Dependent) sequence, which means a signal change that is due to the hemodynamic and metabolic sequelae of neuronal responses.

Hearing is one of the most important senses in the human body where the Human auditory cortex represents 8% of the surface of the cerebral cortex. Five healthy females volunteers of age 24 years have been included in the experi-ment. Brain imaging studies were performed with 1.5T MRI scanner TOSHIBA MRI Vantage ATLAS x MRT equipped with an 8-channel head coil in Inde-pendent Public Clinical Hospital No.1 in Katowice. All paradigms to stimulate the auditory cortex were prepared by using ParaPlayer software. The stimula-tion used seven sinusoidal beeps of frequencies: 250, 500, 1000, 2000, 3000, 5000, 8000 Hz. Analysis of brain activations based on EPI sequence was per-formed in SPM8 package in MATLAB (MathWorks, Inc.) environment.

The aim was to examine the auditory tract in healthy women and presented the structural and functional basis of human brain lateralization in the auditory mo-dality. The author focused on hemodynamic and electromagnetic data of healthy participants concerning sound encoding. Next, the author raised the top-ic of Lateralization which is also often referred to as functional asymmetry of the human body what is a result of differences in construction and function of cerebral hemispheres. Optimization is presented taking into account a selected set of parameters such as kernel (FWHM 5 and 6 mm) and different p-value af-ter applying the mask

Keywords: preprocessing data, auditory cortex, fMRI 2

Decision support system for IBD

Anna Kasperczuk [(1,a),] Agnieszka Dardzinska [(1,b)]
[(1)]Bialystok University of Technology, Faculty of Mechanical Engineering
[(a)]Institute of Biomedical Engineering
[(b)] Department of Mechanics and Applied Computer Science
ul. Wiejska 45c, 15-351 Bialystok, Poland
a.kasperczukuk@pb.edu.pl

Crohn's disease (CD) and ulcerative colitis (UC) have been known to physicians for decades. Unfortunately, so far there are many unknowns, regarding CD and UC. There are numerous descriptions of clinical cases, different locations of disease symptoms, and descriptions of symptoms located both in the gastrointestinal tract and symptoms accompanying these diseases. All this information sheds light on the etiology of inflammatory bowel disease (IBD) do not completely resolve their complexity. An analysis of the literature presented in the work indicates that the characteristics of diseases are often unambiguous. This contributes to the fact that IBD diagnostics are often difficult and create many problems [1, 2]. The aim of the analysis was to find symptoms that differentiate the analysed diseases among popularly tested laboratory exponents.

The study concerned the analysis of patient data with inflammatory bowel diseases. Data were collected using data about patients of the Department of Gastroenterology and Internal Diseases of the Medical University of Bialystok Clinical Hospital, The data was collected based on the analysis of patient records. In the first group, ulcerative colitis was diagnosed (N = 86, women N = 32, men N = 54), and the second group were patients with Crohn's disease (N = 66, women N = 32, men N = 34). The work combines statistical methods and selected data mining algorithms. The research part consists of two main stages of work: the first concerning the issue of classification and searching for the best classifier, and the second one is based on mining the classification rules [3].

The classification model was built. Model contains only variables which in the selection process of features turned out to be significantly different in two analyzed groups (from feature selection).
For the built classifier with available variables, the sensitivity was 100%.The specificity value, describing the ability to detect people with UC, fluctuates within 98.48%.

The results obtained by us are extremely promising and indicate new markers for IBD that may be an alternative to the currently used ones. The analysis showed that preliminary research results may aid in the diagnosis of UC and CD. Laboratory tests alone may be a reason to make a proper diagnosis. The constructed classification system can undoubtedly help doctors in a situation of uncertainty. The level of sensitivity fluctuates at 100% and specificity has reached 98.48%. This indicates that the model is perfectly able to recognize patients on both CD and UC. The results obtained by us are extremely promising and indicate new markers that may be an alternative to the currently used ones. In further studies, it is necessary to apply and verify a model comparing the group of patients with healthy people, which will contribute to systemize the of knowledge about the analysed diseases

References:

[1] M. Krzystek .al. (2020), Biochemical Biomarkers of Mucosal Healing for Inflammatory Bowel Disease in Adults. *Diagnostics*, vol. 10, no. 6, pp. 367.
[2] J. Daniluk, U. Daniluk, J. Reszec, M. Rusak, M. Dabrowska, A. Dabrowski (2017), Protective effect of cigarette smoke on the course of dextran sulfate sodium-induced colitis is accompanied by lymphocyte subpopulation changes in the blood and colon. *Int J Colorectal Dis*, 32, pp. 1551-1559.
[3] A. Kasperczuk, A. Dardzinska (2016), Comparative evaluation of the different data mining techniques used for the medical database. *Acta Mech Autom*, 10, pp. 233-238.

Biochemical anomalies of nervous tissue resulting from mechanical brain injury can be characterized using the techniques of vibrational microspectroscopy

Kamil Kawon[1], Zuzanna Setkowicz[2], Agnieszka Drozdz[1], Krzysztof Janeczko[2], Joanna Chwiej[1]

[1]AGH University of Science and Technology, Faculty of Physics and Applied Computer Science, Al. Mickiewicza 30, 30-059 Krakow, Poland
[2]Jagiellonian University, Institute of Zoology and Biomedical Research, Ul. Gronostajowa 9, 30-387 Krakow, Poland
kawon@agh.edu.pl

Traumatic brain injury (TBI), meaning functional or structural damage which appear as a result of the application of the external physical force, constitutes the main cause of death and disability of individuals and a great socioeconomic problem. To search for the new therapeutic strategies for TBI, better knowledge about posttraumatic pathological changes occurring in the brain is necessary.

The Fourier transform infrared microspectroscopy and Raman microscopy were used to examine local and far-distant biochemical changes occurring in the rat brain as a result of focal cortex injury. The site of the injury and the dorsal part of the hippocampal formation together with the above situated cortex and white matter were the subject of the study.

The topographic and quantitative biochemical analysis followed with the statistical evaluation using principal component analysis (PCA) showed significant biomolecular anomalies within the lesion site but not in the remote brain areas. The observed abnormalities included the decreased accumulation of lipids (the intensity of 2955 cm^{-1} band was two times lower in the scar comparing to the surrounding tissue) and their structural changes. Also the levels of compounds containing phosphate groups (intensity of 1080 cm^{-1} band decreased 2.5 times) and carbonyl groups (intensity of 1740 cm^{-1} was 30% lower) were significantly lower within the lesion site comparing to the surrounding cortex. The opposite relation was, in turn, found for the bands characteristic to proteins and cholesterol/cholesterol esters and the intensity of amide I band and the massif at 1360-1480 cm^{-1} were around 20% higher in the scar than in the surrounding cortex.

The observed changes in the biochemical composition occurring within the region of injury and involving the increased level of proteins and their structural changes probably result from the remodeling of the extracellular matrix and the secondary damage connected with the process of astrogliosis [1]. In turn, the reduction of lipid content at this region is likely a result of the destruction of cell membranes [2] during the primary tissue damage.

References:

[1] M. V. Sofroniew, “Astrogliosis*,” Cold Spring Harb. Perspect. Biol*., vol. 7, no. 2, p. a020420, Feb. 2015
[2] R. M. C. Dawson, “The anima phospholipids: their structure, metabolism and biological significance,” *Biol. Rev.*, vol. 32, no. 2, pp. 188-229, May 1957

Characteristics of nerve roots mechanical properties exposed to uniaxial stretching tests

Tomasz Klekiel, Agnieszka Mackiewicz, Monika Palmerska
Uniwersytet Zielonogórski, ul. Licealna 9, 65-417 Zielona Góra
tklekiel@uz.zgora.pl
20000884@stud.uz.zgora.pl
A.Mackiewicz@ibem.uz.zgora.pl

The article presents the issues of the mechanical response of nerve roots under stretching conditions. There is assumed a relation between deformation, blood flow characteristics, and nerve root impulse transmission. Research proves that vascular hypofusion of peripheral nerves occurs at a deformation of 15%. Impulse conduction disturbances at 6% strains were also observed. From this account it follows that the cause of diseases of the nervous system may be excessive deformation of its structures. One of such diseases is radiculopathy.

Lumbar radiculopathy affects 3 to 5% of the general human population. It is a condition caused by chemical or mechanical factors that destroy the nerve roots, such as herniated discs, inflammation, and iatrogenic causes. Radiculopathy is accompanied by various types of pain and functional deficits that make life difficult for patients. In addition to compression, nerve roots may be exposed to tensile stress, e.g. by adhesions with the surrounding structures as a consequence of inflammation. This phenomenon is often unnoticeable during follow-up MRI examinations, which makes correct diagnosis difficult. It is essential to understand the development of the pathology of nerve roots exposed to mechanical stress to understand the relationship between stresses, strains and the structural and functional reaction of the nerve roots.

Understanding the mechanical response of tissues exposed to certain clinical conditions requires special techniques and complex constitutive models that cannot be solved analytically. Tissue material parameters are therefore tested using numerical approximation methods. In order to do this, it is necessary to experimentally investigate the material characteristics that allow to determine the parameters for the numerical models used.

The aim of investigation was to define the material characteristics of nerve roots. The analysis was performed to obtain data allowing to simulate conditions that can lead to disease states of nerve roots using the finite element method.

The material was obtained from the rabbit's lumbar spine, which was stored in the transplant fluid in a freezer at 5°C by 6 hours. Paraspinal muscles and spinous processes were removed. Samples of the neural structures originating from the spinal cord with the spinal nerve were obtained individually with a scalpel and tweezers, just before the examination. To prevent drying, the samples were soaked in water. Tensile tests were performed with a speed of 0.17 mm / s on testing machine ZWICK. The samples were mounted on specially made holders. The obtained data showed that the rabbit nerve root strength 0.9 ± 0.53MPa, the relative deformation 12.73 ± 4.03%, and Young's modulus 2.53 ± 1.00MPa. The results of the experiment were compared with the results from the literature. The obtained results are partly in line with the results of other researchers, but none of the data is fully consistent with each other. The tensile strain achieved in the studies and data reported in the literature exceed 9%, which in clinical conditions would result in vascular hypofusion, conduction disturbances and tissue changes.

References:
[1]Berthelot J. et al. Stretching of roots contributes to the pathophysiology of radiculopathies. - Joint Bone Spine, 2018 vol.85, pp. 41-45.
[2] Barry J.A. et al. A Review of Lumbar Radiculopathy, Diagnosis, and Treatment, Cureus, 2019, 11.10.
[3]Lin J.H. et al. Lumbar radiculopathy and its neurobiological basis. World J Anesthesiol,2014, vol.3(2), pp.162–173.

Atomic force spectroscopy as a nanoscopic tool for assessing nanomaterials toxic effects *in vitro*

Agnieszka M. Kołodziejczyk[1], Paulina Sokołowska[1,2], Aleksandra Zimon[1], Magdalena Grala[1], Marcin Rosowski[1,3], Małgorzata Siatkowska[1], Piotr Komorowski[1,4], Bogdan Walkowiak[1,4]
[1]Bionanopark Ltd, Dubois 114/116, 93-465 Lodz, Poland
[2]Department of Pharmacology and Toxicology, Medical University of Lodz, Zeligowskiego St. 7/9, 90-752 Lodz, Poland
[3]Lukasiewicz Research Network, Textile Research Institute, Brzezińska 5/15, Lodz, Poland
[4]Department of Biophysics, Institute of Materials Science and Engineering, Lodz University of Technology, Stefanowskiego 1/15, 90-924 Lodz, Poland
a.kolodziejczyk@bionanopark.pl

Atomic force spectroscopy (AFS) is one of the useful methods to assess the toxic effects of different agents in cell culture. The aim of our work is to develop a model for the assessment of the toxic effects of nanomaterials in *in vitro* studies using AFS [1]. Such the model, based on cell elasticity, rearrangement of cytoskeleton fibers, levels of reactive oxygen species and apoptosis for cells exposed to nanostructures, has not been considered in the literature so far. The present study was devoted to the effects of silver nanoparticles (SNPs), multi-walled carbon nanotubes (MWCNTs) and poly(amidoamine) (PAMAM) dendrimers of 4th generation on functioning of EA.hy926 endothelial cell line.

The AFS method was used to investigate the mechanical properties of the cells – measurements of the elasticity modulus. The innovative nature of our work is the comparison of cell elasticity performed with various AFS probes of ball-shape and conical geometries, which enabled detection of local and global elasticity alteration caused by the nanostructures. Cells elasticity modulus was calculated using Hertz-Sneddon model. Results of the cell elasticity were supplemented by measurement of reactive oxygen species (ROS) level, apoptosis detection and labelling of actin cytoskeleton. The cell morphology and the presence of nanostructures on / inside the cells were examined by both atomic force microscopy, scanning and transmission electron microscopies.

Trend of changes in local and global elasticity of cells exposed to nanostructures was similar, but the magnitude of the response was dependent on the selected AFS probe. SNPs and MWCNTs evoked cells stiffening, which was correlated with changes in ROS production levels and the cytoskeletal alteration revealed as thick actin fibers located in the central parts of the cells. In the case of cells exposed to PAMAM dendrimers decrease in the elasticity modulus was obtained accompanied with increased number of apoptotic cells and elevated levels of ROS production. Although the ROS generation along with the induction of apoptosis in various cell lines under the influence of PAMAM dendrimers is considered in the literature [2], the originality of our work lays in the pioneering approach towards elasticity study. Softening of cells exposed to dendrimers can be connected to depolymerization of actin fibers leading to theirs apoptosis.

Scanning and transmission electron microscopies confirmed that tested nanostructures are accumulated on the cell membrane and penetrate inside the cells. Therefore, they can induce numerous intracellular processes related to elastic properties alteration, cytoskeleton remodeling, ROS production and even the induction of apoptosis. The mechanical properties of cells exposed to nanostructures provide information not only about cellular nano and micro-structure, but also about cell physiology. Based on the obtained results we conclude, that the structure and the type of nanostructure (nanoparticle) is essential for their localization inside the cells and for the toxic effect on the endothelial cells.

Presented results are the part of the project funded by The National Science Centre, agreement no. 2017/26/D/ST4/00918.

References:

[1] Kolodziejczyk A.M. Dysfunction of endothelial cells exposed to nanomaterials assessed by atomic force spectroscopy, *Micron* 145 (2021) 103062.
[2] Naha, P.C., Byrne, H.J. Generation of intracellular reactive oxygen species and genotixity effect to exposure of nanosized polyamidoamine (PAMAM) dendrimers in PLHC-1 cells in vitro. Aquat. Toxicol. 132 (2013) 61–72.

Microstructural analysis of fractured orthopedic implants

Mateusz Kopec[1,2], Adam Brodecki[1], Zbigniew L. Kowalewski[1]
[1]Institute of Fundamental Technological Research, Polish Academy of Sciences, Pawińskiego 5B, 02-106 Warsaw, Poland;
[2]Department of Mechanical Engineering, Imperial College London, London SW7 2AZ, UK;
mkopec@ippt.pan.pl

Despite the undeniable advantages of medical implants, their fractures remain a problem. The main factors considered as potential causes of fracture were assigned to the patient's condition, geometry of the implant and
its mechanical loads. Nevertheless, the microstructural mechanisms of fracture occurrence have not been investigated in detail as yet. Thus, fracture mechanisms and their causes were studied in the case of selected types of four implants with different geometries (pure titanium locking plate, pure titanium femoral implant, Ti-6Al-4V titanium alloy pelvic implant, X2CrNiMo18 14-3 steel femoral implant). Each implant fractured in the human body. The scanning electron microscopy (SEM) was used to qualitatively examine and determine the potential cause of implants fracture.

It was found that the implants destructions mainly occurred in consequence of mechanical overloads resulting from repetitive, banned excessive limb loads or singular, un-intendent, secondary injures. The design of implants leads to the generation of stress concentrators that serve as initiators of cracks. The microscopic analysis of the fractured surfaces of the implants revealed that, regardless of the initial material state and geometry, the fracture was caused by the concentration of the stress forces in its holes, including the threaded parts, where the crack initiated and propagated within the material (Figure 1). Most probably, the implants were subjected to an excessive fatigue load with additional effects caused by the interaction between the screws and threaded holes. The very tight connection between the screws and threated holes of the implant initiated cracks that led to significant wear between the working surfaces. The wear of threads of screws and plates might reduce the rigidity of the connection between the bone and the implant, thus enhancing the temporary loads between them that promoted the propagation of the implant’s cracks.

The results of this work enable to conclude that the construction of orthopedic implants is not fully sufficient to transduce mechanical loads acting over them due to an increasing mass of treated patients and much higher their physical activity. One can require to increase the thickness of implant dimensions, especially in the areas with holes in order to reduce the risk of implant fracture.

Keywords: medical fixation devices; orthopedic prostheses and implants; titanium; titanium alloy; stainless steel; microscopic fracture analysis

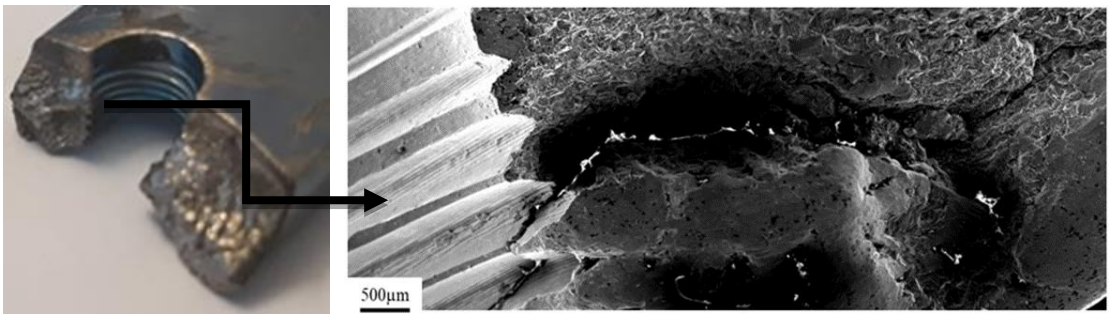

Figure 1. General view of the exploited titanium implant with localized crack propagation initiated in the central part of the thread captured by SEM.

Examination of pneumatic bellows for the rehabilitation of the human jaw

Katarzyna Koter and Witold Szulc
Institute of Machine Tools and Production Engineering, Lodz University of Technology, Lodz, Poland
katarzyna.koter@p.lodz.pl

From 3% to about 18% of the population struggle with the problem of improper functioning of the temporomandibular joint, especially trismus. It affects the range of mouth opening, by decreasing it from 35-55m to couple millimeters only [1]. Existing mechanical devices as TheraBite [2], don't fully cover the needs of effective therapy. Robotic and exoskeleton concepts of trismus treatment equipment, which support a full range of jaw mobility are not widely available.

To eliminate all the drawbacks of existing devices, a complex device of human jaw rehabilitation [3] has been designed. The device uses a pneumatic propulsion system to conduct jaw movement in all required planes, by a system of pneumatic actuators and custom-made pneumatic bellows. There were manufactured several bellows of different shapes and sizes to test the impact of the bellow dimensions on its work.

The bellows were tested by filling them with air at a pressure of 0.05 and 0.1 MPa with simulating the jaws opening from 4 to 16 mm (gap), with a 2 mm stroke. Based on the test there were calculated average values of the generated force, as shown in Fig. 1.

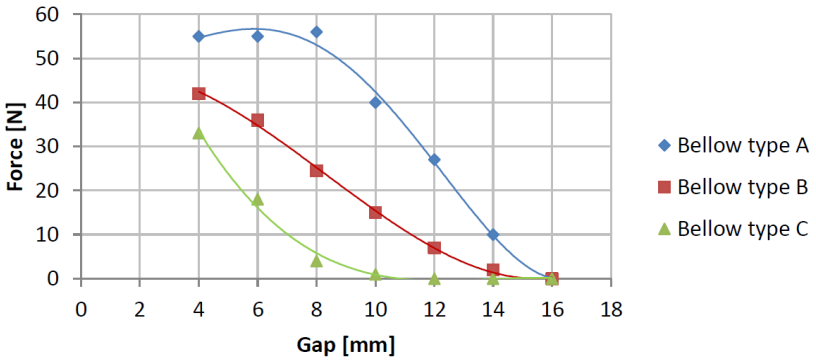

Figure 1 Characteristics of the measured response as a function of the gap for various types of bellows, supplied with air pressure of 0.1 MPa

By using the appropriate type of bellows and their appropriate location, it is possible to get a precise value of force applied, which will allow for the rehabilitation adapted to the individual needs of the patient.

References:

[1] Sharma, S., Gupta, D. S., Pal, U. S., & Jurel, S. K. (2011). Etiological factors of temporo-mandibular joint disorders. National journal of maxillofacial surgery, 2(2), 116–119. https://doi.org/10.4103/0975-5950.94463

[2] Lee R, Yeo ST, Rogers SN, Caress AL, Molassiotis A, Ryder D, Sanghera P, Lunt C, Scott B, Keeley P, Edwards RT, Slevin N. Randomised feasibility study to compare the use of Therabite(®) with wooden spatulas to relieve and prevent trismus in patients with cancer of the head and neck. Br J Oral Maxillofac Surg. May;56 (4) pp. 283-291, 2018

[3] K. Koter, P. Żak, A novel automated device for jaw rehabilitation, International Journal of Mechanical Engineering and Robotics Research, Vol. 9, No. 8, pp. 1176-1181, August 2020

The paper will be available as a full article in the conference proceedings within the "Advances in Intelligent Systems and Computing" series; the book title: "Biocybernetics and Biomedical Engineering – Current Trends and Challenges. Proceedings of the 22nd Polish Conference on Biocybernetics and Biomedical Engineering, Warsaw, Poland, May 19-21, 2021."

Identification of amyloid proteins and their interactions – bioinformatics versus experiment

Małgorzata Kotulska[1], Michał Burdukiewicz[2], Witold Dyrka[1], Marlena Gąsior-Głogowska[1], Katarzyna Hubicka[1], Monika Szefczyk[3], Natalia Szulc[1], Jakub W.Wojciechowski[1]

[1] Department of Biomedical Engineering, Faculty of Fundamental Problems of Technology, Wroclaw University of Science and Technology, Wybrzeże Wyspiańskiego 27, 50-370 Wrocław, Poland;
[2] Clinical Research Centre, Medical University of Białystok, Jana Kilińskiego 1, 15-089 Białystok, Poland
[3] Department of Bioorganic Chemistry, Faculty of Chemistry, Wroclaw University of Science and Technology, Wybrzeże Wyspiańskiego 27, 50-370 Wrocław, Poland;
malgorzata.kotulska@pwr.edu.pl

A wide range of diseases, e.g. Alzheimer's or Parkinson's, are related to amyloid aggregation of proteins. Amyloid proteins form fibrils with regular aggregated cross-beta structures, which is preceded by occurrence of preamyloid oligomers – the most cytotoxic species. Another class of amyloids includes functional amyloids, involved in physiological processes in many organisms. The nature of these proteins is still little understood. Discovering cross-interactions between functional and pathological amyloids is of great interest. Our research on amyloids aims at facilitating recognition of amyloid propensity and interactivity of a protein, mostly with the support of bioinformatics methods. To obtain this objective, an appropriate representation of instances in the reference datasets is needed, effectively supporting development of accurate modeling methods. Unfortunately, databases of amyloids are not sufficiently representative, including too few instances, combining non-compatible sources of data, and neglecting effects of different experimental conditions on amyloid classification. Optimal and correct data representation in databases may propagate to more effective classification methods using machine learning. So far, we have developed a few such methods, including FISH Amyloid, AmyloGram, and PATH. The predictors are based on different premises, using a variety of classical or our original classification methods. They were trained on data collected in databases gathering peptides from a variety of sources, mostly hexapeptides, which are best available. Obtained accuracies and area under ROC curve values are very high, however their sensitivities are still not satisfactory enough. Other available methods have not surpassed those obtained in our studies. One of the reasons could be unsatisfactory training data, either due to their structure or redundancy profile, or misannotation.

In this study, the bioinformatics tools were applied as prefiltering methods to test the consistency of databases, from which training data are obtained, especially with regard to these instances for which predictors contradicted database annotations. Subsequently, the instances selected automatically by the predictors were tested experimentally. For this task we used vibrational spectroscopy methods, Thioflavin T staining, and high-resolution microscopy methods – transmission electron microscopy (TEM) or atomic force microscopy (AFM). The results confirmed misannotations in databases. We observed that these errors may have been partly related to incompatible experimental conditions in different data sources. Therefore, we extended our studies to better characterize the effects of experimental conditions on amyloid aggregation, such as different experimental methodologies and related them to bioinformatics predictors. The studies also included functional amyloid peptides, scarcely represented in experimental amyloid databases. We observed several important factors affecting aggregation characteristics of peptides.

In conclusion, we observed that a source of limited effectiveness of the computational predictors of amyloid propensity could be attributed to insufficiently accurate and representative datasets, which underlie newly developed methods [1]. Reference databases need knowledgeable selection of instances, stratification, and well-defined experimental conditions related to final data annotations. More rigorous data representation may help in discovering the aggregation ***mechanisms*** and build better computational methods, including functional amyloids and cross-talk between amyloids.

Acknowledgements: This project is supported by the National Science Centre, Poland, Grant 2019/35/B/NZ2/03997.

Reference:

[1] Szulc N., Burdukiewicz M., Gąsior-Głogowska M., et al. Bioinformatics methods for identification of amyloidogenic peptides show robustness to misannotated training data, *Scientific Reports*, 2021, 11(1):8934.

The stochastic mathematical model predicts angio-therapy could delay the emergence of metastases in lung cancer

Emilia Kozłowska and Andrzej Świerniak
Department of Systems Biology and Engineering, Silesian University of Technology
emilia.kozlowska@polsl.pl
andrzej.swierniak@polsl.pl

Abstract. Lung cancer is the most common type of cancer across the world. There are known two main types of lung cancer non-small cell lung (NSCLC) and small cell one (SCLC). Here, we focus on NSCLC that is known to dissem-inate to distant organs such as the brain or bones. What is more, the death of a patient with this type of cancer is caused usually by metastases. It justifies tack-ling the problem of the emergence of metastases in NSLC in this paper. Here, we investigated which mathematical parameters affect the emergence of metas-tases using the mathematical oncology approach. We developed a mathematical model of lung cancer growth and metastasis dissemination by taking into ac-count stochasticity in the process. We incorporated into the model two paths of metastasis dissemination through lymphatic and blood vessels. We performed a global sensitivity analysis to identify parameters that affect the model output (metastasis-free survival) the most. We discover that four model parameters have dominating effect on the output and two of them are controllable - the growth rate of primary tumor cells (through the administration of chemothera-peutic agents) and carrying capacity (through the administration of angio-therapy). In conclusion, a mathematical oncology approach could be applied to investigate which treatment modalities in cancer could delay the emergence of metastases.

Keywords: Stochastic differential equations, Lung cancer, Metastases, Angio-therapy. 2

Numerical simulations of air flow and particle deposition in the model human airways during independent lung ventilation

Katarzyna Kramek-Romanowska[1], Agata Dorosz[2], Anna Stecka[1], Piotr Okrzeja[1,3]
[1]Nalecz Institute of Biocybernetics and Biomedical Engineering PAS, Ks. Trojdena 4, 02-109 Warsaw
[2]Faculty of Chemical and Process Engineering WUT, Waryńskiego 1, 00-645 Warsaw
[3]Research Department, CBS Okrzeja, Janówek 11, 07-111 Wierzbno
kkramek@ibib.waw.pl

Aims. Independent lung ventilation (ILV) is a rescue strategy for patients with severe unilateral lung pathology, e.g. lung injury due to unilateral pneumonia, pulmonary hemorrhage or contusion [1]. Computational predictions of the actual flow distribution, aerosol transport and deposition in the in model human respiratory tract can assist in evaluating the effectiveness of pulmonary drug delivery during ILV in clinical conditions. Thus, as there is hardly any work on understanding the role of ILV on pulmonary fluid flow with use of computational fluid dynamics (CFD), this study focuses on this topic.

Methods. ANYSYS Kampus 19.1 Licence was applied for the geometry preparation and further numerical operations. The computational domain consisted of the right side of trachea and two consecutive bronchial bifurcations (computer model obtained from RDD Online, USA) with implemented left side double-lumen endotracheal tube – ETT (Bronchopart, Rusch) fitting the tracheobronchial tree. The unstructured, fully tetrahedral computational mesh was refined to properly resolve the boundary layer. Wall distance was calculated for the maximum value of volumetric flow rate at the inlet of the fluid domain, equal to 10.17 L/min (based on own experimental results). Mesh density was locally increased in the following regions: (1) near the bifurcation points (two carinas); (2) in the regions below the upper cuff and above the lower cuff of the ETT – in the peripheral ridges; (3) near the outlet of the ETT.

Results. In the picture below (a), there is presented the air velocity profile obtained in the analyzed computational domain during inhalation phase (steady air flow assumed). Thanks to properly established inlet and outlet boundary conditions, no back flows at both outlets were observed (b – upper outlet, c – lower outlet), which is an important achievement [2]. Regarding flow features, a considerable jet caused by the ETT was observed as well as the impingement at the carina ridge (black arrow in picture a).

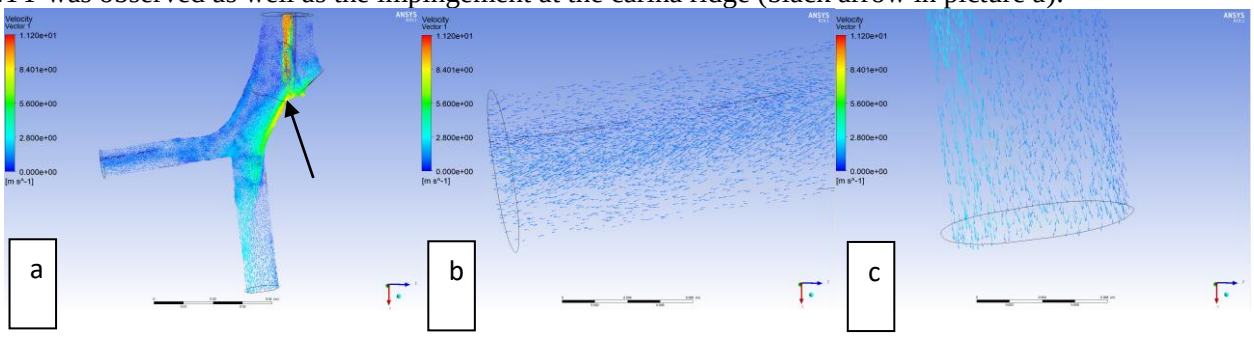

Conclusion. Obtained results indicate the regions of enhanced particle deposition in the bronchial tree during ILV accompanied by inhalation. The ETT jet enhances the particle deposition, especially at the jet impingement sites [2] and also imposes a high risk of lung injury as high wall shear stress appears in these places. This is of important clinical significance while conducting ILV with inhalations. Summarizing, CFD is a powerful tool to understand the role of mechanical lung ventilation on pulmonary fluid dynamics and also give invaluable information considering the deposition of inhalable drugs during ILV, that cannot be obtained solely with the use of experimental techniques.

Work supported by NCBR project no. LIDER/19/0107/L-8/16/NCBR/2017.

References:

[1] Berg S., Bittner E.A., Berra I., Kacmarek R.M., Sonny A. Independent lung ventilation: Implementation strategies and review of literature. *World J Crit Care Med* 8(4), 2019, pp. 49-58.
[2] Van Rhein T., Alzahrany M., Banerjee A., Salzman G. Fluid flow and particle transport in mechanically ventilated airways. Part I. Fluid flow structures. *Med Biol Comput* 54, 2016, pp. 1085-1096.

Dynamic *vs.* static cell culture PLGA microspheres for "bottom-up" tissue engineering

Małgorzata Krok-Borkowicz, Bartosz Mielan1, Elżbieta Pamuła
AGH University of Science and Technology, Faculty of Materials Science and Ceramics,
Department of Biomaterials and Composites, al. Mickiewicza 30, 30-059 Kraków, Poland
krok@agh.edu.pl

"Bottom-up" tissue engineering is different than standard, classical tissue engineering, which is based on large porous scaffolds to form tissue constructs [1]. Classical tissue engineering has many limitations for example low cell density and their non-uniform distribution, limited diffusion of nutrients and impeded new tissue vascularization. In the case of "bottom-up" tissue engineering large scaffolds corresponding to the size of the lesion are replaced by many small modules made of biomaterial-cell constructs [2]. It is believed that "bottom-up" tissue engineering has the potential to reduce the shortcomings of the traditional approach because it ensures more natural conditions for tissue growth that mimic the phenomena occurring in nature, e.g. healing and self-regeneration of tissues. The main aim of this study was (I) to develop a new class of biomaterials – microcarriers for cell culture, made of resorbable polymer poly(L-lactide-*co*-glycolide) (PLGA) in the form of microspheres (MS) and (II) to compare the effect of cell culture conditions (static *vs.* dynamic) on cell morphology and proliferation.

MS were manufactured by oil-in-water emulsification where as an oil phase we used 2% PLGA in dichloromethane and as a water phase 1% polyvinyl alcohol (PVA) aqueous solution. 1 mL of PLGA was dropped into 50 mL PVA and leaved on magnetic stirrer (1000 rpm, 24 h). Diameter of MS was measured by optical microscopy. MG-63 osteoblast-like cells were cultured on MS placed in antiadhesive cell culture plates in static and dynamic conditions, i.e. on the rocker stirrer. Live-dead and Alamar Blue test were performed to assess cell viability and proliferation on days 1, 3 and 7 according to a method described previously [3].

Size distribution of MS was found normal with average diameter of 134.0±19.5 μm (Fig. 1a). Biological evaluation show that cell culture condition have a significant impact for cell proliferation and morphology. In dynamic condition cells were growing on the MS and around them and their number was much higher than in static conditions (Fig. 1b). Cell proliferation was also higher in dynamic than in static conditions as shown by Alamar Blue test (Fig. 1c). We have confidence that produced MS will fulfil the role and objectives of the modular cell carrier in "bottom-up" tissue engineering.

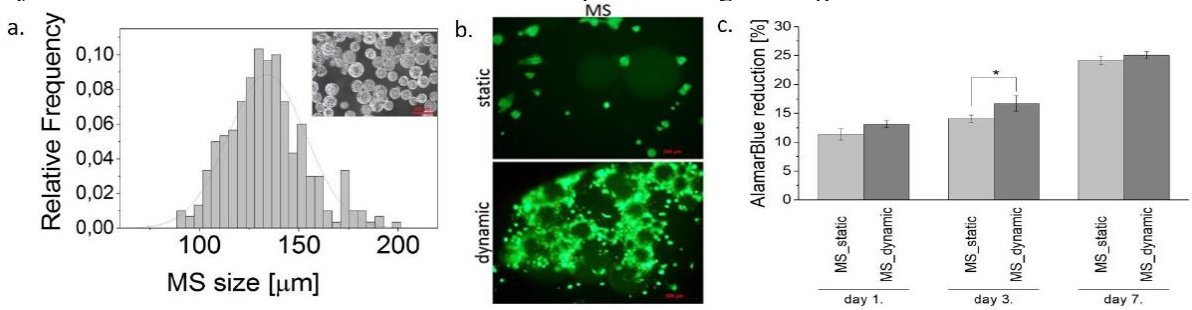

FIG 1 Diameter distribution PLGA MS (n=300) and MS appearance observed under optical microscope (insert) (a.); MG-63 osteoblast-like cell morphology on day 3 of culture in static and dynamic conditions (live/dead staining – all cells are stained green thus alive) (b.); cell proliferation assessed by Alamar Blue test (one-way-ANOVA with post-hoc LSD Fisher, p*<0.05) (c.)

Acknowledgements

This study was supported by the National Science Centre Poland (No 2016/21/D/ST8/01685) and by the Program "Excellence Initiative – Research University" for the AGH University of Science and Technology.

References

[1] R. Langer, J. Vacanti, Tissue engineering, Science 260 (1993) 920-926.

[2] J. W. Nichol A. Khademhosseini, Modular Tissue Engineering: Engineering Biological Tissues from the Bottom Up, Soft Matter 5 (2009) 1312-1319.

[3] U. Cibor, M. Krok-Borkowicz, M. Brzychczy-Włoch, Ł. Rumian, K. Pietryga, D, Kulig, W. Chrzanowski, E. Pamuła, Pharm Res 34 (2017) 2075-2083.

Analysis and comparison of heart rate variability signals derived from PPG and ECG sensors

Aleksandra Królak, Edyta Pilecka
Lodz University of Technology, Institute of Electronics,
Wólczańska 211/215, 93-005, Łódź, Poland
aleksandra.krolak@p.lodz.pl

One of the methods of diagnosis and prevention of cardiovascular diseases is monitoring and analysis of heart rate variability (HRV). However, in order to accurately detect the RR intervals, the ECG signal must be acquired. The advances in optical sensors made photoplethysmography (PPG) to be considered as an alternative for heartbeat interval measurements as it is more convenient. The aim of this study is to compare the HRV signals calculated from ECG and PPG measurements based on the data from two Physionet datasets and assess the reliability and accuracy of time-domain, frequency-domain and nonlinear HRV parameters derived from the ECG and PPG signals. The results achieved suggest that the PRV can be used as an alternative for HRV analysis in static measurements, with significant correlation coefficient values above 98% for nonlinear, time and frequency features. In the dynamic measurements, performed during sports activities, especially non-linear and frequency-domain parameters derived from PPG signals should be used with caution, as in some cases the correlation was inverse.

Keywords: ECG, PPG, HRV, PRV, HRV parameters.

Paper will be available as a full article in the conference proceedings within the "Advances in Intelligent Systems and Computing" series; the book title: "Biocybernetics and Biomedical Engineering – Current Trends and Challenges. Proceedings of the 22nd Polish Conference on Biocybernetics and Biomedical Engineering, Warsaw, Poland, May 19-21, 2021."

Manufacturing of poly(ester-anhydride) microparticles as drug delivery systems for pulmonary administration

Konrad Kwiecień[1], Katarzyna Reczyńska[1], Katarzyna Bąk[1], Daria Niewolik[2], Katarzyna Jaszcz[2], Elżbieta Pamuła[1]
[1]AGH University of Science and Technology, Al. A. Mickiewicza 30 30-059 Kraków, Poland
[2]Silesian University of Technology, Ul. Akademicka 2A, 44-100 Gliwice, Poland
kkwiecien@agh.edu.pl

Conventional therapy methods of pulmonary infections – oral or intravenous administration of antibiotics – are not always effective due to limited drug delivery to the lower respiratory tract. Moreover, such treatment requires high doses of drugs that may cause side effects and the development of resistance to antibiotics. One of the possible ways to solve these problems is to use biodegradable microparticles with a short degradation time as inhaled antibiotic delivery systems [1]. Poly(ester-anhydride)s (PEA)s are considered materials for such purposes thanks to their controllable degradation kinetics. This work aimed to optimize manufacturing parameters of PEA microparticles, so most of them have a diameter in the range of 1-5 μm, i.e. the optimal size for pulmonary administration via inhalation [2]. The second goal was to evaluate the encapsulation efficacy of gentamycin (Gent), i.e. the antibiotic used in the treatment of pulmonary infections.

PEA was obtained by co-polymerization of oligo(3-allyloxy-1,2-propylene succinate) (OSAGE) and poly(sebacic acid)(PSA) at a weight ratio of 40:60, according to a method described earlier [3]. Microparticles (MP) were manufactured using oil-in-water emulsification with poly(vinyl alcohol) (PVA) water solution (concentration of 50, 60, 70, or 80 mg/ml) as water phase and dichloromethane (DCM) solution of PEA (concentration of 20, 25, or 30 mg/ml) supplemented with Gent suspension as oil phase. To prepare the oil phase Gent (2, 4, or 6 mg/ml) was added to PEA solution in DCM and homogenized by ultrasounds for 1.5 or 3 min. MP were obtained by adding oil phase to the water phase and evaporation of the organic solvent under constant stirring (1500, 2000, or 2500 rpm) for 1, 2, 3, 4.5, 6 h. Then, MP were washed to get rid of surfactant residues, and freeze-dried. MP were observed using both optical and scanning electron microscopes (SEM) to assess their microstructure, size, and size distribution. Gent encapsulation efficacy in MP was evaluated by o-phthaldehyde (OPA) assay.

Several batches of MP were obtained at manufacturing conditions differing in: 1) concentration of PEA and Gent in oil phase; 2) concentration of PVA in water phase; 3) steering speed of water phase and 4) evaporation time of DCM. MP produced at the following conditions: 20 mg/ml PEA, 80 mg/ml PVA, 1500 rpm, and 4.5 h evaporation time were round and of regular shape. However, at higher magnification their surface appeared rough. For optimal manufacturing parameters, the batch contained over 90% of MP within the range of 1-5 μm (n=1800). Encapsulation effectiveness of gentamycin was 25.6 ± 0.9% (average ± SD, n = 3) and drug loading was 12.2 ± 0.4% (average ± SD, n = 3) of MP mass. Based on these data we will design dry powder formulations which assure concentration of gentamycin in the septum higher than MIC (minimally inhibition dose) of strains responsible for pulmonary infections. [4]

The results of this work show a great potential of investigated PEA in the treatment of pulmonary bacterial infections. The size of the MP can be controlled by changing parameters of the process such as polymer/gentamycin/PVA concentration or stirring speed of the water phase. It is also possible to encapsulate antibiotics inside the MP with acceptable efficiency to assure clinically relevant doses of Gent. Further studies will also focus on evaluating drug release kinetics as well as assessment of antimicrobial properties and biocompatibility of the system with lung endothelial cells.

References:

[1] Traini D. and Young P. M. Delivery of antibiotics to the respiratory tract: an update, 2009, *Expert Opin. Drug Deliv.*, vol. 6, no. 9, pp. 897–905.
[2] Paranjpe M. and Müller-Goymann C. C. Nanoparticle-Mediated Pulmonary Drug Delivery: A Review, *Int. J. Mol. Sci.*, 2014, vol. 15, no. 4, Art. no. 4.
[3] Jaszcz K. Synthesis and Characterization of New Functional Poly(ester-anhydride)s Based on Succinic and Sebacic Acids, 2007, *Macromol. Symp.*, vol. 254, no. 1, pp. 109–116.
[4] Twiss J., Byrnes C., Johnson R., and Holland D. Nebulised gentamicin—suitable for childhood bronchiectasis, 2005, *Int. J. Pharm.*, vol. 295, no. 1–2, pp. 113–119.

This study was supported by National Science Centre (project No 2019/35/B/ST5/01103) and by the Program "Excellence Initiative – Research University" for the AGH University of Science and Technology.

Modeling acid-base balance for in-series extracorporeal carbon dioxide removal and continuous venovenous hemofiltration devices

John K. Leypoldt,[1] Jörg Kurz,[2] Jorge Echeverri,[3] Markus Storr,[4] Mauro Pietribiasi,[1] Kai Harenski[2]
[1]Nalecz Institute of Biocybernetics and Biomedical Engineering Polish Academy of Sciences, Ks. Trojdena 4 st., 02-109 Warsaw, Poland
[2]Baxter, Baxter Deutschland GmbH, Unterschleissheim, Germany
[3]Baxter Healthcare Corporation, Deerfield, Illinois, USA
[4]Baxter International, Research and Development, Hechingen, Germany
kenleypoldt@gmail.com

Aims: Critically ill acute kidney injury (AKI) patients may require treatment by extracorporeal carbon dioxide removal ($ECCO_2R$) devices to allow protective or ultraprotective mechanical ventilation and avoid hypercapnic acidosis. Continuous venovenous hemofiltration (CVVH) and $ECCO_2R$ devices can be arranged in series to form a single extracorporeal circuit; such a circuit has been proposed to be optimal, based carbon dioxide removal efficacy, if the $ECCO_2R$ device is placed proximal to the CVVH device [1].

Methods: We developed a mathematical model of whole-body, acid-base balance during extracorporeal therapy using in-series $ECCO_2R$ and CVVH devices for treatment of mechanically ventilated AKI patients. Acid-base chemistry in blood was assumed as described previously [2], an approach that has been prospectively validated using laboratory data [3]. Published clinical data [1] of mechanically ventilated (6 mL/kg predicted body weight or PBW) AKI patients treated by CVVH without $ECCO_2R$ were used to adjust model parameters to fit plasma levels of arterial partial pressure of carbon dioxide ($PaCO_2$) and arterial plasma bicarbonate concentration ($[HCO_3]$). The effects of applying $ECCO_2R$ at an unchanged tidal volume and a reduced tidal volume (4 mL/kg PBW) on $PaCO_2$ and $[HCO_3]$ were then simulated assuming carbon dioxide removal rates from the $ECCO_2R$ device measured in the clinical study (91 mL of CO_2/min when $ECCO_2R$ was proximal and 72 mL of CO_2/min when CVVH was proximal).
Results: Agreement of model predictions with the clinical data was good, and model predictions were relatively independent of the in-series position of the devices (see Table below). Total carbon dioxide removal from the CVVH device via ultrafiltration predicted by the model was lower after applying $ECCO_2R$ at both the unchanged tidal volume (25 mL of CO_2/min when $ECCO_2R$ was proximal and 39 mL of CO_2/min when CVVH was proximal) and the reduced tidal volume (30 mL of CO_2/min when $ECCO_2R$ was proximal and 44 mL of CO_2/min when CVVH was proximal). The reduced removal of total carbon dioxide via ultrafiltration when $ECCO_2R$ was proximal resulted from the lower total carbon dioxide concentration in blood entering the CVVH device. Thus, independent of the in-series position of the devices, the magnitude of this difference in total carbon dioxide removal by the CVVH device (14 mL of CO_2/min) approximately cancels out the relative greater efficacy of the $ECCO_2R$ device (19 mL of CO_2/min).

Table: Measured and Model Predicted Values of $PaCO_2$ and $[HCO_3]$

	$PaCO_2$ (mmHg)/$[HCO_3]$ (mEq/L)		
Tidal Volume	6 mL/kg PBW	6 mL/kg PBW	4 mL/kg PBW
	Without $ECCO_2R$	With $ECCO_2R$	With $ECCO_2R$
Clinical Data [1]	47/22	37/22	48/23
Model ($ECCO_2R$ Proximal)	47/22	34/20	49/23
Model (CVVH Proximal)	47/22	35/20	51/23

Conclusion: The described mathematical model has quantitative accuracy. These results suggest that overall acid-base balance when using $ECCO_2R$ and CVVH devices in a single, combined extracorporeal circuit will be similar, independent of their in-series position.
References:
[1] Allardet-Servent et al, *Crit Care Med* 43:2570-2581, 2015
[2] Rees and Andreassen, *Crit Rev Biomed Eng* 33:209-264, 2005
[3] Rees et al, *Eur J Appl Physiol* 108:483-494, 2010

Various approaches to modify Ti13Nb13Zr alloy surfaces for improving biocompatibility

Julia Lisoń, Anna Taratuta, Magdalena Antonowicz, Zbigniew Paszenda, Marcin Basiaga
Silesian University of Technology, Faculty of Biomedical Engineering
Department of Biomaterials and Medical Devices Engineering
ul. Roosevelta 40, 41-800 Zabrze
julia.lison@polsl.pl

The presence of biofilm can lead to decline in the surrounding bone tissue which can result in disturbing the osteointegration process. Nowadays combating of bacterial infection is done by antibiotherapy, however, because of numerous problems regarding medicine application and effective activity, new methods of application are still sought. Unfortunately, both in case of implant instability and long-term bacterial infection there is often a need of reoperation or implant replacement [1,2]. This in turn often leads to extended costs and more importantly discomfort for the patient linked to a long-term hospitalization. In order to limit this unfavorable process molding of physicochemical properties of implants surface was proposed. Today many different methods of application techniques of biomaterials modification they are employed [3]. However, until now fully acceptable effects were not achieved in this field of science. Multiple publications in global literature, mainly in medical magazines confirm this action. Unfortunately, presented in them are piecemeal of research results which do not allow for usefulness assessment of created layers in full.

The aim of this examination was assessment of impact of physicochemical and mechanical properties of modified Ti13Nb13Zr alloy. The specimens were then divided into three groups of 4 specimens each, according to the preparation of the surface as follows: vibration treatment, polishing and sandblasting. The use of various surface treatment methods were resulted in obtaining various roughness values. Subsequently, ZnO layer was applied to these samples by Atomic Layer Deposition ALD. Diethyl zinc was used as the zinc oxide precursor, which reacted with deionized water, allowing the deposition of thin films. The application process was carried out for a different temperature and number of cycles.
In order to assess to suitability of the surface modification method proposed in this way, the authors proposed a series of tests. In the first stage, pitting corrosion resistance tests using the potentiodynamic, potentionstatic methods and tests using electrochemical impedance spectroscopy were carried out. These tests provided information concerning the structural characteristics of the layers, possible defects, lack of sealing, substrate reactivity and the presence of barrier properties involving the electrolyte. In the paper, surface roughness, wettability, coating adhesion to the substrate were also complemented. The obtained data showed different physicochemical properties of antibacterial films generated under different parameters (temperature and number of cycle) in ALD process. These results directly assist the optimisation of the ZnO layer creation process using ALD-based methods on surfaces of Ti13Nb13Zr alloy implants intended for skeletal system, thus improving their functional properties. Obtained results may form the basis for the development of more detailed criteria for the assessment of the final quality of medical devices used in the skeletal system and comparison between different variants, which will ensure the required biocompatibility of implants and contribute to minimizing the risk of postoperative complications.

The results have obtained can be used as a base to develop more detailed criteria of final quality of medical devices which will ensure the required biocompatibility of implants. It has contributed the risk mineralization of postoperative complications. As a result it has increased effectiveness, decreased the indicator of complications and improved life of the patients.

Acknowledgements
The project was funded by the National Science Centre, Poland allocated on the basis of the decision No. 2018/29/B/ST8/02314.

References:

[1] Khatoon Z, McTiernan CD, Suuronen EJ, Mah TF, Alarcon EI. Bacterial biofilm formation on implantable devices and approaches to its treatment and prevention, *Heliyon*, vol. 4, no. 12.
[2] Ribeiro M, Monteiro FJ, Ferraz MP. Infection of orthopedic implants with emphasis on bacterial adhesion process and techniques used in studying bacterial-material interactions. *Biomatte*r vol. 2, no. 4, pp. 176-194.
[3] Qiu ZY, Chen C, Wang XM, Lee IS. Advances in the surface modification techniques of bone-related implants for last 10 years, *Regen Biomater,* vol. 1, no. 1, pp. 67–79.

Mechanical properties of New Zealand White Rabbit urethra tissue under urinal fluid flow

Agnieszka Mackiewicz[1], Tomasz Klekiel[1], Jagoda Kurowiak[1], Tomasz Piasecki[2], Romuald Będziński[1]

[1] Department of Biomedical Engineering, Institute of Material and Biomedical Engineering, University of Zielona Gora, Licealna 9 Street, 65-417 Zielona Gora, Poland
[2] Department of Epizootiology and Clinic of Birds and Exotic Animals, Faculty of Veterinary Medicine, Wroclaw University of Environmental and Life Sciences, C. K. Norwida 25 Street, 50-375 Wroclaw, Poland
a.mackiewicz@iimb.uz.zgora.pl

The urethra is a single organ comprising the mucosa, the muscularis and the adventitious membrane. Due to the anatomical structure, the urethra consists of two parts—pelvic (close to the bladder) and penile (close to the external orifice) [1]. Urethral stenosis is an important problem affecting mainly the male organ. In developed countries, the most common cause of urethral stenosis is idiopathic or iatrogenic origin (inappropriate endoscopic manipulation). To date, no optimal treatment has been developed for this condition. The most effective method seems to be to introduce stents as elements restoring proper flow. Rigid metal stents are most often introduced, which can cause secondary fibrosis in adjacent areas. The use of new materials with characteristics similar to those of the urethra requires knowledge of its mechanical properties and the influence of boundary conditions such as urine flow [2]. Therefore, the aim of the study was to determine the deformability of the urethra and urine flow parameters such as pressure and velocity, which occur during the urination process.

The object of research was the urethra of the New Zealand White Rabbit (male). The most common material tests are carried out using flat or tubular specimens stretched in special grips by testing machines or by cutting out the whole urethra and introducing fluid into it. It should be noted that in both cases, the results obtained may be inadequate to the reality, as the effect of the muscles and internal organs located near the urethra is ignored. The authors obtained approved by the Local Ethics Committee in Wroclaw performed a rabbit urethra deformability test using fluoroscopy. During the test, a 0-80ml saline solution was introduced into the urethra using a syringe (the amount of urine corresponding to a rabbit's bladder filling). A measuring system has been prepared for testing the deformability of the urethra under conditions of urine pressure load, allowing the internal pressure and urine flow velocity to be measured. Based on the graphic conversion of photographs and films from fluoroscopy, the maximum deformation of the urethra during flow was determined.

The test determined the level of urethra deformation, internal pressure and urine flow velocity in the urination process, which was about 110 ml/sec. Geometric measurements were made using a graphical method. The change of urethral diameter and internal pressure are presented in Table 1.

Table 2. Measurement of the change in the lumen diameter of the urethra filled with saline and internal pressure.

Volume of fluid [ml]	Diameter of the urethra [mm]	Pressure inside urethra [kPa]
20	4.19	1.5
40	6.41	1.5
60	7.54	1.5
80	10.66	1.5

The presented studies allowed to determine the behavior of the urethra under the conditions of urinary filling. Mean pressure in the system, which could be assumed to occur under normal operating conditions, was determined. The fluid-filled bladder and urethra made its dimensions increase significantly. Such large changes require that the stents used for the treatment of urethral stenosis should not have a fixed diameter but should adapt to changing urethral dimensions. The research presented in this paper allows us to gain knowledge about the mechanical conditions inside the urethra, which allows us to better understand how an implant should function.

References:

[1] Skonieczna J., et al. Accessory Genital Glands in the New Zealand White Rabbit: A Morphometrical and Histological Study. J.Vet. Res. 2019; 63: 251–257.

[2] Kurowiak J., et al. Analysis of the Degradation Process of Alginate-Based Hydrogels in Artificial Urine for Use as a Bioresorbable Material in the Treatment of Urethral Injuries. Processes 2019; 8(3): 304.

The demands for designing the patient-specific, anti-microbial bioactive finger implants for durable functional reconstruction after amputation

Roman Major[1], Adam Byrski[1], Maciej Gawlikowski[2], Katarzyna Kasperkiewicz[3], Marcin Dyner[4], Juergen M. Lackner5, Boguslaw Major[1]
[1] Institute of Metallurgy and Materials Science, Polish Academy of Sciences, Cracow, Poland
[2] Silesian University of Technology, Faculty of Biomedical Engineering, Department of Biosensors and Processing of Biomedical Signals, Roosevelt Str. 40, Zabrze, Poland.
[3] University of Silesia in Katowice, Faculty of Natural Sciences, Institute of Biology, Biotechnology and Environmental Protection, Jagiellońska St. 28, 40-032 Katowice, Poland;
[4] Faculty of Science and Technology, Jan Dlugosz University in Czestochowa, Armii Krajowej Av, 13/15, 42-200 Czestochowa, Poland,
[5] JOANNEUM RESEARCH Forschungsges.m.b.H., Institute of Surface Technologies and Photonics, Functional Surfaces, Leobner Strasse 94, 8712 Niklasdorf, Austria
r.major@imim.pl

Finger amputation is surgical treatment for ~69.000 patients in EU after traumatic injury, in which replantation microsurgery fails due to severity of tissue damage [1-5]. However, absence of even a single finger results in major impairment in hand function (precise grasping, grip power) and affects the completely social and professional life of the frequently young victims. Surgical reconstruction is currently only possible by autograft transplantation, e.g. toe-to-hand transfer, leading to impairment at the foot site. Some motion functional restoration is possible by bone-anchored silicone prosthesis, but without sensations available.

Reasonable, our current research focuses on alternatives for surgical reconstruction by novel patient-specific, durable, biomimetic, bioactive and antibacterial implants for reconstruction of lost bone and joints. The implant design – and the beyond the project improved micro(neuro)surgery – will include soft-tissue related mobility, implantation of state-of-the-art nerve conduits and aesthetic appearance for fast, successful rehabilitation.

Key issues for long-term functionality of biomaterial-based reconstruction of hard tissue are based on surgical demands: (1) Perfect integration of bone substituting metal to the surrounding bone tissue (a) without loosening due to stress shielding at the interface and (b) with protection against bacterial inflammation (antimicrobial properties and formation of vascularized bone tissue (ossification)) even months to years after the injury. (2) biomimetic finger joints based on nonwearing materials without ossification tendency to prevent loss of motion function.

Acknowlegement
This research was financially supported by the Polish National Centre of Research and Development (Grant no. fingerIMPLANT M-ERA.NET2/2019/7/2020, “Patient-specific, anti-microbial bioactive finger implants for durable functional reconstruction after amputation”).

References:
[1] J.P. Leigh, S.B. Markovitz, M. Fahs, C. Shin, P.J. Lnadrigan, Occupational Injury and Illness in the United States, Arch. Intern. Med. 157 (1997) 1557.
[2] K.C. Chung, M.J. Shauver, Table Saw Injuries, Plast. Reconstr. Surg. 132 (2013) 777e-783e.
[3] E. Davis Sears, K.C. Chung, Replantation of Finger Avulsion Injuries: A Systematic Review of Survival and Functional Outcomes, J. Hand Surg. Am. 36 (2011) 686–694.
[4] E. Mahmoudi, P.R. Swiatek, K.C. Chung, J.Z. Ayanian, Racial Variation in Treatment of Traumatic Finger/Thumb Amputation, Plast. Reconstr. Surg. 137 (2016) 576e-585e.
[5] J.M. Conn, J.L. Annest, G.W. Ryan, D.S. Budnitz, Non–Work-Related Finger Amputations in the United States, 2001-2002, Ann. Emerg. Med. 45 (2005) 630–635.

Liposomal carrier as a phospholipid depot for tear film lipid layer supplementation in patients with evaporative Dry Eye Syndrome

Krzysztof Makuch[1,2], Jolanta Zegarlińska[2,3], Aleksander Czogalla[2,3], Tomasz Borowik[2], Magdalena Przybyło[2,4], Marek Langner[2,4]

[1] Department of Computational Biophysics and Bioinformatics, Faculty of Biochemistry, Biophysics and Biotechnology, Jagiellonian University, 30-387 Kraków, Poland. [2] LipoTech sp. z o. o., Liszki 563, 32-060 Liszki, Poland. [3] Department of Cytobiochemistry, Faculty of Biotechnology, University of Wrocław, 50-383 Wrocław, Poland. [4] Faculty of Biomedical Engineering, Wrocław University of Sciences and Technology, 50-370 Wrocław, Poland.

t.borowik@lipotech.pl

Dry Eye Syndrome (DES) is a multifactorial disorder of preocular tear film leading to ocular surface damage and corresponding ocular discomfort. DES, if untreated, might result in cornea erosion, punctate keratopathy and finally corneal ulcer. The most common DES subtype is known to be due to increased evaporation of tear film aqueous layer from the ocular surface (evaporative DES), accounting for up to 58% off all cases. The first line of treatment for dry eye patients with evaporative DES are so-called artificial tears, used to treat the dryness and irritation associated with tear film deficiency [1]. It is recognized, that local supplementation of tear film lipid layer with lipids, can greatly enhance treatment output when compared with conventional strategies, namely non-liposomal products [2].

In order to design an efficient liposomal carrier for ocular application acting as a phospholipid depot for tear film lipid layer (TFLL) supplementation we have performed a series of MD simulations based on Martini Coarse Grain particle models. The dimensions of the modeled system were 46x46x47 nm simulation time-scale up to 0.5ms. The TFLL was a mixture of polar (POPC, POPE) and neutral (TOG:CHYO) lipids in a ratio of 1:2.2. The liposome carrier was constructed from a mixture of polar lipids. Fusion in the simulated system occurred freely, with no external force forcing the bilayer and TFLL closer together. Along with the modeling we have performed a series of Langmuir-Blodgett experiments to identify the lipid layer tear film components crucial for its stability. Based on the findings pilot liposomal formulations were manufactured in a lab-scale and tested for potential cytotoxicity towards corneal epithelial cells.

We have identified the crucial components engaged in an interaction, enabling lipid transfer from the liposomal carrier to the tear film lipid layer, as shown on the snapshots below. Polar lipids are in green. Non-polar lipids are in yellow and nude. Simulation time starting from the left are 0.2 ns, 12 ns and 15 ns respectively.

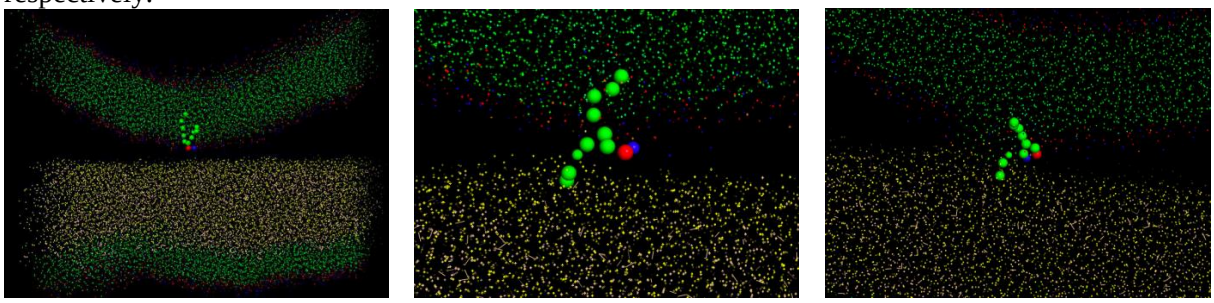

Results obtained in this study indicate, that it is possible to design a liposomal delivery vehicle acting as a phospholipid depot for patients with tear film lipid layer deficiencies suffering from evaporative DES. The predicted performance of liposomal phospholipid depo, potential alteration of water activity by the introduction lipid bilayer interface and the effect of liposome size on the retention time on the eye surface will be used when designing upcoming medical experiment.

[1] Suvarna P. et al. "A Comprehensive Review on Dry Eye Disease: Diagnosis, Medical Management, Recent Developments, and Future Challenges", *Advances in Pharmaceutics*, vol. 2015.

[2] Lee S. et al. Ein neues Therapiekonzept zur Behandlung des Trockenen Auges--die Verwendung von Phospholipid-Liposomen [A new therapy concept for the treatment of dry eye--the usefulness of phospholipid liposomes]. Klin Monbl Augenheilkd. 2004 Oct;221(10):825-36.

Web Application with Semiautomatic Algorithm for Renal Blood Flow Estimation

in Dynamic Scintigraphy

Mateusz Midura, Damian Wanta,
Przemysław Wróblewski, Jacek Kryszyn, Waldemar T. Smolik
Warsaw University of Technology, Institute of Radioelectronics and Multimedia Technology,
Warsaw, Poland
mmidura@ire.pw.edu.pl

The function of the kidneys can be estimated in vivo using diagnostic medical imaging, such as nuclear medicine imaging, computed tomography (CT), and magnetic resonance imaging (MRI). Dynamic scintigraphy using Tc^{99m}-DTPA is considered a silver standard for glomerular filtration rate (GFR) calculation and also a valuable method for estimation of renal blood flow. Both parameters can be calculated from a series of dynamic scintigraphy images using the Peters [3] and Gates [1] method respectively. The modified approach of calculating GFR and renal blood flow presented in [2] was implemented in the NMS system for nuclear medicine imaging, developed at our Institute by P. Brzeski & R. Szabatin years ago. The aim of this work was to make these procedures available in Orthanc - a modern mini-PACS system with a standalone DICOM server and Web-based user interface. Orthanc is an open source system designed to improve the DICOM flowsin hospitals and to support research about the automated analysis of medical images. The application programming interface (API) and a plugin mechanism, that allows to add new modules that extends the core system capabilities, were used in the implementation of the NMwebViewer plug-in for Orthanc. Detailed analysis of regions of interest (ROIs) and time–activity graph functions were added to the system. ROIs have to be defined (manually drawn by the user) on different organs including the left ventricle, descending aorta or right lung. Two J-shaped background regions are automatically drawn under the left and right kidneys.

The output screen with dynamic curves, calculated renal dynamic parameters, flow values and GFR for each kidney is presented in Fig. 1. An assessment of NMwebViewer using NMS software on the same data set representing dynamic renal scintigraphy study, proved the correctness of calculations. Since the manual ROIs drawing is subjective, troublesome and influences the result of the study, further study will be focused on developing methods of automatic region selection.

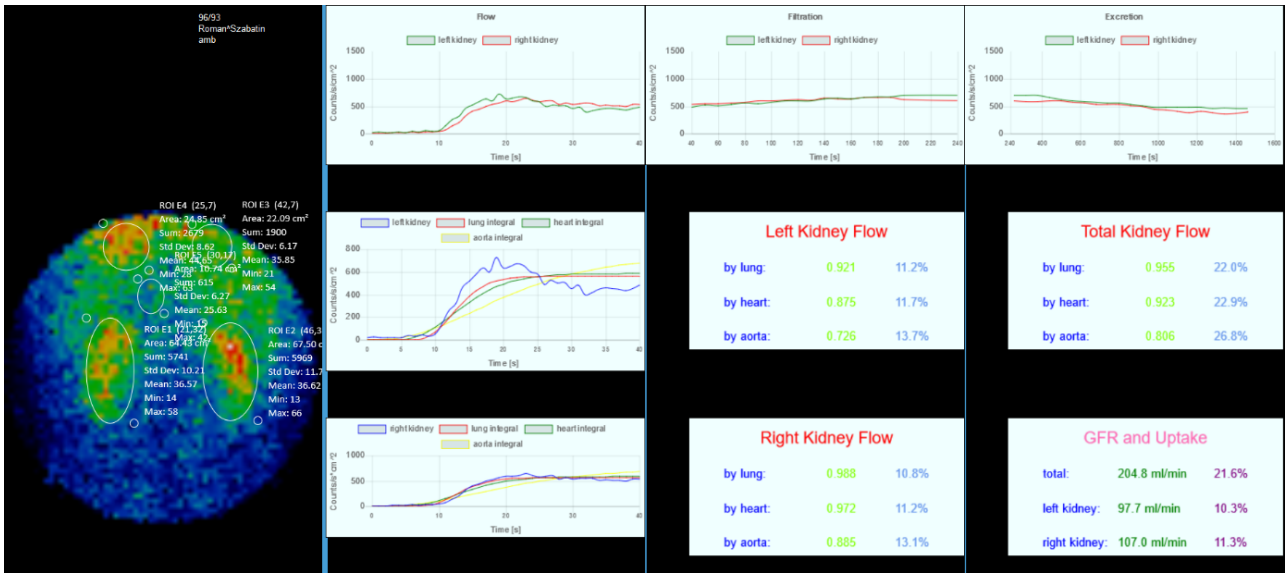

Fig. 1, NMWebViewer results window with calculated renal dynamic curves, flow values and Glomerular Filtration Rate (GFR).

[1] G. F. Gates, "Split Renal Function Testing Using Tc–99m DTPA: A Rapid Technique for Determining Differential Glomerular Filtration," *Clin. Nucl. Med.*, vol. 8, no. 9, 1983.

[2] J. P. Kelleher, P. Brzeski, P. J. Anderson, I. Gordon, and M. E. Snell, "Reproducibility of renal blood flow estimation in the miniature pig using 99Tcm-DTPA: introducing semiautomatic processing," *Nucl. Med. Commun.*, vol. 12, no. 8, 1991.

[3] A. M. Peters *et al.*, "Noninvasive measurement of blood flow and extraction fraction.," *Nucl. Med. Commun.*, vol. 8, no. 10, pp. 823–837, Oct. 1987.

Gait patterns classification in hemiplegia patients based on biclustering algorithm

Katarzyna Minta-Bielecka, Jolanta Pauk
Bialystok University of Technology, Wiejska 45C, 15-351 Bialystok
j.pauk@pb.edu.pl, kasia.minta@gmail.com

1. Aims

Clinical gait analysis is a helpful tool to support clinicians in diagnosing and treating hemiplegia patients' disabilities. Previous approaches to gait patterns classification did not provide adequate evidence of the reliability and validity of the patients' classification results. Therefore, this work aims to provide a new classification algorithm based on gait patterns obtained from kinematics in hemiplegia patients.

2. Methods

The dataset used in this work was derived from a motion tracking system (Motion Analysis Corp., USA) and included the joint angles of 40 hemiplegia patients (156 gait cycles in total), an average age was 56.6±7.2 years. Inclusion criteria for patients were the first-ever stroke, ischemia or intracerebral haemorrhage assessed by computerized tomography or magnetic resonance imaging, ability to walk minimum independently. A new biclustering algorithm called KMB which is based on Cheng and Church algorithms [1-3] was used to classify gait patterns. The different values of parameters α (a threshold describing when the multiple node deletion steps are used) and δ (which controls the target mean square residue score of the resulting biclusters) were tested.

3. Results

The algorithm extracted the largest possible biclusters from the data set **while optimizing the mean square residue score**. For simplicity, we describe only the best classifiers for the datasets: a) hip joint – biclaster 1 (δ=4, α=1.2); b) knee joint – biclaster 2 (δ=4.0, α=1.4); ankle joint – biclaster 3 (δ=2, α=1.2), Fig.1.

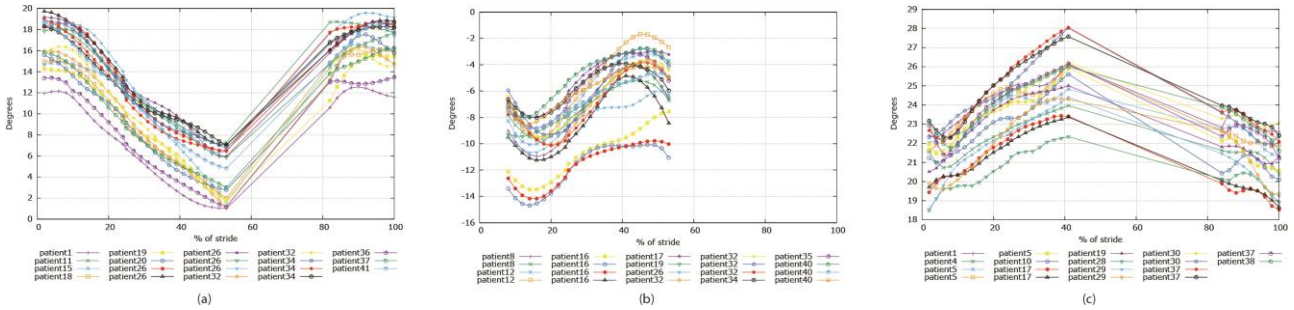

Fig.1. Biclusters discovered by KMB algorithm

Bicluster 1 contains 12 patients and 19 gait cycles; bicluster 2 contains 20 gait cycles derived from 10 patients with hemiplegia; bicluster 3 includes 11 patients and 18 cycles.

4. Conclusion

Biclustering algorithm has been applied to classify groups of stroke patients with similar local kinematic data features. The presented method allows to obtain results of better quality compared to the state of the art. In the future, more complementary analysis of human gait should be support by the sets involving the kinetic and EMG data classification.

References:

[1] Pauk J., Minta-Bielecka K. Gait patterns classification based on cluster and bicluster analysis, *Biocybernetics and Biomedical Engineeri*
ng, vol. 36, pp. 391-396, 2016
[2] Cheng Y., Church, G.M. Biclustering of expression data. In *8th International Conference on Intelligent Systems for Molecular Biology*, San Diego, USA, 2000
[3] Pauk J., Minta-Bielecka K. A new classification of hemiplegia gait patterns based on bicluster analysis of joint moments, *Acta of Bioengineering and Biomechanics*, vol. 18, no. 4, pp. 33–40, 2016.

How to create the electrospun polymeric mats of desired structure for biomedical applications?

Adam Mirek, Paulina Korycka, Katarzyna Kramek-Romanowska, Marcin Grzeczkowicz, Dorota Lewińska
Nalecz Institute of Biocybernetics and Biomedical Engineering Polish Academy of Sciences,
Ks. Trojdena 4 St. 02-109 Warsaw, Poland
amirek@ibib.waw.pl

Polymeric nano- and microfibrous mats obtained in the electrospinning process are being extensively investigated paying special attention to their biomedical applications like drug delivery systems (wound healing, inhalation therapy, cancer therapy) or tissue regeneration and cell cultures [1]. By modifying the electrospinning setup and controlling the properties of the polymer solutions, it is possible to obtain fibers of different structure: porous, smooth, core–shell, with beads etc. allowing their various uses [2]. Although a significant number of studies on the influence of various parameters on the electrospinning process have been carried out so far, the selection of optimal conditions is still a serious challenge. One of the methods that may solve this problem is the concept of factorial design, which enables one to determine the influence of the analyzed factors (process parameters) on the system response (polymeric structure sizes) and the mathematical relationships between them with a minimum number of experiments [3].

In the work, experimental factorial design was carried out to determine the effect of selected electrospinning process parameter values on the diameter of the uniform and heterogeneous (with spheroidal structures) fibers and the size of the spheroidal fragments (beads) which were obtained in this process. The electrospinning process was carried out with poly(vinyl pyrrolidone) ethanolic solutions of different viscosities under various applied electrical voltage and solution flow rate. A full 2^3 factorial design was performed in order to establish the influence of selected factors on the average diameter of fibers and beads that were produced by the electrospinning process. The method and the calculation results were verified – the analysis of variance and the *t*-test were used to determine the significance of the mathematical equation coefficients and the F test was used to test the adequacy of equations.

As a result of the research it was found that the greatest effect on the size of the beaded fibers and beads was observed for the solution viscosity whereas the voltage had the greatest effect on the diameter of the bead-free fiber. The conducted analysis proved that the electrical voltage has the most significant influence on the diameter of fibers without beads, while the dynamic viscosity of the polymer solution has the greatest impact on the diameter of the beaded fibers. On the other hand, the both factors (voltage and viscosity) have the most significant influence on the size of beads. The flow rate of the polymer solution and the correlation between the parameters have no significant effect on the size of the fibers and beads.

This work proved that in order to obtain fibrous mats with desired characteristics features, there is no need to perform many laboratory tests, as the influence of process conditions on the properties of the final material can be determined using presented mathematical methods. Although the number of conducted experiments is small (in the described study it is only sixteen), subjecting their results to factorial design leads to a complete picture of the influence of the process parameter values on the electrospinning process. The proposed method can be used as a tool to optimize the electrospinning process by determining the process factors of the highest statistical significance in the regression equations and selecting their values that will allow to obtain electrospun mats with the specific, desired structure.

References:

[1] Greiner A., Wendorff J. H., Electrospinning: a fascinating method for the preparation of ultrathin fibers, *Angewandte Chemie*, 2007, vol. 46, no. 30, pp. 5670–5703.
[2] Li D., Xia Y., Electrospinning of nanofibers: reinventing the wheel?, *Advanced Materials*, 2004, vol. 16, no. 14, pp. 1151–1170.
[3] Korycka P., Mirek A., Kramek-Romanowska K., Grzeczkowicz M., Lewińska, D., Effect of electrospinning process variables on the size of polymer fibers and bead-on-string structures established with a 2^3 factorial design, *Beilstein Journal of Nanotechnoly*, 2018, vol. 9, pp. 2466–2478.

Hybrid diffuse optical system for the tissue perfusion and oxygenation assessment

Neda Mogharari[1], Saeed Samaei[1, 2], Stanisław Wojtkiewicz[1] Adam Liebert[1], Michał Kacprzak[1]
[1]Nalecz Institute of Biocybernetics and Biomedical Engineering Polish Academy of Sciences, Warsaw, Poland
[2] Institute of Physical Chemistry, Polish Academy of Sciences, Warsaw, Poland
nmogharari@ibib.waw.pl

The blood flow is responsible for distributing nutrients and oxygen to all organs in the body. Any disorders in blood flow may lead to irreversible diseases or injuries. So, modalities for perfusion measurements would be essential at the clinical sites, especially in monitoring patients with cerebral blood flow (CBF) impairments. On the other hand, a sufficient level of tissue oxygenation could be achieved even with a low blood flow. Thus monitoring both parameters (blood flow and tissue oxygen saturation) is desirable and important, especially in neuromonitoring [1].

The optical methods such as diffuse correlation spectroscopy (DCS) and time-domain near-infrared spectroscopy (tdNIRS) are non-invasive methods enabling us to estimate the blood flow index (BFI) and oxygenation of the biological tissue, respectively [2]. Unlike traditional clinical CBF measurements, such as xenon-133 computed tomography and positron emission tomography, patients are not exposed to ionizing radiation in these optical methods. Also, in comparison to the other more safe methods such as ASL-MRI, DCS is relatively inexpensive and portable. Besides, it is possible to use these measurements on the patient's head to assess regional cortical microvascular flow and carry out these tests frequently during a patient's hospital stay [3].

Near-infrared spectroscopy is based on the specific chromophores absorption for various wavelengths in the near-infrared spectrum. So, the number of applied wavelengths depends on the number of measured chromophores. In time-domain near-infrared spectroscopy (tdNIRS), by analyzing the temporal broadening of light pulses at two wavelengths, we can assess the absorption coefficient in absolute value, and then it allows us to evaluate the concentration of HbO2 and HB. In DCS, the tissue is illuminated with a near-infrared long-coherence length laser, and fluctuation of light intensity is observed in the distance of few centimeters from the emission spot by single-photon detectors. The decay of the detected signal autocorrelation function reveals information about the velocity of the moving scattering components in the tissue, such as red blood cells. Fast decay of intensity autocorrelation function indicates high blood flow level, while slow decay reflects slow blood flow. To estimate the BFI, the theoretical autocorrelation function is fitted to the experimental curve, taking into account the optical properties and measurement geometry.

To optimize the DCS system and validate the capability of detecting BFI changes in turbid media, we designed a liquid phantom model which is composed of milk (3.2% fat). In our experiments, due to the reason that quantitation of the biological compounds of interest (hemoglobin, etc.) can not be tested, the medical utility is limited. The instrument was equipped with a 785 nm CW laser (CrystaLaser, USA) and four single-photon avalanche diode (SPAD) detectors (PDM, Micro Photon Devices, Italy) which each was connected to a time-correlated photon counting (TCSPC) board (SPC-130, Becker&Hickl, Germany). In this report, we described the design of a dynamic phantom with the controlled flow inside, which permits direct testing of CW-DCS-derived blood flow index and characterizing the fluid dynamics and optical properties of this phantom brain model. We also performed measurements on tissue during the cuff occlusion experiment and observed a drop of the BFI during occlusion and postocclusive hyperemia, which the results were comparable to the literature.

Acknowledgments
The studies were financed by the National Science Centre of Poland (NCN) in the framework of project 2019/33/B/ST7/01387.

References:

[1] T. Durduran, Diffuse correlation spectroscopy for non-invasive, micro-vascular cerebral blood flow measurement, *NeuroImage*, Vol. 85, pp. 51-63.

[2] E. Sathialingam, Hematocrit significantly confounds diffuse correlation spectroscopy measurements of blood flow, *Biomedical Optics Express*, Vol. 11, No. 8, pp. 4786-4799.

[3] E. M. Buckley, Diffuse correlation spectroscopy for measurement of cerebral blood flow: future prospects, *Neurophotonics*, Vol. 1(1), pp. 1-7.

Flexible electrochemical biosensor fabricated from *Bombyx mori* silk

Denise Molinnus [1], Kevin A. Janus [1], Aleksander Drinic [2], Heiko Iken [1], Nadja Kröger [3], Max Zinser [3], Ralf Smeets [4], Marius Köpf [2], Alexander Kopp [2], Michael J. Schöning [1,5]

[1]Institut of Nano- and Biotechnologies (INB), Aachen University of Applied Sciences, Heinrich-Mußmann-Straße 1, 52428 Jülich, Germany

[2]Fibrothelium GmbH, TRIWO Technopark Aachen, Philipsstraße 8, 52068 Aachen, Germany

[3]Department of Plastic, Reconstructive and Aesthetic Surgery, University Hospital of Cologne, Kerpener Straße 62, 50937 Cologne, Germany

[4]Department of Oral and Maxillofacial Surgery, Division of Regenerative Orofacial Medicine, University Medical Center Hamburg-Eppendorf, Martinistraße 52, Hamburg, Germany

[5]Institute of Biological Information Processing (IBI-3), Forschungszentrum Jülich GmbH, 52425 Jülich, Germany

janus@fh-aachen.de

Implantable biocompatible electronics play a key role in future medicine [1]. For the realization of `green electronics`, silk from the silk worm *Bombyx mori* represents a promising approach. Silk is a natural biopolymer with high biocompatibility and adjustable biodegradation [2]. Therefore, silk-based electronics in medicine is a widely discussed topic in the literature. For instance, it is used to detect *Staphilococcus aureus* infections and other bacteria by applying a graphene-based biosensor based on transient silk fibroin onto a tooth [3].

In this work, a proof of concept experiment was conducted, in which thin- (for Pt working and counter electrode) and thick-film (for Ag/AgCl quasi-reference electrode) technologies were combined to fabricate a biosensor based on a natural, biodegradable fibroin from the silk worm *Bombyx mori* as substrate. The biosensor was developed exemplarily as glucose sensor by applying the enzyme glucose oxidase. A biocompatible silicon rubber encapsulated the flexible biosensor. The sensor set-up was demonstrated by glucose measurements in buffer and Ringer's solution, while the stability of the quasi-reference electrode was investigated versus a commercial Ag/AgCl reference electrode. Repeated bending studies as well as cross-sensitivity against ascorbic acid, noradrenaline and adrenaline were investigated. Additionally, biocompatibility-, cytotoxicity- and degradation tests of the silk fibroin with and without thin-film platinum electrodes were carried out.

In conclusion, the experiments demonstrated the potential of flexible, biocompatible silk-based sensors for future application in medicine.

Acknowledgements: The authors thank S. Fuest and A. Baranowsky for support on the biological testing and D. Rolka for the SEM and EDX images. Also many thanks to J. Kiesel and S. Woege for their assisting during the electrochemical measurements.

References:

[1] K. Bazaka and M. V. Jacob Implantable Devices: Issues and Challenges, *Electronics*, 2013, 2, 1 – 34.

[2] Y. Cao and B. Wang Biodegradation of Silk Biomaterials, *Int. J. Mol. Sci.*, 2009, 10, 1514 – 1524.

[3] M. S. Mannoor, H. Tao et al. Graphene-based Wireless Bacteria Detection on Tooth Enamel, *Nat. Commun.*, 2012, 3, 763.

Novel Bluetooth Low Energy wireless endoscopic capsule for gastrointestinal diagnostics

Jakub Niemczuk[1], Dawid Michałowski[1], Bartosz Pośpiech[1], Marek Langner[2]
[1]Biocam Sp. Z o.o., Rynek 39/40 r.421, 50-102 Wrocław, Poland
[2]Wrocław University of Science and Technology, wybrzeże Wyspiańskiego 27, 50-370 Wrocław, Poland
jakub.niemczuk@biocam.pl

An endoscopic capsule is a device used for non-invasive examination of the human digestive system. The diagnostic method is not widely used due to the high cost generated by expensive hardware and long examination time. In addition, most diseases of gastrointestinal track are located in the esophagus, stomach and large intestine. Regions that are easily reached with traditional endoscopic procedures. However, the traditional endoscopic methods, due to accompany pain and inconvenience, have low patient compliance. This has serious epidemiological consequences emanating from low patient participation in national, free of charge, screening programs. The enrollment rate in Poland is typically lower than dozen percentage [1]. The need for effective, noninvasive, easily to implement diagnostic procedure is therefore obvious. The issue is addressed by interdisciplinary effort aiming at designing and implementing a cost effective diagnostic procedure based on new generation of endoscopic capsule.

The new endoscopic capsule is developed using novel universal silicon SoCs (System on Chip), which enables the use of flexible and energy efficient method of wirelesses bulk data transmission. The Bluetooth Low Energy connection between capsule and portable image acquisition mobile device opens the possibility to perform a diagnostic procedure without direct participation of the medical personnel and most important at the patient location. All that will make the capsule-based diagnostics feasible for general application due to its convenience and high level of acceptance by patients.

The size of the designed capsule do not exceed that a medium sized drug pill (11 mm x 28 mm). The already available prototype can capture HD images and transmit data with the speed up to 1,4 Mb/s. The use of two-ways Bluetooth communication and a build in ARM microcontroller enables the dynamic adjustment of image quality, FPS (Frames Per Second) and make possible for the implementation of additional features, what will dramatically extend capsule capability as an non-invasive diagnostic device for gastrointestinal track and affected tissues by the addition of temperature, pH and pressure sensors. The research efforts resulted in the functional prototype, which has been approved for clinical studies. This work presents the advantages of the proposed technique in comparison with other capsule endoscopes available on the market.

References:
[1] Program Badań Przesiewowych Raka Jelita Grubego, http://pbp.org.pl/program/statystyki/

This work was co-financed by NCBiR (National Center for Research and Development) „Poddziałanie 1.3.1, program Bridge Alfa“

Thermosensitive hydrogel/short electrospun fibers as a smart scaffold for tissue engineering

Beata Niemczyk-Soczyńska, Paweł Sajkiewicz
Laboratory of Polymers and Biomaterials, Institute of Fundamental Technological Research, Polish Academy of Sciences, Pawińskiego 5b, 02-106 Warsaw
bniem@ippt.pan.pl

The aim of these studies was to obtain a thermosensitive injectable hydrogel system consisting of methylcellulose (MC)/agarose hydrogel and short electrospun poly(l-lactide) acid (PLLA) nanofibers as a scaffold for tissue engineering application. Hydrogel components provide many benefits such as biocompatibility, high processability, and 3-D highly hydrated structure. The thermosensitivity of this biomaterial allows it to remain as a sol at room temperature and become a highly crosslinked gel in the physiological temperature after injection. It is an effect of reversible crosslinking of MC starting from dehydration known as "water cages destruction," followed by fibril formation. Agarose plays a supportive role in MC crosslinking as a dehydration accelerator [1]. Filling hydrogel with short electrospun nanofibers strengthens hydrogel mechanically and enriches its structure with bioactive fibers. Such an approach improves the mimicry of native ECM, providing an appropriate environment and support for cell growth and regeneration.

In these preliminary studies, scanning electron microscopy (SEM) was used to determine the hydrogel/short fibers system's morphology. The viscosity measurements allowed to assess hydrogels' injection ability after fibers addition by comparing viscosities with the literature reports.

The morphology of 5 wt. % MC/ 5 wt. % Agarose filled with 7.5 mg/ml of PLLA fibers (Fig. 1.) showed a structure, which according to Padhi et al. [2], are similar to native ECM of rats spinal cord. Table 1 shows a few examples of the viscosity results for hydrogels vs. hydrogels loaded with PLLA fibers at room temperature. The viscosities are below 1000 mPa • s, which according to Bradshaw et al. [3], is the limit of liquid injectability through 23 and 25 gauge needles.

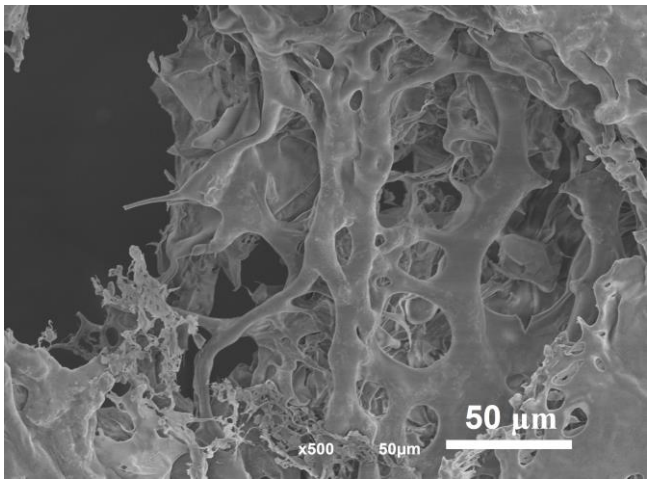

Fig. 1. SEM image of a hydrogel loaded with fibers.

Material	Viscosity [mPa • s]
3 MC/3 Agarose	121.44 ± 11.7
3MC/3 Agarose/7.5 mg/ml PLLA fibers	179.7 ± 15.2
5 MC/ 5 Agarose	725.2 ± 55.6
5 MC/ 5 Agarose/7.5 mg/ml PLLA fibers	890 ± 90.9

Table. 1. Viscosities of hydrogels before and after the addition of short fibers.

The SEM imaging showed a resemblance between the structure of the obtained hydrogel system and native ECM. Simultaneously, viscosity studies confirmed hydrogel/short fibers systems' injectability, thereby demonstrating its high potential in tissue engineering applications.

References:

[1] B. C. Martin, E. J. Minner, S. L. Wiseman,R. L. Klank, R. J. Gilbert *2008 J. Neural Eng* 5, pp. 221
[2] A. Padhi, A.S. Nain, 2020 *Ann Biomed Eng* 48**,** pp. 1071–1089
[3] J. Bradshaw, S. White, 2018 *ONdrugDelivery Magazine* 91, pp.16-21

EEG Based Image Reconstruction Using Transformers

Kacper Ogórek[1], Paweł Poryzała[2], Paweł Strumiłło[2]
[1,2] Institute of Electronics, Lodz University of Technology, Lodz, Poland
[1]kacperoglo3@gmail.com
[2]{pawel.poryzala, pawel.strumillo}@p.lodz.pl

Abstract. In this work the possibility of creating an end-to-end system being able to reconstruct natural images based on the subject's EEG response has been evaluated. Herein, various Transformer-based model's configurations have been implemented and tested in order to find the optimal solution for the given problem, taken into account the limitations of 16-channel EEG apparatus. Pretrained BigBiGAN neural network model has been used for the purpose of image featurization that is essential for the proper EEG feature mapping. The resulting image reconstruction performance was compared between the BigBiGAN and the model that is based on an original implementation of a simple DNN autoencoder. The presented implementation and obtained results show that on a limited amount of data it was very possible to build a system that is capable of successful reconstruction of images that are similar according to quantitative measures to the original graphical stimuli.

Keywords: EEG, Deep Neural Networks, Image reconstruction, SOM, GAN, Transformers.

That the paper will be available as a full article in the conference proceedings within the "Advances in Intelligent Systems and Computing" series; the book title: "Biocybernetics and Biomedical Engineering – Current Trends and Challenges. Proceedings of the 22nd Polish Conference on Biocybernetics and Biomedical Engineering, Warsaw, Poland, May 19-21, 2021."

Independent Lungs Ventilation impact on the cardiovascular system – a computer simulations

Piotr Okrzeja, Krzysztof Zieliński, Marcin Michnikowski, Marek Darowski
Nalecz Institute of Biocybernetics and Biomedical Engineering Polish Academy of Sciences,
Ks. Trojdena 4 st., 02-109 Warsaw, Poland
research@okrzeja.com

The first use of Differential Lungs Ventilation in thoracic surgery dates back to 1931, but in intensive care therapy – in 1976 [1]. A lot of research was conducted since this date. The most popular methods use two ventilators. The special solutions for Independent Lung Ventilation are developing since 80th years of XX century [2]. Independent Lung Ventilation was successfully used for post-traumatic ARDS therapy [3]. The aim of the analysis was to demonstrate the effect of artificial ventilation on the circulatory system, independent for each lung.
For the purposes of this study, the VirRespir application was used. A simplified computer model of the ventilator, operating in a controlled volume mode with a rectangular flow signal during the inspiration phase, was used . The research stand has been expanded by external model of the trachea intubated with a twolumen endotracheal tube. To complete the system authors used a model of a flow divider that allows for independent synchronous ventilation of each lung with a different value of pressure, flow and volume. The research work was divided into two stages. The first was the analysis of the influence of artificial mechanical ventilation of the lungs on the mechanics of the circulatory system. The second stage of the work included the analysis of the relationship between ventilation and perfusion in individual lobes.
The differences in the mean parameters of the circulatory system are on the verge of statistical error. The used of different flow rates for the ventilation of each lung does not improve the hemodynamics, but also does not negatively affect it. The lobe segment share of the lung and the amount of blood flowing through the lobe is constant. Instead, the amount of breathing gas required to maintain a given level of perfusion changes. The conducted research shows that the most favorable division of tidal volumes in relation to the obtained perfusion was obtained for the divisions in the ratio 50/50 and 30/70.
Based on preliminary research, we can see then the use of independent ventilation in severe obstruction does not cause changes in the mechanical activity of the circulatory system, which allows it to be used not only in asymmetrical diseases. It should be noted that the two-lumen intubation is more invasive then classical intubation. Therefore, the assessment of whether in symmetrical diseases the classical intubation, or the twolumen tube intubation is optimal, requires more research. The next step will be test on physical device dedicated to Independent Lung Ventilation and physical ventilator. Its more important considering still increased interest about Independent Lung Ventilation.

References:
[1] Anantham D. Jagadesan R. Tiew P.E. Clinical review: Independent lung ventilation in critical care,Critical Care, 2005 december, vol. 9, no. 6; 9:594-600 10.1186/cc3827. published online: 10 october 2005 http://ccforum.com/content/9/6/594.
[2] Darowski M. Hedenstierna G. Beahrendtz S. Development and evaluation of a flow-dividing unit fordifferential ventilation and selective PEEP, Acta Anaesth. Scand., 1985, 29, 61-66.
[3] Sawulski S. Nestorowicz A. Wośko J. Dąbrowski W. Kowalczyk M. Fijałkowska A. Independent lungventilation for treatment of post-traumatic ARDS, Anaesthesiology Intensive Therapy, 2012, vol. 44, no. 2, 85-88, ISSN 0209-1712, www.ait-viamedica.pl.

An SVM-based peptide identification algorithm integrated into a database search engine

Katarzyna Orzechowska, Tymon Rubel
Warsaw University of Technology, Institute of Radioelectronics and Multimedia Technology
Nowowiejska 15/19, 00-665 Warsaw, Poland
orzechowska@ire.pw.edu.pl

Mass spectrometry has recently become the method of choice for the identification of proteins in biological samples. In typical proteomic experiments proteins are digested into short peptides, which are analyzed in a tandem mass spectrometer (MS/MS) and identified by comparing the measured spectra to peptides originating from a protein database. This process involves a scoring function to evaluate the similarity of the observed spectra to theoretical spectra of candidate peptides. For each spectrum the best scoring candidate is selected to create a peptide-spectrum match (PSM). This general scheme is currently widely used and implemented by numerous proteomic database engines. However, despite major advances in MS/MS data analysis, search results are still affected by high error rates, and to achieve better discrimination of correct and incorrect identifications external tools must be used, with Percolator being probably the most popular one [1]. Here we present a machine-learning algorithm inspired by Percolator but integrated directly into the MScanDB search engine (available at proteom.ibb.waw.pl/mscandb). Such approach not only eliminates the need for additional postprocessing steps but also allows for the full utilization of specific features of MScanDB, including its ability to compute multiple scoring functions.

The input data for the algorithm consists of a list of scored PSMs obtained from searching the MS/MS spectra against a database composed of target protein sequences and the same number of randomly generated decoy records. This strategy, referred as target/decoy search, is commonly used in proteomic studies to estimate the false discovery ratio (FDR). Initial scores of the search engine are used to create a training set containing confidently identified target PSMs (with FDR below a predefined threshold, typically equal to 0.01) as positive examples, and decoy PSMs as negative examples. The selected PSMs are then converted into numeric feature vectors, and the resulting data matrix is used to train a classifier capable of discriminating between correct and incorrect sequence identifications. The learned classifier is used to rescore all PSMs, and finally, new FDR estimates are computed. In contrast to Percolator, which utilizes a linear support vector machine (SVM), our algorithm allows the selection of a nonlinear kernel with parameters optimized by cross-validation. We also redefined the feature vectors to take full advantage of the MScanDB scoring scheme.

The algorithm was tested on a large dataset originating from a study on the proteome composition of pancreatic cysts fluid [2]. In total 715 972 high resolution MS/MS spectra were searched against 40 758 human proteins from the SwissProt database and an equal-sized set of decoy records. As a first step, the proposed algorithm was compared in terms of identification performance with the default scoring function of the MScanDB search engine. The results demonstrated the superiority of the SVM-based approach, which identified 17.1% more PSMs at an FDR threshold of 0.01. A second comparison was made with Percolator executed as an external postprocessing tool. As expected, both methods performed similarly, however, our algorithm assigned 4.4% more sequences to spectra than Percolator (FDR $\leq$ 0.01). An additional test was conducted to verify the possibility of using distributed computations to reduce the time needed to fit the SVM model to large proteomic datasets. For this purpose, a dedicated version of the algorithm was implemented using the Apache Spark platform. The results revealed that, although the distributed version ensures faster computations, the observed scalability is not yet satisfying (speed-up equal to 6.6 on 16 cores), and further improvements are needed.
The main idea behind the incorporation of a machine-learning algorithm into the search engine was to simplify the MS/MS data processing pipeline. But, as we demonstrated above, the integration also improves the results of database protein identification, thus it might be beneficial for the quality of preotemic studies.
References:

[1] Käll L. et al. Semi-supervised learning for peptide identification from shotgun proteomics datasets, *Nature Methods*, vol. 4, no. 11, pp. 923-925
[2] Paziewska A. et al. Mass Spectrometry-Based Comprehensive Analysis of Pancreatic Cyst Fluids, *BioMed Research International*, vol. 2018, article ID 7169595

Customizable transepithelial/endothelial electrical resistance device with integrated multi-microelectrodes for the measurement of cellular barrier integrity

K. Orzeł[1], T. Gajowik[2], M. Zielińska[1]
[1]Department of Neurotoxicology, Mossakowski Medical Research Centre, Polish Academy of Sciences, 5 Pawińskiego St. Warsaw, Poland
[2]Institute of Control and Power Electronics, Warsaw University of Technology, 75 Koszykowa St. Warsaw, Poland

Endothelial cells are a specialized type of cells that make up a single layer of polarized inner lining of blood vessels, a passive and active barrier in the human body. Disturbance of barrier properties by destabilizing homeostasis lead to a number of diseases, including hypertension or inflammatory bowel disease. In *in vitro* experiments, proper control of barrier integrity is crucial. Trans Endothelial Electrical Resistance (TEER) measurement is a popular and easy technique of barrier integrity monitoring. However, commercially available systems are invasive and offer an imprecise method of measuring, based on the forced current flow with a voltage wave frequency of 12.5 Hz, causing undesirable electrolysis of the culture media. Moreover, commercial devices comprise complicated mechanics and large size rising problems with placing in the incubator.

In turn, a newly introduced commercial multi-functional systems offering additional TEER recordings are of high costs of the usage (a large amount of the culture medium, clogging of the flow channels) that limit wide laboratory usage of the method. For this purpose, we designed a proprietary non-invasive automatic measuring system (MS) offering more accurate measurement parameters and versatility of use at a significantly lower production (components) and operating cost. The monolayer resistance measured in ohms (Ω) or modulus of electrical impedance, with a long-range frequency spectrum of the excitation signal, offers a quantitative analysis of barrier integrity. To measure cells' monolayer integrity, growing on semipermeable inserts placed in the wells of the culture plates, we use two electrodes located at different positions 1) in the insert 2) in the medium of the well. The multiple measurement channels allow parallel simultaneous recordings of several dozen wells are competitive for so-far offered systems. The signal duration of the measurement (<1 ms per 5 min cycle) minimizes the biological effect on cells

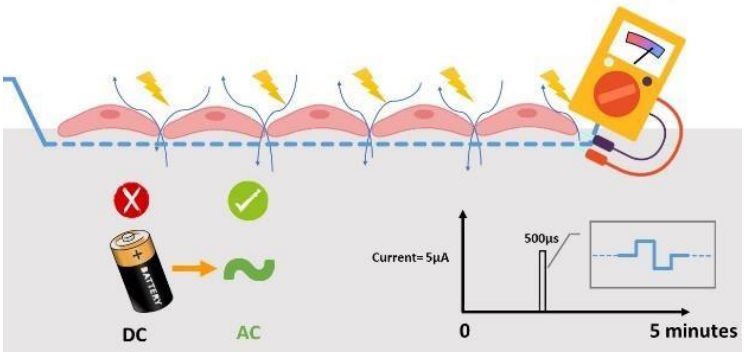

Figure 1 Scheme and measurement basis of TEER using MS .

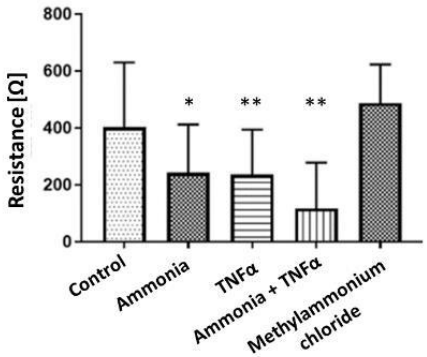

Table 1 Resistance recordings of rat brain endothelial cell ammonia and TNF α using MS.

Supported by National Science Centre grant 2015/19/8/NZ/01902 and by Knowledge Education Development Programme.

A cell-based biosensor: “All-in-one” and “off-the-shelf” format for on-site monitoring of cell response

Dua Özsoylu[1,2], Tuğba Isık[3,4], Mustafa M. Demir[4], Michael J. Schöning[1,5], Torsten Wagner[1,5]
[1]Institute of Nano- and Biotechnologies (INB), Aachen University of Applied Sciences, Heinrich-Mußmann-Straße 1, 52428 Jülich, Germany
[2]Medical Biology and Genetics, Graduate School of Health Sciences, Dokuz Eylül University, Mithatpasa Street 1606, Balcova, 35340 Izmir, Turkey
[3]School of Chemistry, University of Bristol, Great George Street 31, BS1 5QT Bristol, UK
[4]Department of Materials Science and Engineering, Izmir Institute of Technology, 35430 Izmir, Turkey
[5]Institute of Biological Information Processing (IBI-3), Forschungszentrum Jülich GmbH, 52425 Jülich, Germany
oezsoylu@fh-aachen.de

There are only a few cell-based biosensors available on the market despite an increased number of publications and efforts, usually focusing on their capability to detect substances of interest such as pollutants [1], toxins [2], or viruses like SARS-CoV-2 [3]. As the sensor chip contains a ‘living’ component such as adherent mammalian cells, efficient preservation of these biosensors during transportation to end-users is still a major challenge, which hinders their practical applicability and commercialization [1-3]. Thus, there is an urgent need for preservation tools and methods to enable ready-to-use on-site systems.

Herein, we studied a strategy named on-sensor cryopreservation, a method for preserving this living component by freezing them (-80 °C) directly on the biosensor surface. To protect the cells from cryo-injury, the rigid sensor surface was modified with elastic electrospun fibers composed of a polymer (polyethylene vinyl acetate), which has a high thermal expansion coefficient and low glass-transition temperature. The modified sensor chip is then integrated into a microfluidic system to obtain a cryo-chip (Figure 1).

This cryo-chip system is found to be effective for keeping cells viable during cryopreservation as well as for post-thaw detection of the extracellular acidification of CHO-K1 cells. Cryopreservation of the chips containing cells at the manufacturing stage and transporting them via cold-chain transport could pave the way for “all-in-one” format and “off-the-shelf” possibility for on-site applications.

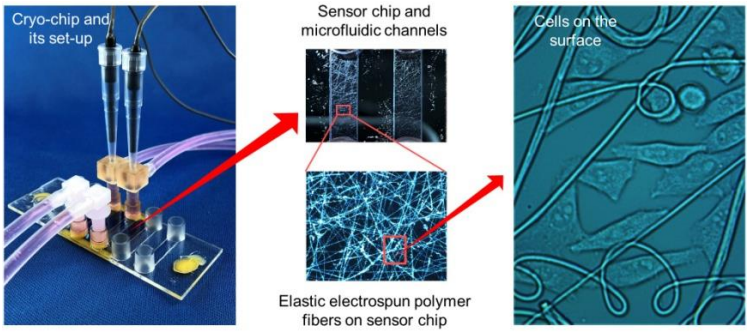

Figure 1: Elastic electrospun polymer fibers-modified light-addressable potentiometric sensor (LAPS) integrated into a microfluidic system (cryo-chip).

Acknowledgments: DÖ would like to acknowledge the Ph.D. research scholarship grant from the Scientific and Technological Research Council of Turkey (TÜBITAK). The authors gratefully thank the Federal Ministry of Education and Research of Germany (Opto-Switch FKZ: 13N12585).

References:

[1] Q. Gui, T. Lawson et al. The Application of Whole Cell-Based Biosensors for Use in Environmental Analysis and in Medical Diagnostics, *Sensors*, 2017, 17, 1623.
[2] Y. Ye, H. Guo et al. Recent Progress on Cell-Based Biosensors for Analysis of Food Safety and Quality Control, *Biosens. Bioelectron.*, 2019, 126, 389 – 404.
[3] S. Mavrikou, G. Moschopoulou et al. Development of a Portable, Ultra-Rapid and Ultra-Sensitive Cell-Based Biosensor for the Direct Detection of the SARS-CoV-2 S1 Spike Protein Antigen, *Sensors*, 2020, 20, 3121.

Hybrid cardiovascular simulator – an application for the mechanical assistance by an intra-aortic balloon pump

Raman Pasledni and Krzysztof Zieliński
Nalecz Institute of Biocybernetics and Biomedical Engineering, Polish Academy of Sciences, Warsaw, Poland
rpasledni@ibib.waw.pl

The United States Food and Drug Administration agency is encouraging to use modeling and simulation in medical device evaluation, in order to reduce reliance on animal models and human data, and reduce costs and speed innovation. To address this challenge various models and simulators have been developed that play the role of artificial/virtual patients.

A previously elaborated in IBBE PAS a hybrid (hydro-computer) simulator was adapted to perform simulations of the left ventricular mechanical assistance by the intra-aortic balloon pump (IABP).
To implement this, some hardware and software changes were made to the simulator, in particular the following functionalities were added: connecting a physical aorta model; variable aortic compliance by introducing a numerical capacitor into the hybrid circulatory model; a rigid tube model of the aorta with an orifice system to simulate IABP support. Static characteristics were measured for both physical models of the aorta (silicone tubes) and the model with a numerical capacitor. IABP assistance was simulated using the developed aortic model.

The preliminary simulation results show that the system is behaving correctly. The effects of IABP mechanical assistance of the left ventricle observed in the simulator are consistent with clinical practice. The application for simulations of IABP mechanical assistance extends the whole IBBE PAS hybrid simulator functionalities in terms of the mechanical heart assistance simulations.

References:
[1] Zieliński, K., Darowski M., Kozarski, M., et al. The need for hybrid modeling in analysis of cardiovascular and respiratory support, *Int J Artif Organs*, 2016, vol. 39, no. 6, pp. 265–271.
[2] Sintek, M., Gdowski, M., Lindman, B., et al. Intra-aortic balloon counterpulsation in patients with chronic heart failure and cardiogenic shock: clinical response and predictors of stabilization, *J Card Fail*, 2015, vol. 21, no. 11, pp. 868-876.
[3] Ferrari, G., Khir, A., Fresiello, L. Hybrid model analysis of intra-aortic balloon pump performance as a function of ventricular and circulatory parameters. *Artif Organs*, 2011, vol. 35, no. 9, pp. 902-911.

Estimation of the fraction of area covered by cells and cell clusters in WSI patches

Antonina Pater[1], Łukasz Roszkowiak[1], Krzysztof Siemion[1,2], Anna Korzyńska[1]
[1] Nałęcz Institute of Biocybernetics and Biomedical Engineering PAS,
Ks. Trojden 4 st. Warsaw, Poland
[2] Medical University of Białystok, Kiliński 1 st. Białystok, Poland
a.pater@ibib.waw.pl

Introduction Cervical smears are commonly used in industrialized countries as a screening test for detection of precancerous lesions [1]. However, the evaluation of the test material is still done manually by experts. Automation of the part of the process can lead to faster, cheaper and more precise results. The first step towards the process automation may be a detection of cells in the smear image. Nowadays Deep Neural Networks gain popularity as image segmentation tools due to their powerful learning abilities [2]. The aim of this investigation is to estimate area of patch covered by cells. It's done by detection of singular or clustered cells using deep neural networks. This investigation is a primary step towards developing a support system for expert's evaluation of samples.

Materials and Method Dataset consisted of 50 patches cut out from various WSI of cervical smears. 10 additional patches were used for testing. Images were annotated with bounding boxes by author. Objects in the images were divided into 3 classes: background, single cells and clustered cells.

Images were augmented randomly applying horizontal or vertical flip and rotation up to 90 degrees. Supervised learning process was performed using the preprocessed data on Region Based Convolutional Neural Network (RCNN), using VGG16 architecture as a backbone. Prepared model was evaluated on test set with F1 score calculated on manually revised detections. A detection was defined as true positive if its area covered significantly with ground truth for specific cell.

Result and Conclusions Mean F1 score was 0.81 ± 0.11 on test set. This not so high result may be caused by low contrast between cytoplasm and background, insignificant for cell detection color difference or presence of artefacts in the background. Impact of these issues may be lowered with use of color normalization or conversion to grayscale, contrast alteration, noise filtration.

References

[1] E. Gakidou, S. Nordhagen and Z. Obermeyer, "Coverage of Cervical Cancer Screening in 57 Countries: Low Average Levels and Large Inequalities," *PLoS Medicine,* vol. 5, p. e132, 6 2008.

[2] A. Janowczyk and A. Madabhushi, "Deep learning for digital pathology image analysis: A comprehensive tutorial with selected use cases," *Journal of Pathology Informatics,* vol. 7, p. 29, 2016.

The outcome of breast chemotherapy based on Gray Relational Coefficient of ultrasound images

Anna Pawłowska[1], Norbert Żołek[1], Katarzyna Dobruch-Sobczak[2], Ziemowit Klimonda[1], Hanna Piotrzkowska-Wróblewska[1], Jerzy Litniewski[1]
[1]Institute of Fundamental Technological Research, Polish Academy of Sciences, ul. Pawinskiego 5B, 02-106 Warsaw, Poland
[2]Maria Sklodowska-Curie Institute - Oncology Center, ul. Wawelska 15B, 00-001 Warsaw, Poland
nzolek@ippt.pan.pl

Breast cancer is the most common malignancy in women and the second most common cause of cancer-related death of women in Poland [1]. One of the treatment modalities used is neoadjuvant chemotherapy (NAC), which aims to reduce tumor mass, limit metastases and enable surgical treatment. The tumor response to NAC is variable. Detection of tumors that respond well to NAC prior to surgery allows for breast-saving surgery. Current methods of monitoring therapy are based primarily on assessing changes in tumor size. Techniques for measuring tumor size are subject to significant error, and a change in tumor size does not always yield a good response rate to treatment [2].

In the presented study, we analyzed the ultrasound data from 38 breast tumors collected before the NAC therapy and after each of the six subsequent treatment cycles. An ultrasound scanner with a research option was used, allowing for the recording of RF data. Gray Relational Coefficient (GRC) was used to evaluate the therapy. The parameter was determined for three data types (for RF images, envelope images and envelope after log compression) and for four areas of interest (including both tumor tissue and surrounding tissue). The tumor sizes were also recorded. The usefulness of GRC and tumor size changes in predicting the effects of NAC was statistically evaluated based on the area under the ROC curve (AUC) and the post-mastectomy histopathology result was used as a reference.

Considering all the results of the prediction of treatment effects obtained, the highest AUC values were obtained when using RF data after envelope detection. After the first dose of NAC, data collected from the entire tumor and its surroundings predicted a good tumor response with AUC not less than 0.85. Only the data from the inside of the tumor gave a worse result = 0.81. For subsequent NAC doses, data collected from the tumor margin and surrounding tissues turned out to be the best. After the fifth dose, by far the best response to NAC was obtained using data from the tumor alone and strict center of the tumor, AUC > 0.93. The results of the classification of tumors by GRC have always been significantly better than by their size (Figure 1).

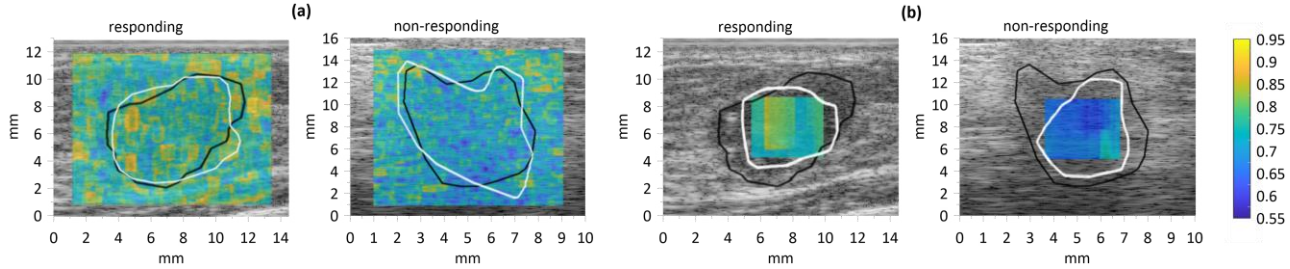

Figure 2. Parametric images of the responding and non-responding breast tumor after the first (a) and fifth (b) NAC cycle. The color scale shows the values of the GRC parameter. The lines represent the border of the lesion before chemotherapy (black line) and after the first/fifth cycle (white line)

The number of cases considered is insufficient to draw more general conclusions. However, our results indicate that the values of the GRC parameter may reflect the changes in tumor tissue structure as a result of chemotherapy. Thus, it may support the physician in evaluating the effects of NAC and contribute to an increase in the number of breast-saving procedures.

References:

[1] Nowotwory złośliwe w Polsce w 2018 roku. *Krajowy Rejestr Nowotworów*, Ministerstwo Zdrowia 2020
[2] Reig B., et al. Role of MRI to assess response to neoadjuvant therapy for breast cancer, *Journal of Magnetic Resonance Imaging*, 2020, vol. 52, no. 6, pp. 1587–1606

A multimodal, optical and electrochemical, approach towards detection of endogenous immunomodulators

Agnieszka Paziewska-Nowak, Marcin Urbanowicz, Anna Sołdatowska, Kamila Sadowska, Dorota G. Pijanowska
Nalecz Institute of Biocybernetics and Biomedical Engineering, PAS, Ks. Trojdena 4, Warsaw, Poland
apaziewska@ibib.waw.pl

The endogenous immunomodulators: cortisol (Cort) and lactoferrin (Lf), display various immune functions by either down- or up-regulation of the immune system. Several diseases of autoimmune background are associated with Cort and Lf excessive or insufficient secretion, thus the need for their determination arises [1]. Both are known for their anti-inflammatory activity, however, differ significantly in size and physicochemical properties, which implies several challenges in their determination [2, 3]. Since current methods of Cort and Lf determination are not sufficient, new sensing layers of high sensitivity, selectivity and stability towards these analytes are necessary. A multimodal detection method based on surface plasmon resonance (SPR, optical) and voltammetry (electrochemical) is proposed along with two strategies of affinity-based sensing, in particular using biological and biomimetic recognition sites for each analyte.

The biosensing layers were obtained due to the immobilization of antibodies via linkers of various length and degree of branching. The influence of cross-linker type, ligand dilution, running buffer type and pH on immobilization was established. The investigation on ligand-analyte interaction at fixed analyte concentration was performed using developed biosensing layers. Biosensor with antibodies immobilized via linear linker enabled to determine Lf within physiologically-relevant linear concentration range (12.5-250 nM) with the sensitivity of 1.51 m_0/nM and $R_2 = 0.97$. The biosensor was characterized by good stability and repeatability represented by low SD values. The advantage of hyperbranched linkers over linear was observed in terms of loading density of antibodies at the SPR sensors' surface. However, further measurements with Lf revealed the lower response for dendrimer-modified biosensors compared to results obtained with the linear linker-functionalized biosensor, most plausibly due to steric hindrance.

Another approach based on biomimetic sensing was carried out via molecular imprinting of whole analyte molecule (bulk imprinting), forming artificial cavities of adequate affinity for target analytes, that mimic the functionalities of biological receptors. The procedure of molecularly imprinted polymeric (MIP) layer made of conductive polymeric matrix consisted of two following steps: (1) electropolymerization of analyte/functional monomer mixture onto amperometric sensors (gold, glassy carbon, platinum), and (2) elution of template (analyte) molecules from cavities. The impact of electrical parameters during electropolymerization, as well as template/monomer solution composition on the sensor performance, were checked. For comparative measurements, non-imprinted layers were fabricated. Since chosen analyte is electrochemically inactive, the differential electrochemical analysis was carried out using $K_4[Fe(CN)_6]$ as a redox indicator. Preliminary results obtained using biomimetic sensors with molecularly imprinted polypyrrole doped carboxylic acid derivative showed decrement of recorded signal for the following concentrations of Cort. The most noticeable difference in signal height was received in the case of glassy carbon MIP-modified electrodes, while the lowest response drop was obtained in the case of platinum MIP-modified sensors. On the other hand, polyazulene-based MIP-modified sensors showed positive results using a glassy carbon electrode exclusively.

The SPR biosensor for Lf was successfully developed using linear linkers to immobilize the bioreceptor. Further adjustment of immobilization procedure is needed in the case of hyperbranched linker-modified biosensors to achieve well-defined spatial orientation of antibodies – the reduction of steric hindrance and improvement of stability and reproducibility is expected. Promising preliminary results using MIP-modified amperometric sensors were received for Cort detection. Future research will be focused on searching for new nanostructurized layers of improved metrological parameters for selective molecular recognition of chosen analytes.

References:

[1] K.C. Navegantes, R. de Souza Gomes, P.A.T. Pereira, et al., *J Transl Med* 2017, vol. 15:36, pp. 1-21.
[2] K. Hogenelst, M. Soeter, V. Kallen, *Sensing and Bio-Sensing Research* 2019, vol. 22, pp. 100249.
[3] H. Kudo, K. Maejima, Y. Hiruta, D. Citterio, *SLAS Technol* 2020, vol. 25, pp. 47-57.

Subject Specific Atlas Based Frequency Domain Diffuse Optical Tomography

Guy Antony Perkins[a,b] Samuel J. E. Lucas[c], Hamid Dehghani[b]
[a]Sci-Phy-4-Health Centre for Doctoral Training,
[b]School of Computer Science,
[c]School of Sport, Exercise and Rehabilitation Sciences, University of Birmingham,
Birmingham, UK, B15 2TT
g.perkins@pgr.bham.ac.uk

Frequency Domain Diffuse Optical Tomography (FD-DOT) has a wide range of applications in human brain imaging. DOT relies on the accurate determination of the source-detector (SD) locations on the subjects scalp aswell as the geometry of the domain being imaged, as the accuracy of tomographic reconstruction will directly depend on this. The locations of the SD probes can be estimated, however, to improve the spatial accuracy of the tomographic reconstruction, registration of an subject specific model can be performed. It is possible to register the subject's head on a model based on a MRI scan. In some clinical environments an MRI scan is not possible, therefore SD locations have to be obtained using a different method. Typically, these SD locations can be obtained using a device like the Polhemus digitizer (Polhemus, VT, USA), however this can't be used in environments or subjects where metal-electromagnetic interaction is unsafe.

This work investigates the use of a 3D camera (Artec Leo, Artec 3D, Luxembourg) to perform subject specific atlas based registration. A subject was scanned using the 3D camera, figure 1a. Five landmark (LM) points were selected on the subject scan and atlas., figure 1b. These are the nasion (LM1), the left (LM2) and right (LM3) pre-auricular point, the inion (LM5) and the vertex (LM4). Then, the atlas was registered (figures 1c-e) into the subject space using an algorithm which produces an alignment matrix, T, such that the difference between the 5 LM points of the subject and atlas are minimised. T is then applied to every node in the atlas, such that each atlas node is registered into subject space. FD-DOT measurements were then performed on the subject performing a hand grip experiment, figure 1b. These measurements were performed at 690 nm and 830 nm at 140.625 MHz using the ISS Imagent (ISS, Champaign, IL, USA). Figure 1 d-f. shows the results of the 3D scan, registration and tomography. Changes in the total hemoglobin (HbT) are tomographically reconstructed using NIRFAST [1].

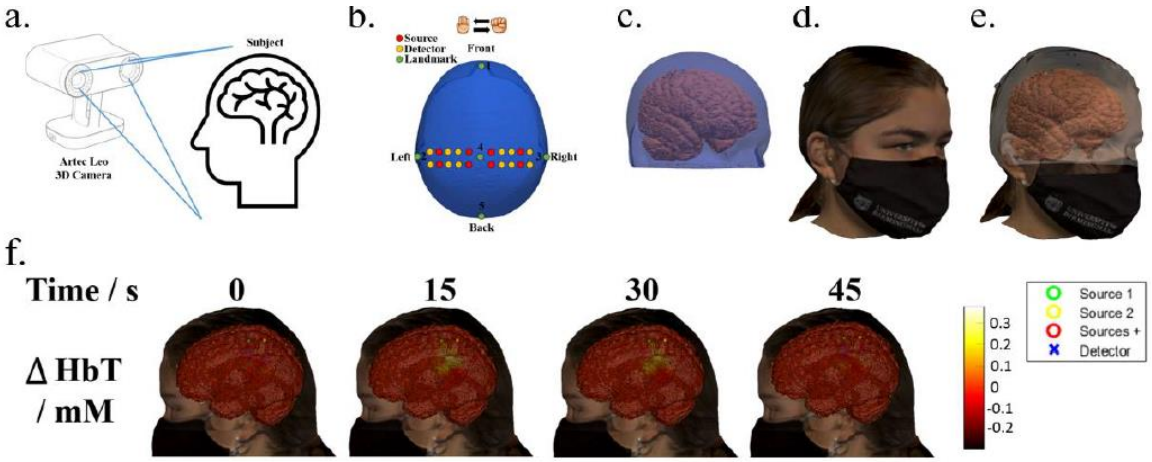

Figure 1 a. A representation of the 3D camera scanning the subject. b. The SD set up and five LM points on the subject. c. The atlas model. d. The 3D scan of the subject. e. The atlas model registered to the subject. f. Tomographic reconstruction of HbT at four time points after the start of the stimulus.

This work has shown that subject specific atlas based registration can be performed using a 3D camera and five LM point registration. This registration can then be used for FD-DOT and this can be visualised on a subject specific scan. Future direction of this work would be to collect data on multiple subjects, and perform 3D scans of subjects with and without SD probes on. This would allow for an accurate placement of SD probes on the subject's scalp for DOT. Due to the cloud point nature of the 3D scan, other registration

methods could be used, which utilize more than five LM points. The authors would like to acknowledge financial support from the Engineering and Physical Sciences Research Council through a studentship from the Physical Sciences for Health Centre for Doctoral Training (Grant No. EP/L016346/1).

References:

[1] Dehghani H, Eames M, Yalavarthy P, Davis S, Srinivasan S, Carpenter C et al. Near infrared optical tomography using NIRFAST: Algorithm for numerical model and image reconstruction. Communications in Numerical Methods in Engineering. 2009;25(6):711-732.

Modelling bicarbonate and CO_2 dialysance in the haemodialyzer

Mauro Pietribiasi, Jacek Waniewski, John K. Leypoldt
Institute of Biocybernetics and Biomedical Engineering Polish Academy of Sciences
Ks. Trojdena 4, Warsaw, Poland
mpietribiasi@ibib.waw.pl

Bicarbonate is added to the dialysis fluid in haemodialysis sessions to replenish buffer reserves in end-stage renal disease patients who lost the physiologic ability of the kidney to regulate the concentration of metabolic acids.
The transport of bicarbonate, from dialysis fluid to patient's blood, is quantified by its dialysance, usually assumed constant for given haemodialyzer and treatment settings. However, a recent discussion in the American Journal of Physiology [1], highlighted how the simple calculation of bicarbonate dialysance might not be enough to describe the net buffer balance at the end of a dialysis session.
The classical approach of constant dialysance neglects the transport of dissolved carbon dioxide (CO_2) between dialysate and plasma, and the chemical interconversion of bicarbonate and CO_2 within blood. We assessed the impact of dissolved CO_2 transport on the calculation of bicarbonate dialysance with a comprehensive mathematical model of acid-base transport in haemodialyzers.

The model simulates the transport of bicarbonate and dissolved CO_2 in a haemodialyzer using one-dimensional mass conservation equations for blood and dialysate, while assessing blood acid-base biochemistry with a previously developed model [2]. The model was solved numerically and fitted to published data [3] to estimate mass transfer coefficients for both bicarbonate and dissolved CO_2. Simulations were then carried out using different bicarbonate concentrations at the inlet of the dialyzer, with and without transport of dissolved CO_2. In the latter case, the same total CO_2 balance was assured by adjusting the bicarbonate mass transfer coefficient.

In both cases the model was able to fit the available clinical data, with different fitted parameters. Dialysances were calculated as solute lost in dialysate over the difference between inlet concentrations of dialysate and plasma, for bicarbonate (Dbic), dissolved CO_2 (DCO_2), and in simulations without dissolved CO_2 transport (Dbic2).
The values of [Bic] were tested ranging from 20.4 mEq/L (Dbic = 164 mL/min, DCO_2 = 448 mL/min, Dbic2 = 211 mL/min) to 24.4 mEq/L (Dbic = 139 mL/min, DCO_2 = 518 mL/min, Dbic2 = 220 mL/min), with BE = -4 mEq/L.

DCO_2 exceeded the blood flow rate (300 mL/min) because of the conversion of bicarbonate into dissolved CO_2 after its transport into blood within the haemodialyzer. Calculated Dbic2 values to achieve identical overall total CO_2 transport required mass transfer-area coefficients that increased with plasma bicarbonate concentration at blood inlet.
Quantification of acid-base transport in haemodialyzers requires dialysance values for bicarbonate and dissolved CO_2 that are dependent on the plasma bicarbonate concentration at the blood inlet. The characterization of acid-base transport neglecting transmembrane transport of dissolved CO_2 may also be appropriate if the dialysance for bicarbonate is adjusted based on the plasma bicarbonate concentration at blood inlet.

References:
[1] F. J. Gennari and J. A. Sargent, Acid-base events during hemodialyis (letter to the Editor). *Am J Physiol Renal Physiol* 320, F130-132, 2021.
[2] S.E. Rees and S. Andreassen, Mathematical Models of Oxygen and Carbon Dioxide Storage and Transport: The Acid-Base Chemistry of Blood. *Crit Rev Biomed Eng* 33(3), 209-264 2005.
[3] K.I Sombolos et al., pO2 and pCO2 Increment in Post-dialyzer Blood: The Role of Dialysate. *Artificial Organs* 29(11), 892-898, 2005.

Indirect 3D-printing of viscous hydrogel in poly(vinyl alcohol) molds as a method to obtain tissue engineering scaffolds

Krzysztof Pietryga, Angelika Kiełbasa, Elżbieta Pamuła
AGH University of Science and Technology, Faculty of Materials Science and Ceramics,
Department of Biomaterials and Composites, al. Mickiewicza 30, 30-059 Kraków, Poland
pietryga@agh.edu.pl

Indirect 3D printing method of the scaffolds involves material casting in 3D printed mold and subsequently dissolving soluble mold material (in organic solvent or water). The method is ideal to shape more demanding naturally derived biomaterials [1]. Due to printing limitations molds of simple grid lattice is usually produced. Casting in simple grid mold results in formation of top-bottom channels in the scaffold. This may be not favorable for cell seeding when medium and cells flow easily through material. In our research two alternative mold models were designed, which can produce scaffolds without straight top-bottom channels. However, it might be difficult to fill in such type of molds, particularly with hydrogels of higher viscosity. Therefore, before laboratory experiments fluid dynamic simulations were performed to illustrate the process of fast vacuum infiltration.

Mold models of three different lattice shapes were designed in Fusion 360 software (Autodesk) (Fig.1A, grey structure): standard grid lattice (GRID), grid lattice shifted for half distance between layers (GRID-SHIFT) and the model in which every layer was twisted 15° relative to previous layer (TWIST). The models were imported into fluid dynamics simulation software (CFD, Autodesk) to simulate flow of viscous (0.5 Pa*s) fluid through the syringe containing a cylindrical mold. Simulation represented vacuum infiltration when liquid was pulled through the syringe by negative pressure of 0.1 atm. Information of flow and pressure was analyzed. In experimental part models of molds were sliced by Cura 3 (Ultimaker) and printed from poly(vinyl alcohol) (PVA) filament on FDM 3D printer. 0.5% w/v gellan gum (GG) and 10% w/v gelatin (Gel) and 0.03% $CaCl_2$ mixture was molded into PVA by vacuum method in the syringe. After complete gelation (30 min at 4°C) PVA mold was dissolved in water to obtain GG/Gel hydrogel scaffold crosslinked with calcium ions.

Performed simulation showed that the flow of viscous liquid is more resisted by GRID-SHIFT and TWIST geometries. It is illustrated by pressure buildup in a bottom part of syringes (Fig. 1B). Additionally flow in TWIST mold was also less uniform and tended to fill in the central part earlier. Simulations were confirmed by the observations during infiltration of the real PVA molds. All geometries resulted in a proper scaffold molding. Most of imperfections were attributed to PVA swelling during its dissolution.

Infiltration of sacrificial mold during indirect 3D printing process may be demanding for fast gelling and viscous hydrogel especially in connection with dense and complex mold geometry. Vacuum infiltration method proved to be effective to infiltrate all molds despite of considerable flow resistance in GRID-SHIFT and TWIST due to a high viscosity of the hydrogel.

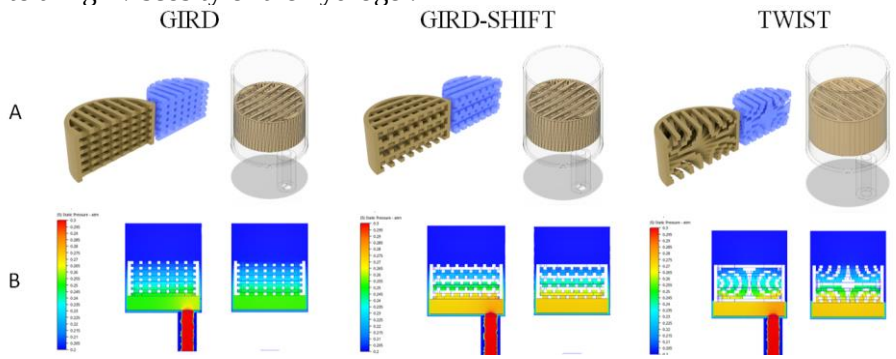

Fig 1. 3D models of PVA molds (grey) and corresponding hydrogel scaffold (blue) (A). Pressure distribution during infiltration of PVA molds with hydrogel matrix in FEM simulation (B).

References:

[1] W. Y. Yeong, *et al*. Comparison of drying methods in the fabrication of collagen scaffold via indirect rapid prototyping. J. Biomed. Mater. Res. B Appl. Biomater., 2007, 82B(1): 260–266

Acknowledgements:

This study was supported by the National Science Centre Poland (No 2018/29/N/ST8/01544)

Mathematical modelling of phosphate kinetics, its peculiarity and adequacy indices for patients on maintenance hemodialysis

Joyce Pinto, Malgorzata Debowska, Jacek Waniewski
[1]Nalecz Institute of Biocybernetics and Biomedical Engineering, Polish Academy of Sciences,
Ks. Trojdena 4 St., 02-109 Warsaw, Poland
mdebowska@ibib.waw.pl

Phosphate imbalance is a part of mineral disturbances in dialysis patients. Serum phosphate kinetics during hemodialysis (HD) session is different from other standard adequacy markers, i.e., urea and creatinine. The rebound for serum phosphate after dialysis is much faster compared to urea and creatinine, however the detailed interdialytic profiles are not known. *Equivalent continuous clearance* (ECC) was proposed for phosphate as an adequacy index, although its values were studied based on the limited clinical data [1]. Our objective was to estimate and compare ECC for phosphate, urea and creatinine at different serum concentration reference values of peak, peak average, time average and treatment time average, c.f. [2], based on numerical simulation of one-week cycle of HD sessions.

The kinetic equations for urea and creatinine were drawn from the two-compartment model and for phosphate from the pseudo-one compartment model [2]. Standard HD conducted three times per week was simulated using MATLAB 2019b. Models were fit to the average clinical data from a previous study [1] and ECCs were calculated for the three solutes.

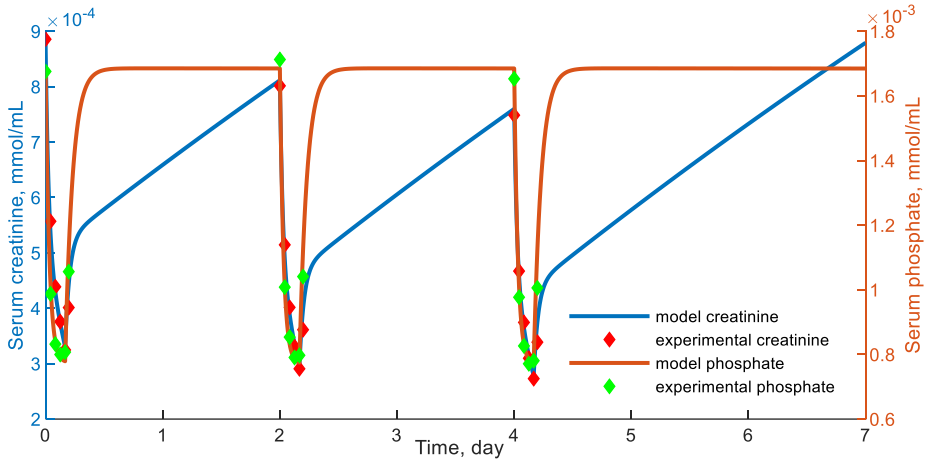

Fig. 1. Phosphate and creatinine serum concentrations for one week cycle of three hemodialysis sessions.

The predicted peak (i.e., pre-dialytic) phosphate concentrations were the same for all three sessions in contrast to urea and creatinine with decreasing peak levels throughout the week (Fig. 1). ECC values at peak, peak average, time average and treatment time average reference concentrations were 6.79, 7.78, 11.30 and 12.57 for urea; 4.98, 5.36, 6.76 and 7.11 for creatinine and 5.28, 5.29, 5.54 and 9.45 mL/min for phosphate, respectively. The difference between peak average and time average ECC value, much discussed for urea, was very low for phosphate. In contrast, the treatment time average ECC for phosphate was relatively much higher than time average ECC compared to low difference of these two indices for urea and creatinine.

It was observed that ECC - hemodialysis adequacy index - for phosphate at peak, peak average and time average reference concentrations behaves differently when compared with the ECC values of urea and creatinine. This difference is the result of quick post-dialytic phosphate rebound due to the tight short-term regulation of serum phosphate levels in the body as described by the pseudo-one compartment model.

References:

[1] Debowska M., Wojcik-Zaluska A., Ksiazek A., Zaluska W., Waniewski J. Phosphate, urea and creatinine clearances: Haemodialysis adequacy assessed by weekly monitoring, *Nephrology Dialysis Transplantation*, 2015, vol. 30, no. 1, pp. 129–136

[2] Waniewski J, Debowska M., Lindholm B. Theoretical and numerical analysis of different adequacy indices for hemodialysis and peritoneal dialysis, *Blood Purification*, 2006, vol. 24, no. 4, pp. 355–366

Biomolecular topography of glioblastoma multiforme developed in the rat brain – a FTIR study

Karolina Płaneta[a], Zuzanna Setkowicz-Janeczko[b], Damian Ryszawy[c], Natalia Janik-Olchawa[a], Agnieszka Dróżdż[a], Joanna Chwiej[a]
[a]Faculty of Physics and Applied Computer Science, AGH University of Science and Technology, Krakow, Poland; [b]Institute of Zoology and Biomedical Research, Jagiellonian University, Krakow, Poland; [c]Faculty of Biochemistry Biophysics and Biotechnology, Jagiellonian University, Krakow, Poland
Karolina.Planeta@fis.agh.edu.pl

Anomalies in distribution of biochemical compounds are often observed in pathologies of different origin, including cancers [1]. One of the most malignant brain tumor is glioblastoma multiforme (GBM). Despite devasting therapies, the survival rate of patients suffering from GBM is very poor [2]. Based on the current knowledge, the etiology of GBM is not clear and therefore various researches are aimed at better understanding of its nature [3].

The aim of our study was the assessment of anomalies in accumulation of biomolecules occurring in the rat brain after implantation of three different GBM cell lines. To achieve this goal the brain tissue slices were analyzed using Fourier Transform Infrared Spectroscopy (FTIR). These results were correlated with histological evaluation of examined nerve tissue. The obtained data allowed us to indicate potential biomolecular markers of the degree of GBM invasiveness.

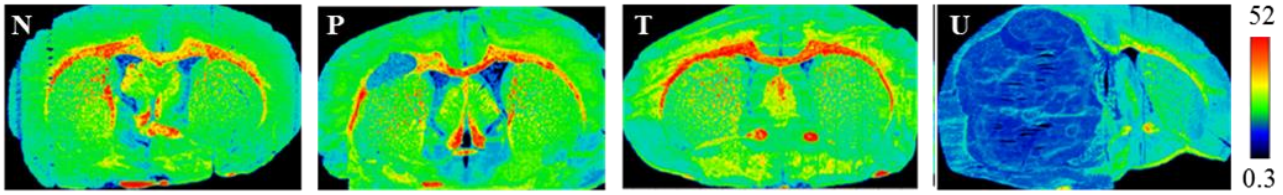

Figure 1. The example of distribution of saturated lipids (2924 1/cm) in the analyzed rat brain tissues. N correspond to control group while P, T and U correspond to animal groups subjected to implantation of three GBM cells lines. Each of the experimental group consisted of six rats. Decreased accumulation of saturated lipids in the regions of tumor development for groups P and U is clearly visible.

The FTIR qualitative analysis allowed us to indicate biologically important compounds, which may be involved in processes of GBM development. The observed differences in the distribution of biomolecules between experimental groups correlate with regions of tumor development determine during histological examination. Based on the biochemical maps, obtained especially for saturated lipids and compounds containing carbonyl groups, the GBM areas can be differentiated from surrounding brain tissue. These observations allowed us to state that 1740 1/cm and 2924 1/cm absorption bands may be considered as potential biomarkers of glioma invasiveness.

References:
[1] Su K. Y. and Lee W. L. Fourier Transform Infrared Spectroscopy as a Cancer Screening and Diagnostic Tool: A Review and Prospects, *Cancers (Basel)*, vol. 12,1 115.
[2] Czapski B, Baluszek S., Herold-Mende C., Kaminska B. Clinical and immunological correlates of long term survival in glioblastoma, *Contemp Oncol (Pozn)*, vol. 22, 1A, pp. 81-85.
[3] Wehbe K., Travo A., Eimer S., Cinque G., Barron E., Déléris G. and Forfar I. Investigation of blood vessels in glioblastoma at a micrometric scale: a comparative study by synchrotron and conventional micro-FTIR, Analytical Methods, vol. 5, pp. 6925-6932.

Microsimulation-based optimization of colorectal cancer screening strategies

Jan Poleszczuk[1], Niklas Krupka[2], Benjamin Misselwitz[2]
[1]Nalecz Institute of Biocybernetics and Biomedical Engineering, Polish Academy of Sciences, Warsaw, Poland
[2]Department of Visceral Surgery and Medicine, Inselspital Bern and Bern University, Bern, Switzerland
jpoleszczuk@ibib.waw.pl

Colorectal cancer (CRC) is a substantial public hearth burden and is in the top three cancers with respect to incidence and mortality in US and many other industrialized countries. CRC screening tests based on the endoscopic visualization of the colon have proven effective in reducing mortality, both by allowing CRC at earlier stages and by CRC prevention since adenomatous precursors of CRC can be removed during endoscopy. However, the starting age and time intervals of screening colonoscopies for optimal protection against CRC are unknown. We used microsimulation to systematically optimize screening colonoscopy schedules.

We advanced our established open-source microsimulation model CMOST [1,2] to simulate the effects of colonoscopy screening on the natural history and medical costs of CRC. In CMOST, carcinoma develops via early and advanced adenoma precursors. Altogether six adenoma stages and four carcinoma stages are considered in the model. CMOST accounts for the gender- and age-dependent risks for adenoma development, the presence of multiple adenomas, as well as their locations within the colon. CMOST microsimulation tracks the history of a general population from birth until death for a maximum age of 100 years. Adenoma initiation, progression to advanced adenoma and cancer, cancer progression, screening and surveillance are all modeled in time increments of 3 months. We used CMOST to optimize colonoscopy schedules with one, two, three and four screening colonoscopies between 20 and 90 years of age. For each scenario, we calculated life years gained, incidence and mortality reduction, and cost-effectiveness.

A single screening colonoscopy is most effective in reducing life years lost from CRC when performed at 55 years of age. Two, three and four screening colonoscopy schedules are optimal at earlier ages. For maximum reduction of incidence and mortality, screening colonoscopies need to be scheduled later in life compared to optimal age for life years lost. The optima are influenced by adenoma detection rates, individual CRC risk, and adherence to screening, with lower values for these parameters favoring a later starting age of screening. Incremental cost-effectiveness remained below 100’000 discounted US dollars per discounted life year gained except for an optimal four-colonoscopy schedule, which was not cost-effective. In a personalized approach, optimal screening would start earlier for high-risk patients and later for low-risk individuals.

Our results support screening recommendations involving an early starting age of 45 years. Our optimized screening strategies are cost-effective and save more life years than currently recommended in some countries screening starting at 50 years of age. However, efforts should be directed to personalize screening recommendations.

References:
[1] Prakash MK, Lang B, Heinrich H, et al. CMOST: an open-source framework for the microsimulation of colorectal cancer screening strategies. BMC Medical Informatics and Decision Making 2017; doi: 10.1186/s12911-017-0458-9.
[2] Deibel A, Deng L, Cheng CY, et al. Evaluating key characteristics of ideal colorectal cancer screening modalities: the microsimulation approach, GIE Gastrointestinal Endoscopy, 2021; doi.org/10.1016/j.gie.2021.02.013.

Automatic detection of intracranial aneurysms on MRA data sets

Krzysztof Psiuk-Maksymowicz[1,2], Martyna Szczyrba[3], Damian Borys[1,2]
[1]Dept. of Systems Biology and Engineering, Silesian University of Technology,
[2]Biotechnology Centre, Silesian University of Technology
[3]Faculty of Automatic Control, Electronics and Computer Science, Silesian University of Technology
ul. Akademicka 2A, 44-100 Gliwice, Poland
krzysztof.psiuk-maksymowicz@polsl.pl

Aims

Detection of the intracranial aneurysm is very important due to risk of subarachnoid hemorrhage and a very high mortality rate in case of its rupture. Intracranial aneurysms are diagnosed and monitored with imaging techniques, most often the computed tomography angiography (CTA) and the magnetic resonance angiography (MRA). Aneurysms of the cerebral arteries are relatively common [1], hence a tool that can be supportive for the radiologist in the diagnosis is desirable. The aim of this work was to develop an algorithm for an automatic detection of the intracranial aneurysms of the saccular (the most common) type. The methods found in the literature distinguish shape-based, skeleton-based, difference image based approaches [2], and recently also very often the deep learning-based approaches [3].

Methods

The developed method belongs to the skeleton-based type of approach. We used both the synthetic and the non-contrast Time-of-Flight (ToF) MRA imaging data sets. The overall workflow consists of a number of steps. The preprocessing step included the skull stripping. The next steps necessary to extract the arterial structure of the cerebrum consisted of filtering, segmentation of the blood vessels based on the region growth method, skeletonization, and detection of a branch- and end-points of the skeleton. The rules for the detection of the saccular type aneurysms were based on measures based on the morphological characteristics.

Results and Conclusion

Developed algorithm allowed for the creation of a three-dimension model of the vascular network/tree as well as quantification of each branch of the network/tree. Received three-dimensional model representing the structure and features of the indicated vascular network allowed for further analysis. It included characterization of morphological features of the vessels. The developed rules were able to find the aneurysms, but they still need to be validated on more clinical cases. The algorithm has potential both in clinical applications as well as in scientific works.

Acknowledgements

This work was supported by the National Centre for Research and Development grant No. TANGO3/420990/NCBR/2019 (KPM, DB) and by the internal grant of the Silesian University of Technology for student research groups (MS). Calculations were carried out using the computer cluster Ziemowit (http://www.ziemowit.hpc.polsl.pl) funded by the Silesian BIO-FARMA project in the Computational Biology and Bioinformatics Laboratory of the Biotechnology Centre in the Silesian University of Technology.

References:

[1] Keedy A: An overview of intracranial aneurysms. Mcgill J Med. 2006; 9(2):141-146.
[2] Hentschke CM, Beuing O, Nickl R, and Tönnies KD: Automatic cerebral aneurysm detection in multimodal angiographic images, 2011 IEEE Nuclear Science Symposium Conference Record, Valencia, Spain, 2011, pp. 3116-3120.
[3] Sichtermann T, Faron A, Sijben R, Teichert N, Freiherr J, and Wiesmann M: Deep Learning-Based Detection of Intracranial Aneurysms in 3D TOF-MRA. AJNR Am J Neuroradiol. 2019; 40(1):25-32.

Contribution of albumin and globulins to plasma oncotic pressure

Leszek Pstraś, Jacek Waniewski
Nalecz Institute of Biocybernetics and Biomedical Engineering, Polish Academy of Sciences
Ks. Trojdena 4, 02-109 Warsaw
lpstras@ibib.waw.pl

Colloid osmotic (oncotic) pressure of blood plasma is one of the major factors affecting fluid filtration or absorption across the capillary walls, thus governing the fluid balance between the vascular and extravascular space. It is widely accepted that fluid exchange between plasma and interstitial fluid takes place across various capillary endothelial gaps (pores) of different size and limited, though varied, permeability to proteins. For a quantitative analysis of transcapillary transport processes using the pore theory (e.g. to study microvascular fluid exchange during haemodialysis or fluid resuscitation), it is hence necessary to distinguish between the oncotic pressures exerted by different protein fractions characterized by different capillary reflection coefficients. This is, however, not straightforward given a nonlinear relationship between protein concentration and oncotic pressure due to the Gibbs-Donnan effect as well as protein-solvent and protein-protein interactions.

In 1981, based on the famous equations by Landis and Pappenheimer for the oncotic pressure of whole plasma and pure albumin solutions [1], Nitta et al. proposed a plausible equation for oncotic pressure exerted by non-albumin plasma proteins (treated collectively as globulins) and a combined equation for the whole plasma oncotic pressure (π, in mm Hg), based on total plasma protein concentration (TP, in g/dL) and albumin and globulins mass fractions (a and b) [2]: $\pi = a[2.8TP + 0.18TP^2 + 0.012TP^3] + b[0.9TP + 0.12TP^2 + 0.004TP^3]$. Using this approach, the first part of the above equation has been treated by some researchers as a contribution of albumin to the total plasma oncotic pressure (π_{alb}). In another approach, some researchers calculated π_{alb} using the original Landis-Pappenheimer equation for pure albumin solutions: $\pi_{alb} = 2.8A + 0.18A^2 + 0.012A^3$, where A is plasma albumin mass concentration (in g/dL). This approach, however, underestimates the oncotic pressure exerted by albumin, as it neglects the presence of other proteins in the solution and their interactions with albumin, water molecules, and ions. Here, we propose another approach, in which π_{alb} is calculated as the product of total plasma oncotic pressure and the albumin molar fraction of TP (n_{alb}, calculated assuming the average molecular weight of globulins of 170 kDa): $\pi_{alb} = \pi \cdot n_{alb}$.

We compared the performance of our proposed approach with the Nitta-based approach using random combinations of TP (range 3-12 g/dL) and various albumin/globulin ratio (AGR, range 0.5-3.0). For normal or above normal AGR ($\geq$ 1.5) and normal TP (6-8 g/dL), the discrepancies between the two approaches are negligible (error < 1%). For low AGR (<1.5) and high TP (> 8 g/dL), our approach provides values higher by 2-3%, whereas for very low AGR (<1.0) and very low TP (< 4 g/dL), the Nitta-based approach provides values higher by 1-3%. In general, the higher the globulins fraction, the higher the discrepancy between the two approaches.

Given the relatively small differences observed, the two studied approaches can be treated as practically equivalent, especially for normal or close to normal AGR and TP. Nevertheless, for detailed modelling studies, we suggest using our approach that breaks down the total oncotic pressure into the contributions of individual protein fractions according to their relative molarity in the solution, which seems to be more in line with the theory, given that osmotic pressure is a colligative property. For cases with abnormal proportions between individual globulins fractions (α_1, α_2, β, γ), more complex equations are needed to accurately describe the contributions of individual protein fractions to the total oncotic pressure [3].

References:
[1] Landis EM & Pappenheimer JR. Exchange of substances through the capillary walls. In: Handbook of Physiology, Sec. Circulation, American Physiological Society, Washington DC, 1965, pp. 961-1034.
[2] Nitta S, Ohnuki T, Ohkuda K, Nakada T, Staub NC. The corrected protein equation to estimate plasma colloid osmotic pressure and its development on a normogram. Tohoku J Exp Med, 135, 1981, pp. 43-49.
[3] Ahlqvist J. Equation for osmotic pressure of serum protein (fractions). J Appl Physiol, 96, 2004, pp.762-764.

Solid lipid nanoparticles loaded with antibacterial peptides as versatile drug delivery systems for the treatment of bacterial infections

Katarzyna Reczyńska[1], Magdalena Bialik[2], Natalia Nowosińska[2], Elżbieta Pamuła[1]
[1] AGH University of Science and Technology, Faculty of Materials Science and Ceramics, Al. Mickiewicza 30, 30-059 Kraków, Poland
[2] AGH University of Science and Technology, Faculty of Electrical Engineering, Automatics, Computer Science and Biomedical Engineering, Al. Mickiewicza 30, 30-059 Kraków, Poland
kmr@agh.edu.pl

Bacterial infections (e.g. with *Pseudomonas aeruginosa* and *Staphylococcus aureus*) are causing life-threatening pulmonary infections or extensive abscesses. Conventional treatment methods based on oral or intravenous administration of antibiotics are not always effective [1]. Antibacterial peptides (ABPs) – cationic molecules consisting of 12 – 45 amino acids are able to hamper bacterial proliferation as effectively as antibiotics, whereby bacteria are not able to develop resistance for ABPs [2]. The aim of this study was to fabricate delivery carriers for ABPs protecting them from premature degradation and allowing their direct delivery to infected sites.

Solid lipid nanoparticles based on stearic acid were manufactured using oil-in-water emulsification/solvent evaporation method. Stearic acid was dissolved in different organic solvents (i.e. dichloromethane, chloroform, acetone, ethanol) and homogenized using ultrasound probe with external water phase consisting of aqueous solution of polyvinyl alcohol (PVA). After solvent evaporation, the morphology of the obtained nanoparticles was evaluated using atomic force microscopy (AFM). Further studies focused on optimization of other processing parameters such as concentrations and volumes of organic and aqueous phases or time and amplitude of homogenization. The nanoparticles were evaluated in terms of their morphology (AFM), size and size distribution (dynamic light scattering, DLS). In the end, different ABPs (i.e. bacitracin, nisin and LL-37) were encapsulated in lipid nanoparticles. The morphology, size and encapsulation efficacy of ABPs were determined along with the evaluation of cytocompatibility of the nanoparticles in contact with lung epithelial cells and fibroblasts.
The selection of organic solvent was crucial for fabrication of lipid nanoparticles, as it was found out that only the use of chloroform and dichloromethane enabled formation of relatively uniform, spherical nanoparticles. Further studies utilized only chloroform as a solvent for stearic acid. AFM characterization and DLS measurements showed that the nanoparticles were spherical with diameters ranging from 300 nm to 450 nm. The increase of concentration of stearic acid from 2%w/v to 5% w/v lead to formation of larger and less uniform nanoparticles. On the other hand, the increase in concentration of the surfactant in water phase (i.e. PVA) or prolongation of homogenization time (i.e. from 1 min to 3 min) resulted in fabrication of smaller nanoparticles. The addition of ABPs did not influence nanoparticle morphology, however a slight decrease in nanoparticle size was observed. The encapsulation efficacy of ABPs differ depending on their hydrophilicity. It was the lowest for bacitracin, which is highly soluble in water (below 30%), while in the case of less soluble in water LL-37 over 80% of the peptide was successfully loaded into the nanoparticles. The nanoparticles were found non-cytotoxic for both lung epithelial cells and fibroblasts as long as their concentration did not exceed 50 μg/ml.
Optimized oil-in-water emulsification/solvent evaporation method allowed for successful fabrication of stearic acid based nanoparticles. The nanoparticle size and size distribution can be controlled via modification of different processing parameters such as concentration of organic and aqueous phase or homogenization intensity. The encapsulation efficacy of ABPs strongly depends on their properties, mainly solubility in water – the higher is the hydrophilicity of ABPs, the least successful is its encapsulation in lipid nanoparticles. The developed nanoparticles will be further modified to allow their efficient delivery to the lungs via inhalation or will be embedded within hydrogel to obtain antibacterial wound dressing.

This study was supported by the National Science Centre Poland (No 2018/29/N/ST5/01543) and by the Program ”Excellence Initiative – Research University” for the AGH University of Science and Technology
References:
[1] Lázár V. et al., *Nature microbiology*, 2018;3(6):718.
[2] Tong Z. et al., *Peptides*, 2014;60:32-40.

An In Vitro System To Study Suction Events In Ventricular Assist Devices In Different Pathophysiological Conditions

Maria Rocchi[1]; Libera Fresiello[1,2]; Bart Meyns[1,3]; Steven Jacobs[3]; Anna Stecka[4]; Maciej Kozarski[4]; Krzysztof Zieliński[4]
[1]Department of Cardiovascular Sciences, Katholieke Universiteit Leuven, Leuven, Belgium
[2]Institute of Clinical Physiology, National Research Council, Pisa, Italy
[3]Department of Cardiac Surgery, University Hospitals Leuven, Leuven, Belgium
[4]Nalecz Institute of Biocybernetics and Biomedical Engineering, Polish Academy of Sciences, Warsaw, Poland
maria.rocchi@kuleuven.be

Objectives: Ventricular Assist Devices (VADs) are unable to adequately adjust their flow to meet the changing cardiac demand due to their insufficient sensitivity to changes in preload. This characteristic might lead to an overpumping of the ventricle causing suction. In this study, a suction module (SM) was developed and embedded in a hybrid (hydraulic-computational) cardiovascular simulator so to test different pathophysiological conditions.

Methods: The developed SM consisted of a compliant latex tube reproducing a simplified 3D model of the ventricular apex. The SM was connected on one side to a hydraulic chamber of the simulator reproducing the pressures and flows of the left ventricle, and to the other side to a HVAD system (Medtronic). The tube was immersed in another hydraulic chamber with a controllable pressure (Pext) to actively induce suction by occluding the tube when specific hemodynamic conditions were met. The hemodynamic of two heart failure patients were simulated. Namely a dilated cardiomyopathy and an heart failure with preserved ejection fraction (HFpEF). Hypovolemia was induced in both profiles by decreasing the total circulating blood volume stepwise to induce suction events. Data collected were: HVAD flow, power, current and speed, distal and proximal ventricular pressures.

Results: Data collected for the two profiles and for decreasing preload levels evidenced suction profiles differing in terms of frequency (intermittent vs. every heart beat), amplitude (partial or complete stoppage of the HVAD flow) and shape. Typical indicators of suctions were observed in the HVAD flow patterns, e.g. plateaus on top of the peaks, a mean value close to the maximum value, saddle sequences in the falling arch of the peak and falling flanks considerably steeper than the rising ones. Different HVAD flow patterns were observed for the two patient profiles due to the different mechanical properties of the simulated ventricles.

Discussions: Results confirmed that the suction module can be used to test the sensitivity to changes in preload of VADs for different pathophysiological conditions. Overall, the HVAD flow patterns showed typical indicators of suctions observed in clinics. As such, the SM can be used in the future to test VADs and control algorithms aimed at preventing suction phenomena.

Acknowledgements: This project was supported by the internal KU Leuven C1 project (C1-18-00576), by the FWO project 1SD0321N and by the FWO International Cooperation Program VS03119N.

Split point assessment for HRnet dual model

Lukasz Roszkowiak, Jakub Zak, Krzysztof Siemion, Antonina Pater, Anna Korzynska
Nalecz Institute of Biocybernetics and Biomedical Engineering Polish Academy of Sciences
Ks. Trojdena 4 st., 02-109 Warsaw, Poland
lroszkowiak@ibib.waw.pl

Cell segmentation in bright-field microscopy image modality is still a valid scientific problem. In the literature, there are already solutions utilizing simple methods, such as automatic thresholding, clustering or active contours. Unfortunately, these methods are not robust enough to overcome the problem of background non-uniformity and luminescence irregularity. Nowadays, convolutional neural networks (CNNs) are a common solution for various segmentation tasks. These methods often overcome the limitations of classical image processing techniques, but unfortunately they require a large dataset to properly learn for a given task.
Cell segmentation often provides a basis for evaluation of cells' behavior based on shape and movement. To increase the accuracy of such evaluation, not only accurate segmentation of the cell's boundary is necessary but also combining it with the segmentation of nuclei has a positive impact. To provide co-localized cell boundary and cell nucleus segmentation we proposed a dual model. This solution consisted of two base models set in conjunction. Two models worked in parallel providing two corresponding segmentation results. One vein was trained to segment only nuclei while the other one was segmenting the whole cell area.
In this experiment, we tested the different placement of the split in the dual model. The further from the input the split is localized, the less computationally complex will be the model. Also, more parameters will be shared providing a more cohesive model. We proposed the use of HRnet [1] as a CNN backbone for this dual model. Since the used implementation of HRnet consisted of four stages (see Figure), the experiment tested if the split of the process should be after first (Model1), second (Model2) or third (Model3) stage. As a reference for this experiment we used a dual model with separation after so called *stem* part of the HRnet (Model0). Additionally, we tested the dual model with separation just after the Input layer (Model00).
For testing purposes, the input was a monochromatic image of size 128x128. The models were trained and evaluated on the publically available EVICAN dataset (providing both cell and nuclei masks), for 20 epochs (with *Adam* optimizer) and 5-fold cross-validation. The results are detailed in the following Table.

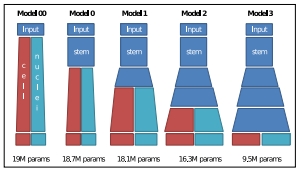

		Model00	Model0	Model1	Model2	Model3
Average Epochs		11±2	11±3	14±2	8±0	11±4
Average Accuracy	Nuclei	95.04±0.04	95.07±0.02	95.08±0.01	94.66±0.70	95.11±0.02
	Cell	92.34±3.71	95.06±0.02	95.05±0.02	94.64±0.67	95.08±0.03
Parameters:		19M	18.7M	18.1M	16.3M	9.5M

In deep CNN models, initial parts are considered to learn about image priors [2], i.e. colors, lines at a specific angle. Consequently, subsequent parts of the network learn about more complex structures, i.e. patterns. The last parts of the network have the information about objects of interest in general, i.e. faces for the face detection task.
In this study we want to segment cell as well as nuclei boundary. Both of them are much different from the biological point of view, but there are partly similar features contrasting them from the surroundings. Seeing as all models' achieved accuracy is comparable, it could be assumed that the priors useful for both types of objects are similar.
Based on the acquired results it could be concluded that positioning of the split point has little impact on final accuracy, in the case of both cell and nuclei segmentation. Given that, the accuracy is similar for all tested models, the less complex model (with fewer parameters) seems to be the optimal solution, hence we establish that Model3 is the most favorable. In the future, we plan to further investigate this problem with the increased size of images and including segmentation specific metrics like Intersection over Union (IoU).

References:
[1] Sun, Ke, et al. "Deep high-resolution representation learning for human pose estimation." *Proceedings of the IEEE/CVF Conference on Computer Vision and Pattern Recognition*, 2019.
[2] Jacobsen, Jorn-Henrik, et al. "Structured receptive fields in CNNs." Proceedings *of the IEEE Conference on Computer Vision and Pattern Recognition*. 2016.

The use of FTIR microspectroscopy for the investigation of molecular changes in the hippocampal formation after repetitive electrical stimulation

Marzena Rugiel[1], Justyna Kutorasinska[1], Agnieszka Drozdz[1], Zuzanna Setkowicz[2], Joanna Chwiej[1]
[1] AGH University of Science and Technology, Faculty of Physics and Applied Computer Science, Al. Mickiewicza 30, 30-059 Krakow, Poland
[2] Jagiellonian University, Institute of Zoology and Biomedical Research, Gronostajowa 9, Krakow, Poland
rugiel@agh.edu.pl

Temporal lobe epilepsy (TLE) is the most common form of the focal epilepsy, in which the cases of drug resistance are the most numerous [1]. There is still little known about the epidemiology of this disease [2] and therefore, there is a great need to deepen the knowledge on the pathomechanisms of TLE. For this purpose animal models of disease can be used both to develop new anticonvulsants and to observe processes associated with the epileptogenesis [3].

In the study, the influence of the repetitive transauricular electrical stimulation on the biochemical composition of the dorsal part of rat hippocampal formation was analyzed. For this purpose two groups of animals were compared, namely the rats subjected to the repetitive electroshocks and controls. After 21 days of stimulation, the brains of animals were taken, cut in cryomicrotome into 12 μm thick slices and placed on the MirrIR slides for the measurements using FTIR microspectroscopy. The accumulation and distribution of main macromolecules (proteins, lipids, cholesterol, compounds containing phosphate and carbonyl groups) in brain specimens containing the dorsal part of hippocampus was examined using the chemical mapping of the main absorption bands and their ratios and followed by the statistical evaluation of the obtained data. Additionally, the results of the biochemical analysis were correlated with the data describing animal behavior after stimulation such as the cumulative intensity and the duration of the clonic and tonic seizures. Cluster analysis based on behavioral parameters allowed to divide them into subgroups characterized by the weak or severe tonic and clonic seizures.

Performed investigation showed that the repetitive electrical stimulation leads to the biomolecular hippocampal abnormalities including the changes in protein secondary structure (increased relative level of proteins with β-sheet secondary structure) and in the distributions of saturated fatty acids, cholesterol or its esters as well as the compounds containing phosphate and carbonyl groups The observed anomalies in the protein secondary structure together with the increased accumulation of compounds containing carbonyl groups, suggest that the repetitive electroshocks induce oxidative stress and subsequent lipid peroxidation which products probably lead to the conformational changes of proteins. Decreased intensity of 1240 cm^{-1} absorption band and the increased intensity of the band at the wavenumber of 1080 cm^{-1} seem to point at the DNA damages and abnormalities in the composition phospholipids building the cell membranes but also the mobilization of glucose connected with the increased demand to energy during the post-electroshocks seizures.

References:
[1] Bodini B., Ciccarelli O. Diffusion MRI in Neurological Disorders, *Diffusion MRI (Second Edition)*, 2014, pp. 241-255.
[2] Téllez-Zenteno JF, Hernández-Ronquillo L. A review of the epidemiology of temporal lobe epilepsy, *Epilepsy Res Treat*, 2012, vol. 2012, pp. 1-5.
[3] Löscher W. Animal Models of Seizures and Epilepsy: Past, Present, and Future Role for the Discovery of Antiseizure Drugs, *Neurochem Res.*, 2017, vol. 42, no. 7, pp. 1873-1888.

Analyzing the sensitivity of a procedure for obtaining a spherical contact pair to model the hip joint

Joanna Rymek, Adam Ciszkiewicz
Faculty of Mechanical Engineering, Cracow University of Technology,
Cracow, Poland
adam.ciszkiewicz@pk.edu.pl

The hip joint is a very important structure in the leg, which is formed by the femur and a port of the pelvis called acetabulum. These bones are connected through a layer of soft tissue – called cartilage – and a complex system of ligaments. In the literature many different approaches to the modeling of the cartilage have been proposed [1, 2]. In most of the studies, the geometry of this layer is substituted with simple contact pairs – for instance: a spherical pair. Obtaining such a pair is a complex process, which encompasses 3D modeling and shape fitting. To the best of our knowledge, the sensitivity of this process has not yet been analyzed. Therefore, our main aim in this study was to analyze how the different aspects of obtaining a spherical pair for the hip joint affect the obtained results.

In order to assess the sensitivity of obtaining the contact pair, five computer tomography scans of the hip joint were segmented using *3D Slicer*. Furthermore, one of the scans was additionally segmented two times, but with different segmentation settings – to imitate the subjective aspects of medical image segmentation. In total, seven 3D models of the bones were obtained. The meshes of the femur and the pelvis were then imported into *Meshmixer*, in which the parts of the meshes corresponding to the contact regions in the joint were selected and cut. For each model, four different cuts were obtained, which included a lunar-shaped patch assumed after [3]. This resulted in twenty-eight pairs of contact meshes between the femur and the pelvis. These surfaces were then imported into *Python*, in which a sphere fitting procedure was performed. The procedure used two different numerical methods for fitting – optimizational and with linear approximation, and returned fifty-six spherical contact pairs. The pairs were then analyzed in terms of their validity and fit quality with both: visual assessment and statistics.

The obtained results showcased the sensitivity of the procedure for obtaining contact pairs. Firstly, the contact region selection had a major impact on the quality of the obtained contact pair. The best results were obtained when selecting a lunar-shaped patch on both the femur and the pelvis. Secondly, the optimizational approach to sphere fitting was more robust, as it returned more valid contact pairs and lower standard deviation for the fitted spheres. Thirdly, the lunar-patch selection was affected the least by the subjective aspects of the segmentation process.

To summarize, the study focused on analyzing the sensitivity of the procedure for modeling the hip joint using a spherical contact pair. Our findings indicated that process of selecting the contact region highly affected the obtained results. The most viable results were obtained when using lunar-shaped patches for the contact regions. Lunar patches were also the least sensitive to the subjective aspects of medical image segmentation.

References:
[1] Lopes D.S., Neptune R.R., Gonçalves A.A., Ambrósio J.A., Silva M.T. Shape Analysis of the Femoral Head: A Comparative Study Between Spherical, (Super)Ellipsoidal, and (Super)Ovoidal Shapes. *J. Biomech. Eng.*, 2015, vol. 137, no. 11, pp. 1–8.
[2] Cerveri P., Marchente M., Chemello C., Confalonieri N., Manzotti A., Baroni G. Advanced computational framework for the automatic analysis of the acetabular morphology from the pelvic bone surface for hip arthroplasty applications, *Ann. Biomed. Eng.*, 2011, vol. 39, no. 11, pp. 2791–2806.
[3] Hammond A.S., Plavcan J.M., Ward C. V. A validated method for modeling anthropoid hip abduction in silico, *Am. J. Phys. Anthropol.*, 2016, vol. 160, no. 3, pp. 529–548.

Non-invasive brain perfusion and oxygenation assessment with combined use of time-domain diffuse correlation spectroscopy and time-domain near-infrared spectroscopy

Saeed Samaei[1,2], Neda Mogharari[1], Dawid Borycki[2] Adam Liebert[1], and Michał Kacprzak[1]
[1]Nalecz Institute of Biocybernetics and Biomedical Engineering, Polish Academy of Sciences
Ks. Trojdena 4 st. 02-109, Warsaw, Poland
[2]Institute of Physical Chemistry, Polish Academy of Sciences, Kasprzaka 44/52, 01-224 Warsaw, Poland
ssamaei@ibib.waw.pl

Diffuse optical methods, such as near-infrared spectroscopy (NIRS) [1] and diffuse correlation spectroscopy (DCS) [2], enable us to monitor cerebral hemodynamics non-invasively and can be employed in clinical applications. In this study, we developed an optical instrument based on the combination of time-domain DCS (TD-DCS) and TD-NIRS to measure cerebral blood flow index (BFI), hemoglobin concentrations, and tissue oxygen saturation (StO2) at the same time. The time-domain approach, achieved by employing picosecond pulsed lasers and time-resolved single-photon detection, minimizes the influences of superficial layers by separating photons based on their traveling time from source to detector.

Our hybrid system is equipped with two picosecond diode lasers, electrically driven at 80 MHz, and generates pulses at wavelengths of 830 nm (LDH-P 830, PicoQuant, Germany) and 765 nm (VisIR-765-HP "STED", PicoQuant, Germany). To implement the TD-NIRS method, each laser was connected to a 200 μm multi-mode fiber, and the tip of the fibers was located close to each other at the sample surface. The laser modules were operated simultaneously, and the injected photons were propagated across different depths. The diffusively reflected photons were collected by two fiber bundles, with a 4 mm core diameter located 3 cm apart from the illumination points. Each detection bundle was coupled to a photomultiplier tube (PMT) detector (R7400U-02, Hamamatsu Photonics, Japan). To distinguish the detected photons based on their wavelength, two optical filters (800 nm cut-off wavelength, short-pass filter, and 790 cut-off wavelength, long-pass filter) were placed in front of the active area of the detectors. On the other hand, VisIR laser provides light of an adequate coherence length to keep path-length-resolved photons correlated at the detector and satisfies the TD-DCS technique conditions. For this aim, two single-mode fibers with 1.5 cm source-detector separations were located at the sample surface, each connected to a single-photon avalanche diode (SPAD) detectors (PDM, Micro Photon Devices, Italy). Four time correlated photon counting (TCSPC) boards (SPC-130, Becker&Hickl, Germany) were employed for time tagging the detected photons.
To validate the capability of our hybrid system to quantify depth-resolved BFI changes and StO2, we carried out an *in vivo* measurement on four healthy volunteers. The fibers were secured on the forehead, and the experiment started with a 1 min baseline, followed by a 30 s Valsalva maneuver [3]. To quantify the brain oxygenation, the distributions of time-of-flight (DTOF) of photons were acquired every 2 s. Then, by applying the modified Beer-Lambert law, the oxy- and deoxy-hemoglobin concentrations were estimated for the brain and the extra-cerebral layers based on the absolute value of variance and the total number of photons of the DTOF, respectively. The signals obtained by the TD-DCS method were recorded with 10 s temporal resolution, and by employing the time gate strategy, the photons propagated along different path-lengths were separated. Eventually, the path-length-resolved BFIs were estimated by fitting the theoretical model to the experimentally obtained autocorrelation curves.

The VM causes a reduction of the signal in both intra- and extra-cerebral layers. We observed a drop of the StO2 in the extra-cerebral layers with a larger amplitude than in the brain cortex. This result corresponds with the data published in reference [3]. The influence of VM on blood flow changes was also detected by the TD-DCS method, although due to the instrument response function broadening, separating the BFI changes at different layers is challenging.

This study is supported by the National Science Centre of Poland (NCN) in the framework of Opus 2019/33/B/ST7/01387, Preludium 2019/33/N/ST7/03024, and Maestro 2016/22/A/ST2/00313 projects.
[1] M. Kacprzak, et al., J. Biomed. Opt., vol. 12, no. 3, p. 34019, 2007.
[2] D. A. Boas, et al., Phys. Rev. Lett., vol. 75, no. 9, p. 1855, 1995.
[3] M. Clancy et al. ECBO 2015, Proc. of SPIE, Vol. 9538.

Analyzing the geometry of the articular surfaces of the bones in the radioulnar and the radiohumeral joint

Mikołaj Schabowski, Adam Ciszkiewicz
Faculty of Mechanical Engineering, Cracow University of Technology,
Warszawska 24, 31-155 Cracow, Poland
adam.ciszkiewicz@pk.edu.pl

The modeling of the elbow joint has been the focus of many biomechanical studies. Arguably, the most versatile method for modeling the joint is the finite element approach [1], which offers great flexibility in terms of element geometry and material parameters. It comes, however, at a significant numerical cost and, in some cases, convergence problems. On the other hand, the multibody framework can be used to represent the elbow using simplified mechanical constraints, usually in the form of kinematic pairs [2] – spherical, revolute and prismatic. Nevertheless, this approach limits the degrees of freedom of the joint elements. The multibody method can also be used to represent the particular elements of the joint with their simple, mechanical counterparts, as seen in [3] for the knee joint. This procedure creates a more general model, which is both inexpensive computationally and contains, in some form, all the elements of the original joint. To the best of our knowledge, such an approach has not been tested for the elbow joint yet. Therefore, our main goal in this study was to analyze the geometry of contact regions in two subjoints of the elbow, the radius-ulna joint and the radius-humerus joint, in terms of whether these regions could be replaced with spherical contact pairs.

In order to do so, three computer tomography scans of the elbow were segmented using *3D Slicer*. The obtained bone meshes were then further processed in *Meshmixer*. *Meshmixer* was also used to select and cut the parts of the meshes corresponding to the contact regions in the joint. The obtained mesh cuts were then imported into Python and two sphere-fitting procedures – optimizational and with linear approximation – were applied to obtain the contact pairs. In total, sixteen unique contact pairs of the sphere-sphere type were obtained analyzed (twelve for the radius-humerus and four for the radius-ulna).

The obtained results showcased that both the contact regions in both the radius-ulna joint and the radius-humerus joint could be successfully represented with a simple sphere-sphere contact pair. All of the obtained pairs represented proper ball-and-socket joints. Furthermore, in all of the studied cases, the standard deviation obtained for the fitted spheres did not exceed 0.35 mm and was as low as 0.02 mm. Considering that the radii of the spheres varied from 8.23 mm to 30.15 mm, the fitted spheres were of good quality. In terms of the sphere-fitting approach, higher quality sphere-fits were obtained with the opimizational approach. While both of studied methods returned mostly viable contact pairs, the spheres obtained with using optimization had lower standard deviation.

To summarize, the obtained results proved that simple, spherical contact pairs could be a valid approach to model contact regions in the two studied subjoints of the elbow. Nevertheless, it should be noted that obtaining the contact pair is a complex problem and the obtained pairs were affected by the numerical approach used for sphere fitting. This issue should be studied more in future research.

References:
[1] Renani M.S., Rahman M., Cil A., Stylianou A.P. Ulna-humerus contact mechanics: Finite element analysis and experimental measurements using a tactile pressure sensor, *Med. Eng. Phys.*, 2017, vol. 50, pp. 22–28
[2] Lemay M.A., Crago P.E. A dynamic model for simulating movements of the elbow, forearm, and wrist, *J. Biomech.*, 1996, vol. 29, no. 10, pp. 1319–1330
[3] Machado M., Flores P., Ambrosio J., Completo A. Influence of the contact model on the dynamic response of the human knee joint, *Proc. Inst. Mech. Eng. Part K J. Multi-body Dyn.*, 2011, vol. 225, no. 4, pp. 344–358

Impact of micron-sized diamond particles on barrier cells of the human small intestine

Małgorzata Siatkowska[1], Paulina Sokołowska[1,2], Kamila Białkowska[1,3], Aleksandra Zimon[1], Magdalena Grala[1], Marcin Rosowski[1,4], Kinga Kądzioła-Długołęcka[1], Piotr Komorowski[1,5], Krzysztof Makowski[1], Daniel Reda[6], Bogdan Walkowiak[1,5]
[1]Bionanopark Laboratories Sp. z o.o., Dubois Str. 114/116, 93-465 Lodz, Poland
[2]Department of Pharmacology and Toxicology, Medical University of Lodz, Zeligowskiego Str. 7/9, 90-752 Lodz, Poland
[3]Department of General Biophysics, University of Lodz, Pomorska Str. 141/143, 90-236 Lodz, Poland
[4]Lukasiewicz Research Network, Textile Research Institute, Brzezinska Str. 5/15, 92-103 Lodz, Poland
[5]Division of Biophysics, Institute of Materials Science, Lodz University of Technology, Stefanowskiego Str. 1/15, 90-924 Lodz, Poland
[6]NPR Medical, LLC, 1011 Varsity Ct, Mountain View, CA 94040, USA
m.siatkowska@bionanopark.pl

Due to their outstanding features, diamond and diamond-like materials have shown great potential in variety of biomedical applications, especially as coatings for implantable materials, drug delivery systems, or tools for bioimaging. This wide use of diamond materials calls for detailed determination of their potential health hazards, especially as some adverse cellular effects of diamond particles used in nano form have been already reported [1,2]. At the same time there is a lack of experimental data concerning micron-sized diamond particles, whereas they can serve as a good prospect for drug delivery systems competitive to their counterparts in nano form that are more prone to evoke toxic biological responses. In this context, the aim of our study was to assess the influence of micron-sized diamond particles on epithelial cells of small intestine (FHs 74 Int). These cells constitute the barrier between the gastrointestinal tract and internal environment of the human body, thus serving as one of the first routes of exposure to particles administered orally.

Human small intestine FHs 74 Int cells (ATCC® CCL-241) were used as *in vitro* model for the assessment of cell viability, apoptosis and formation of micronuclei after treatment of cells with microdiamond particles added to the culture to the final density of 18 particles per cell (that corresponded to a concentration of 12.5 μg/mL). The treatment time was specified for each test. Various microscopic methods i.e., scanning electron microscopy (SEM), transmission electron microscopy (TEM), automated bright field observations (BF) and flow cytometry were also employed to evaluate epithelial cells' movement, particle uptake and accumulation after exposure to microdiamond particles. Basic characterization of microdiamonds was also performed with the use of Raman spectroscopy and SEM.

Our results, confirmed a good biocompatibility of microdiamond particles towards FHs 74 Int cells when used at tested concentration. We did not observed cytotoxic effects of microdiamonds after 24, 48 and 72 h of incubations with barrier cells, and also microdiamonds did not induce formation of micronuclei in epithelial cells. The rate of apoptosis was not significantly different than that of untreated control cells. However, TEM imaging showed the presence of diamond particles in semi-thin slices of treated cells, while SEM showed association of diamond particles with cell surface. Additionally, according to flow cytometry analysis time-dependent accumulation of diamond particles by FHs 74 Int cells was observed up to 48 h with a subsequent plateau.

Our studies demonstrated that diamond particles of micro size can be effectively accumulated inside the cells even at very low concentration and at the same time they do not show any harmful effects on barrier intestinal cells. This renders them very promising candidate for drug delivery systems, competitive towards diamond particles of nano size that are in general more prone to evoke size-dependent toxicity. We strongly believe that the use of microdiamonds in biomedical filed, especially as drug carriers is still undervalued, and should be developed with the same attention as is paid for the diamonds of nano size.

References:

[1] Huang, YA., Kao, CW., Liu, KK. et al. The effect of fluorescent nanodiamonds on neuronal survival and morphogenesis. *Sci Rep* 4, 6919 (2014), pp. 1-10
[2] Karpeta-Kaczmarek J., Dziewięcka M., Augustyniak M., et al., Oxidative stress and genotoxic effects of diamond nanoparticles, *Environ Res* 148 (2016) pp. 264–272

Application of image analysis methods to evaluate histopathological slides in the study of prognostic factors of inflammatory spindle cell lesions

Krzysztof Siemion[1,2], Anna Korzyńska[1], Łukasz Roszkowiak[1], Jakub Żak[1], Antonina Pater[1], Joanna Reszeć-Giełażyn[2]
[1]Nalecz Institute of Biocybernetics and Biomedical Engineering PAS, Warsaw, Poland
[2]Medical University of Białystok, Poland
krzysztof.siemion@ibib.waw.pl

Inflammatory spindle cell lesions encompass benign reactive processes, pseudoinflammatory tumors (IPTs), and intermediate grade neoplasms, inflammatory myofibroblastic tumors (IMTs) [1]. IMTs can be localized most frequently in the abdominal cavity of children and adolescents [2, 3]. IPT never recurs after resection and does not metastasize [1]. IMT is characterized by a high recurrence rate after excision and low metastatic potential [4]. Assessment of the histological slides by pathologists is highly subjective [5]. Therefore, the idea of automatic (independent from human control) and semiautomatic (partly dependent on human control) image analysis method application was invented to support and objectify a diagnostic process [5]. Actually, deep learning methods are thought to be a solution to the problem and their application results seem to be promising [6]. They are based on the learning of artificial neural networks. The networks gain discriminative abilities by being presented with desired and adverse elements of an image, to manage to classify image fragments into definite categories [6]. The presence of myxoid intercellular content, necrosis, ganglion-like cells, giant cells, high mitotic activity, and increased cellularity are adverse factors, which worsen the prognosis after resection [2].
In this study, we would like to verify, if histopathologic diagnostics, supported by the use of image analysis, correlates more strongly with prognostic and predictive factors of inflammatory myofibroblastic tumors in comparison with the conventional assessment provided by a pathologist without computational assistance.
Prognostic factors have already been assessed manually by independent pathologists.

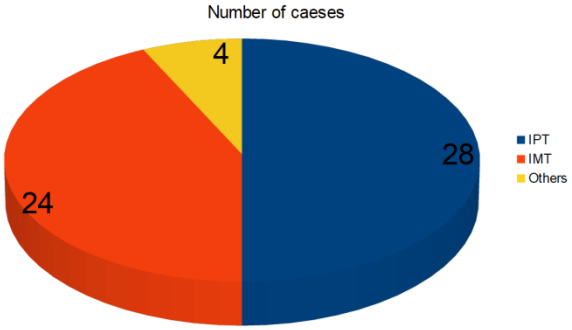

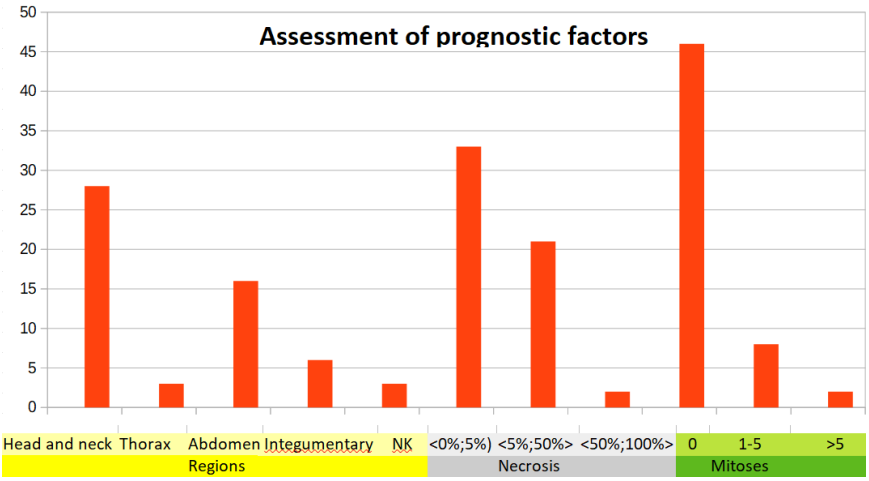

NK – not known
Deep learning methods will be applied to assess prognostic factors of inflammatory spindle cell lesions and their results will be compared with manual estimation provided by humans.

References:

[1] Kutok JL, Pinkus GS, Dorfman DM, Fletcher CDM. Inflammatory pseudotumor of lymph node and spleen: An entity biologically distinct from inflammatory myofibroblastic tumor. Human Pathology. Vol. 32, no. 12 pp. 1382-1387.
[2] Lindberg MR, Cassarino DS, Gardner J, Lucas D, Quick CM, Stallings-Archer K. Diagnostic Pathology – Soft Tissue Tumors. Third edition Elsevier 2019. pp. 196-201.
[3] Mocellin S. Soft Tissue Tumors: A Practical and Comprehensive Guide to Sarcomas and Benign Neoplasms. Springer Nature. pp. 439-442.
[4] Antonescu CR, Blay JY, Bovee JVGM, Bridge JA, Cunha IW, Dei Tos AP, et al. WHO Classification of Tumours: Soft Tissue and Bone Tumours. Fifth edition. Lyon: International Agency for Research on Cancer, 2020. pp. 109-111.
[5] Leveque L, Liu H et al.: On the Subjective Assessment of the Perceived Quality of Medical Images and Videos, 2018 Tenth International Conference on Quality of Multimedia Experience (QoMEX), IEEE.
[6] Alom MZ, Yakopcic C et al.: Microscopic Nuclei Classification, Segmentation and Detection with improved Deep Convolutional Neural Network (DCNN) Approaches, arXiv:1811.03447.

Feasibility analysis of suppressed water peak in single voxel 1H MRS thermometry

Marcin Sińczuk[1], Jacek Rogala[2], Nikodem Hryniewicz[1], Ewa Piotrowska-Janko[1,3], Piotr Bogorodzki[1,3]
[1]Nalecz Institute of Biocybernetics and Biomedical Engineering - Polish Academy of Sciences, Warsaw, Poland, Ks. Trojdena 4
[2]Nencki Institute of Experimental Biology – Polish Academy of Sciences, Warsaw, Poland, Ludwika Pasteura 3
[3]Faculty of Electronics and Information Technology, The Institute of Radioelectronics and Multimedia Technology,Warsaw, Poland, Nowowiejska 15/19
msinczuk@ibib.waw.pl

Introduction: 1H-Magnetic resonance spectroscopy (MRS) thermometry is a non-invasive method of measuring internal temperature of the brain. This method exploits the temperature dependence of the water proton chemical shift in reference to temperature-independent compounds in single voxel MRS (svMRS) spectra. This temperature dependency correlates linearly with the water–chemical shift by approximately −0.01 ppm/°C [1]. Therefore, the water peak frequency is a key element of the temperature measurements, giving brain temperature estimates with 0.2-0.8°C [2] accuracy. In our study we compare two point resolved spectroscopy (PRESS) spectra: one with water signal suppressed and one with unsuppressed water signal in order to evaluate an influence of water suppression pulses on water peak frequency.

Methods: 180 healthy adult subjects (87 female, 93 male, mean age 28±6 y) have been recruited. The MR in vivo scans were completed on a 3T GE Discovery MR 750w scanner (IBBE PAS, Warsaw, Poland) fitted with a standard 8-channel head coil. All spectral data was acquired using single-voxel point-resolved spectroscopy (PRESS) sequence using following settings: TR(ms)/TE(ms) = 1500/25; 96 averages; voxel 20x20x20 mm^3; 5 kHz bandwidth; 4096 samples. Two PRESS scans per subject have been performed with voxel of interest (VOI) positioned in the right inferior parietal lobule. Data from 360 spectral scans were processed using home written scripts developed on MATLAB platform based on an open source software package FID-A [3]. Signal preprocessing was composed of RF coil and average combination and phase correction. Parametrization (amplitude, FWHM, central frequency) of the peaks was performed using Lorentzian line shape fit. Parametrization datasets have been analyzed using a two-sided Student's t-test where $p<0.01$ was considered as statistically significant.
Results: Peak frequency difference 0.06 ppm is significant at $p<0.001$. Significant changes with $p<0.001$ in amplitude at -1.791·10^7 signified that water suppression occurred correctly. FWHM change of 0.042 Hz was significant at $p<0.001$.

	Frequency [ppm]	Amplitude [u.i.]	FWHM [Hz]
Water Suppressed	4.613	7.4622·10^5	0.1604
Water Unsuppressed	4.607	1.866·10^7	0.1562
Difference	0.06	-1.791·10^7	0.042

Discussion: The comparison shows statistically significant ($p<0.001$) shift in peak frequency between suppressed and unsuppressed water peaks which may in turn result in temperature overestimation in the 0.5°C range. Therefore we conclude that in order to measure temperature unsuppressed water spectra in tandem with suppressed spectra are necessary.
References:
[1] Hindman, J. C. (1966). Proton resonance shift of water in the gas and liquid states. The Journal of Chemical Physics, 44(12), 4582-4592.
[2]Childs, C., Hiltunen, Y., Vidyasagar, R., & Kauppinen, R. A. (2007). Determination of regional brain temperature using proton magnetic resonance spectroscopy to assess brain–body temperature differences in healthy human subjects. Magnetic Resonance in Medicine: An Official Journal of the International Society for Magnetic Resonance in Medicine, 57(1), 59-66.
[3] Simpson, R., Devenyi, G. A., Jezzard, P., Hennessy, T. J., & Near, J. (2017). Advanced processing and simulation of MRS data using the FID appliance (FID-A)—an open source, MATLAB-based toolkit. Magnetic Resonance in Medicine, 77(1), 23-33.

Cell nuclei detection in breast cancer cytology images with U-Net neural network

Marcin Skobel, Marek Kowal and Józef Korbicz
Faculty of Computer, Electrical and Control Engineering,
University of Zielona Góra, Poland, Licealna 9, 65-417
M.Skobel@issi.uz.zgora.pl

The quantification of cell nuclei in cytological or histological images is essential for disease diagnosis and clinical trials. To implement such systems, we need algorithms for precise detection and segmentation of cell nuclei. One of the important challenges tackled is to detect cell nuclei when cellular material creates complex clumps with overlapped cells. Recent studies have shown that deep learning usually yields promising results in this case. To train such a neural network, we need large amounts of manually segmented images. The preparation of such data is very time-consuming. It is much simpler and faster to label only the centers of the cell nuclei [1]. Therefore, we propose and test the cell nuclei detection method based on the automatic extraction of cell nuclei centers with the U-Net neural network's help.

The developed system takes as the input an RGB image of any size and determines coordinates of cell nuclei centers. The heart of the system is the U-Net neural network, which is used to determine the probability map of cell nucleus centers. Compared to the original U-Net structure, ours is equipped with Batch Normalization and Dropout layers. It has 3 downsampling and upsampling layers instead of four, and the number of filters in convolutional layers is reduced by half [2]. The U-Net generates the probability map by scanning the input image using a sliding window (128x128px) with stride 64px. Resulted probability map is thresholded (T=0.2, 0.4, 0.6, 0.8); thus, we obtain a binary mask of cell nuclei centers. Finally, we find connected components in the binary mask and calculate their centroids. The neural model was trained using the ADAM algorithm and the binary cross-entropy loss function. At each training epoch 95000 input patches (128x128px) were sampled from 95 breast cancer cytological images (1583x828px) coming from 25 patients. We generated validation patches (85000) only once before training from 17 images (6 patients). All patches were subjected to a random augmentation with a probability of 0.8. The test set consisted of 28 images from 10 patients. Training, validation, and test datasets were disjoint.

The quality of nuclei detection was assessed by comparing the detected nuclei centroids with reference centers marked manually. For each reference nuclei center, the nearest detected center was determined using the Hungarian algorithm with Euclidean distance. If the distance between these positions is at most r_{max}=150, it is considered a match (True Positive). Unmatched reference centers and unmatched detected centers are evaluated as False Negatives and False Positives, respectively.

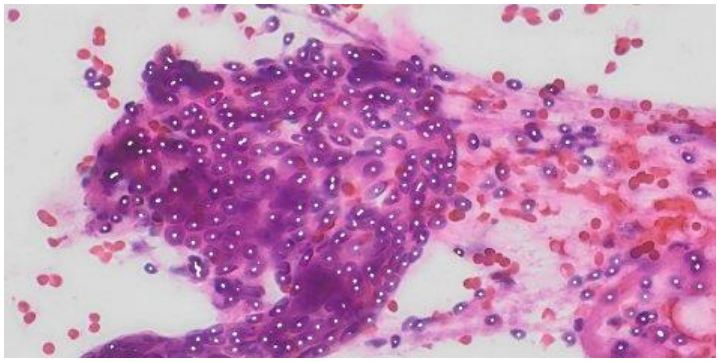

Fig 1. Result of cell nuclei detection

T	Precision	Recall	F1-score
0.2	0.62	0.92	0.74
0.4	0.62	0.87	0.73
0.6	0.63	0.83	0.72
0.8	0.63	0.75	0.69

Table 1. Quality of detection

The experiment shows that the method has a relatively high sensitivity (recall = 0.92) but unfortunately generates too many false centroids (precision = 0.63). Further research work will focus on solving this problem. After solving this problem, we plan to use the developed model to generate cell nuclei seeds for a more advanced segmentation algorithm that will deal with overlapping cells.

References:

[1] Höfener H., Homeyer A., Weiss N., Molinb J., Lundströmb C., Hahn H.: Deep learning nuclei detection: A simple approach can deliver state-of-the-art results, Computerized Medical Imaging and Graphics, vol. 70, pp. 43-52, 2018.
[2] Ronneberger O., Fischer P., Brox T.: U-Net: Convolutional Networks for Biomedical Image Segmentation, Medical Image Computing and Computer-Assisted Intervention (MICCAI): LNCS, vol. 9351, pp. 234-241, 2015.

A framework for modeling and efficacy evaluation of treatment of cancer with metastasis

Jaroslaw Smieja, Krzysztof Psiuk-Maksymowicz, Andrzej Swierniak
Silesian University of Technology, Akademicka 16 44-100 Gliwice, Poland
Jaroslaw.Smieja@polsl.pl

Abstract. The paper is concerned with modeling of tumor growth, taking into account chemo- and radiotherapy and metastasis. The model consists of two compartments, one representing the primary tumor, sensitive to chemo- and radiotherapy and another, representing metastatic tumor. A population of virtual patients is created by sampling model parameters. Kaplan-Meier survival curves are used to analyze the inuence of model parameters on treatment efficacy, with one standard treatment protocol.

Keywords: Chemotherapy, Radiotherapy, Metastasis, Modeling.

The authors were supported by NCN grant (National Science Centre, Poland) DEC-2020/37/B/ST6/01959 and SUT statutory research funds.
Calculations were partially performed on the Ziemowit computational cluster (http://www.ziemowit.hpc.polsl.pl) created in the PO G.02.01.00-00-166/08 project (BIO-FARMA) and expanded in the POIG.02.03.01-00-040/13 project (Syscancer) and PBS3/B3/32/2015 project (Biotest).

Osteosarcoma cells in early and late passages as the cancer progression model *in vitro* for assessing responsiveness of cancer cells to silver nanoparticles

Paulina Sokołowska[1,2], Małgorzata Siatkowska[1], Kamila Białkowska[1,3], Marcin Rosowski[1,4], Piotr Komorowski[1], Bogdan Walkowiak[1,5]
[1]Molecular and Nanostructural Biophysics Laboratory, Bionanopark Sp. z o.o., Lodz, Poland
[2]Department of Pharmacology and Toxicology, Medical University of Lodz, Lodz, Poland
[3]Department of General Biophysics, University of Lodz, Pomorska 141/143, 90-236 Lodz, Poland
[4]Lukasiewicz Research Network, Textile Research Institute, Department of Chemical Textiles Technologies, Brzezinska Str. 5/15, 92-103 Lodz, Poland
[5]Department of Biophysics, Institute of Materials Science, Lodz University of Technology, Stefanowskiego 1/15, 90-924 Lodz, Poland
p.sokolowska@bionanopark.pl

The aim of study was to investigate whether cancerous progression of osteosarcoma cells can affect mechanisms of action of silver nanoparticles (SNPs). Antiproliferative and pro-apoptotic properties of SNPs render them an interesting candidate for cancer therapy. They can be used in medical imaging, in drug delivery and biosensing systems [1] However, the use of SNPs as a safe and efficient material in cancer treatment needs understanding of all the mechanisms related to their anticancer activity. We established an *in vitro* model of cancer progression closely resembling processes occurring *in vivo* in terms of protein profile. Differentially Expressed Proteins (DEPs) derived from cancer cells or tissue samples have been widely investigated as biomarkers for diagnosis or prognosis assessment as they may significantly contribute to better understanding of cancer biology and the development of new treatment strategies [2-3].
We established a model of cancer progression using osteosarcoma cell line Saos-2 in early (6-21) and late (167-182) passages. To study whether cancerous progression of cultured osteosarcoma cells could affect vulnerability to polydispersed SNPs, we compared the cytotoxic and genotoxic potentials and performed comparative proteomic analysis of Saos-2 cells in early and late passages after contact with SNPs.
Evaluation of cytotoxic and genotoxic potentials of SNPs demonstrated that cells in the early stage of cancerous progression, i.e., Saos-2 cells in early passages were significantly more vulnerable to SNPs toxicity than the cells in advanced stage of cancer development, i.e., Saos-2 cells in late passages. Altered cell responsiveness to SNPs was reflected by a significant shift towards higher concentrations of nanoparticles in Saos-2 cells in late passages compared to the early passage cells. Our study also showed that effects of SNPs on proteomic profile of osteosarcoma cells were dependent on the passage number (early/late) resembling characteristics of cancer progression. We identified considerably higher number of DEPs in Saos-2 cells in early passages compared to the late passage cells. SNPs-induced upregulation of proteins involved in oxidative stress, ER stress response and mitochondrial damage was observed only in Saos-2 cells in early passages.
Significantly reduced responsiveness of the late passage Saos-2 cells to SNPs toxicity may partly result from diminished accumulation of nanoparticles on the cell membrane and inside the cells. Comparing proteomic profile, we also hypothesize that Saos-2 cells in advanced stage of cancerous progression may develop additional mechanisms protecting them from SNPs toxicity.

References:
[1] G.M. Vlasceanu, S. Marin, R.E. Tiplea, I.R Bucur, M. Lemnaru, M.M. Marin, A.M. Grumezescu, E. Andronescu. Silver nanoparticles in cancer therapy. In *Nanobiomaterials in Cancer Therapy. Applications of Nanobiomaterials* Volume 7; Grumezescu, A.M., Ed.; William Andrew, 2016; pp 29-56
[2] J. Burns, C.P. Wilding, R. Jones, P. Huang. Proteomic research in sarcomas – current status and future opportunities. *Semin. Cancer Biol*. 2020, 61, pp. 56-70.
[3] Y. Suehara, D. Kubota, K. Kikuta, K. Kaneko, A. Kawai, T. Kondo. Discovery of Biomarkers for Osteosarcoma by Proteomics Approaches. *Sarcoma* 2012, 425636, pp. 1-15.

Bioplatform development for DNA-azathioprine interaction studies

Anna Sołdatowska, Marcin Urbanowicz, Agnieszka Paziewska-Nowak, Kamila Sadowska, Dorota Pijanowska
Nalecz Institute of Biocybernetics and Biomedical Engineering Polish Academy of Sciences
Ks. Trojdena 4 st. Warsaw, Poland
asoldatowska@ibib.waw.pl

The mechanism of drugs interaction with DNA has been searched thoroughly during the past decades. Understanding these procesess can provide information of undoubted importance, such as a prompt alert to harmful substances, explain most of the biological mechanisms or increase the effectiveness of the therapies – while minimizing side effects of drugs, which mode of action is still unknown [1]. An example of such molecule is an azathioprine (AZA) – the most commonly used immunosuppressive prodrug. Like any pharmacological therapy, the one with AZA also has many side effects that are related to the mechanism of action, which has not been clearly described so far [2]. To provide safety and efficency of therapy, the patient must undergo regular tests, but unfortunately there it is not always possible to obtain conclusive results. Therefore, there is a need for comprehensive description of AZA-DNA interactions, wich could be the first step in developing an effective and selective method for AZA determination, and thus improvement of applied therapies.

The aim of this research was to develop reliable, stable and reproducible biosensing platform for the study of the AZA – DNA interaction. In this work, various strategies of oligonucleotides immobilization on gold surface were tested: (1) chemisorption of thiolated DNA (HS-DNA), (2) covalent immobilization of H_2N-DNA on self-assembled monolayer (SAM) with carboxyl terminal groups, (3) covalent immobilization of H_2N-DNA on fourth generation poly(amidoamine) dendrimer (PAMAM 4G) layer. The immobilization of single-stranded oligonucleotides was followed by hybridization reaction, to obtain a double-stranded DNA biosensing layer. Each step of gold surfaces modification was monitored by surface plasmon resonance (SPR), a technique which gives a measurable values representing efficiency of the process.

The best results were obtained with the use of H_2N-DNA, which required the usage of additional compounds forming the intermediate layer on the surface. It gave a better control over the distribution of the immobilized H_2N-DNA strand compared to HS-DNA, which was directly applied to the gold surface, resulting in increased efficiency of the hybridization process. The final outcome of the performed modifications was a double-stranded DNA layer, with a packing density of approximately 2 ng/mm^2. The constructed biosensors were used for the first experiments with azathioprine, confirming the existing interaction. Conclusions regarding the possible interaction were also verified by electrochemical methods.

The results and conclusions drawn from this study will be used for further detailed analysis of the azathioprine interaction with DNA strands of various sequences and lengths. In the future, the obtained knowledge may form the basis for extending research on other substances with immunosuppressive activity, e.g. azathioprine metabolites. More investigation studies in this area may result in the design of DNA specific sequences for the needs of biosensors. Such a broad understanding of the topic can provide modern tools for selective detection of immunosuppressive substances in complex real samples and significantly improve the control of the therapy and its effectiveness.

References:
[1] Sirajuddin M.; Ali S.; Badshah A.; Drug-DNA interactions and their study by UV-Visible, fluorescence spectroscopies and cyclic voltammetry, *Journal of Photochemistry and Photobiology B: Biology*, 2013, vol. 124, pp. 1-19
[2] Kim M.J.; Choe Y.H. Monitoring and Safety of Azathioprine Therapy in Inflammatory Bowel Disease, *Pediatric Gastroenterology, Hepatology & Nutrition*, 2013, vol. 16, no. 2, pp. 65-70

Mathematic modeling of automated peritoneal dialysis: Effect of schedules with variable temporal patterns of administration of dialysis fluid with different glucose concentration

Joanna Stachowska-Pietka[1], Beata Naumnik[2], Ewa Suchowierska[2], Jacek Waniewski[1], Bengt Lindholm[3]
[1] Nalecz Institute of Biocybernetics and Biomedical Engineering, Trojdena 4 Street, 02-109 Warsaw, Poland.
[2] The I[st] Department of Nephrology and Transplantation with Dialysis Unit, Medical University of Bialystok, Zurawia 14 Street, 15-540 Bialystok, Poland
[3] Department of Clinical Science, Intervention and Technology, Division of Renal Medicine and Baxter Novum, Karolinska Institutet, Novum Research Center, level 5, SE-141 57 Stockholm, Sweden.
jstachowska@ibib.waw.pl

In automated peritoneal dialysis (APD) with so-called dry day regimen, the APD cycler infuses dialysis fluid into the peritoneal cavity during consecutive exchanges during the night, leaving the cavity empty during the day. One strategy - thought to be conducive to achieve targets for water removal - is to stepwise increase the concentration of glucose in infused dialysis fluids during the APD session by connecting dialysate bags with increasing glucose content. However, the evidence that this strategy is effective is lacking. We investigated the impact of different APD schedules - with same total amount of glucose administrated and same volumes of dialysis fluid infused - for different temporal combinations of dialysis fluid with two different glucose concentrations, on net ultrafiltration (UF) during each consecutive exchange, total water removal during the whole APD session in case of a dry day APD regimen, and glucose efficiency to remove water.

Peritoneal transport of fluid and solutes was modeled using the spatially distributed model that considers the kinetics in the peritoneal cavity and the transport across the peritoneal tissue. A typical 8-hour APD session was simulated with 5 exchanges of 2 L of dialysis fluid with glucose 1.36% (G1) and 2.27% (G2), each stored in a 5 L container. Five schedules of fluid delivery were considered: S1) mixing both containers and delivering the same mean glucose concentration infused at each exchange throughout the session, S2) glucose concentration increasing between consecutive cycles starting from the lower concentration G1 (refilling of the G1 container occurring after each infusion from G2 container), S3) glucose concentration increasing from G1 (no refilling, dialysis fluid from G2 container applied after emptying G1 container), S4) as in S2 but with decreasing glucose concentration from G2 to G1, S5) as in S3 but with decreasing glucose concentration from G2. Glucose efficiency was calculated as the total UF divided by the glucose mass administered during the APD session.
Numerical simulations of S1, with a constant mean glucose concentration of 1.82% administered in each exchange, predicted lower UF during the first (UF1) as compared with second (UF2) exchange, Table 1. Similarly, lower initial UF was obtained also for schedules (S4 and S5) with higher initial glucose concentration while schedules (S2 and S3) with lower initial glucose concentration resulted in even slightly negative UF during the initial exchange. The simulated values of UF for the whole APD session, and glucose efficiency to remove water, were similar for the different administration schedules, being the highest (UF 1250 mL) for S4 and the lowest (1180 mL) for S3.

Table 1. Simulated water removal (in mL) during consecutive night exchanges (UF1, ..., UF5), total UF of whole APD session, and glucose efficiency (mL/g) for each administration schedule.

Schedule	UF 1	UF2	UF 3	UF 4	UF 5	Total UF	Glucose Efficiency
S1	131	263	267	269	274	1204	6.64
S2	-24	217	320	342	378	1234	6.80
S3	-24	90	241	419	454	1180	6.50
S4	288	319	245	201	196	1250	6.89
S5	274	429	297	123	97	1221	6.73

The observed lower UF efficiency of the initial APD exchange is a phenomenon that, as reported previously, appears to be due to adaptative changes of the peritoneal tissue following APD treatment after a dry day. The model suggests that while the administration schedule influences UF of the initial exchange(s), it has a negligible impact on the overall water removal during the APD session. However, different schedules might influence patient comfort, depending on catheter function, fluid status and residual renal function.

Lung function impairment in CDH – from fetus diagnostics to young child examination

Barbara Stankiewicz, Krzysztof J. Pałko, Marek Darowski
Nalecz Institute of Biocybernetics and Biomedical Engineering Polish Academy of Sciences,
4 Trojdena Street, 02-109 Warsaw, Poland
bstankiewicz@ibib.waw.pl

Aim. Congenital diaphragmatic hernia (CDH) is a rare newborn disease (1/2500) with a high mortality rate (20-40%). Severe hypoplasia and inhomogeneity of lungs make ventilation therapy of the infants very difficult, especially at the beginning of treatment, aimed at infant stabilization and preparation for hernia repair. Lung function impairment in CDH survivors was reported in long-term outcome studies. Availability and usefulness of different diagnostics tools of lung assessment in fetus, infant and young child, described in the literature, were analyzed in this study.

Methods. The studies, published between 2016 and 2021, concerning diagnostics of fetus lung hypoplasia, postnatal lung examination and outcomes pulmonary function tests made in CDH survivors (<12 years) have been searched using Google Scholar, PubMed, Web of Science.

Results. 2D/3D Ultrasound (US) and MRI constitute the gold standard in fetus lung assessment in CDH, made between the 24^{th} and 34^{th} week of pregnancy. Besides liver herniation, LHR (lung-to-head ratio) and (observed/expected) O/E LHR (in %), O/E TFLV (observed/expected total fetus lung volume), PPLV (% predicted lung volume) are the most widely used parameters in fetus diagnostics. They have prognostic value regarding CDH severity, need for ECMO use in ICU or survival rate, but do not translate directly into ventilation management. In the postnatal period, prior to hernia repair, usually, thorax X-ray scan is carried out, constituting the gold standard, to date. More rarely, MRI is repeated and CT scans are made [1]. In other cases, single-breath- or multi-breath washout techniques (SBW or MBW) are applied, if adequate equipment is available in the ICU. They enable to determine accurately FRC (funtional residual capacity) and the parameters of lung ventilation inhomogeneity (e.g. LCI, moments ratio, etc.), which can be useful in ventilation therapy. However, they remain in the experimental stage [2]. Most studies using MBW/SBW published, so far, had been carried out with CDH survivors within outcome studies. In the last, FOT (forced oscillation technique), body plethysmography and spirometry are utilized [3].

Conclusion There is a gap between prenatal lung diagnostics and guidelines for postnatal ventilation management. For more effective and safer treatment of CDH infants, a new method of lung inhomogeneity assessment which might be directly applied in ventilatory support is needed. It is unlikely that MBW will be utilized in the nearest future in everyday clinical practice, due to the time-consuming, cost of the method and difficulty with standardization. However, lung tests using MBW or FOT constitute a good alternative to spirometry, in the case of neonates, infants and preschool children, born with CDH

References:

[1] K.G. Snoek, I.K.M. Reiss, A. Greenough, et al. Standardized Postnatal Management of Infants with Congenital Diaphragmatic Hernia in Europe: The CDH EURO Consortium Consensus - 2015 Update, *Neonatology*, 2016, vol. 110, pp. 66-74. https://doi.org/10.1159/000444210.

[2] R. Auten, C. Ren, O. Yilmaz, T.L. Noah. Pediatric pulmonology year in review 2016: Part 2. *Pediatric Pulmonology*, 2017, vol. 52, pp. 1219– 1225. https://doi.org/10.1002/ppul.23719.

[3] L.C.C Toussaint-Duyster, M.H.M. van der Cammen-van Zijp, M. Spoel, et al. Lung function in school-aged congenital diaphragmatic hernia patients; a longitudinal evaluation, *Pediatric Pulmonology*, 2019, vol. 54, pp. 1257- 1266. https://doi.org/10.1002/ppul.24375.

Cough: is this seemingly unfavorable phenomenon profitable during thoracentesis?

Anna M Stecka[1], Marcin Michnikowski[1], Elżbieta M Grabczak[2], Monika Zielinska-Krawczyk[2], Rafał Krenke[2], Tomasz Gólczewski[1].
[1]Nalecz Institute of Biocybernetics and Biomedical Engineering, Polish Academy of Sciences; Księcia Trojdena 4, 02-109 Warsaw, Poland
[2]Department of Internal Medicine, Pulmonary Diseases & Allergy, Medical University of Warsaw, Banacha 1a, 02-097 Warsaw, Poland
astecka@ibib.waw.pl

Too excessive pleural pressure (Ppl) fall, which may follow pleural fluid withdrawal during therapeutic thoracentesis (TT), carries the risk of several complications, e.g., pneumothorax or re-expansion pulmonary edema. Cough during TT is commonly considered as an unfavorable phenomenon and it is frequently treated an indication for TT termination. The aim of the work was to verify our initial hypothesis that cough protects against too significant Ppl fall [1].

With the use of a pleural manometer of own construction [2], Ppl was measured during intervals between periods of fluid withdrawal (Fig.1). Changes in Ppl (ΔPpl) at functional residual capacity between the ends and beginnings of both these intervals and withdrawal periods were considered. Statistical significance of cough influence on the ΔPpl distribution shape was analyzed by means of the two-sample Kolgomorow-Smirnow test, whereas the nonparametric skew was used to determine the influence nature.

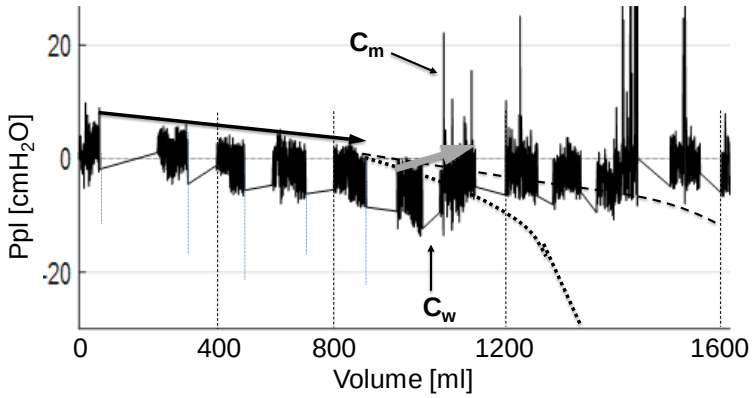

Fig.1. An example of Ppl measurements between periods of fluid withdrawal.
Bold grey arrow – Ppl increase associated with a cough episode (during fluid withdrawal, thin black long arrow – a trend of Ppl (at FRC) decline before this first cough episode, dashed and dotted lines – expected Ppl decrease assuming normal lungs and lungs entrapment, respectively. Cm – cough identified by rapid changes of Ppl during measurement. Cw – cough noted manually during withdrawal.

Data from 59 patients (59% females; median age 66 years, IQR=21; withdrawn pleural fluid volume 2±1 L) were analyzed. Cough caused statistically significant changes in ΔPpl distributions both for withdrawal and measurement periods ($p<0.001$); in particular, it decreased the left tail of the distribution for withdrawal periods and increased the right tail of the distribution for measurement periods. Thus, in average, Ppl fall during withdrawal was less significant and ΔPpl during measurement period was more positive if cough was present (Fig.1).
Our results confirm a profitable influence of cough on Ppl changes during TT and suggest that it may protect against excessive Ppl fall caused by pleural fluid withdrawal. Thus, cough should not be suppressed during TT; on the contrary, it may be applied as a very simple maneuver to reduce the risk of TT complications.
References:

[1] Zielinska-Krawczyk M, Michnikowski M, Grabczak EM, Palko KJ, Korczynski P, Golczewski T, Krenke R. Cough during therapeutic thoracentesis: Friend or foe? *Respirology* 2015;20(1):166-168.
[2] Krenke R, Guc M, Grabczak EM, Michnikowski M, Pałko KJ, Chazan R, Gólczewski T. Development of an electronic manometer for intrapleural pressure monitoring. *Respiration* 2011;82:377-85.

Hemoglobin spectra affect estimation of concentration and oxygen saturation: blood-lipid phantom study

Aleh Sudakou[a,], Anna Gerega[a], Helene Isler[b], Piotr Sawosz[a], Daniel Ostojic[b], Martin Wolf[b], and Adam Liebert[a]
[a]Nalecz Institute of Biocybernetics and Biomedical Engineering, Warsaw, Poland
[b]University Hospital Zurich, University of Zurich, Zurich, Switzerland
asudakou@ibib.waw.pl

Aims: Near-infrared spectroscopy (NIRS) is an established optical tool that can be used to monitor non-invasive, in real-time, and at the patient's bedside, the concentration of hemoglobin inside tissue, which can help e.g. study physiological conditions or monitor clinical interventions [1]. A number of extinction coefficients (ε) of hemoglobin have been measured by different groups, which have visible differences. Small variations in ε may cause significant differences in the calculations of concentrations [2]. In this work, we study the effect of ε spectra on quantification of concentrations of oxy- (HbO_2), deoxyhemoglobin (Hb), and oxygen saturation (StO_2) using multi-wavelength time-resolved NIRS measurements performed on a series of blood-lipid phantom measurements.

Methods: The data were obtained on blood-lipid phantoms during a series of controlled dynamic deoxygenation cycles with various amounts of blood using the phantom and a similar protocol as in [3]. The main components of the phantom were water, Intralipid, and blood. Blood was added before oxygenating the phantom, resulting in 20, 35, 55, and 70 ml of blood. The optical properties of the mixture containing 55 ml of blood are close to the typical optical properties of tissue. The blood was deoxygenated by yeast and oxygenated by bubbling oxygen from an oxygen bottle. The oxygen saturation covered a continuous range from 100% to 0%. The following were controlled: 7.4 pH level, 37 °C temperature and a constant mixing speed of 500 rpm.

The time-domain NIRS system [1] recorded the distribution of times of flight of photons (DTOFs) simultaneously at 16 spectral channels of approximately 12.5 nm width in the range from 680 to 880 nm. The concentrations of HbO_2 and Hb were calculated using the fitting method and the Beer-Lambert law. The calculations were repeated for four ε data sets to study the effect of the choice of the hemoglobin spectra on the estimation of concentration and oxygen saturation. The residuals of absorption coefficients were used to show the goodness of fit for each wavelength.

Results: The ε data set provided by Moaveni *et al.* [2] is found to be the optimal as it provided the most consistent results as expected from the blood-lipid phantom measurement protocol: StO_2 range is close to 100 and 0% for each deoxygenation cycle and C_{HbT} remains roughly constant. The analyses were repeated with different combinations (subsets) of 11 wavelengths and, as expected, the choice of wavelengths strongly influences the findings of this study, i.e. the effect of ε data set on the estimation of hemoglobin concentrations and oxygen saturation.

Conclusions: The extinction coefficients were shown to be an important parameter for quantifying hemoglobin concentration and oxygen saturation. The optimal ε data set was identified as the data set provided by Moaveni *et al.* [2]. The hemoglobin spectra are a factor that needs to be considered for future developments and applications of NIRS.

References:

[1] Gerega, A., Milej D., Weigl W., Kacprzak M., Liebert A., "Multiwavelength time-resolved near-infrared spectroscopy of the adult head: assessment of intracerebral and extracerebral absorption changes," Biomed. Opt. Express, 9(7): p. 2974--2993, (2018).
[2] Zhao, Y., Qiu, L., Sun, Y., Huang, C., and Li, T., "Optimal hemoglobin extinction coefficient data set for near infrared spectroscopy," Biomed Opt Express 8(11), 5151-5159 (2017).
[3] Kleiser, S., Nasseri, N., Andresen, B., Greisen, G., and Wolf, M., "Comparison of tissue oximeters on a liquid phantom with adjustable optical properties," Biomed Opt Express 7(8), 2973-2992 (2016).

Two methods for recording and classifying cough signals

Dominika Szuberla[1], Włodzimierz Łukasik[1], Elżbieta Magdalena Grabczak[2], Krzysztof Jakub Pałko[3] and Tadeusz Pałko[1]
[1]Warsaw University of Technology, Faculty of Mechatronics, Institute of Metrology and Biomedical Engineering, A. Boboli 8 St., 02-525 Warsaw, Poland
[2]Department of Internal Medicine, Pulmonary Diseases and Allergy, Medical University of Warsaw, Banacha 1a, 02-097 Warsaw, Poland
[3]Nalecz Institute of Biocybernetics and Biomedical Engineering, Polish Academy of Sciences, Ks. Trojdena 4 st., 02-109 Warsaw, Poland
d.szuberla17@gmail.com

Aim: Cough is one of the most common symptoms of chronic lung diseases [1] and even pulmonary malignancies. It is also one of the main symptoms of COVID-19 [2]. There is a need for a device that can accurately detect, identify, distinguish and parameterize a given type of cough, or find its cause. The main purpose of the work was to design and implement two portable cough recording systems.

Methods: The first device is a recorder with an accelerometer with a digital memory, this sensor is responsible for measuring accelerations in 3 axes (x, y, z) and for recording and counteracting vibrations or changes in the position of the sensor. The second device is a portable cough detection system, in which a microphone sensor TONSIL MEO 55 has been used, thanks to which it is possible to record the cough signal in the acoustic band. The recorder modules are placed on a special belt fastened on the patient's abdomen.

Results: The main result of the work was verification of the correctness of the devices operation and carrying out initial registration of acoustic and accelerometric signals and the possibility of their further analysis.
An integral part of the topic was the performance of tests on volunteers at the Department of Internal Medicine, Pneumology and Allergology in Warsaw. The analysis was carried out in Microsoft Visual Basic 6.0.
The written application made it possible to easily compare, check and analyze selected cough parameters, including: amplitude, number of cough incidents, sum of all incidents, the longest and the shortest pause between signals, duration, intensity or vibration assessment. Five registrations were made, each taking approximately 40 minutes. Registrations took place with two devices simultaneously.

Conclusions: A very interesting phenomenon was observed, i.e. a slight delay (30-40 msec) of the microphone in relation to the accelerometer, the delay occurs with every cough incident. It can be concluded that the delay is the result of the propagation time of the acoustic and accelerometric signals . Another conclusion developed after a thorough literature analysis of vibroacoustic tests on the described group of patients [3] showed that the value of vibration amplitudes during coughing incidents did not exceed about 8-12dB (maximum values). The preliminary tests are promising and the scientific work will be continued.

References:

[1] Mlynczak M, Pariaszewska K, Cybulski G. Automatic cough episode detection using a vibroacoustic sensor. *Annu Int Conf IEEE Eng Med Biol Soc.* 2015 Aug;2015:2808-11. doi: 10.1109/EMBC.2015.7318975.
[2] Sharma N., Krishnan P., Kumar R., Ramoji S., Chetupalli S. R., Ghosh P. K., Ganapathy S. et al. Coswara–a database of breathing, cough, and voice sounds for COVID-19 diagnosis. *arXiv preprint* arXiv:2005.10548, 2020.
[3] Krajnik M., Damps-Konstańska I., Grabowski M., Pozański P., Jassem E. An evaluation of cough-generated sound and body surface vibration by the MEPIM Vibroacoustic System of Cough Registration (MEPIM VSCR), *Advances in Palliative Medicine* 2008, vol. 7, no. 1, pp. 3-8.

The effect of deuterium oxide on the aggregation process of CsgA fragments

Natalia Szulc[1,2,] Marlena Gąsior-Głogowska[1], Jakub W. Wojciechowski[1], Monika Szefczyk[3], Andrzej M. Żak[4], Michał Burdukiewicz[5], Malgorzata Kotulska[1]

[1] Department of Biomedical Engineering, Faculty of Fundamental Problems of Technology, Wroclaw University of Science and Technology, Wybrzeże Wyspiańskiego 27, 50-370 Wrocław, Poland;
[2] CNRS, University of Lorraine, F-5400 Nancy, France;
[3] Department of Bioorganic Chemistry, Faculty of Chemistry, Wroclaw University of Science and Technology, Wybrzeże Wyspiańskiego 27, 50-370 Wrocław, Poland;
[4] Electron Microscopy Laboratory, Faculty of Mechanical Engineering, Wroclaw University of Science and Technology, Wybrzeże Wyspiańskiego 27, 50-370 Wrocław, Poland;
[5] Clinical Research Centre, Medical University of Białystok, Jana Kilińskiego 1, 15-089 Białystok, Poland
natalia.szulc@pwr.edu.pl

Aims: This work aims to investigate the effect of D_2O on the aggregation process of major curli subunit (CsgA) fragments in Gram-negative bacteria strains. CsgA protein is the most frequently studied functional amyloid. The structures of amyloids are widely studied by spectroscopic methods, i.e. nuclear magnetic resonance (NMR) and Fourier-transform infrared spectroscopy (FTIR). In these techniques, especially in FTIR measurements, D_2O is a commonly used solvent. Using D_2O is a popular method to solve the "water problem" [1]. In this work we studied if application of D_2O could influence the amyloid aggregation process, thus affecting the results credibility.
Methods: The studies were performed on five imperfect repeat fragments, labelled as R1-R5, of the curli CsgA protein from *Sallmonella enterica (S. enterica)*. The protein belongs to the class of functional amyloids forming fibrils in bacterial biofilm. The repeat fragments, as isolated peptides, aggregate. The only exception is non-amyloid R2 fragment. Secondary structure investigations was carried out with Attenuated Total Reflectance – Fourier-Transform InfraRed (ATR-FTIR) and Fourier Transform Infrared Microscopy (μIR) using transmission mode. Additionally, the transmission electron microscopy (TEM) was performed to observe the fibril morphology. Peptides were synthesized and purified using preparative HPLC method, lyophilized and dissolved. Spectroscopic studies and imaging were conducted using two different solvents: D_2O and phosphate-buffered saline (PBS) containing H_2O.
Results: D_2O affected the stability of peptides and enhanced the fibrillation process. For example, fibrils were observed in case of R2 fragment, generally considered as non-amyloid. We also observed, immediately after dissolving in D2O, the position of Amide I maximum at ca. 1630 cm^{-1}, which is typical of amyloid fibrils. In contrary, for water samples the band maximum was located at higher wave numbers. We hypothesize that the exchange of NH group protons with solvent deuterons may have caused some distortion of the hydrogen bonding network and led to the peptide misfolding. The secondary and tertiary structures of studied fragments were different in D_2O and H_2O, as observed with infrared spectroscopy and TEM techniques.
Conclusions: The results of our study proved that D_2O accelerates the aggregation process of the studied fragments of CsgA of *S. enterica*. It can also change the amyloid propensity of a non-amyloid. We observed significant differences in the aggregation process using ATR and transmission modes in infrared measurements. Shifts in the Amide I position were noted. Additionally, compared to other techniques, the ATR-FTIR spectra indicate the presence of more advanced forms (longer and more rigid fibrils) in the studied aliquotes. They are caused by the peptide interaction with the hydrophobic diamond surface of ATR accessory.
Acknowledgements: This work was partially supported by the National Science Centre, Poland, Grant 2019/35/B/NZ2/03997(MK, MB, MGG, JW) and Grant No. 2017/26/D/ST5/00341 (MS), National Centre for Research and Development, Poland under POWR.03.02.00-00-I003/16 (NS), and Wroclaw Center of Biotechnology program "The Leading National Research Center (KNOW) for years 2014- 2018" (MB).

References:
[1] Zuber G., Prestrelski S.J., Benedek K. Application of Fourier transform infrared spectroscopy to studies of aqueous protein solutions, *Anal Biochem*,1992, vol. 207, no. 1, pp. 150–156

A new low-range biosensor for glutamate based on hyperbranched linkers

Marcin Urbanowicz[a], Bartłomiej Lemieszek[b], Kamila Sadowska[a], Anna Sołdatowska[a], Agnieszka Paziewska-Nowak[a], Marek Dawgul[a], Dorota G. Pijanowska[a]
[a]Nalecz Institute of Biocybernetics and Biomedical Engineering Polish Academy of Sciences, Ks. Trojdena 4, 02-109 Warsaw, Poland
[b]Gdańsk University of Technology, Faculty of Chemistry, Department of Chemistry and Technology of Functional Materials, Narutowicza 11/12, 80-233 Gdańsk, Poland
murbanowicz@ibib.waw.pl

Glutamate is the major excitatory neurotransmitter in the nervous system. Elevated glutamate level in body fluids is associated with a wide array of nervous system diseases and disorders, among others, Alzheimer's, Parkinson's, Huntington's disease or brain injury [1]. Therefore, there is a particular need for reliable tools for neurodegenerative diseases diagnosis and patients monitoring during treatment.

The main problem in the determination of glutamate is the wide concentration range which depends on the sample type (serum, saliva, urine, cerebrospinal fluid). Currently, the standard methods of glutamate determination are optical methods, which have many disadvantages, such as costly and labor-intensive analysis process [2]. Alternative tools for glutamate determination are electrochemical sensors with a bioreceptor layer. Among electrochemical biosensors, the most successful are the ones based on electron transfer, therefore belonging to the amperometric sensors. Glutamate is not electrochemically active, however glutamate oxidase (GluOx) enables the breakdown of glutamate into three products, of which hydrogen peroxide is electrochemically active. The formed H2O2 is oxidized at the electrode surface. The number of electrons produced in this reaction is proportional to the concentration of glutamate. Platinum is preferentially used as an electrode material, due to the highest sensitivity to hydrogen peroxide formed by enzymatic reaction with glutamate [3]. However, in our studies, we observed the lowest detection limit of glutamate as reported so far, when using gold electrodes prepared by direct printing and then chemically functionalized using hyperbranched linkers, followed by GluOx immobilization.

Surface plasmon resonance (SPR) was successfully used to control the process of designing procedures for the modification of gold surfaces. The analysis of sensorgrams showed that the length and degree of branching of the linker has a significant influence on the level of bioreceptor loading on the surface - which has a significant impact on the biosensors sensitivity. The effectiveness of modification of gold surfaces was confirmed by the presence of characteristic functional groups (-COOH, -NH2) using the FTIR technique. Contact angle analysis revealed changes in the hydrophobicity of modified surfaces. Non-modified gold substrates were hydrophobic, while modified gold substrates changed properties to hydrophilic. More hydrophilic character of functionalized surface is important due to functionality of bioreceptors in water environment. The biosensors constructed on the gold electrodes were characterized for glutamate sensitivity using the CV technique. Electrochemical studies have shown that the linear range of biosensors are from 10 fM to 10 pM with a sensitivity of from several to several hundred μA·pM-1. Sensitivity increased with the surface loading by the bioreceptor and was the highest when using highly branched linkers.

In summary, the results of our research show that the hyperbranched linkers influence the sensitivity of the glutamate biosensor. The SPR analysis of the bioreceptor loading on the sensor surface enabled establishing the modification procedure that ensured the highest sensitivity of the developed biosensor. In the future this results may allow to construct ultra-sensitive analytical tools that can be useful in the diagnostic process of neurodegenerative diseases.

References:

[1] Haris M, Nath K, Cai K, et al. Imaging of glutamate neurotransmitter alterations in Alzheimer's disease. *NMR Biomed*, **2013** vol. 4, no. 26, pp. 386-391.

[2] Ferreira C.P, Antunes F.T.T, Rebelo I.N, et al., Application of the UV–vis spectrophotometry method for the determination of glutamate in the cerebrospinal fluid of rats, *J Pharm Biomed Anal*, **2020** vol. 186, pp. 113290.

[3] Schultz J, Uddin Z, Singh G, et al. Glutamate sensing in biofluids: recent advances and research challenges of electrochemical sensors, *Analyst*, **2020** vol. 2, no. 145, pp. 321-347.

The utility of using non-invasive arterial blood pressure to estimate the time constant of cerebral arterial bed

Agnieszka Uryga1, Marek Czosnyka2, Magdalena Kasprowicz1
1Department of Biomedical Engineering, Wroclaw University of Science and Technology, Wroclaw, Poland; e-mail: agnieszka.uryga@pwr.edu.pl
2 Brain Physics Laboratory, Division of Neurosurgery, Department of Clinical Neurosciences, University of Cambridge, UK
agnieszka.uryga@pwr.edu.pl

The time constant of the cerebral arterial bed (τ) is defined as the time required to fill the arterial bed distal to the level of the insonated vessel after a heart constriction. The estimation of τ requires monitoring of arterial blood pressure (ABP), intracranial pressure (ICP) and cerebral blood flow velocity (CBFV). However, in some clinical scenarios, where characterization of cerebral haemodynamics may be profitable, measurement of invasive ABP is not compulsory [1]. It has been shown in the previous studies that invasive ABP measurement could be successfully replaced by non-invasive one in assessing dynamic cerebral autoregulatory indices [2] or evaluation of the cerebrovascular pressure reactivity index [3]. However, using non-invasive ABP measurement in the assessment of pulsatile changes in cerebral blood volume has not been yet investigated. Therefore, this study aimed to evaluate whether invasive ABP could be replaced by non-invasive ABP in the estimation of the τ.

Forty-six recordings from ten head injury patients hospitalised in the Neurosurgical Critical Care Unit of Addenbrooke's Hospital, Cambridge, UK were retrospectively analysed. The τ was calculated using a modelling approach using a constant flow forward model [CFF, pulsatile blood inflow and steady blood outflow] and pulsatile flow forward [PFF, blood inflow and outflow are pulsatile]). ABP was measured invasively using an arterial line in a radial artery and noninvasively using photoplethysmography Finapres 2300. ICP was measured invasively using ICP intraparenchymal probe. CBFV was monitored using transcranial Doppler ultrasonography. The signals recorded were analysed using algorithms embedded in the ICM+ system.

The Bland–Altman analyses showed that noninvasive ABP was on average 10.36 mm Hg less than invasive one. However, transfer function analysis showed that median coherence and transfer function gain between noninvasive and invasive ABP, calculated within a range of 40–140 beats/minute, were 0.90 (0.85–0.96) [a.u.] and 0.78 (0.67 – 0.90) [a.u.], which reflects appropriate linear coupling between them. The noninvasive τ was significantly higher than invasive one, both when estimated using the CFF model (197.96 (151.08-238.15 [ms] vs. 145.40 (104.52-182.63) [ms]; $p < 0.001$) and the PFF model (93.30 (58.25-112.75 [ms] vs. 43.48 (10.49 – 81.26) [ms]; $p < 0.001$). Based on Bland–Altman analysis the bias between noninvasive and invasive τ, estimated using the CFF model, was 55.72 [ms], while they correlated strong ($r_S = 0.63$). For the PFF model, the range between the lower and upper limits of agreement was also wide: the mean ratio of noninvasive to invasive τ was 2.34 and the correlation was moderate ($r_S = 0.40$).
Our study showed that differences between noninvasive and invasive τ are meaningful, regardless of the model used for estimation. Thus estimation of τ using non-invasive ABP monitoring could be insufficient in head trauma patients. However, despite there was rather poor agreement between noninvasive and invasive τ estimation, the noninvasive approach could be beneficial in patients where invasive ABP is clinically impossible. Further study needs to be done using the latest generation of non-invasive photoplethysmography (Finometer Midi or Finapres NOVA) in a larger cohort of patients.

Acknowledgements
A. Uryga is supported by Foundation for Polish Science.

References:

[1] Czosnyka Z, Czosnyka M, Pickard J et al.Who needs a revision? 20 years of Cambridge shunt lab Acta Neurochir. Suppl. 2016; vol.122, pp. 347–51.
[2] Lavinio A, Schmidt E A, Haubrich C et al. Noninvasive evaluation of dynamic cerebrovascular autoregulation using finapres plethysmograph and transcranial Doppler. Stroke. 2007; vol. 38, pp. 402–404.
[3] Kasprowicz M, Schmidt E, Kim DJ et al. Evaluation of the cerebrovascular pressure reactivity index using non-invasive Finapres arterial blood pressure. Physiol. Meas. 2010; vol. 31, pp. 1217–28.

A combined chemical/biosensor for simultaneous online monitoring and sterility assurance in aseptic food packaging

Farnoosh Vahidpour [1], Torsten Wagner [1], Michael J. Schöning [1,2]
[1]Institute of Nano- and Biotechnologies (INB), Aachen University of Applied Sciences, Heinrich-Mußmann-Straße 1, 52428 Jülich, Germany
[2]Institute of Biological Information Processing (IBI-3), Forschungszentrum Jülich GmbH, 52425 Jülich, Germany
vahidpour@fh-aachen.de

Hydrogen peroxide is one of the most common sterilants used for packaging in aseptic filling machines [1]. To validate the sterilization of the packages, spores are exposed to the sterilant, their kill rate is determined and the sterilization is concluded accordingly. However, as the results of such method can be obtained only after 48-72 hours, it has a drawback of tedious physical work and slow response. To overcome this issue, a novel sensing platform, a spore-based biosensor, has been previously introduced [2]. In this work, the combination of such spore-based biosensor with a calorimetric H_2O_2 gas sensor on a single chip is introduced to assess the viability of spores and to control gaseous H_2O_2 concentration and temperature.
Here, interdigitated electrodes functioned as impedimetric sensors (see Fig. 1) at the top part of the sensor chip. Furthermore, two meander structures were used as temperature sensors (see Fig. 1), at the bottom part of the sensor chip. For both, the calorimetric gas sensor and spore-based biosensor, a differential measurement set-up was used. As for the former case, one sensor was used as a reference (i.e., inert to H_2O_2 exposure), whereas the other one was employed as an active element (i.e., functionalized with MnO_2 which catalyzes H_2O_2). Upon exposure to H_2O_2, a temperature difference between both sensors could be correlated to the H_2O_2 concentration. Similarly, on the spore-based biosensor, spores were immobilized on the active part of sensor. After H_2O_2 exposure, changes in the morphology of the spores could be correlated to the viability of spores.
The calorimetric gas sensor response depended linearly to different concentrations of gaseous H_2O_2. The biosensor was investigated with different types of spores. Signal responses (impedance) of the spore-based biosensors at various H_2O_2 concentrations were studied, showing a correlation between H_2O_2 concentration and the spores' impedance. Figure 1 represents a schematic alteration of the impedance and calorimetric signals regarding the H_2O_2 concentrations.
In conclusion, the synergy of these two sensor types as one combined sensor array allows us more specific multi-parameter-based fault indication in aseptic filling machines in comparison to isolated microbiological state-of-the-art- or hydrogen peroxide detection methods.

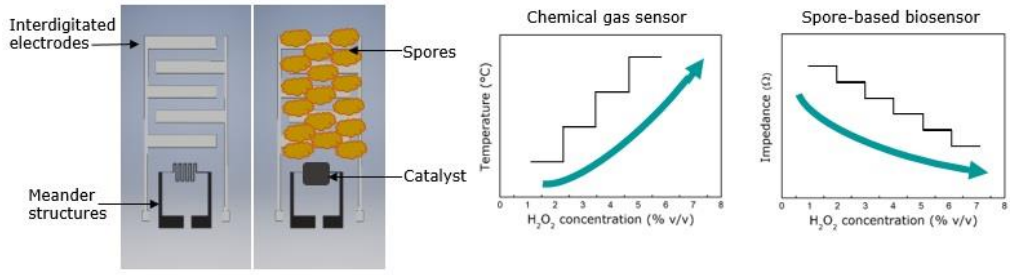

Figure 1: Combined sensor array consisting of a calorimetric H_2O_2 sensor and a spore-based biosensor (left) with their respective calorimetric and impedance responses (middle and right).

Acknowledgements: Part of this work was supported by the Federal Ministry of Education and Research (BMBF) within the project "SteriSens" (Entwicklung eines Chip-basierten Sensorarrays zur Echtzeiterfassung kritischer Prozessparameter in Sterilisationsprozessen an Sterilgütern, Fund. No.: 03FH057PX5). The authors thank J. Arreola and E. Guthmann for valuable discussions and H. Iken for assisting the sensor fabrication.

References:

[1] I. A. Ansari, A. K. Datta, An Overview of Sterlization Methods for Packaging Materials Used in Aseptic Packaging Systems, *Food Bioprod. Process*, 2003, 81, 57 – 65.
[2] J. Oberländer, M. Mayer, et al. Spore-based Biosensor to Monitor the Microbicidal Efficacy of Gaseous Hydrogen Peroxide Sterilization Processes, Biosens. Bioelectron., 2018, 104, 87 – 94.

Can molecular biology and photoelectron spectroscopy methods be used to identify nanotechnology products?

Bogdan Walkowiak[1,2], Magdalena Walkowiak-Przybyło[1], Piotr Komorowski[2]
[1]Department of Biophysics, Institute of Materials Science and Engineering, Lodz University of Technology Stefanowskiego 1/15, 90-924 Lodz, Poland
[2]Bionanopark sp. z o.o, Dubois 114/116, 93-465 Lodz, Poland
bogdan.walkowiak@p.lodz.pl

Despite the intensive progress in the field of nanotechnology, the basic problem remains the correct and effective identification and grouping of nanotechnology products for registration under the REACH Directive. It remains a problem to explain why nanoparticles composed of the same type of atoms exhibit different chemical reactivity and cause different biological effects depending on the size, and on the other hand, very similar or even identical biological effects can be caused by nanoparticles of different chemical composition and size.

It is now well known that the ordering of elements in the Mendeleev's periodic table can be made on the basis of the knowledge of the electronic orbitals of these elements, which in turn implies chemical reactivity and biological effects of the elements. The basis for this ordering can be the knowledge of the energy eigenvalues of the states and the wave functions corresponding to these energies, which define the orbital of electron. Although such a task is not easy, this information can be obtained from solving the Schrödinger equation.

Naturally, the question arises whether by analogy it would be possible to differentiate, identify and group nanotechnology products (nanoparticles, nanostructures) based on the knowledge of molecular orbitals identified on the surface of nanostructures? Technologically, this problem seems to be solvable, because modern science has the possibility of imaging orbitals using scanning tunneling microscopy (STM) [1] and computerized tomography of orbitals using photoelectron spectroscopy (PES) [2], and quantum physics with the Density Functional Theory (DFT) provides theoretical tools to solve this unfortunately complicated task.

Unexpectedly, molecular biology tools also provide promising tools to solve this problem. It turns out that the metabolic response of cells, observed at the transcriptome and proteome levels, shows highly selective and specific properties, which very likely translates into the ability of cells to recognize stress caused by contact with nanoparticles. These observations became the basis of the patent claim [3] and was described in more detail in the previous work [4] with the use of the evaluation of gene expression profiles (RNA microarrays technique) and peptides/proteins profile (2D-DIGE electrophoresis technique). This specific metabolic response of cells should come as no surprise, since the biochemical processes taking place in a living cell are subject to the same laws of the formation and dissociation of molecular bonds as in chemical reactions, and the decisive factor in the occurrence of such a reaction is the formation of a bonding molecular orbital, when new bond is formed, and the formation of an anti-bonding molecular orbital - the case of dissociation of the existing bond. The conditions for the formation of such molecular orbitals may result from the presence of a nanostructure presenting the appropriate energy potential modulating the solutions of the Schrödinger equation and affecting the resultant molecular orbital.

Summarizing this report, we pay attention to the potential possibility of identifying, differentiating and grouping nanotechnology products in order to register them with the use of quantum properties of these products and their recognition by biological objects, and both approaches should be seen as complementary in terms of materiomics.

References:

[1] Z. Cheng, S. Du, W. Guo, L. Gao, Z. Deng, N. Jiang, H. Guo, H. Tang, J. Gao. Nano Res. 4(6) 2011, 523–530, DOI 10.1007/s12274-011-0108-y.

[2] H. Offenbacher, D, Lüftner, T. Ules, E.M. Reinisch, G. Koller, P. Puschnig, G. Ramsey, J. Electron Spectroscopy and Related Phenomena, 204 (2015), 92–101, https://doi.org/10.1016/j.elspec.2015.04.023.

[3] B. Walkowiak, P. Komorowski, M. Walkowiak-Przybylo, PL patent – PAT.223224, 11.07.2012.

[4] P. Komorowski, M. Siatkowska, T.Wasiak, K. Działoszyńska, S. Kotarba, K. Kądzioła, N. Bartoszek, P. Sokołowska, M Elgalal, A. Sobol-Pacyniak, K. Makowski, B. Walkowiak. Simultaneous transcriptome and proteome analysis of EA.hy926 cells under stress conditions induced by nanomaterials. Journal of Biomedical Materials Research - Part B Applied Biomaterials, 2019, 107(4):1024-1034, DOI: 10.1002/jbm.b.34195.

Quantitative real-time polymerase chain reaction (qRT-PCR) technique as a useful tool for the assessment of cancer risk caused by medical implants

Magdalena Walkowiak-Przybyło[1], Marta Walczyńska[1], Marta Kamińska[1], Małgorzata Siatkowska[2], Piotr Komorowski[2], Bogdan Walkowiak[1,2]
[1]Department of Biophysics, Institute of Materials Science and Engineering, Lodz University of Technology Stefanowskiego 1/15, 90-924 Lodz, Poland
[2]Bionanopark sp. z o.o, Dubois 114/116, 93-465 Lodz, Poland
magdalena.walkowiak-przybylo@p.lodz.pl

There is a growing number of reports about the formation of neoplastic changes adjacent to the implant or in places distant but temporally correlated with the implantation. At the moment there is no indisputable data on the induction of carcinogenesis by implants used in orthopedics, although this subject has been often discussed and some malignant neoplasms like osteoma, osteosarcoma, lymphoma or squamous cell carcinoma have frequently been reported [1]. A literature review on clinical reports indicates that cancer changes situated in the bone and affecting not typically osteoblasts but chondrocytes and cartilage tissue may be the reason of failure in orthopedic implantation process [2]. What is more, some benign tumors like enchodroma that are very often difficult to diagnose, can transform to chondrosarcoma over the years [3]. In the light of above disturbing information, the aim of this project was to verify whether immortalized cell lines with neoplastic phenotype show an altered response to contact with implant material compared to primary cells of the same type.

The study was carried out for two types of materials used for implant production (medical steel AISI 316L and titanium-aluminum-niobium alloy Ti6Al7Nb). Nineteen genes promoting cancer formation were selected and a custom RT-PCR plate was designed. The HC-a primary chondrocytes (ScienCell Research Laboratories, Cat. #4650) and secondary chondrosarcoma line SW 1353 (ATCC-HTB-94) were used. Seven independent RNA isolation experiments from the cells grown on the surfaces of the tested biomaterials were carried out. The cells grown on the surface of a standard culture flask were used as a control. RNA quality and purity was assessed by capillary electrophoresis (Agilent's 2100 bioanalyzer). Seven independent qRT-PCR reactions (CFX96 Touch thermal cycler and Universal SYBR Green Supermix reagent, both from BIO-RAD) were performed. t-Student test was used for statistical analysis of obtained results of fold change values (Fc or $\log_2$Fc). Changes in gene expression were observed for 16 and 17 genes, for HC-a and SW1353 cells, respectively. The predominant direction of changes for HC-a cells was gene suppression whereas for SW1353 chondrosarcoma the genes were mainly overexpressed.

The differences in the expression of genes observed in primary and cancer cells seems to be gentle, but even these subtle differences should be taken into account. Gaining more knowledge in this area requires further intensive research, however it was proved that qRT-PCR (quantitative real-time polymerase chain reaction) technique plays a vital role in the assessment of risk of induction or intensification of carcinogenesis by the biomaterials used for implants production. Compilation of qRT-PCR experiments carried out on primary and cancer cells in parallel will allow to identify possible future contraindications for patients with a genetic predisposition to cancer or with cancer history and may be a crucial step in the selection of the right biomaterial for a specific patient.

References:
[1] V. Levašič, I. Milošev, V. Zadnik: *Acta Orthop*. 2018 Apr;89(2):252.
[2] L. Mustaki, P. Goetti, N. Gallusser, B. Morattel, H. Rüdiger, S. Cherix: *Arthroplast Today* 2021 Jan 11;7:84-90.
[3] GW. Herget, P. Strohm, C. Rottenburger, U. Kontny, T. Krauß, J. Bohm, N. Sudkamp, M. Uhl: *Neoplasma* 2014;61(4):365-78.

Hydration and swelling of non-perfused tissue: spatially distributed mathematical model for nonlinear poroelasticity

Jacek Waniewski[1], Joanna Stachowska-Pietka[1], Roman Cherniha[2]
[1] Nalecz Institute of Biocybernetics and Biomedical Engineering, Ks Trojdena 4 Street, 02-109 Warszawa, Poland
[2] Institute of Mathematics, NASU, 3 Tereshchenkivs'ka Street, Kiev, Ukraine
jwaniewski@ibib.waw.pl

The change of tissue hydration caused by variable environmental hydrostatic and osmotic pressure can occur in some medical treatments, as peritoneal dialysis, or due to fluctuating physiological conditions. Although mathematical modeling of such phenomena is known, the problem of the tissue swelling or shrinkage is typically assumed negligible or omitted. Our objective was to predict the change of tissue size after the change in hydrostatic or/and osmotic pressure of fluid that surrounds the tissue using a mathematical model.
The model is based on the theory of momentum, fluid and solute transport in poroelastic flat sheet of tissue with the assumption that the transport occurs only in the direction x perpendicular to the tissue surface. The stress-strain relationship for generalized Terzaghi stress tensor τ is assumed quadratic in deformation rate $\partial u/\partial x$: $\tau = -p^* + \lambda^*(\partial u/\partial x) + \kappa(\partial u/\partial x)^2$, where λ^* is reduced Lame coefficient, κ describes the contribution of quadratic term to stress, the hydrostatic and osmotic combined pressure is defined as $p^* = p - \sigma RTC$. We assess the change of the steady state tissue width from the tissue in physiological equilibrium of width L_0 to the tissue with modified hydrostatic and/or osmotic pressures of the surrounding fluid, of width L_S, which is unknown. The steady state version of the model involves three nonlinear ordinary differential equations of the second order that describe the profiles of deformation (dilation) u, intra-pore fluid hydrostatic pressure and osmotic agent concentration as a function of distance from the tissue surface. We assume that both tissue surfaces are permeable for fluid and solute.
The mathematical analysis of the model provided a closed (analytical) expression for L_S / L_0 as a function of normalized pressure difference $DP_{sc} = (p^*_{ex} - p^*_0)/\lambda^*$ that for $\kappa = 0$ reduces to the formula published previously (Cherniha et al, Symmetry 2020; doi:10.3390/sym12030396), see Figure 1:

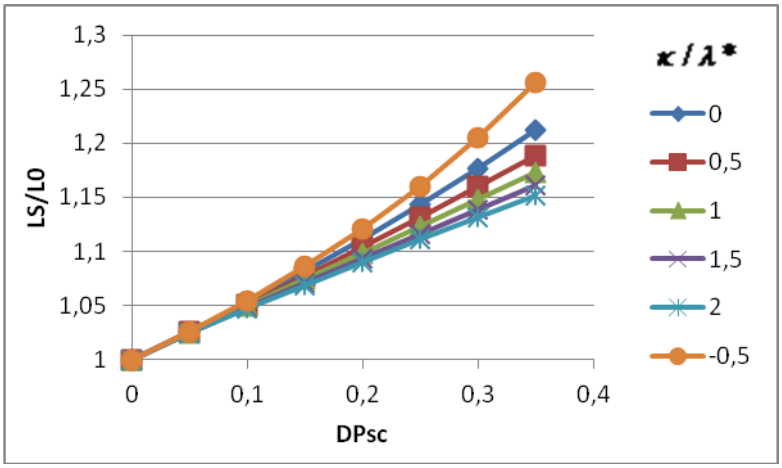

Figure 1. The ratio of the equilibrium tissue widths L_S / L_0 as a function of normalized pressure change $DP_{sc} = (p^*_{ex} - p^*_0)/\lambda^*$ for a few values of the ratio of κ/λ^* from -0.5 to 0 to 2.0.

The presented model provides a simple generalization of linear poroelastic theory and allows for more flexible description of the swelling/shrinking of the tissue. The closed formulas for linear and nonlinear versions of the theory facilitate the general analysis of the relationship between the change of the tissue width, the boundary conditions and the tissue parameters and reveal a useful scaling method for the problem.

Capacitively coupled electrical tomography for anatomical and functional imaging of thorax

Damian Wanta, Mateusz Midura, Przemysław Wróblewski, Grzegorz Domański,
Jacek Kryszyn, Waldemar T. Smolik
Warsaw University of Technology, ul. Nowowiejska 15/19, 00-665 Warsaw, Poland
d.wanta@ire.pw.edu.pl

Electrical Impedance Tomography (EIT) has the potential to be an alternative method of obtaining imaging information in medical diagnostics without exposing the patient to ionizing radiation. The latest scientific works show diagnostic possibilities of EIT, including monitoring of intracranial pressure and the assessment of changes in regional pulmonary ventilation [1]. The problem of transmitting electrical signals through the skin barrier limits the development of this noninvasive technique. It is necessary to acquire new knowledge to overcome existing limitations. The contactless electrical tomography uses electrodes capacitively isolated from the skin as opposed to ohmic skin contact in classic EIT. In the last 2 years, first promising attempts to use this concept of measurements in AC-based (sine-wave excitation) electrical tomography were presented in [2]. The aim of this study is to investigate a concept of electrical tomography with the use of capacitively coupled electrodes to monitor the respiratory cycle and the regional ventilation distribution.

A simplified numerical thorax models for inhalation and exhalation phases were designed using six different permittivity values, each corresponding to real dielectric constant of inflated lungs - 3, deflated lungs - 6.7, heart - 9 and connective tissue - 5 [3]. The forward and inverse problem were calculated using ECTsim toolbox for MATLAB. The finite volume method (FVM) and octree data structures were applied to compute electrical field distributions in the thorax phantom. Values of the mutual capacitances of 16 electrodes surrounding the sensing area were simulated using the sensitivity matrix that had been previously determined based on the calculated distributions of the electric field. Two reconstructions for different numerical models of chest were obtained with linear Levenberg-Marquardt method.

An elaborated model with inflated lungs is presented in Fig. 1a. Permittivity distribution reconstructed from simulated measurements for different levels of lung aeration is presented in Fig. 1b-c. The difference between the reconstructed permittivity values measured in the center of the left lung for different phases of the respiratory cycle was about 4. It corresponds to the values assumed in the model.

Results obtained with numerical simulation led us to believe that capacitively coupled electrical tomography can be suitable for monitoring of the respiratory cycle. The sensitivity of real measurements as well as contrast and spatio-temporal resolution of images should be assessed during further research.

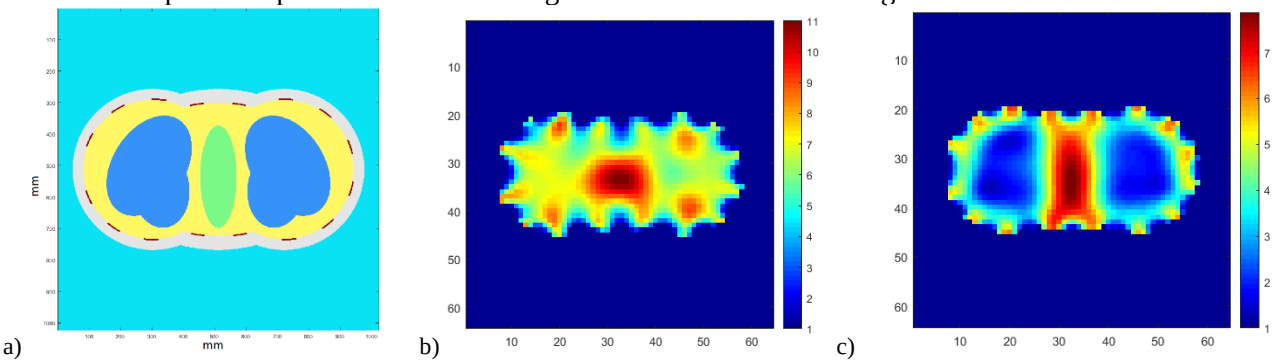

Fig. 1 Numerical model of the thorax (a) and reconstructed permittivity distribution for deflated (b) and inflated (c) lungs

References:

[1] Tomicic V. and Cornejo R. Lung monitoring with electrical impedance tomography: Technical considerations and clinical applications, *Journal of Thoracic Disease*, vol. 11, no. 7. pp. 3122–3135, 2019.
[2] Jiang Y. and Soleimani M. Capacitively Coupled Phase-based Dielectric Spectroscopy Tomography, *Sci. Rep*., vol. 8, no. 1, pp. 17526, 2018.
[3] Gabriel C. Compilation of the Dielectric Properties of Body Tissues at RF and Microwave Frequencies, *Report N.AL/OE-TR- 1996-0037*, 1996.

Light-addressable electrodes induce pH changes in microfluidic channels

Rene Welden [1,2,] Michael J. Schöning [1,3,] Patrick H. Wagner [2,] Torsten Wagner [1,3]
[1]Institute of Nano- and Biotechnologies (INB), Aachen University of Applied Sciences, Heinrich-Mußmann-Straße 1, 52428 Jülich, Germany
[2]Laboratory for Soft Matter and Biophysics, KU Leuven, Celestijnenlaan 200D, B-3001 Leuven, Belgium
[3]Institute of Biological Information Processing (IBI-3), Forschungszentrum Jülich GmbH, 52425 Jülich, Germany
welden@fh-aachen.de

Actuating electrochemical electrodes can manipulate biological and chemical specimens in microfluidic systems, e.g., by changing the local pH. Often, noble metal (Pt, Au) electrodes are integrated inside complex systems, like lab on a chip or micro total analysis systems. Electrode geometry and location are defined during the design and fabrication process for the specific task. In combination with biological systems this can serve as a drawback, since the exact location and geometry of the point of interest is only determined after e.g., cell culture cultivation and visual inspection. A different approach is the use of a semiconductor as electrode material, with a light-induced generation of charge carriers [1]: Combining these light-addressable electrodes (LAE) with a digital light-processing (DLP) projector, a flexible spatio-temporal adjustment of the conductive area is enabled.

In this work, we present a sol-gel fabrication method for a glass/SnO_2:F/TiO_2 heterostructure and discuss morphological and photoelectrochemical parameters. The structure of the LAE is depicted in figure 1. For the fabrication, a thin TiO_2 film was deposited on the glass/SnO_2:F substrate by a sol-gel process with subsequent spin-coating (2500 rpm) and heating steps (95 °C, 550 °C) [2]. The impact of the TiO_2 thickness for the application as an LAE was characterized by means of scanning electron microscopy and photocurrent measurements. Additionally, to evaluate the spatio-temporal addressing of the LAE visualised by a local pH change, a microfluidic chamber was adapted on top of the LAE, and fluorescence measurements with a pH-sensitive dye were performed.

The results indicate the feasibility of the LAE, fabricated by a non-aqueous sol-gel approach, for the light-directed addressing inside a microfluidic system.

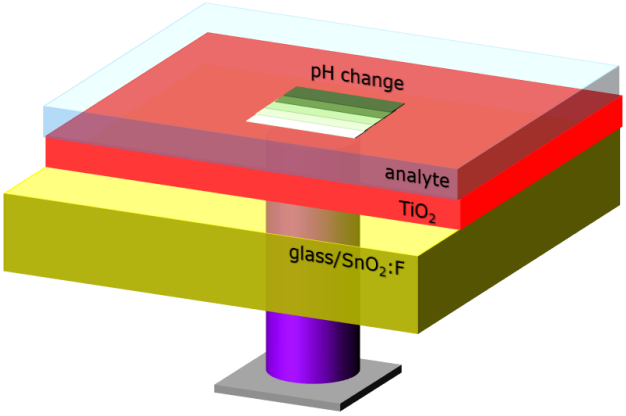

Figure 1: Schematic of the glass/SnO_2:F/TiO_2 structure with a local pH change at the illuminated area.

Acknowledgements: This work was supported by the German Federal Ministry of Education and Research (BMBF) within “NanoMatFutur” (13N12585).

References:

[1] R. Welden, M. J. Schöning et al. Light-addressable Electrodes for Dynamic and Flexible Addressing of Biological Systems and Electrochemical Reactions, *Sensors*, 2020, *20*, 1680.
[2] R. Welden, S. Scheja et al. Electrochemical Evaluation of Light-Addressable Electrodes Based on TiO_2 for the Interation in Lab-on-Chip Systems, *Phys. Status Solidi A*, 2018, 215, 1800150.

Individualized mathematical models for Covid-19 pandemic in European countries

Agata Wilk, Krzysztof Łakomiec, Krzysztof Psiuk-Maksymowicz, Krzysztof Fujarewicz
Silesian University of Technology, Dept. of Systems Biology and Engineering
Akademicka 16, 44-100 Gliwice, Poland
agata.wilk@polsl.pl

Aims

The aim of the presented research is to build mathematical models of the spread of the Covid-19 pandemic in various European countries. The models take into account the impact of control policies applied in different countries on virus transmission rates. A typical approach presented in the current world literature [1-3] is the construction of independent models for separate countries (areas, regions) and the estimation of their parameters on the basis of separate data sets. However, limited amount of data makes estimation of multiple parameters numerically problematic and the results difficult to compare. One solution may be to construct a common model for all regions, yet it would not reflect the specific character of individual countries. In the presented approach, we propose the simultaneous construction of many individualized models. In each of these models, a subset of parameters is common and estimated from a combined dataset for all countries, while other parameters are estimated separately for each country.

Methods

As the basic model of an epidemic in a single country, we used the classic SEIR model, in which we treated the virus transmission intensity as a time-dependent parameter, expressed as a function of variables depending on the degree of restrictions applied in individual countries.
In order to estimate the parameters, we used linear least squares method combined with a gradient approach in which we calculated the derivatives of the objective function with respect to the parameters of the models using adjoint sensitivity analysis.

Results and Conclusion

As a result, we obtained a set of models with estimated values of their parameters. Compared with the independent models and common model approaches, the individualized solution yields best results for largest number of countries. The analysis of the obtained values leads to conclusions regarding SARS-CoV-2 pandemic development in individual countries. In addition, we obtained information on how the transmission intensity depends on introduced restrictions, suggesting which of them are more effective and whose impact is smaller.

Acknowledgements

This work was supported by statutory research funds by Silesian University of Technology, Dept. of Systems Biology and Engineering. Calculations were carried out using the computer cluster Ziemowit (http://www.ziemowit.hpc.polsl.pl) funded by the Silesian BIO-FARMA project in the Computational Biology and Bioinformatics Laboratory of the Biotechnology Centre in the Silesian University of Technology.

References:

[1] IHME COVID-19 Forecasting Team., Reiner, R.C., Barber, R.M. *et al.* Modeling COVID-19 scenarios for the United States. *Nat Med* **27,** 94–105 (2021) https://doi.org/10.1038/s41591-020-1132-9.
[2] Carcione J.M, Santos J.E, Bagaini C, Ba J. A Simulation of a COVID-19 Epidemic Based on a Deterministic SEIR Model. *Front Public Health*. **8** (2020) https://doi.org/10.3389/fpubh.2020.00230.
[3] López L., Rodó X. A modified SEIR model to predict the COVID-19 outbreak in Spain and Italy: simulating control scenarios and multi-scale epidemics *Results in Physics*, **25** (2020) https://doi.org/10.1016/j.rinp.2020.103746.

Analysis of the mechanical properties of impact absorbing structures used in military helmets

Kamila Wiśniewska[1], Aleksandra Jędrzejewska[1,2], Monika Ratajczak[1], and Tomasz Klekiel[1]
[1]Department of Biomedical Engineering, Faculty of Mechanical Engineering, University of Zielona Góra, 65-516 Zielona Góra, Poland.
[2]Science and Technology Park of University of Zielona Góra, 66-002 Zielona Góra, Poland.
m.ratajczak@iimb.uz.zgora.pl

This article deals with the issues of head protection against dynamic effects. The current design of the helmets does not fully protect against the destruction of the soft tissues of the head resulting, for example, as a result of an impact. Damage to these tissues is usually caused by dynamic loads, and soldiers are one of the most vulnerable groups to craniocerebral injuries. Hence, the study undertook the development of a model and numerical research on determining the optimal design solution for materials absorbing impact energy.
The work analyzes proprietary solutions of tubular and honeycomb structures for four different construction materials. The conducted research allowed to determine the mechanical properties of the proposed geometries of the helmet's dynamic load absorbing layer and the possibility of their use for head protection. Various solutions were analyzed in terms of geometry and material characteristics. In order to obtain the desired features of the analyzed structures, optimal values of parameters such as diameter or wall thickness were searched for. Two structures were analyzed in terms of the use of diferent materials.

The performed numerical analysis showed that one of these structures exhibits special energy absorbing properties, thanks to which it can be an effective solution for protecting the skull and soft tissues of the head against the effects of dynamic loads and impacts.

Construction of Hollow Fiber Bioreactors for Hepatic Cell Culture

Monika J. Wiśniewska, Małgorzata Jakubowska, Agnieszka Wencel,
Dorota G. Pijanowska, Krzysztof D. Pluta
Nalecz Institute of Biocybernetics and Biomedical Engineering Polish Academy of Sciences,
Ks. Trojdena 4, 02-109 Warsaw
mwisniewska@ibib.waw.pl

The capacity to regenerate is one of the most desirable feature of the liver, but when liver loses its functions, transplantation of the organ is the only method to extend patients life. Approximately 10% of patients from transplant waiting list die every year worldwide, because of donor shortage. One of the most promising alternative therapies of liver failure is the use of Bioartificial Liver devices - BALs. Hepatocytes isolated from human liver would be the best source of cells for these hybrid systems. Until today the most promising results were obtained for the Extracorporeal Liver Assist Device (ELAD). ELAD entered the phase II and III, of controlled, randomized clinical trials. Unfortunately, the results of the study were not satisfying and treatment with the ELAD did not improve patients survival. The aim of the study was to construct improved hollow fiber bioreactor for hepatic cell culture, which ensure better *ex vivo* cell growth conditions than standard 2D culture and become upgraded biologically active block of a new BAL.

The culture of hepatic cells will be carried out in hollow fiber bioreactors. The cells will be seeded on the outer surface of the membrane. Commercially available polysulfone membranes with a large pores of declared size of 0.2 µm were used to prepare the bioreactor modules. The bioreactors construction was performed in cooperation with the Laboratory of Semipermeable Membranes and Bioreactors IBBE PAS. The finished modules consist of 20 capillaries. The ultrafiltration of prepared modules was evaluated. Scanning electron microscope (SEM) was used to identify the membrane structure, such as membrane surface, actual pore size or to measure the outer and inner diameter of the fiber. To improve cells' attachment the growth surface was coated by collagen. Additionally, the roughness of the membrane surface covered and not covered with collagen was analyzed using laser scanning microscope.

This study showed that the structure of the membrane varied: the inner surface of the capillary had larger pores, while the outer surface had smaller pores. The results obtained from SEM showed that the layer of collagen on membrane surface sealed parts of pores, which can affect compounds diffusion. Line roughness measurements revealed that collagen increase the membrane roughness and can improve the cells attachment to the growth surface.

Obtained results are promising for successful culture of hepatic cells in the hollow fiber bioreactors. Hollow fiber bioreactors are widely used in BAL devices and have a great application potential, because of their ability to better reflect *in vivo* conditions. The optimized modules, populated with self-produced hepatic cell line, will be tested as the improved biologically active function block of new BAL.

Wavelet Decomposition in Analysis of Impact of Virtual Reality Head Mounted Display Systems on Postural Stability

Piotr Wodarski, Jacek Jurkojć, Marek Gzik
Silesian University of Technology, Biomechatronics Department, ul. Roosevelta 40, 41-800 Zabrze
piotr.wodarski@polsl.pl

Aims: Maintaining the balance system in good working condition requires regular exercise and training, particularly in the case of elderly people, in the context of an aging society[1]. Physical exercises are becoming more and more popular and desirable thanks to development of modern techniques including the use of Virtual Reality Technology. Virtual Reality Technology increases the attractiveness of physical training and provides feedback in real time, which can positively influence the therapy results[2][3]. However, the introduced disturbances make the standard analysis of measurement results determined in the time domain insufficient.Analyzing precisely defined frequency bands of movements of the center of pressure makes it possible to determine the effectiveness of the balance system's response to disruptions and disorders, and may be used as an indicator in the diagnosis of motor dysfunction. The aim of the study was to determine the influence of spatial projection systems on body balance, including postural stability.

Methods: The study involved 28 participants (14 women and 14 men, average age 22 SD 1.3, average height 173 cm SD 9, average weight 66 kg, SD 11.6) for whom the center of pressure was assessed in a test with open eyes, closed eyes and with virtual reality projection. The study was performed using a measurement platform (WinFDM-S, Zebris) and Oculus DK2 HMD system. VR application was prepared in the Unity3D system and consisted of a simple scenery presented in Fig. 1. Percent distributions of energy during wavelet decomposition were calculated (selected wavelet function was Coiflets 5). The results were averaged and statistical analysis was performed. The CoP signals courses for a selected subject and signals occurring at the subsequent 12 levels of following wavelet decomposition were determined. In the next step, medians of percentage energy values for the signals occurring in the decomposition process were calculated. The above-mentioned medians were calculated for the whole study group within the range of 25%-75%. The values were calculated separately for displacements in the AP planes with open eyes, closed eyes and with virtual reality projection.

Results: The results present percentage energy values for individual signals occurring during the decomposition process of the CoP displacement signal in the AP and ML directions. Results are for the tests with open eyes OE, closed eyes CE and VR projection in the HMD VR system. An exemplary energy distribution for the CoP signal for AP direction for the OE, CE and VR tests is shown in fig. 2.

Figure 1. The scener presented in the study.

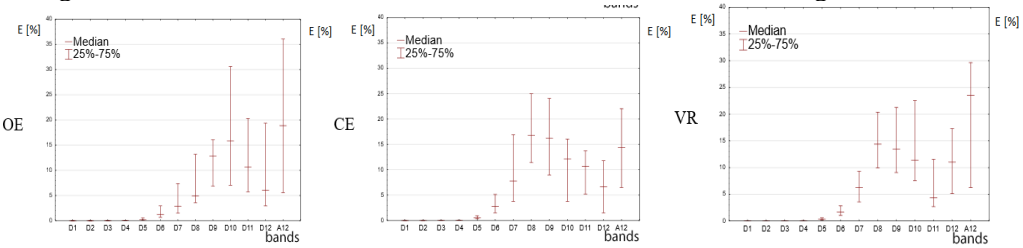

Figure 2. Percentage energy values for individual signals occurring during the decomposition process of the CoP displacement signal in the AP directions. Example results are from the tests with open eyes OE, closed eyes CE and with virtual reality projection VR.

Conclusion: The conducted wavelet analysis shows differences in postural stability between real and virtual environments. What seems to be important some of main differences can be noticed for low frequencies – the energy analysis revealed them for frequencies lower than 0.1 Hz. Such analysis is impossible to perform not only in time domain analysis but also in FFT analysis whereas this information may be crucial in diagnosis process of some diseases. The results shows as well that destabilization effect may be stronger in closed eyes conditions than in virtual environment.

References:

[1] Wodarski, P.; Jurkojć, J.; Gzik, M.: Wavelet Decomposition in Analysis of Impact of Virtual Reality Head Mounted Display Systems on Postural Stability, Sensors 2020, 20(24), 7138.

[2] Robert, M. T.; Ballaz, L.; Lemay, M.: The Effect of Viewing a Virtual Environment through a Head-Mounted Display on Balance. Gait Posture 2016, 48, 261–266.

[3] Gzik, M.; Wodarski, P.; Jurkojć, J.; et al.: A. Interactive System of Enginering Support of Upper Limb Diagnosis. In Advances in Intelligent Systems and Computing; Springer Verlag, 2017; Vol. 526, pp 115–123.

Statistical potential and energy maps in prediction of amyloids

Jakub W. Wojciechowski, Małgorzata Kotulska
Department of Biomedical Engineering, Wroclaw University of Science and Technology,
Wybrzeże Wyspiańskiego 27, 50-370, Wrocław, Poland.
jakub.wojciechowski@pwr.edu.pl

Amyloids are fibrillar protein aggregates, rich in beta structures. They were first observed in patients suffering from severe diseases, such as Alzheimer's and Parkinson's disease or type II diabetes. However, more recent studies have shown that similar structures can play important roles in many physiological processes in many organisms, including animals, fungi, and bacteria. Experimental techniques of identification of amyloids are expensive and time consuming, hence nowadays they are often accompanied by computational tools. Such bioinformatics methods often rely on complex statistical and machine learning models, which provide good accuracy, but are difficult to interpret, or utilizes time consuming molecular modeling approaches [1].

In this work, we aimed on developing a highly interpretable, physicochemical model based on a newly proposed statistical potential. We investigate the frequency of contacts between amino acids in 8000 globular proteins, 510 aggregates models obtained using PATH software [1], as well as those in nearly 150 amyloid fibrils deposited in Protein Data Bank, and used them to estimate pairing statistical potentials, considered as energy. These energies were then used to generate energy maps for known amyloidogenic and non-amyloidogenic fragments from the Waltzdb database [2]. In order to prove the usability of the concept, we have built the classifier by taking an average value of the energy map within an analyzed fragment of a protein sequence.

We have shown that the prediction method based on the statistical potential derived from the set of globular proteins outperforms other tested variants. Furthermore, even such a simple classifier as a mean value of energy map can provide a quite good distinction between amyloids and non-amyloids and obtain AUC = 0.81. This value is only slightly worse than AUC of state-of-the-art methods that utilize machine learning techniques, such as AmyloGram [3], and is orders of magnitude faster than structural modeling techniques like PATH [1].

The results show the great potential of the proposed methodology in developing a highly interpretable amyloid prediction tool. Furthermore, as the method does not rely heavily on training data, it may prove vary useful in the prediction of functional amyloids, which are currently underrepresented in databases of amyloids.

Acknowledgements: This work was partially supported by the National Science Centre, Poland, grant 2019/35/B/NZ2/03997.

References:
[1] Wojciechowski, Jakub W., and Małgorzata Kotulska. "PATH - prediction of Amyloidogenicity by threading and Machine Learning." *Scientific reports* 10.1 (2020): 1-9.
[2] Louros, Nikolaos, et al. "WALTZ-DB 2.0: an updated database containing structural information of experimentally determined amyloid-forming peptides." *Nucleic acids research* 48.D1 (2020): D389-D393.
[3] Burdukiewicz, Michał, et al. "Amyloidogenic motifs revealed by n-gram analysis." *Scientific reports* 7.1 (2017): 1-10.

Homodyne detection of brain-origin signals in near infrared spectroscopy

Stanislaw Wojtkiewicz, Karolina Bejm and Adam Liebert
Nalecz Institute of Biocybernetics and Biomedical Engineering, Warsaw, Trojdena 4, 02-109, Poland
swojtkiewicz@ibib.waw.pl

The diffuse scattering of light travelling through a tissue limits optical imaging resolution. As such, methods of improving the near infrared spectroscopy (NIRS) spatial resolution were proposed: e.g. the tomography approach applying high-density mesh of sources and detectors linked at all possible combinations, creating thousands of spatially overlapping measurements [1]. Furthermore, the tissue volume visited by the diffusely scattered light is broad and information carried in an optical signal originate somewhere within this volume. Therefore, methods of narrowing the volume of information origin are in high demand, e.g. using a spatial differentiation of signals measured by in-line source-detector pairs with slightly shifted positions [2, 3].
Here we aim to focus the NIRS sensitivity region within the brain tissue, canceling out the extracerebral sensitivity. Furthermore, we aim to use the biological variability in brain-originating components to lock-in amplify (homodyne detect) signals as measured on a head surface. Hence, amplifying components of brain-origin.

We propose a following hardware solution: two source-detector pairs (e.g. 3 cm separation) 90-degree rotated (forming the ‘x’ shape) and fixed on a human head surface. A product of the symmetrical spatial sensitivity profiles of such x-shaped pairs is non-zero in common volume located towards the brain and approaches zero outside of the common region, i.e. cancels out the sensitivity in the extracerebral volume. Furthermore, the proposed data processing algorithm based on the lock-in amplification of signals at both arms of the ‘x’, leads to amplification of signals originating within the common sensitivity region. Signals are locked-in amplified against each other (wide-band homodyne detection). The interference strength follows brain-originating components as the same components are present in both arms at the same time.
In-vivo tests on three healthy volunteers under visual cortex stimulation condition showed the proposed solution provides real-time, high signal to noise ratio brain activation signals with auto-filtered movement artefacts and other non-physiological components. The lock-in filtering characteristics follow signals variability and change constantly, auto-adjusting to the measured locked-in signals. Please refer to [4] for detail on the stimulation condition. The protocol as reported in [4] was adapted here to epochs of 20 s of stimulation and 20 s of rest. A round black and white checkerboard, flickering at 8 Hz, was displayed to stimulate the visual cortex.

We have developed mathematical formalism for simple two-channel measurements and high-density diffuse optical tomography, followed by data processing and analysis algorithms (the Beer-Lambert law and the tomography reconstruction) and hardware solutions. All adoptable in current systems and tested numerically and in-vivo on healthy volunteers. The proposed solution is ready to be used in e.g. brain-computer interfaces or brain hemodynamic monitoring devices.

References:

[1] K. M. Bergonzi, T. M. Burns-Yocum, J. R. Bumstead, E. M. Buckley, P. C. Mannion, C. H. Tracy, E. Mennerick, S. L. Ferradal, H. Dehghani, A. T. Eggebrecht, and J. P. Culver, "Lightweight sCMOS-based high-density diffuse optical tomography," Neurophotonics **5**, 035006 (2018).
[2] P. Sawosz and A. Liebert, "Method to improve the depth sensitivity of diffuse reflectance measurements to absorption changes in optically turbid medium," Biomedical optics express **10**, 5031-5041 (2019).
[3] S. Fantini, G. Blaney, and A. Sassaroli, "Transformational change in the field of diffuse optics: From going bananas to going nuts," Journal of Innovative Optical Health Sciences **13**, 1930013 (2020).
[4] K. Bejm, S. Wojtkiewicz, P. Sawosz, M. Perdziak, Z. Pastuszak, A. Sudakou, P. Guchek, and A. Liebert, "Influence of contrast-reversing frequency on the amplitude and spatial distribution of visual cortex hemodynamic responses," Biomedical optics express **10**, 6296-6312 (2019).

“Pulse wave propagation modeling for non-invasive assessment of heart function”

Kamil Wołos, Jan Poleszczuk
Nalecz Institute of Biocybernetics and Biomedical Engineering
ul. Księcia Trojdena 4, 02-109 Warszawa
kwolos@ibib.waw.pl

Pulse wave propagation modeling can help to predict blood pressure and flow in a system of arteries. It can also augment our understanding of cardiovascular system and help to develop non-invasive methods to assess the state of the cardiovascular system. In our current work, we aimed at extending previously proposed pulse wave propagation model with more detailed model of the heart. Such an extension, after confronted with clinical pulse wave recordings, might provide additional actionable information about patient’s status.

Proposed system is described by a bifurcation tree that includes 55 main arteries. A single blood vessel is modeled as an axis-symmetric, elastic cylinder with an impermeable wall. Equations governing blood flow are derived from conservation of mass and momentum equations. We assume that blood is a Newtonian fluid with constant density. We also assume that the blood velocity profile is parabolic across a cross-sectional area (Poiseuille profile). At arterial tree bifurcations we impose standard conditions i. e. continuity in the case of pressure and no leakage in the case of flow. At each end of the terminal arterial segments, we impose a three-element Windkessel model. In our previous work phenomenological heart ejection profile was considered as an inflow boundary condition [1], [2]. We propose an elastance model as an inflow boundary condition. It is a lumped model based on elastance function describing a relationship between pressure and the volume in the left ventricle. In our case elastance function is given by the time-dependent parametrized equation [3].

We have calibrated parameters that are connected with the heart elastance model to reflect results from the previous model – the mean pressure (MP) and the cardiac output (CO). The developed model faithfully reflects the most prominent characteristic features observed in measured flow and pressure profiles: the maximum pressure along the arterial tree increases (due to the tapering of the vessels), mean pressure drops toward the periphery (according to the distribution of flow and impedance of vascular bed) and dicrotic notch (a secondary upstroke in the descending part of the pulse which corresponding to the increase of the pressure in the aorta during the closure of the aortic valve) propagate along the periphery and becomes more separate and more prominent. We also performed a simple sensitivity analysis and examined the influence of the parameters related to the heart model on the basic characteristics predicted by the whole system: stroke volume, and diastolic, systolic and mean pressure.

The analysis of the developed model which uses inflow boundary condition with elastance function showed that it can previously obtained qualitative and quantitative results. Moreover, thanks to a more accurate description of the heart, the shape of the pulse wave can include reflections from the aortic valve which implies a more prominent dicrotic notch in the ascending aorta level. The simple sensitivity analysis provided us information about changing basic characteristics in dependency on values of the parameters.

[1] Poleszczuk, Jan, et al. "Subject-specific pulse wave propagation modeling: Towards enhancement of cardiovascular assessment methods." *PloS one* 13.1 (2018): e0190972.
[2] Poleszczuk, Jan, et al. "Patient-specific pulse wave propagation model identifies cardiovascular risk characteristics in hemodialysis patients." *PLoS computational biology* 14.9 (2018): e1006417.
[3] Ottesen, Johnny T., Mette S. Olufsen, and Jesper K. Larsen. *Applied mathematical models in human physiology*. Society for Industrial and Applied Mathematics, 2004.

Differentiation between single fiber potential (SFP) from one muscle fiber and SFP contaminated by other fibers

Ewa Zalewska
Nalecz Institute of Biocybernetics and Biomedical Engineering, Polish Academy of Sciences,
Ks. Trojdena 4 str., 02-109 Warsaw, Poland
ewa.zalewska@ibib.waw.pl

Introduction. Single-fiber electromyography is used as a routine procedure to study physiological and morphological parameters of motor unit. The most important usefulness is to evaluate neuromuscular transmission and fiber density. The variations in the time interval between firing of adjacent single muscle fibers from the same motor unit reflect abnormalities in the transmission time in axonal derivations and synapses and are called neuromuscular jitter [1]. For the accuracy of jitter measurement an identification of single fiber potential that is of one muscle fiber only is a crucial issue [3]. This is volid in case when jitter is measured using single fiber electrode as well as in case of concentric needle electrode [2].

Objectives. The aim was to improve the identification of potentials recorded using single fiber electrode contaminated by potentials from other muscle fibers, which might affect measured jitter value, by defining more selective criteria of SFPs discrimination. We were looking for solution suitable for automatization.

Methods. Standard parameters characterizing SFP and their combinations were analysed to define an analytical discriminating function able to verify if potentials recorded using single fiber electrode is due to single fiber or due to two (or more) fibers. The discriminating function is based on combination of standard SFP parameters. The procedure was tested on a set of simulated data and on samples of clinical data. To examine the procedure we have performed a series of simulations of contaminated SFP and analyzed the SFP parameters. We calculated SFP for a selected value of the principal fiber diameter and then added a second fiber. For each studied principal fiber diameter, we determined a range of acceptable second fiber diameters in such a way that the resulting potential was smooth, looked like a SFP and fulfilled the amplitude and rise time criteria of the SFP.

Results. Extention of the SFP criteria was proposed to improve identification of SFP. The tests on simulated data confirmed assumed properties of discriminating function. The percentage of contaminated SFP in simulated data was around 7% and in the sample of clinical data may be estimated to be at least 38%. The present data indicates that determination of jitter from this data set may be significantly influenced by the presence of second fiber potentials. Preliminary results suggest ability of proposed method for differentiation between potentials of one fiber and contaminated ones. Identification of potentials that are contaminated by the presence of a second fiber allows eliminating spurious potentials from the analysis of SFP.

Conclusion. Results suggest that proposed discriminating function when supplementing standard criteria would help to promote SFP recordings and enable to improve relevancy of jitter measurements and of jitter values norms.

References

[1] Sanders DB, Arimura K, Cui L, et al. Guidelines for single fiber EMG. Clin Neurophysiol 2019;130(8):1417-39.
[2] Stålberg E, Sanders DB. Jitter recordings with concentric needle electrodes. Muscle Nerve 2009;40:331-9.
[3] Zalewska E, Gawel M. Influence on jitter measurement of components from distant fibers in potential recorded by single fiber electrode. Acta Physiol 2018; 222(4): 1-5.

Designing Three-Dimensional Piezoelectric Scaffolds for Neural Tissue Engineering

Angelika Zaszczyńska, Paweł Ł. Sajkiewicz
Laboratory of Polymers and Biomaterials, Institute of Fundamental Technological Research Polish Academy of Sciences, Pawińskiego 5B, 02-106, Warsaw, Poland
azasz@ippt.pan.pl, angelika.zaszczynska@gmail.com

Piezoelectric materials are a class of inorganic and organic materials that can transform electricity into mechanical force and vice versa. In crystals, piezoelectricity is explained by the displacement of ions in materials that have a nonsymmetrical unit cell. [1,2].

The overall objective is devoted to designing and developing a novel smart piezoelectric polymer scaffold belonging to the type of conducting and stimuli-responsive scaffolds dedicated to neural engineering applications. The smart scaffold will significantly improve the effectiveness and safety of medical nerve reconstruction procedures. Polyvinylidene fluoride (PVDF) was chosen as one of the most piezoelectric polymer with various piezoelectric crystal modifications, depending on the forming conditions.

PVDF (Mw = 180 000 g/mol) nanofibers were electrospun from 25% solution of dimethylformamide and acetone (DMF/Ac 4:1 weight ratio) at the positive voltage of 16 kV applied to the needle, feed rate 0.2 mL/h (3 mm needle) and collected on drum collector (diameter 40 mm) at a distance between the needle and collector 180 mm. Human adipose-derived stromal cells (ADSCs) were cultured in osteogenic medium on the piezoelectric PVDF scaffolds electrospun with different collector rotational speed (200, 1000, and 2000 rpm) and subjected to ultrasound stimulation (power 80 mW, frequency 1.7 MHz) for 30 minutes every 24 hours. ADSCs seeded on piezoelectric PVDF scaffolds without ultrasonic stimulation were used as a control for each group. In order to confirm the piezoelectric effect on ADSCs viability, PrestoBlue cell viability test was performed on days 3, 14, and 21. Results were statistically analyzed using the Student's t-test. The observations of fibers and cell morphology were conducted using Scanning Electron Microscopy (SEM), Fourier-transform infrared spectroscopy (FTIR), and Differential scanning calorimetry (DSC).

The application of various process parameters allows for electrospinning of thin PVDF fibers with the preferred spatial arrangement and high polar phases content. Our cellular studies under in vitro conditions show that such nonwovens constitute promising smart scaffolds for tissue engineering applications, especially when stimulated by ultrasounds in order to activate their piezoelectric properties. PVDF nonwovens stimulated by ultrasounds is advantageous for cell viability. The obtained preliminary results are promising from the perspective of tissue engineering applications.

References:
[1] Zaszczyńska A., Sajkiewicz P., Gradys A., Piezoelectric scaffolds as smart materials for neural tissue engineering, Polymers, Vol.12, No.1, pp.161-1-25, 2020.
[2] Zaszczyńska, A., Sajkiewicz, P. Ł., Gradys, A., Tymkiewicz, R., Urbanek, O., Kołbuk, D. Influence of process-material conditions on the structure and biological properties of electrospun polyvinylidene fluoride fibers. Bulletin of the Polish Academy of Sciences. Technical Sciences, 68(3), 2020.
[3] Della Pietra, A., Mikhailov, N., Giniatullin, R. The emerging role of mechanosensitive piezo channels in migraine pain. International journal of molecular sciences, 21(3), 696, 2020.

Bioinspired glucose sensor based on a smart nanoarchitecture hydrogel composite

Yasamin Ziai, Chiara Rinoldi, Paweł Nakielski, Tomasz A. Kowalewski, and Filippo Pierini
Institute of Fundamental Technological Research Polish Academy of Sciences, 02-106 Warsaw, Poland.
fpierini@ippt.pan.pl

Smart biopolymers have attracted a lot of interest in the development of platforms for biomolecule sensing. One of the most common explored areas is the design of soft materials for glucose monitoring, which is of great significance in the diabetic therapeutic market. Multifunctional biomimetic, biocompatible, and stimuli-responsive materials based on hydrogels with physical properties similar to living tissues have attracted great attention. In this frame, designing nanostructured materials that do not require any external energy source is a key parameter for developing a platform for sensing glucose in body fluids.

Here, the fabricated material to fulfill this aim consisted of two outer layers of a nanocomposite plasmonic hydrogel, and one electrospun nanofibrous mat, resulting in a compact and stable device. Inspired from exceptional chameleon skin features, plasmonic silver nanocubes were embedded in poly(N-isopropylacrylamide)-based hydrogel. Using UV irradiation, fabricated network achieve enhanced thermoresponsive and antibacterial properties. Introduction of an electrospun mat consisted of poly(ε-caprolactone) and poly(ethylene oxide) (PCL/PEO) into the hydrogel layers creates a compatible environment for homogenous hydrogel coating, while providing necessary mechanical and structural properties to the final system.

Chemical, morphological, and optical characterizations were performed to investigate the proposed platform's structure in both scales of layers and the whole construct. The synergetic effect of thermoresponsivity and antibacterial properties of the composite material was investigated. Glucose detection was done using urine as a sample of a body fluid, revealing that the system has the limit of detection befitting the level of glucose in healthy and diabetic people. These characterizations, signify the proposed platform as a potential candidate for glucose sensing application.

Acknowledgments: This work was supported by the FNP First TEAM grant number POIR.04.04.00-00-5ED7/18-00

References

[1] Xu, X.D., Wei, H., Zhang, X.Z., Cheng, S.X. and Zhuo, R.X., 2007. Fabrication and characterization of a novel composite PNIPAAm hydrogel for controlled drug release. Journal of Biomedical Materials Research Part A: An Official Journal of The Society for Biomaterials, The Japanese Society for Biomaterials, and The Australian Society for Biomaterials and the Korean Society for Biomaterials, 81(2), pp.418-426.
[2] Eskitoros-Togay, Ş.M., Bulbul, Y.E., Tort, S., Korkmaz, F.D., Acartürk, F. and Dilsiz, N., 2019. Fabrication of doxycycline-loaded electrospun PCL/PEO membranes for a potential drug delivery system. International journal of pharmaceutics, 565, pp.83-94.

An innovative approach for a hip disorders rehabilitation

Jolanta G. Zuzda[1] PhD, Jakub Kacpura[2] MSc, Jakub Dziura[3] MSc, Piotr Borkowski[4] PhD Robert Latosiewicz[5] MD, PhD.

[1] Bialystok University of Technology, Institute of Management and Quality Science, Bialystok, Poland, j.zuzda@pb.edu.pl
[2]Rehabilitation Center, „Przystanek Zdrowie", Warsaw, Poland, e-mail: jbkacpura@gmail.com
[3]Rehabilitation Center, „Przystanek Zdrowie", Warsaw, Poland, jakub.dziura.0420@gmail.com
[4] Bialystok University of Technology, Institute of Biomedical Engineering, Bialystok, Poland, p.borkowski@pb.edu.pl
[5] Medical University of Lublin, Poland, Department of Physiotherapy and Rehabilitation, Lublin, Poland, r.latosiewicz@umlub.pl
corresponding author jakub.dziura.0420@gmail.com

Abstract
Aims: With growing rate of aging population, importance of efficient and cost-effective methods to cope with musculoskeletal system disorders is essential. Almost all people at some part of life will experience problems from aforementioned system [1]. It could be osteoarthritis, or rheumatoid arthritis or injuries and syndromes which result from daily living in a rushing world, where not only people overexert themselves, but from factors resulting from bad eating habits leading to obesity or malnutrition, spending many hours in one position working. There are many factors which could lead ultimately to problems with musculoskeletal diseases. Hip joint is one of the most important joints in body, as it through pelvic girdle it allows to walk, but in the same time it could be overloaded, as it transfers body weight [2].

Methods: The aim of this article is the review how important is rehabilitation in hip joint problems not only to reduce present problems but also to prevent possible forthcoming injuries. Next aim is to present specially developed device to be used in addition to Hip Conditioning Program, which is special training regime and it could be great addition to physical therapy or standalone training regimen that is not only effective, but also cost-efficient.

Results: The aiding device has been designed using CAD software. The main design assumptions are: hip joint rehabilitation and co-operating muscles, active one-legged exercises without resistance or dosed resistance, two configurations (flexion–extension and internal–external rotation) with adjustable angular range. Device is simple in construction, small sized and easy to handle.
Conclusion: Basing on the lower limb anatomy and biomechanics and the review of existing devices for rehabilitation special device with a new hip joint rehabilitation program has been developed. The device was reported in the Polish Patent Office (P. 426698)
Key words: hip joints, rehabilitation, exercise therapy, physical therapy, osteoarthritis

References:
1. Kuryliszyn-Moskal A, Hryniewicz A, Dziura J, Balneotherapy in the treatment of rheumatoid arthritis and osteoarthritis. Forum Reumatol. 2017, 3(3): 168–172.
2. Kulig K, Burnfield JM, The role of biomechanics in orthopedic and neurological rehabilitation. Acta Bioeng Biomech. 2008, 10(2):3-14.

The paper will be available as a full article in the conference proceedings within the "Advances in Intelligent Systems and Computing" series; the book title: "Biocybernetics and Biomedical Engineering – Current Trends and Challenges. Proceedings of the 22nd Polish Conference on Biocybernetics and Biomedical Engineering, Warsaw, Poland, May 19-21, 2021.

The Influence of Hip Conditioning Program with Rotational Movements on Thermal Response of Lower Limbs

Jolanta G. Zuzda[1], Jakub Kacpura[2], Jakub Dziura[3] Manuel Sillero Quintana[4], Robert Latosiewicz[5]

[1] Bialystok University of Technology, Tourism and Recreation Department, Bialystok, Poland, fitness2004@wp.pl
[2] Rehabilitation Center, „Sprawność", Zielonka, Poland, e-mail: jbkacpura@gmail.com
[3]Rehabilitation Center, „Sprawność", Zielonka, Poland, e-mail: jakub.dziura@gmail.com
[4]Universidad Politecnica de Madrid, Departmento de Deportes, Madrid, Spain, manuel.sillero@upm.es
[5] Medical University of Lublin, Department of Rehabilitation and Physiotherapy, Lublin, Poland, rlatos@umlub.pl
corresponding author jakub.dziura@gmail.com

Abstract

Purpose: The purpose of this study was the evaluation of differences in skin temperature on the body surface and of the impact of level of physical activity, characteristics of leg muscles and flexibility on the skin temperature during Hip Conditioning Program with Rotational Movements (HCP).

Methods: The study included 35 healthy volunteers of the Bialystok University of Technology. A thermographic camera and dedicated software were used for the acquisition and processing of thermographic images of body muscles before and after the HCP training regime.

Results: Hip Conditioning Program with Rotational Movements results in alignment of thermoregulatory processes in groups with lower fitness level and lower lean body mass in comparison to groups better developed in this matter. Individuals which has less developed muscles shows higher differences in skin temperature than groups more fit and muscle-developed.

Conclusion: Hip Conditioning program with Rotational Movements proved to be one of forms of physical activity that are suited to track and study the change of skin temperature measured by thermographic camera in subjects with different levels of lean body mass.
The usage of infrared thermography proved to be potent investigation tool in assessing relationship between thermoregulatory processes and forms of physical activity with taking into account the individual traits and characteristics of participants.

Keywords
Thermography, Hip Conditioning Program, Skin temperature, Muscles, Flexibility, Physical Activity

The paper will be available as a full article in the conference proceedings within the "Advances in Intelligent Systems and Computing" series; the book title: "Biocybernetics and Biomedical Engineering – Current Trends and Challenges. Proceedings of the 22nd Polish Conference on Biocybernetics and Biomedical Engineering, Warsaw, Poland, May 19-21, 2021.

Fourier Transform Layer for fast foreground segmentation in samples' images of tissue biopsies

Jakub Żak[a], Krzysztof Siemion[a,b], Lukasz Roszkowiak[a], Anna Korzynska[a]
[a]Nalecz Institute of Biocybernetics and Biomedical Engineering
[b]Medical University of Bialystok
jzak@ibib.waw.pl

Sjögren's Syndrome is a systemic disease, presenting itself in a spectrum of symptoms and signs throughout the body. Its diagnosis can include the examination of minor salivary gland biopsies. The image processing of digital images, specifically large-scale Whole Slide Images can aid in diagnosis, but unfortunately requires a lot of processing power and time for automatic analysis. This paper presents a new method for fast foreground (tissue) segmentation in fragments of Whole Slide Images containing biopsies of minor salivary glands taken from patients with diagnosed Sjögren's Syndrome. The method involves training a neural network with a novel type of layer, which calculates Fourier transform of data within the network. The neural network achieved accuracy of 89% on a test dataset.

The method for the approximation of AUC curve for supplements of endogenous biologically active substances

Grzegorz Żurek[1,2] Mateusz Gąbka[3], Paulina Dałek[4,5], Magdalena Przybyło[4,5], Marek Langner[4,5]
[1]Faculty of Pure and Applied Mathematics, Wrocław University of Sciences and Technology
[2]P&T Grzegorz Żurek
[3]Faculty of Fundamental Problems of Technology, Wrocław University of Sciences and Technology
[4] Lipid Systems Ltd.
[5] Department of Bioengineering, Wrocław University of Sciences and Technology
paulina.dalek@pwr.edu.pl

Aims
Due to environmental degradation and changing lifestyle, it becomes necessary to supplement organism with critical compound(s), which at normal circumstances are endogenously produced. An example of such a substance is cholecalciferol (vitamin D_3), which is endogenously produced and only in marginal quantities extracted from the diet. To evaluate its supplementation efficacy, it is necessary to determine the area under the curve (AUC) so the pharmacologically relevant parameters, such as dosage or frequency of application, can be determined. In the case of cholecalciferol, the direct determination of its concentration in blood is not practical since the application of a radiolabeled compound is required, and the patient should be monitor for an extended period (more than months). In addition, the cholecalciferol is not directly determined, but instead, its metabolite (calcifediol) in serum is measured.
Method
The presented new method for the reconstruction of the calcifediol AUC curve combines short-term clinical studies and experimentally derived mathematical function describing metabolic processes responsible for the maintenance of the calcifediol level. The method is founded on the combination of the medical trial performed for one day and the mathematical formula for calcidiol level, which is entirely controlled by metabolic processes.
Results
As a result of implemented method, the entire pharmacokinetic profile of the cholecalciferol formulation can be reconstructed. The method effectiveness has been demonstrated in studies of two different cholecalciferol formylations; oily and liposomal.
Conclusion
Obtained results have shown that the proposed methodology is a convenient and effective tool for the evaluation of the efficiency of an organism supplementation with cholecalciferol. Moreover, with a similar approach, the pharmacokinetic profile for other hydrophobic biologically active molecules could be constructed.

SPECIAL SESSION

Split Ventilation – Lessons From the COVID-19 Pandemic

Peter A Kahn
Section of General Internal Medicine
Yale Medical School
peter.kahn@yale.edu

At the height of the COVID-19 pandemic in the United States, there was significant fear that the number of patients requiring mechanical ventilation would exceed the supply of ventilators. Engineers, physicians, and respiratory therapists rapidly collaborated to produce a series of devices that would enable the sharing of one ventilator until a second critical care capable ventilator became available for use. One such device is the Vent Multiplexor, a 3-D printed venturi tube based device to split and measure ventilator output so as to allow individualization of delivered tidal volumes. Through close partnership between clinicians, industry, and engineers the worst fears of ventilator shortages were able to be averted and an entirely new device category created.

Flow diverters for lung ventilation in clinical practice: state of the art and future perspectives

Giuseppe Marraro
University of Milan, Italy
gmarraro@picu.it

In bilateral lung disease there is a marked disparity in disease severity between lung segments. Consequently the V/Q mismatch is distributed non-uniformly within both lungs because of regional differences in compliance and resistance. This non-uniformity of V/Q is most evident in unilateral lung disease.

Since the late 1980s it has been proposed the simultaneous independent lung ventilation (SILV) to better match the ventilation to the perfusion of each lung for obtaining a better gas exchange.

SILV requires selective intubation and two electronically synchronized respirators. Its clinical application has been hampered by the need to have two synchronized respirators for a single patient and by the increase in the complexity and costs of treatment. But to overcome these obstacles a flow diverter was engineered, whose clinical applications are described in the literature.

The shortage of respirators in intensive care following the COVID-19 pandemic has let to the development of ventilator sharing multisplit methods, whose reliability, benefits and risks still has to be assessed, confirmed and validated.
The COVID-19 pandemic highlighted the need to use a flow diverter for SILV in single patient to treat specific pulmonary pathology and to connect multiple patients per ventilator.

The lecture considers the state of the art on flow deviators for SILV, the actual possibilities of clinical application and the future perspectives.

Sesja specjalna: Inżynieria kliniczna w Polsce – jak przeskoczyć lukę pokoleniową

Ewa Zalewska
Nalecz Institute of Biocybernetics and Biomedical Engineering, Polish Academy of Sciences,
Ks. Trojdena 4 str., 02-109 Warsaw, Poland
ewa.zalewska@ibib.waw.pl

Sesja dotycząca spraw inżynierii klinicznej organizowana jest w cyklu konferencji KBIB po raz trzeci. Na tle rozwiązań wypracowanych w innych krajach, zaproponowane będą konkretne działania, które doprowadzą do tego, że specjaliści inżynierii klinicznej w Polsce będą mieli kompetencje i umiejętności spełniające standardy i wymagania międzynarodowe, a inżynieria kliniczna będzie pełniła właściwą rolę w ochronie zdrowia – rolę filaru, któremu przypisane są unikatowe kompetencje.

Współczesna medycyna nie może funkcjonować bez wsparcia inżynierii klinicznej. Rosnący udział techniki i technologii w ochronie zdrowia powoduje, że specjaliści inżynierii klinicznej są fundamentem i siłą napędową rozwoju opieki zdrowotnej i tylko ta grupa zawodowa mająca kwalifikacje nabyte w szkoleniu podyplomowym (specjalizacja w dziedzinie inżynierii klinicznej zakończona egzaminem państwowym) może zapewnić efektywne i bezpieczne stosowanie aparatury i technologii medycznych w całym cyklu eksploatacji od zakupu do utylizacji. Inżynieria kliniczna stała się filarem w nowoczesnym systemie ochrony zdrowia.

Trzeba jednak zdawać sobie sprawę, że współczesna rola inżynierii klinicznej jest całkowicie inna niż 30 lat temu. Obszar jej działania i odpowiedzialności jest bez porównania większy i obejmuje zupełnie nowe dziedziny takie jak zarządzanie, planowanie strategiczne, analizę kosztów, zarządzanie ryzykiem, zarządzanie zasobami części i akcesoriów zapasowych, systemy informatyczne, automatyzację wspartą systemami sztucznej inteligencji.

Zrozumienie jak funkcjonuje współcześnie inżynieria kliniczna i jak należy ją zorganizować od nowa w Polsce wymaga przede wszystkim oderwania się od myślenia stereotypowego, w którym jest ona kojarzona z serwisem aparatury medycznej, a zatrudnianie inżynierów w placówkach medycznych z kosztem.

Inżynieria kliniczna na świecie rozwijała się bardzo intensywnie w ciągu ostatnich 20-30 lat nadążając za innowacyjnym postępem technicznym i technologicznym, powszechną digitalizacją i informatyzacją, ale także rozwojem nowoczesnych metod zarządzania. Organizacyjnie przebiegała różnie w poszczególnych krajach. Ale w zakresie kształcenia i uzyskiwania kompetencji specjalistów inżynierów klinicznych – rozwijała się spójnie dzięki współpracy międzynarodowej. Syntetycznie można tę ewolucję podsumować następująco: od aparatury medycznej → do systemów oraz od serwisu → do kompleksowego zarządzania środkami technicznymi w ochronie zdrowia na poziomie strategicznym.

W tym czasie w Polsce inżynieria kliniczna, rozwijana od lat 60., przestała funkcjonować, co spowodowało powstanie pokoleniowej luki kadrowej i luki organizacyjnej. Za wyposażeniem placówek ochrony zdrowia na poziomie światowym nie nastąpił właściwy rozwój organizacyjny i kształcenie specjalistów w dziedzinie inżynierii klinicznej. Wyzwaniem jest teraz przeskoczenie obu tych luk, ponieważ globalizacja rynku aparatury i technologii medycznych wymaga równoważnych kompetencji specjalistów we wszystkich krajach, i współpracy międzynarodowej.

Realizacja i osiągnięcie tego celu w Polsce nie wymaga wymyślania jak to osiągnąć, wystarczy skorzystać z doświadczeń innych krajów. Równoległe działania mające na celu osiągnięcie równowagi popyt-podaż dadzą efekt sprawnie działającego systemu – a więc system ochrony zdrowia, w którym jest należne miejsce dla inżynierii klinicznej i zapotrzebowanie na specjalistów, oraz wykształcenie kadry specjalistów.

Przedstawiony będzie projekt rozwiązań legislacyjnych niezbędnych, aby inżynieria kliniczna pełniła właściwą rolę w ochronie zdrowia – rolę filaru, oraz organizacji kształcenia specjalistów, którzy będą mieli kompetencje i umiejętności spełniające standardy i wymagania uprawniające do uzyskania międzynarodowego certyfikatu. Projekt jest odpowiedzią na pytanie – jak przeskoczyć lukę i dorównać do światowych standardów.

Sesja popularnonaukowa pt.: "DLACZEGO POLSKA NIE PRODUKUJE RESPIRATORÓW?"

Zapraszamy do udziału w sesji popularnonaukowej pt.: "DLACZEGO POLSKA NIE PRODUKUJE RESPIRATORÓW?", która odbędzie się w trybie zdalnym 19 maja (środa) o godz. 13.30-14.30 w ramach XXII Międzynarodowej Konferencji Biocybernetyka i Inżynieria Biomedyczna.

Organizatorami Konferencji są:

PAN KOMITET BIOCYBERNETYKI I INŻYNIERII BIOMEDYCZNEJ

PTIB Polskie Towarzystwo Inżynierii Biomedycznej

IBIB PAN Instytut Biocybernetyki i Inżynierii Biomedycznej im. Macieja Nałęcza Polskiej Akademii Nauk

Czas pandemii COVID-19 obnażył słabości systemu ochrony zdrowia wielu krajów na świecie. Braki kadrowe, niedofinansowanie oraz organizacyjne niedomagania to główne czynniki negatywnie wpływające na proces diagnostyczno-terapeutyczny, czego efektem są wysokie wskaźniki umieralności. Przy tej okazji zaczynamy zwracać uwagę na rolę techniki w medycynie. Na podkreślenie zasługuje znaczenie osiągnięć inżynierii biomedycznej dla ratowania zdrowia i życia ludzkiego. W naszym głębokim przekonaniu droga do poprawy funkcjonowania i zwiększenia efektywności ekonomicznej systemu ochrony zdrowia wiedzie poprzez nowoczesne technologie medyczne do zastosowań w prewencji, diagnostyce, terapii oraz systemy informatyczne m.in. do zastosowań w teleopiece .

Zdrowie choć istotnie elektryzuje opinię publiczną nie ma barw politycznych. Dlatego zapraszając Państwa do udziału w sesji chcemy wzbudzić refleksję, zadać pytania:
- Czy my jako kraj jesteśmy dobrze przygotowani do walki z pandemią?
- Czy potrafimy wyciągnąć odpowiednie wnioski z przebiegu obecnej fali zachorowań?

Pandemia pokazała, że w sytuacji walki o przetrwanie poszczególne państwa zapominają o solidarności. Technologie ratowania życia rezerwują w pierwszej kolejności dla swoich obywateli. Stąd też rodzi się kolejne pytanie:
- Czy my jako kraj Unii Europejskiej właściwie inwestujemy środki w rozwój krajowej myśli technicznej na potrzeby medycyny?

Wszystkie te nurtujące pytania chcemy zadać w odniesieniu do prac badawczych nad polskim respiratorem. Urządzeniem, które w obecnej pandemii COVID-19 okazuje się kluczowym dla potrzeb terapii osób w stanie ciężkim. Urządzeniem, które w okresie pandemii stało się niezwykle pożądane, którego ceny zostały nagle wywindowane, a dostępność była bardzo ograniczona. Podczas dyskusji panelowej zadamy istotne dla bezpieczeństwa mieszkańców naszego kraju pytanie:
- Dlaczego Polska nie produkuje respiratorów?

Moderatorzy sesji:

prof. Marek Gzik

wiceprzewodniczący Komitetu Biocybernetyki i Inżynierii Biomedycznej PAN, przewodniczący Rady Dyscypliny Inżynieria Biomedyczna Politechniki Śląskiej,

prof. Adam Liebert

przewodniczący Komitetu Biocybernetyki i Inżynierii Biomedycznej PAN, dyrektor Instytutu Biocybernetyki i Inżynierii Biomedycznej im. Macieja Nałęcza PAN.

Paneliści:

prof. Jarosław Fedorowski

prezes Federacji Szpitali Polskich, kardiolog,

prof. Tomasz Topoliński

rektor Uniwersytetu Technologiczno-Przyrodniczego im. Jana i Jędrzeja Śniadeckich w Bydgoszczy w kadencji 2016–2020, pomysłodawca polskiego respiratora,

dr inż. Krzysztof Zieliński

Instytut Biocybernetyki i Inżynierii Biomedycznej im. Macieja Nałęcza PAN, kierownik zespołu wdrażającego polskie urządzenie Ventil, które może pozwolić na wentylację dwóch pacjentów z użyciem jednego respiratora,

Michał Janasik

wiceprezes Centrum Łukasiewicz ds. Finansów i Komercjalizacji.

Rejestracja do udziału w Sesji oraz całej konferencji jest dostępna bezpłatnie na stronie

https://pcbbe.ibib.waw.pl/